KWAME NKRUMAH UNIVERSITY OF SCIENCE AND TECHNOLOGY, KUMASI.

MINIMUM CARDINALITY FOR GEOMETRIC DISKS COVERING: APPLICATION TO GLOBAL SYSTEM FOR MOBILE COMMUNICATION (GSM) MASTS IN TELECOMMUNICATION NETWORK DESIGN.

By

Elvis Kobina Donkoh, (M.Phil. Mathematics)

A Thesis submitted to the Department of Mathematics, Kwame Nkrumah University of Science and Technology in partial fulfillment of the requirement for the degree of

DOCTOR OF PHILOSOPHY

College of Science

September, 2015

DEDICATION

This piece of work is dedicated to the Almighty God for His protection throughout my academic years in this university.

Part of it goes to Great Men and Women shaping a strong, prosperous and peaceful Ghana.

I also dedicate it to my virtual wife, partner, friend, and lover Elvina and my sister Elizabeth Yaa Donkoh with whom I share this inspiration.

Lastly I dedicate this work to the late Swiss mathematician, Leonhard Euler (1707 - 1783), whose achievements and contributions in Mathematics is immeasurably infinite.

DECLARATION

I hereby declare that this submission is my own work towards the P h D. Applied Mathematics and that, to the best of my knowledge, it contains no material previously published by another person nor material which has been accepted for the award of any other degree of the University, except where due acknowledgement has been made in the text.

PG8107412

Elvis Kobina Donkoh	… ………………………….	22nd September, 2015
Student Name & ID	Signature	Date

Certified by:

Prof. Samuel K. Amponsah	…..…………….…………	22nd September, 2015
Supervisor(s) Name	Signature	Date

Certified by:

Prof. Samuel K. Amponsah	…. …..………...……...	22nd September, 2015.
Head of Dept. Name	Signature	Date

ABSTRACT

This thesis is in computational geometry and optimization. Such problems arise in many application domains, such as communication networks, geographic information systems, crop management (watering of grid pattern crops with sprinkler), robotics, computer graphics and many others. More specifically, in this thesis we conduct research in the context of geometric covering with disks and optimization of overlap difference and overlap area for uniform and non-uniform disks. GSM networks are very expensive. The network design process requires too many decisions in a combinatorial explosion. For example, due to inappropriate location of GSM masts and irregular assignment of frequencies, mobile users experience frequent hard handovers, uneconomical soft handovers, call trafficking, call blocking and higher degrees of interference. As a result it is important to design optimized networks that meet performance criteria. In the telecommunication industry it is well known that wireless communication does not perform well without antennas on GSM masts, but the existence and design of GSM masts becomes an inconvenience to many users and the industry when not properly positioned. These wireless networks have a lot of geometric properties since the multiple sector radiated signal corresponds to circular motion. A unique greedy approximation model, called Hexagonal Tessellation Model (HTM) is proposed to solve the network design problem. Data from MTN and GLO Ghana and Nigeria were collected and analyzed using the developed model. Hexagonal Tessellation Model for uniform cell range accounted for an overlap difference of 5.788km using 35 GSM masts instead of $27.566km$ for 50 MTN masts in Kumasi East, Ghana. This is a 79% reduction in number over the original layout. GLO Accra East,

Ghana accounted for an overlap difference of $9.646km$ using 44 GSM masts instead of $16.624km$ for 50GSM masts. This is a 41.98% reduction over the original layout. Also, non-uniform cell range for MTN River State accounted for 12.367km using 36 GSM masts instead of $26.412km$ for 50 GSM masts. This is 53.18% reduction over the original design. Finally, non-uniform cell range for GLO River State, Nigeria accounted for an overlap difference of $15.541km$ using 38 GSM masts instead of $30.946km$ for 45 GSM masts. This is 49.78% reduction over the original design. Our solution is shown to be optimal in overlap difference and overlap area for both uniform and non-uniform cell range. Theorems on geometry of hexagonal tessellation for GSM network design are stated, conjectures are made followed by a corollary. Also, this research will seek to provide a profound and unifying exposition to telecommunication network theory and the mathematical algorithms that support it.

ACKNOWLEDGEMENT

My deepest, heartfelt thanks, first of all goes to the Almighty God for granting me guidance and knowledge in coming out with this important study.

I especially appreciate the encouragement, guidelines, comments, criticisms, suggestions and the unrelenting efforts of my supervisor and mentor; Prof. S. K. Amponsah from the proposal stage to the completion stage. All these thoughtful comments were considered carefully in the final preparation of the project and they have been of invaluable help in reinforcing my own ideas as to how the findings in this text should be presented.

Besides, I am thankful to all my lecturers in the Mathematics and Statistics Department, Kwame Nkrumah University of Science and Technology (KNUST), Prof. Sagary K. Nokoe, Dean of Graduate School, Prof. E. Owusu-Marfo, Dean of School of Science and my colleague mathematician Dr. Alex A. Opoku, all of University of Energy & Natural Resources, Sunyani for being helpful and impacting knowledge in me in diverse ways. The person who has made the largest contributions to the accuracy of this findings: the Northern Sector Manager (Operations and Management) of ATC Tower (Ghana) Ltd , Mr. Alexander Woahene, OMCR engineer of GLO Ghana , Mr. Eric Frimpong Gyamfi, Site engineers and managers of EATON and Helios Towers, Ghana and Ms. Stella Ofori Ampofo of the Geodetic department, who enlightened me on the use of Fugro and AutoCAD software. I wish to express my thanks and appreciation for a helpful, lively and enjoyable interaction with the afore mentioned people.

TABLE OF CONTENTS

CHAPTER TWO: TELECOMMUNICATION NETWORK CONCEPTS, FUNDAMENTALS, NOTATIONS AND TERMINOLOGIES.

CHAPTER 3 : LITERATURE REVIEW

CHAPTER 4 : HEXAGONAL TESSELLATION MODEL FOR GSM NETWORK DESIGN

LISTS OF TABLES

LIST OF FIGURES

DEFINITION OF TERMS

AMPLITUDE: The maximum value attained by a quantity that varies in periodic cycles i.e. the maximum displacement from its mean position, usually equal to half its total displacement.

ANTENNA: A device for sending and receiving radio waves; a metallic piece of equipment of variable shape, used in the sending and receiving of television or radio signals.

ATTENUATION: The attenuation is the decrease of signal strength between the transmitter and the receiver. In air medium, the attenuation is simply inversely proportional to the square of the distance.

BANDWIDTH: The range of frequencies that is used in any particular broadcast.

CARRIER WAVE: An electromagnetic wave of specified frequency and amplitude that is emitted by a radio transmitter in order to carry information; which is superimposed onto the carrier by means of modulation.

CELLS: The area or country to be covered in a telephone network or a manufacturing unit consisting of a group of work stations and their interconnecting materials-transport mechanisms and storage buffers.

FRACTAL: A geometric figure that consists of an identical motif repeating itself on an ever-reducing scale.

FREQUENCY: The frequency (f) of the oscillations is the number of complete cycles per second made by the oscillating object. The unit of frequency is hertz

GLO: An abbreviation for globacom or global communication.

GLOBAL SYSTEM FOR MOBILE COMMUNICATION (GSM) : GSM is a digital system for mobile telecommunication. Mobile subscribers can make calls to and receive calls from both fixed and mobile subscribers.

MACROCELLS: A macrocell is a cell in a mobile phone network that provides radio coverage served by a high power cellular base station (tower).

MAST: A broadcast tower or a tall broadcasting antenna.

MERCATOR'S PROJECTION: A method of making a map of a globe on a flat surface in which the meridians and latitudes are shown as straight lines that cross at right angles.

MICROCELLS: Are used in areas of high subscriber density such as urban and suburban areas. Base station antennas are placed at an elevations of street lamps, so the shape of the micro cells are defined by the street layout. The cell length is up to 2km.

PERIOD: The time period T of an oscillating object is the time it takes to go through one complete cycle of oscillation. The unit of time period is the second.

PHYLOGENY: The development over time of a species, genus or group as contrasted with the development of an individual from a fertilized ovum to maturity; ontogeny.

PICOCELLS: Are designed for very high mobile user density or high data rate applications, typically in indoor environment. Base station antennas are below roof top or the elevation of book shelves so the coverage is dictated by the shape and characteristics of the rooms and the service quality is affected by the presence of furniture and people. The radius of pico cells is between 10m to 200m.

SERVICE AREA: A number of Location Areas form a Service Area.

SIMPLE HARMONIC MOTION (S.H.M): The straight line motion of a particle whose acceleration is proportional to its displacement from a fixed point (origin) and is always directed towards that fixed point.

SPACE WAVES: Radio waves of frequencies greater than 30MHz that covers the UHF, VHF and microwave bands with a limited range for broadcasting such as direct 'line-of- sight' communications or for satellite links.

TELECOMMUNICATIONS: The study and application of means of transmitting information, either by means of wire or by electromagnetic radiation.

WAVELENGTH: It is the distance from one particle to the next particle in phase with it or the distance in meters between successive points of equal phase in a wave.

WAVESPEED: The speed of propagation or wave speed is the distance covered by the wave in unit time.

CHAPTER 1

INTRODUCTION

Throughout the existence of the human species, we have always communicated with one another. First with simple sounds, later on with words and full sentences. The ability to communicate is a gift that children learn at a very early age. Human communication may be a sophisticated speech or a simple smile. Animals can also communicate. For example, whales and dolphins communicate using high and low pitched sounds that travel through water over many kilometers. This manner of communication is only used at short distance (Mee et al., 2010).

To meet the demand for long distance communication smoke-signals were introduced. But the resulting connectivity was insufficient. After electricity had been invented, long distances were not a problem anymore, e.g. the telegraph was used to send messages in Morse code. Shortly after this period, the telephone allowed voice communications. The telephone is still the most important means of Radio Frequency (RF) communication to the present-day. In most homes one or more telephones are available. This kind of telephone network is fixed meaning that the place from which the subscriber can make call is fixed. The mobility is restricted by the length of the wire connecting the mouthpiece of the telephone and the telephone itself. As technology progressed the telephone became smaller and smaller. At the same time (RF) designs also improved mobile communication possible. First the pagers were introduced which represented only a simplex radio traffic. This means that the subscriber can only send short messages. After the pagers had been introduced the mobile phone was invented. In the course of the early years these phones were very big and you had to carry a big sized batteries on your back.

In the case of humans, the ability to communicate has been developed and extended so that messages and information may be sent over great distances in very short time intervals; sometimes without any underlying cables via free space waves. Since the number of subscribers increased rapidly another system architecture was needed to cope with mass communication. For this purpose the multi cellular radio communication concept was introduced (Matthesijssen, 2000). Most wireless communications devices, such as radios, broadcast television sets, radar and cellular radio telephones, use or are fitted with antennas on mast. These antennas are used to send radio waves to distant sites and to receive radio waves from distant sources. A typical example is the GSM communication system. Today, GSM is the fastest growing communications technology of all time, with the billionth user connected on the first quarter of 2004, which is twelve (12) years after the commercial launch of the first GSM networks
(Raisanen, 2005).

One application is in the evaluation of a grid network design compared to a non-grid design. Consider, for example radio base stations that must cover a set of potential customers (subscribers). The problem is where to position the base stations, according to a distribution of demand points, to achieve optimum quality of service, at minimum costs. In this case, the number of grid stations required to cover the same demand points that are covered by a single non-grid station is given. We point out that facility location problems such as those that represent our motivating application are well-studied problems in Discrete Mathematics, Operation Research and Computer Science, but they also represent abstractions and hence, a simplification of real problems. In reality, GSM antennae and base stations cannot be placed anywhere on the plane, their potential location can be influenced by a variety of physical and economic considerations. Similarly, only some cities (or part of cities) resemble a regular grid pattern that can be exploited by the location of the facilities. It is well known that there are two popular tessellations of a plane with regular polygons of the same kind: square and hexagonal (Stojmenovic, 1997). A lot of designs are based on those two popular tessellations.

This study is devoted to develop a new approach to achieving best site placement in order that operators of GSM network will be empowered to make better choices during network planning which will aid them in meeting the demands of subscribers more efficiently. In this study we shall consider the hexagonal tessellation, which closely approximates the circular radiation patterns and achieves the maximum coverage with a given number of nodes.

1.1 BACKGROUND OF THE STUDY

Recently, development of wireless communication models and networks have been considered as a subject of great interest in telecommunication industry (Rappaport, 2002). A special focus is to study intercell interferences in modern cellular networks. In particular, many techniques for modelling such interferences, between telecom operators, are well developed in many works (Jraifi, 2010). Wireless networks are fundamentally limited by the intensity of the received signals and by their interference. Since these quantities depend on the spatial location of the nodes, mathematical techniques have been developed in the last decade to provide communication-theoretic results accounting for the network's geometrical configuration. Often, the location of the nodes in the network can be modelled as random, following for example a Poisson point process. In this case, different techniques based on stochastic geometry and the theory of random geometric graphs – including point process theory, percolation theory, and probabilistic combinatorics – have led to results on the connectivity, the capacity, the outage probability, and other fundamental limits of wireless networks (Haenggi, 2009).

In Ghana, mobile communication network providers such as MTN, VODAFONE, TIGO, AIRTEL and GLO respectively use the slogan : " Everywhere you go", " Power to you", " It's your time" and " Feel free" among others. Unfortunately, not everywhere we go do we feel free, have our time or power come to us. To allow subscribers the liberty to ramble anywhere within a service area, ample signal strength needs to be made available. As the roaming and number of subscribers increases, the density of the sites needed to meet the demands also increases. It will be shown that the solution of this problem can be articulated around the following approaches:

(i) Location of Global Positioning System (GPS) and

(ii) Geometry of design network for continuous signal by mobile user.

For cellular wireless systems, GSM is facilitated by base stations, which have a proper spatial dispersion. The service coverage area from a single antenna at a base station is made up of a cell. This cell is made of a region where subscribers have to receive ample radiated signal strength. Due to restrictions of the signal strength from various factors such as surrounding terrain, high building, antenna altitude etc multiple cells are required to provide a wide coverage area. The collation of these multiple cells across the service area involves a network design. For this problem industrial mathematicians and cell planners need to investigate the exact position with soft handovers and the geometry of the cell design for the location of GSM mast for better coverage area.

The desire of these communication networks and others in offering its subscribers connectivity at anytime and anywhere is in concert with the optimal design of GSM masts for total coverage area concept and has in turn elicited the fast growth of wireless networks, especially in the area of modern network optimization and geometric topology. Time spent in communication is very crucial to the cost borne by the consumer. This has evoked high-speed and highbandwidths in communication network in combinatorial optimization in an attempt to avert excess time. The advent of this high-speed and high-bandwidth networks has triggered a spate of work in the application of combinatorial techniques from Discrete Mathematics and Computer Science to problems in network design. The geometry of hexagonal tessellation problem is one of the classical examples. This problem arises in applications such as the Honey-Comb

Conjecture (Fan, 2004), the circle packing problem in recreational mathematics (Wikipedia, 2013), phylogeny (Cabrera et al, 2012).

Communication network providers, in an attempt to maximize service area coverage of a country, or reach more people, have resorted to design masts to cover these areas without proper accuracy of the position and the design model. This leaves some parts of towns or communities with no or poor networks. The problem can be stated as follows: given an open area of land scheduled for 900 MHz of bandwidth, what should be the maximum coverage area this GSM antenna should cover and how many of such mast's should be erected? This thesis seeks to investigate the location where a mast should be erected, the maximum service area together with some theorems and conjectures, on masting of GSM antennae's using hexagonal tessellation and geometry; followed by a corollary. The GSM masts and Base Stations (BS) correspond to the centres of circles representing a set of locations (cells) that are required to be interconnected via a communication network in a telecommunication setting. The problem is to find a maximum-size network transmission with minimum number of masts antenna's to route connection.

1.2 STATEMENT OF THE PROBLEM

The demand for wide network transmissions have increase due to competition from various communication networks such as TIGO, MTN, VODAFON, AIRTEL, GLO among others. This has triggered the spate of masting of GSM towers in too many places. In an attempt to offer maximum network transmission, these communication networks need to erect fewer masts with specific cell range at certain positions within a given area; as the number of masts erected has a direct influence on the costs. Telecommunication engineers are faced with the problem of cell planning in order to reduce hard handover (reduce or eliminate signal drop) and optimize coverage area at least costs. This thesis seeks to investigate the exact GPS to erect the GSM masts by proposing hexagonal tessellation model to optimize total service area.

1.3 OBJECTIVES OF THE STUDY

Network design optimization is a fundamental issue in several fields, including Applied Mathematics, Computer Science, Engineering, Operations Management discrete mathematics and Operations Research. Networks provide a useful way of modelling real world problems and are extensively used in many different types of systems including communications, mechanical, hydraulic, logistics among others. Since cellular radio networks are large scale engineering objects and consists of numerous technical entities and represent high financial investments, they need a systematic design approach using precisely stated network design objectives and requirements. In this thesis, we intend to formulate a geometric algorithm to

(i) Determine the best geometric disk covering algorithm.

(ii) Minimize the overlap difference in the disks covering problem

(iii) Establish an analytical proof that the area of any regular polygon inscribed in a disk with fix radius approximates that of a circle as the number of sides increases.

(iv) Establish a formula for computing the overlap dimensions (area and difference) of this geometric plane object with least cost for both uniform and non-uniform disk.

(v) Establish a formula for determining the apothem and dimensions of any regular polygon inscribed in a disk.

(vi) Formulate a non-rigorous geometric disk covering algorithm for point sets, regular and irregular plane.

(vii) Propose a formula for calculating the co-channel re-use distance and ratio in GSM cell design for both uniform and non-uniform cell range.

(viii) Propose theorems and conjectures associated with disks covering via hexagonal tessellation for telecommunication network design.

1.4 SIGNIFICANCE OF THE STUDY

This study will;

(i) serve as a guide for further potential research in other areas such as watering crops using sprinkler, site emergency warning sirens coverage etc. (ii) give telecommunication engineers a geometrical model for cell planning (a formula for computing the co-channel re-use ratio, distance, designing approximation algorithms for better coverage etc);

(iii) aid mathematicians in the field of computational geometry, optimization and geometric topology in their study of disk covering.

(iv) aid in locating a better coordinate (WGS-84 or local) for GSM masts placement for wireless network design.

(iii) evoke some geometric theorems associated with disks covering in a plane.

1.5 METHODOLOGY

The question of mobile service user's network availability, connectivity and signal strength has brought attention to the strategic significance of GPS and GSM antennae location for maximization of area coverage in telecommunication network design. The question is how to optimize total service area of a GSM mast in a GSM network design and how to reduce hard handover network connectivity. Due to the high cost of masting GSM and the complexity associated with optimizing area coverage for different areas, it is therefore meaningful to algorithmize and generalize the rules for disk covering. We therefore employ geometry of hexagonal tessellation in our design.

We first consider the physical design of GSM antenna and their signal propagation in GSM masts. This according to Azad (2012) is known to be cuboid shaped with sector radiating signal. A collection of sectors at a point constitute a circle, so the circular signal radiation pattern is used. Covering with circle is possible and efficient if it is only motivated by tilling using regular polygons. Three tessellable geometrical shapes regular triangle, square and hexagon will be inscribed each in a circle and the ratio of their area to that of the circle will be computed. The shape whose area approximate circles more closely is considered. We then construct a grid using the tessellable regular polygon obtain and superimpose it on a Mercator projected map. The disk covering algorithm for optimizing coverage area with soft handovers will be used to determine the GPS of the base stations as well as the number of GSM antennae's required in a given region. Theorems and conjectures on the geometry of hexagonal tessellation for uniform and non-uniform cell range will be stated.

1.6 ASSUMPTIONS

From the modelling perspective the following assumptions were made.

(i) GSM antennas are placed in such a way that the signal radiation is in sectors (Azad, 2012).

(ii) There is sufficient and constant flow of transmission power. For the antennas on the masts to work there is the need for flow of electric power.

(iii) There are no obstacles (like high buildings, trees etc) to signals. This assumption is natural as GSM masts are higher than any of these obstacles.

1.7 THE SCOPE OF THE STUDY

A network is a system of nodes and interconnecting links. Telecommunication network is the study and application of means of transmitting information, either by means of wire or by electromagnetic radiation. This energy radiates in simple harmonic motion which is equivalent to circular motion. This thesis therefore studies the relationship between the simple harmonic pattern to the circular motion in a GSM antennae radiated energy; the geometrical shape that approximates circles closely and their tessellation in a Mercator projected map that will offer maximum total service area with soft handovers in a telecommunication network. Specific attention is given to telecommunication network layout design in a hexagonal grid which is dual to regular triangular grids, location of GPS in the World Geodetic System 1984 (WGS-84) for base stations. Telecommunication networks of different scales are discussed and studied. The following problems are discussed in detail:

(i) Basics of GSM networks including handover, hexagon inscribed disks coverage and geometry of hexagonal in tessellation.

(ii) Determination of location position (GPS) for base stations in a telecommunication network.

(iii) Development of a method for identifying optimal disks covering for GSM positions in telecommunication network design.

(iv) Illustration of the above methods using local studies such as MTN and GLO for Ghana and Nigeria.

1.8 LIMITATIONS OF THE STUDY

The following are the limitations encountered when conducting the research

(i) Cumbersome nature of working in different coordinate system using Fugro converter and WGS-84 in an Autocad environment.

(ii) Financial constraints; as the researcher has to travel to the offices of various communication network for the exact GPS coordinates and confirmation of GSM masts in Ghana.

(iii) Time taken to compute the overlap difference for the randomly erected GSM masts for GLO and MTN masts.

1.9 ORGANISATION OF THE REST OF STUDY

The ideas contained in this thesis are arranged as follows. Chapter 2 deals with telecommunication network concepts, fundamentals, notations and terminologies. It begins by introducing the problem of area coverage and user capacity and then extends to telecommunication network analysis and routing. Telecommunication network fundamentals are discussed together with related definitions and terminologies that were employed in the thesis. The chapter also provides a groundwork about information theoretic concepts, which will be used throughout the thesis. Chapter 3 provides the theoretical background for this thesis. Particularly, this chapter presents the existing work upon which this thesis is built. The chapter introduces a number of concepts related to network topology, including various degree and link distributions. It describes the concept of hexagonal tessellation at network level and presents the existing research works. Finally, the chapter also briefly reviews a number of real world

telecommunication networks. That is, Chapter 3 describes and discusses relevant research ideas which have been published and shows their importance for this research. Chapter 4 introduces, develops and illustrates the theorems and algorithms for the method of solutions of the problem. In particular, this chapter provides a taxonomy of geometric disk covering methods employed in interconnection networks that considers path set up and selection of GPS for base station locations. Chapter 5 develops and analyzes the algorithm for total service area of two GSM masts using the geometry of hexagonal tessellation.

This chapter also compares the design pattern using MTN and GLO Ghana and Nigeria. The comparison is made using a set of benchmarks, namely overlap difference and area in both hexagonal tessellation and random erecting of masts.

Included in this chapter are theorems and corollary that support the problem. A summary and conclusion derived from this research is presented in chapter six. Addition to this chapter, is the areas of applications, strengths and weakness as well as discussion on areas recommended for further research.

1.10 SUMMARY

The selection of an optimal configuration or design of a network occurs in many different application contexts including transportation (airline, railroad, traffic, and mass transit), communication (telephone and computer networks), electric power systems, and oil and gas pipelines. This section is devoted to geometric disk covering technique applied to telecommunication network design using variants GSM communication network. The classical GDC problems when applied to telecommunication network design need to be modified to take into account different network features in order to provide more realistic models of real-life situations. The Hexagonal Tessellation Model (HTM) is then proposed.

The chapter discusses the intended objectives for which this thesis was conducted and also shows their importance in other research. Demand for quality service by subscribers and telecommunication competition has compelled various networks to seek better GSM masts placement models and cell planning. This has called for both industrial mathematicians as well as telecommunication engineers and geodetic engineers to model using ideas in graph theory and combinatorics for telecommunication network design. The hexagonal tessellation model will be discussed to be the ideal design model. Data from ATC, Helios and Eaton (Ghana and Nigeria) showing local GPS coordinates of GLO and MTN for some selected regions was used as case studies on a Mercator projected map for modelling.

In the next chapter, we shall introduce and consider a plethora of concepts, notations and terminologies as well as symbols employed in the telecommunication network design problem.

CHAPTER 2

FUNDAMENTALS, NOTATIONS, TERMINOLOGIES AND CONCEPTS OF TELECOMMUNICATION NETWORKS.

The traditional problem of balancing the incompatible requirements of maximum area coverage and mobile user capacity has been a challenge to telecommunication engineers and industrial mathematicians alike. These requirements conflicts because to achieve a high and large coverage area, a single, high powered transmitter with a high antenna mounted on a tall mast must be used. Although a good coverage can be achieved by this approach, it is impossible to reuse the same allocated frequencies except in very distant location because of interference (Darweesh, 1999).

It implies that instead of having a large area covered by a single transmitter, that area can be divided into smaller coverage areas called cells, each with a low powered transmitter. This way, it is possible to reuse the same frequencies in different cells. It can be inferred that maximizing the number of times each frequency may be used in a given geographical area while keeping the interference level within tolerable limits is the key to an efficient cellular system design.

The optimize design network model needs to be topologically represented in graphs, symbols and notations, which is a language in the field of discrete mathematics, graph theory, geometric topology and computational geometry. Certain network analysis and routing are to be considered before further design models will be considered. In this chapter, we shall begin by looking at telecommunication network analysis and routing together with fundamental concepts, notations and terminologies that will be useful in the thesis.

2.1 TELECOMMUNICATION NETWORK ANALYSIS

Telecommunication network analysis is used to determine the signal strength, attenuation, and to enhanced network performance in the telecommunication systems. At the microscopic level, network analysis helps to accurately monitor the movement of mobile telephones and to make better decisions on when to hand over from one cell to the next. To a large extent, long-term monitoring of mobile telephone positions provide excellent input to the planning of the cellular network (Drane, 1998). Besides that, it can be used to determine the usage of service by subscribers especially during the peak times. By making the telecommunication network analysis, time of maintenance and bad signal can be measured. The effects of new load on the telecommunication path/line can also be predicted. Generally, telecommunication network analysis can be divided into three types; viz Network Tracing, Network Planning and Network

Allocation. Network tracing is the ability to trace the location of a call or a cell in the system. Network routing is done to find the optimum total service area, which cost less for the system. Network allocation is done in order to relocate all the calls in the cells. Our analysis of network shall focus on telecommunication network routing.

2.2 TELECOMMUNICATION NETWORK ROUTING

In the field of telecommunication network design, a routing process is the procedure of moving information across an interconnected system, from a source to a destination. Usually, along the way, there are at least one network peer, so that the routing protocol uses metric and low interference area to identify which path is the best for the information to travel. In order to dispatch the information, by a more technical point of view, a routing protocol need to organize the information, so that different kinds of network architectures can communicate among them. In the area of network routing, there is an enormous number of kinds of routing problems. Many works, in literature, treat the performance evaluation of routing algorithms (Sperduto, 2009).

In a theoretical scenario, in which the communication network is modelled as a graph, the best known problem is the Polygon Tilling Problem (PTP). In a PTP instance, we are given a number of cities in an area to be covered and a distance function (say maximum cell size 35km) over an area. The question is to find the minimum number of Global System of Mobile Communication (GSM) masts with antenna that will cover maximum total service area for good and continuous signal strength. Since PTP has a mass of application in the real world, this problem has been studied by many researchers belonging to the Operation Research and Discrete Combinatorial areas. Lawler (1985) has an intriguing history of a number of variant PTP such as Travel Salesman Problem (TSP), but in this discussion we limit to describe tilling a plane with disks for

GSM network coverage.

2.3 FUNDAMENTAL CONCEPTS OF GSM ANTENNA COVERAGE IN TELECOMMUNICATION NETWORKS DESIGN.

Telecommunication comprise various communications technologies, which can ensure convenience and mobility. The technologies range from indoor infrared

Wireless Local Area Networks (WLAN) to satellite systems (Miller et al., 1993). Most of the research results performed for this thesis refer to geometry of cellular systems design optimization, which are the most predominant part of telecommunication network design in terrestrial communication. The terrestrial communications also include mobile phone and mobile radio.

Brasche et al., (1997) (cited in Banciu 2003), emphasized that a cellular system is recognized as a network of radio cells, based on frequency reuse, which provides complete coverage of the service area. From all the mobile terrestrial systems, the cellular technology offers voice and data communication services over very large coverage areas. Each cell contains a Base Station (BS) serving more mobile stations (MS's). The MS can be a handset, a computer seen as mobile office (Ioachim et al., 2001), etc. There is no well-defined geometric border (unless for modelling, where discs are used) between the cells. When the signal becomes too weak for being handled by a BS, a neighbor BS takes over the communication after a new Radio Frequency (RF) channel was assigned. This process is called handover. The time over which a call can be maintained within a cell without handover is called the dwell time.

The radio link in a cellular system is subjected to the specific propagation laws of the radio waves. There is a substantial disparity between a transmission channel of a wired communication path and a radio mobile channel. Since the former is virtually constant in time, the latter is random and undergoes shadowing and fast fading (Shankar et al., 2013). Even when a mobile user is standing, ambient motion in the vicinity of the base station can produce fading. Shadowing, also called slow or long-term fading (Balachandran et al., 1999), designates the slow variation in the mean complex envelope of the receiver signal over a distance corresponding to tens of wavelengths. This is caused by variations in the local topography such as buildings, vegetation, and hilly topography. The effect of shadowing is reduced when the transmitter power is increased. Fast fading, also designates the rapid fluctuation of the envelope. Deep fades up to about 40dB can occur within a fraction of wavelength (Banciu, 2008). According to Furuskar (1998), the fluctuations in fast fading are caused by the interference of multiple copies of a transmitted signal each with different amplitude, phase and delay. This subsection outlines the basic concepts needed for the discussion of GSM antenna coverage that follows.

2.3.1 GSM SPECTRUM

GSM spectrum is the range of radiating frequencies in electromagnetic waves. Originally, GSM operated only in 900MHz band but later extended to 1800MHz and 1900MHz bands. Most GSM networks operate in the 900MHz to 1800MHz. Some countries used the 450MHz bands (Hˈmˈlˈinen, 2008). In so called primary GSM 900MHz the uplink frequency band is 890 – 915MHz and the downlink frequency is 935 - 960MHz. This 25MHz bandwidth is subdivided into One hundred and twenty four (124) carrier frequency channels each spaced 200KHz apart (Drane, 1998). This thesis uses the 900MHz GSM for the optimization of MTN and GLO for Ghana and Nigeria network design (World Time Zone,2014).

2.3.2 GSM SYSTEM DESIGN

The design of GSM network requires some physical equipment's as well as engineering knowledge. The physical equipment's include Base Station Controller (BSC), Mobile Switching Centre (MSC), Home Location Register (HLR), Serving GPRS Support Node (SGSN), Gateway GPRS Support Node (GGSN), Gateway

Mobile Switching Centre (GMSC), Mobile Station (MS), Visitor Location Register (VLR), Public Land Mobile Network (PLMN) etc. Figure 2.0 shows the design arrangement, but our optimization design algorithm shall focus between the Mobile Station (MS) and the Base Station Subsystem (BSS).

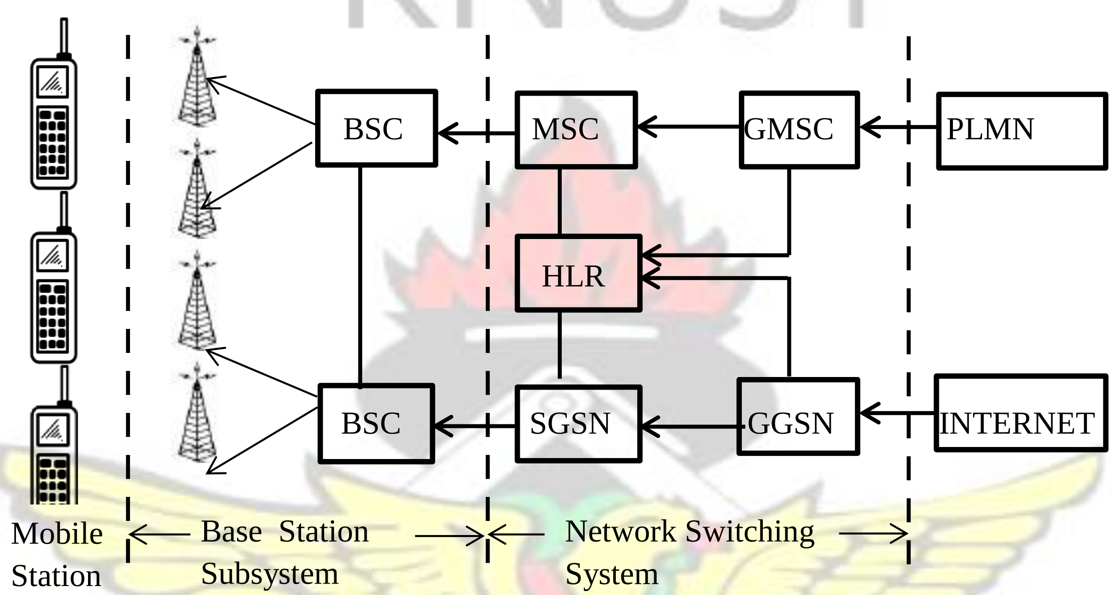

Figure 2.0: GSM System Architecture

2.4 NOTATIONS AND TERMINOLOGY

This subsection outlines the basic terms needed for the discussion of telecommunication networks that follows. A network is a set of points, some or all of which are connected by a set of lines with cycles. The points are known as nodes N or vertices V and the lines are called links, L or arcs A. The concept is illustrated diagrammatically in Figure 2.1. Networks are also sometimes called graphs. A network link between two nodes i and j, is denoted by (i,j) where i is the predecessor node $p(i)$ and j is the successor node $s(i)$.

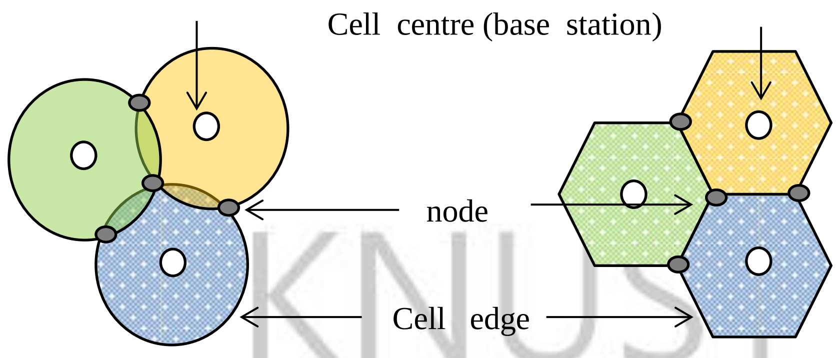

Figure 2.1: A graph or network.

A telecommunication network transmits information either by wires or by electromagnetic radiation. When the transmission is by wires it make use of nodes and links, but our focus will be on transmission by electromagnetic radiation-waves where the nodes represents the base stations or the points of intersection of the circular waves (equivalent to the simple harmonic motion of the radiation pattern) and the edges representing the circumference of these circular radiation waves.

ADJACENCY: Adjacency is a measure of the relation between a cell and its neighbours. A grid possessing uniform adjacency means that a cell with n edges also has n neighbours. A non-uniform grid means that each cell has some neighbours with which only shares vertices (Kidd, 2005). Figure 2.2 illustrates the concept of adjacent cells in some regular polygons.

a) Triangular Cells b) Square Cells c) Hexagonal Cells

Figure 2.2 : Tessellation of Regular Polygon Cells, (Kidd, 2005).

HANDOVER: The process of transferring an in-progress call from one cell or base station to a neighbouring cell without interruption. Handover is the main feature in cellular systems. Its goal is to allow the subscriber to keep its communication while moving from one cell to another.

CONNECTED SET: Intuitively speaking, a connected set is one which can be thought of as one piece. Analytically, a set S is said to be connected if it is such that when expressed as a union of any two disjoint non-empty sets , then either S_1 contains a limiting point of S_2 or S_2 contains a limiting point of S_1. Application of this concepts to Hexagonal Tessellation Model is found in chapter five. Three cases of connectedness have been established but only one case will be considered in our model. Figure 2.8(a) shows the union of a collection of connected sets that have at least one point in common . Figure 2.8(b) shows that if each pair x, y of S lies in some connected subset, say of S then S is connected. Also, if $S = \cup_{n=1}^{\infty} K_n$ where each K_n is a connected subset of S and $K_{n-1} \cap K_n \neq \emptyset$ for $n \geq 2,$ then S is connected (Chidume,1989). $S_1,\ S_2$

This is shown in Figure 2.8(c).

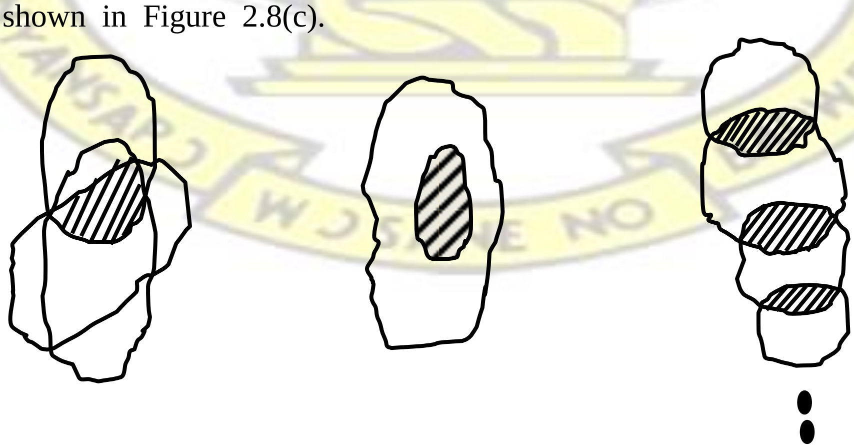

E_{xy}

Figure 2.8(a) Figure 2.8(b) Figure 2.8(c)

Figure 2.3: Variant Topologies in Connected Sets

CONNECTED COVER SET (CCS): Let S_i be a non-empty subsets of the set $\mathbb{R}$, where $i \in \mathbb{N}$. Then the property that $\bigcup_{i=1}^{n} S_i = \mathbb{R}$ such that $\bigcap_{i=1}^{n} S_i \neq \emptyset$ is a connected cover set. That is the members of the quotient set $\mathbb{R}/S_i$ are not pairwise disjoint (mutually exclusive) affording us a connected cover set. Conversely, if some $\bigcap_{i=1}^{n} S_i = \emptyset$ then the set S is not a connected cover set and may only give us a near-optimal solution of the network design. In telecommunication network, for node set S, which denotes the disks (circular motion of a GSM antennae wave) and the target region R, which denote the target flat plane geographical area, if S is a cover set (wave) for R and the hexagonal telecommunication graph is entirely connected, then S is a connected cover set of R. Figure 2.9 illustrates the concepts of connected cover set and disconnected cover set.

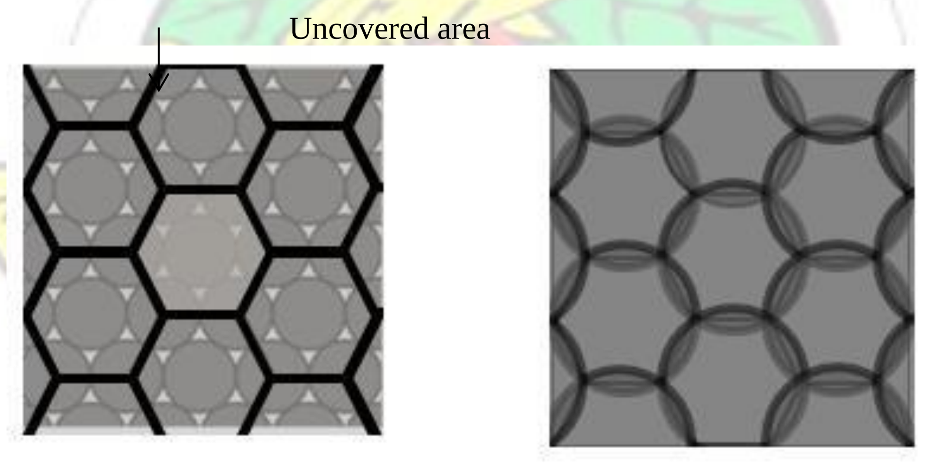

(a) Disconnected cover set (b) Connected cover set

Figure 2.4 Connected sets in GSM Coverage Area

From Figure 2.4(a) the hexagonal tessellation S_i connects the entire geographical area R whereas the disks does not cover the entire target region R, hence a disconnected cover set. This gives us a near-optimal solution or area coverage. On the other hand, figure 2.4(b) is a connected cover set with the hexagonal tessellation S_i and the circular waves connected and covering the entire geographical area R. Mathematically, $\bigcap_{i=1}^{n} S_i \neq \emptyset$. The connectedness is associated with the intersecting circular disks. The square represent the set $\mathbb{R}$ and the hexagonal tessellation as the non-empty cover set (S). Disconnectedness is associated with the mutually exclusive circular disks.

MINIMAL CONNECTED COVER SET (MCCS): Consider positioning a GSM network antennae S_i in a target region R, a MCCS problem equals finding the connected cover set $S_i' \subset S_i$ which has the minimum elements. Figure 2.4(b) shows a minimal connected cover set for our model coverage area. This algebraic topological property will be applied in the actual design of our optimal solution of the GSM antenna coverage as discussed in chapter five.

GEOMETRIC COVERING: These are cover problems in combinatorial and computational mathematics that are induced by geometric settings of the well-known set-cover problem. Given a collection $S = \{D_1, D_2, \dots, D_n\}$ of subsets of a universal set $\mathbb{U}$ and a set $H \subseteq \mathbb{U}$ of size n that is to be covered, the goal is to determine the least cardinality sub-collection $S^* \subseteq S$ such that the union of D_i is a superset of or equal to H where $D_i \in S^*$. Mathematically, $\bigcup_{D_i \in S^*} D_i \supseteq H$. This is illustrated in figure 2.5.

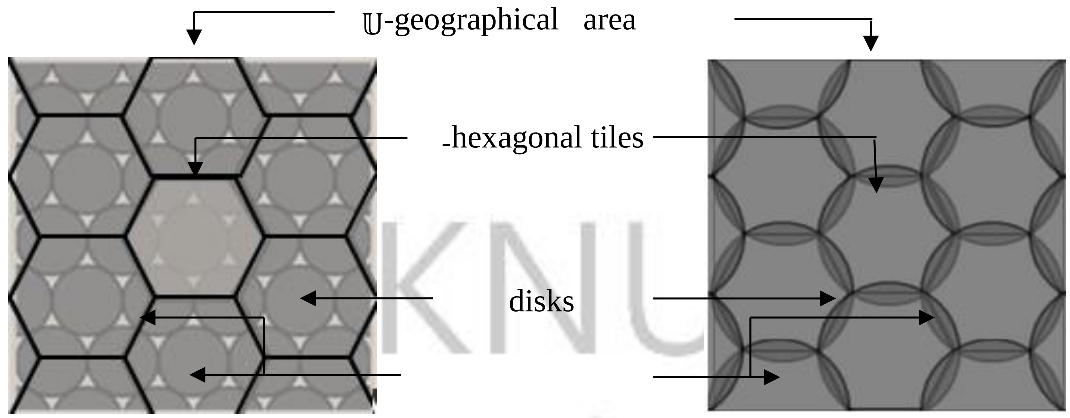

Figure 2.5: Geometric Covering of a Set

In geometric settings, often the subsets $D_1, D_2, \dots, D_n$ are geometric objects, such as strips, half-planes, disks, convex polygons (convex sets) among others. In the disk covering problems mentioned above, the aim is to minimize the number of disks in the cover. In the context of wireless networks, one often wants to minimize the sum of the radii of the covering disks.

CHAPTER 3

LITERATURE REVIEW

The literature review summarizes a number of works in the field of geometric covering and wireless telecommunication networks, which have application to disk covering in computational geometry, GSM antenna coverage area in telecommunication engineering and dispersal of points (settlements, population, seed, species etc) for bounded areas in physical geography, agricultural science and biochemistry. The chapter begins by reviewing publications related exclusively to modelling of cellular communication system, research in wireless network coverage, tiling and covering , geometric disks covering literatures, geometric covering of point sets using convex hull and hexagonal versus circular cells in GSM antenna.

Telecommunication network study, however encompasses more than just communication lines. For this reason, the following sections contain a synopsis of published writings in wireless network coverage. They include developments in each of the analytical, computational and heuristic approaches.

3.1 MODELLING OF CELLULAR COMMUNICATION SYSTEM

For all cellular network systems one major design step is selecting the locations for the base station transmitters and setting up optimal configurations such that coverage of the desired area with sufficient strong radio signals is high and deployment costs are low. A crucial parameter in the modelling of a cellular communication system is the shape of the cells. In real life, cells are irregular and complex shapes influenced by terrain features and artificial structures. However, for the sake of conceptual and computational simplicity, we often adopt approximate approaches for their design and modelling. In the literature, cells are usually assumed hexagonal or circular. The hexagonal approximation will be frequently employed in planning and analysis of wireless networks due to its flexibility and convenience.

However, since this geometry is only an idealization of the irregular practical cell shape, simpler models are often used. In particular, the circular– cell approximation is very popular due to its low computational complexity (Pirinen, 2006; Bharucha et al, 2008). Among various performance degradation factors, CoChannel Interference (CCI) is quite significant since the cells in cellular networks tend to become denser in order to increase system capacity (Stavroulakis, 2003). The development of models that describe CCI generates great interest at the moment. Several reliable models can be found in the published literature (Cho et al., 2000). However, their practical application is restricted by their algorithmic complexity and computational cost, which results in the development of simpler models.

3.2 GEOMETRIC DISKS IN WIRELESS NETWORK DESIGN COVERING LITERATURES.

Coverage is one of the fundamental requirements of wireless networks. There has been considerable research on optimal coverage of infinitely large areas.

However, in the real world, the deployment areas of wireless networks are always geographically bounded. It is a much more challenging and significant problem to find optimal deployment patterns to cover bounded areas using disks (geometric circles) shapes with soft handovers. We design several deployment patterns for circular and other regular tessellable shapes such as hexagons, regular triangle, squares etc. Kershner proved in 1939 that the honeycomb structure, also known as the triangular lattice, is the optimal pattern to cover unbounded areas (Bai, 2006). Simon (2007) (cited in Yu et al., 2008), investigated several optimal patterns for unbounded areas with special constraints, e.g., connectivity among nodes, are proposed in the area of wireless networking.

Yu et al., (2013) investigated the number of nodes needed to cover a bounded area. There are several classical papers on the problem of how large an area congruent shapes can cover.

Bambah et al. (1952) developed a bound on the largest area of a hexagon that can be covered (with simple intersection) by n congruent convex domains , i.e.,

$a(H) \leq nh(K)$, where $a(H)$ is the area of H and $h(K)$ is the maximum inscribed hexagon area in K.

Toth (1987) improved the result by adding a rectifying term on the right hand of the inequality. Later Boroczky (2005) gave a (nearly) optimal bound of node density to cover hyperbolic planes. As the bounds given by Boroczky is generic, it is not as tight as the bounds given by Toth in the research area of interest to us. However, none of them have used geometry of hexagonal tessellation to study coverage of bounded areas optimizing the overlap difference for both uniform and non-uniform cell range. We have improved the results of Toth, and applied the improved results to solving the bounded area coverage problem of sample GSM networks.

Some approximate patterns are proposed for covering certain bounded areas with specific shapes. Melissen and Schur, (1996) studied how to cover a bounded square with a small number of circles, i.e., 6-8 and Nurmela et al. (2000) extended their work up to 30 circles. Their patterns are highly specific, i.e., a unit square can be optimally covered by n discs with a specific radius.

Hochbaum and Maass. (1985) provided an approximation scheme to cover orthogonal bounded rectangles. Though the scheme can provide a pattern infinitely close to optimality, the computation cost is prohibitively high, i.e., not polynomial regarding the approximation ratio $\frac{1}{\epsilon}$. There is also a large body of literature on covering infinitely large, i.e., unbounded, areas with discs, with or without other constraints.

Kershner (1939) gave the most well-known result that the honeycomb structure, also known as the triangular lattice, is the optimal pattern to cover unbounded areas. In the area of sensor networks, optimal deployment patterns to achieve coverage or connected coverage can be intensively studied.

Bai et al. (2009) have reported several optimal regular patterns to achieve full coverage and different degrees of connectivity in two dimensional and three dimensional space.

Yu et al. (2011) designed optimal patterns for connected coverage in wireless networks with directional antenna. Several works focus on how to select the minimum number of sensors to be activated from a set of randomly pre-deployed sensors such that all interested discrete locations (or targets) are k-covered. This problem is known to be NP-hard (Yang, 2006). Centralized and distributed approximation algorithms were then proposed.

3.3 TILINGS AND COVERINGS

Covering has been one of the most fundamental and yet challenging issues in wireless network and found many applications such as routing and broad casting (Xu et al., 2011). A natural dual to covering is the corresponding tiling. Tiling is a countable family of closed sets $\{T_1, T_2, T_3, \dots\}$ which covers the Euclidean plane without any gaps or overlaps (Grünbaum and Shepard, 1986). Here

$T_1, T_2, T_3, \ldots$ are known as the tiles of T. Tiling differs from covering according to Lessard (2000) that the former is a family of sets without overlap whereas the latter covers the entire plane with no gaps but with overlaps. When the set of polygons has the same shape and size then it is a monohedral tiling. The only edge-to-edge monohedral tiling's by regular polygons are tiling of squares, equilateral triangles and regular hexagons (Lessard, 2000).

Sirbu (1992) has shown that plane tiling's and their properties have applications in medicine, where tiling's are used to describe the fight between the immune system and a pathogen agent. Richard et al. (1998) discussed concepts about random tiling's. Paredes et al. (1998) stated that tiling with squares and triangles are very useful tools to study several structural and thermodynamical properties of a wide variety of solids.

Keating and King (1999) worked on tiling's with squares. They have shown a necessary and sufficient condition for a bounded region of the plane with rectangles to be tillable with finitely many squares. The rectangles have the form $[a_1, a_2) \times [b_1, b_2)$ where $a_1 < a_2$ and $b_1 < b_2$.

Grünbaum and Shepard, (1986) shown that there exists precisely eleven (11) edgeto-edge Archimedean tiling's by regular polygons such that all vertices are of the same type. The vertices of the tiling [4.4.4.4] are called lattice points. A polygon with all its vertices at lattice points is called lattice polygon. Figure 3.1 shows the three (3) Archimedean tilling's of lattice polygon.

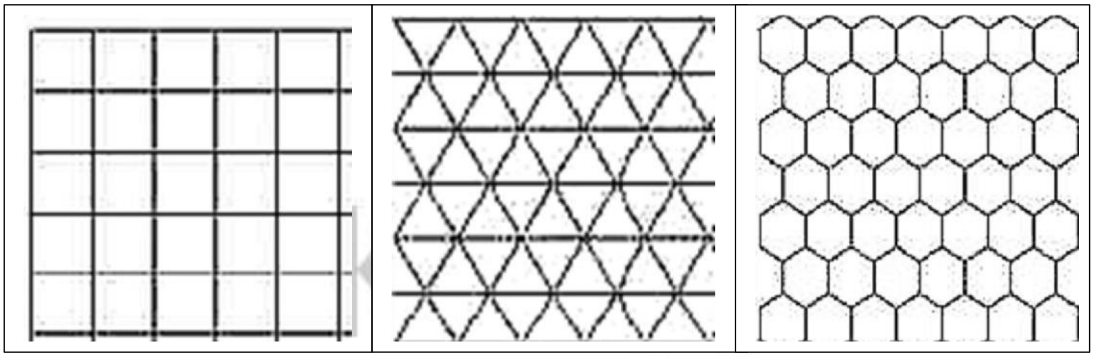

(a) 4.4.4.4 (b) 3.3.3.3.3.3 (c) 6.6.6

Figure 3.1: Archimedean Tiling's of Lattice Polygon (Ding, 2010)

When the vertices of the polygon are not lattice points we call it non-lattice Archimedean tiling polygon. This is illustrated in Figure 3.2.

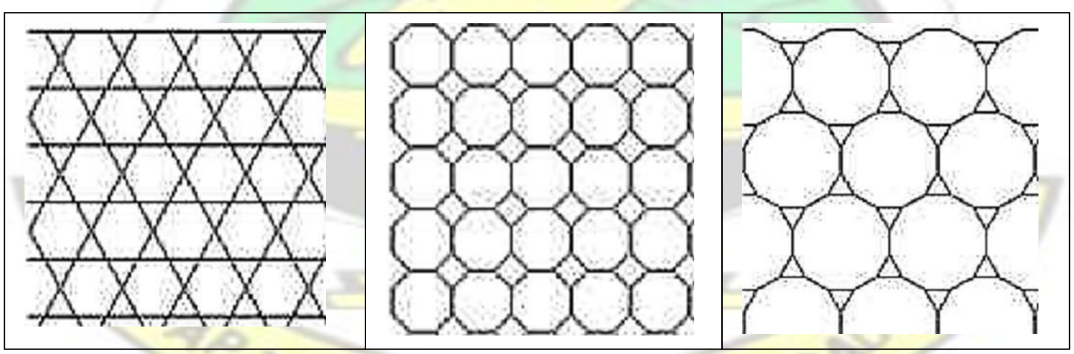

(a) 3.6.3.6 (b) 4.8.8 (c) 3.12.12

Figure 3.2: Archimedean Tiling's of Non-Lattice Polygon (Ding, 2010)

There are five (5) more Archimedean tiling's of no lattice polygon with vertices [3.4.6.4], [4.6.12], [3.3.3.4.4], [3.3.4.3.4], [3.3.3.3.6]. None of these authors

considered finding the minimum approximation algorithm for disks covering in a plane using tiling. The thesis investigate the minimum number of disks of radius r needed to cover any plane with point sets. It make use of Archimedean tiling [6.6.6] together with a geometric covering technique. Graham (1990) tested for anisotropic effects in medical images across three tessellations: a pentagonal approximation of hexagonal tessellation, a non-regular hexagonal grid, and a regular hexagonal grid. He found that tessellation artifacts in the sensor response were consistently lowest in the regular grid. He thus recommends the use of regular hexagonal grids for their superior detection and representation of local variation on a plane. Beyond applications of Christaller's (1933) classic theory, hexagonal tessellation has been advocated for thematic cartography by Carr et al., (2004), and has been used to study cluster perception in animated maps (Griffin et al.,
2006), as well as color perception (Brewer, 1996). Raposo (2011), uses hexagonal algorithm and the implementation of the Li - Openshaw raster-vector algorithm to produce comparably acceptable cartographic lines in Earth and Mineral Science.

3.4. GEOMETRIC DISKS COVERING LITERATURES

Geometric Disks Covering (GDC) is one of the most typical and well studied problems in computational geometry (Hu, 2013) and geometric optimization which arise in carrot crop management (Reid, 2005) as well as wireless network design and various other facility location problems (Alt et al., 2011).

Finding a minimum cover is an interesting combinatorial problem. Many well known problems (e.g., Vertex Cover, Dominating Set, Set Cover, and Covering by

Cliques) Gary (1979), can all be viewed as such problems. Let $D = \{D_0, D_1, D_2, \ldots, D_n\}$ be a set of discs of radius R with all their origins (centers) located inside D_0. Given D, the minimum disc cover problem seeks to identify a minimum subset of D, say D', such that the union of the discs in $'$ D is equal to the union of the discs in D. k

Charikar et. al (2004) in their study of minimizing the sum of cluster diameters using an approximate solution of k clusters noted that these problems are usually NP-hard. Many Polynomial-Time Approximation Schemes (PTAS) have been proposed, including geometric instances of these problems (Arora, 1998). In the context of GSM area coverage, when modeling the energy required for wireless transmission, it is common to assume a super linear $(a > 1)$ dependence of the cost on the radius (coverage): a quadratic dependence $(a = 2)$ models the total area of the served region, and in fact, physically accurate simulation often requires super quadratic dependence $(a > 2)$ for some known GSM antenna coverage

function $f(r) = \pi r^{\alpha}$.

Aloupis et al. (2012) improved the lower bound $11 \leq k$ results of Inaba (2008) to $13 \leq k$ and the upper bound results $k \leq 53$ of Okayama (2011) to $k \leq 45$ when considering a configuration of 50 points on a triangular lattice where is the smallest point set that is not coverable by disjoint unit disks. Aloupis (2012) problem is a variation of our GSM antenna coverage area problem. The variation lies in the fact that Aloupis (2012) was covering sparse point sets in triangular lattice grid using disjoint unit disks whereas the problem investigated is to cover entire GSM area (in a plane) with a condition in a mini-dense (or sparse) point set using intersecting disks of unit (equal) radius. The author use unit radius as a trial model and then generalize to rcm non-unit radius. Figure 3.3 shows a model of Aloupis (2012) configuration and the authors own model.

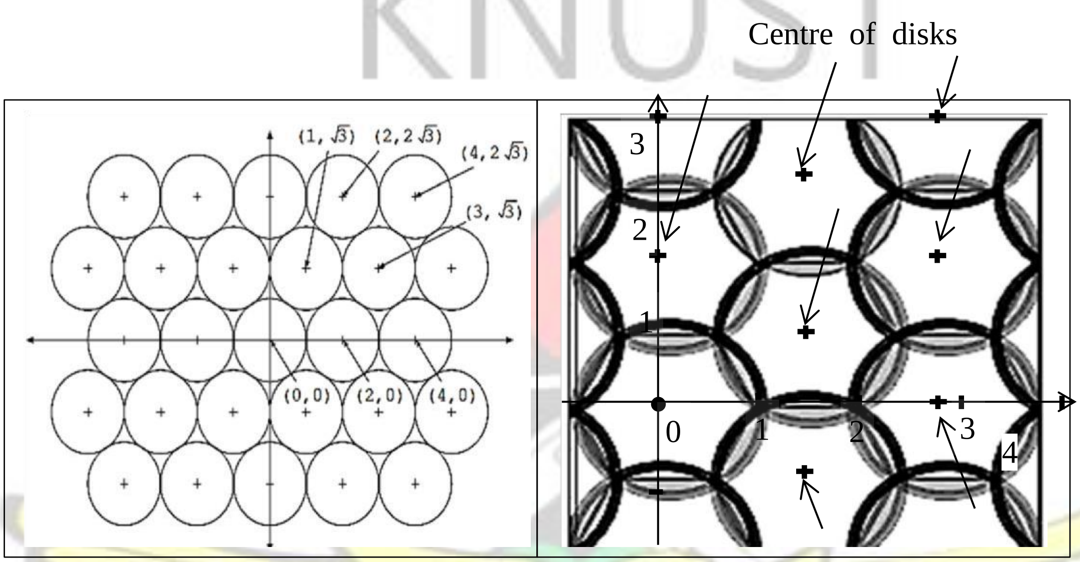

a) Covering using disjoint unit disks (b) Covering using intersecting unit disks

Figure 3.3: Unit disk covering of sparse points (Aloupis, 2012—3.3(a)).

3.5 GEOMETRIC DISKS COVERING OF POINT SETS USING CONVEX HULL

Covering of points is a well-known computational geometric problem that is NP-hard for interior polygons using convex polygons (Culberson et al., 1994). Chan (2005) emphasized that construction of convex hull of a finite set of points in low-dimensional Euclidean space is a fundamental problem in computational geometry. Given an n −point sets $P \subseteq E^2$, the convex hull of P written $Conv\ (P)$ is constructed by first constructing the upper hull of P, which consists of a sequence of hull edges that have an upward normal vector. Then the lower hull can be constructed by reflection and the convex hull can be obtained by joining the two edges.

Convex hull for point set covering is widely used in various fields such as Shape Matching (Corney et al., 2002), Pattern Recognition (Li, 2002), Cover Designing (Igarashi and Suzuki, 2011), Image Processing (Yang and Cohen, 1999), Finger Print Matching (Wen and Guo, 2009), Geographical Information Systems (Wang et al., 2003), (Peng et al., 2005), Path Planning (Meeran and Share, 1997) etc. There are many convex hull algorithms but no proper research has emerge in the geometric disk covering of point sets from convex hull using hexagonal tessellation. [1]The study develops a mathematical technique that is necessary for the disk covering in GSM antenna masting and can be applied to covering of point sets using maximal node covering (this can be extended to regular and irregular polygons).

[1] Both regular and irregular polygons can be thought of us convex hull computed from point set.

3.6 HEXAGONAL VERSUS CIRCULAR CELLS IN GSM NETWORK DESIGN

Cellular networks are infrastructure-based networks positioned throughout a given area. One of their features is the efficient utilization of spectrum resources due to frequency reuse (Baltzis, 2011). In practice, frequency reuse is a defining property of cellular systems. It is the fact that signal power falls off with distance to reuse the same frequency spectrum at spatially separated locations (cells).

In a cellular communication system, cell shape varies depending on geographic, environmental and network parameters such as terrain and artificial structures properties, base station location and transmission power etc. Nevertheless, for representation and analytical simplicity, cells will be approximated as regular shapes such as hexagons and circles. In the following paragraphs, we will discuss the main features of the two approximations. A hexagon is a tessellating cell shape in that cells can be laid next to each other with no overlap; therefore, they can cover the entire geographical region without any gaps. This thesis shall focus on using hexagons to approximate cell shapes in macro cellular systems with base stations on the ground or placed on top of buildings.

3.7 SUMMARY

In this chapter, we review publications related to developments in the GSM network design, tilling and covering and geometric covering disks. They include developments in each of the analytical, computational and heuristic solution approaches. In the next chapter, we shall introduce, develop and illustrate the general approximation algorithms for the method of solutions of the problem.

CHAPTER 4

HEXAGONAL TESSELLATION MODEL FOR GSM NETWORK DESIGN

In this chapter, we shall analyze the problem of designing a geometric disk covering algorithm with minimum cardinality for point sets and proposed an extension for regular and irregular polygons in an efficient time. The procedure employ here are useful for covering in less time complexity and for getting numerous alternative systems of near-optimal and optimal disks covering which can be compared using cost-effective (time and energy) and qualitative analysis, which may be very useful in the industry to determine the most reliable covering procedure.

4.1 OVERVIEW

This section presents an existing historical development as well as an improved and new development of the efficient geometric disks covering algorithm with minimum cardinality. It describes the algorithm that would be implemented. It will include a brief summary of motion of waves in GSM antenna, simple harmonic and circular motion, Geometry of GSM shapes, Co-channel re-use ratio in GSM network, tessellating a plane for maximum area coverage. It also discuss the geometry of GSM cell shapes, Cover patterns using tessellable regular polygons, how antennas are positioned and their characteristics, establishes a formula for calculating the number of overlaps in cluster sizes for the GSM network and the cost function of the network. The section also defines and theorize the Hexagonal Tessellation Model (HTM), algorithmize optimal disks covering techniques for point sets using maximal node covering and proposed extension to regular and irregular polygons. Area loss for placement of uniform disks and area signal loss. Finally, sectoring GSM antenna for area fractals in geometry, apothem theorem of inscribed hexagon as well as theorems and conjectures with their proofs are made.

4.2 MOTION OF WAVES IN GSM ANTENNA MAST

An antenna is a metallic object which acts as a medium for receiving and transmitting electromagnetic energy. It acts as a transitional structure between the transceivers and the free space. An antenna radiation pattern is the angular distribution of the power dissipated by the antenna (Saunders, 1999). It is a graphical explanation of the relative field strength transmitted and received by an antenna. As an antenna radiates through open space, several graphs are sometimes needed to describe the characteristics of an antenna. But antenna's may take different shapes and size used for different purposes. Figure 4.1 shows different antenna's.

(a) Dish Antenna

(b) Grid Antenna

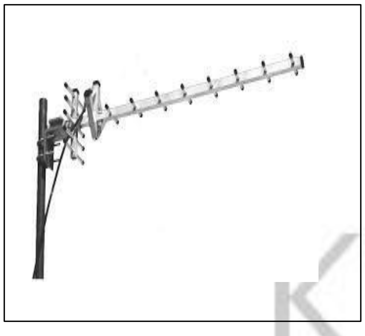

(c) Yagi Antenna

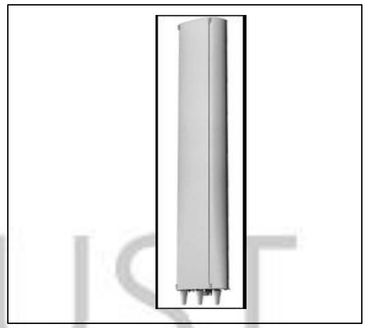

(d) GSM Antenna

Figure 4.1: Some types of antenna's

The dish-shaped type of parabolic antenna shown in Figure (4.1a) is designed to receive electromagnetic signals from satellites, which transmit data transmissions or broadcasts, such as satellite television. The grid antenna is a parabolic antenna designed for the spread spectrum system with long range highly directional applications. It operates in the 2.4-2.5GHz and are commonly used for satellite TV's and WiFi. A Yagi antenna also known as Yagi-Uda antenna commonly used in communications with frequency above 10MHz is a directional terrestrial antenna.

A sector antenna commonly called GSM antenna is a type of directional antenna which has a sector shaped radiation pattern. It is typically used in mobile phone base-stations (Azad, 2012). Due to it convenience and usefulness manufacturers of GSM antenna like Mobile Mark, Multiband Technologies, Global Source, Asian Creation among others have designed GSM antenna's with variety of sector angles including 30^0, 60^0, 90^0 and 120^0 as the common ones. A common sector angle is fitted on a GSM masts is shown in Figure 4.2.

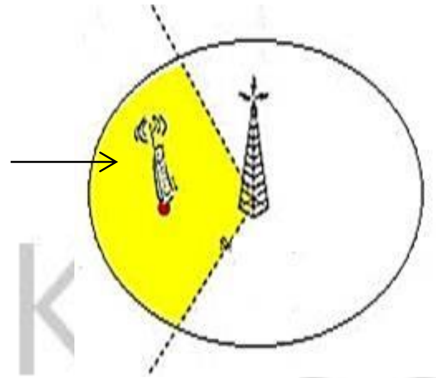

Figure 4.2: 120^0 Sector GSM Antenna

Typically, three sector antennas are used to cover a cell $(120^0 + 120^0 + 120^0 = 360^0)$. Also larger or smaller numbers of sectors are also possible (Balanais et al, 2007). Figure 4.4 shows a typical sectorized systems with three antenna's on GSM masts.

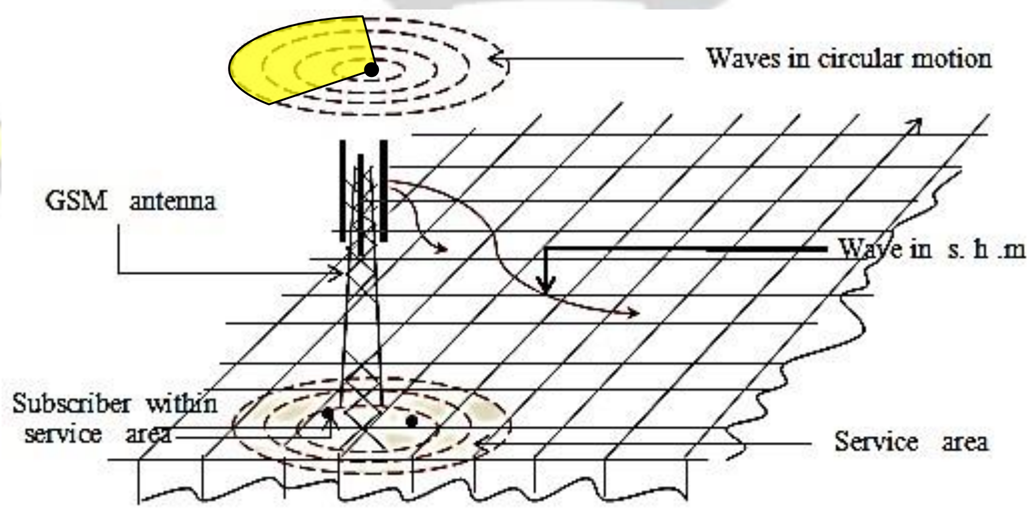

Figure 4.4: Modelling GSM Antenna tower coverage

4.4 GEOMETRY OF GSM CELL SHAPES

In mobile telecommunication networks we may represent the term 'cells' artificially by geometrical shapes such as hexagons or concentric circles. Hexagon is conveniently chosen because it is the only tessellable shape that is closest to being circular with the widest area. The circular shapes are themselves inconvenient as they have overlapping coverage areas. In reality, the ideal coverage of the power transmitted by the base station antenna is non-geometric because of inconsistency in signal strengths. A practical network will have cells of non-geometric shapes, with some areas not having the required signal strength for various reasons. Figure 4.5 shows the various cell shapes in GSM network.

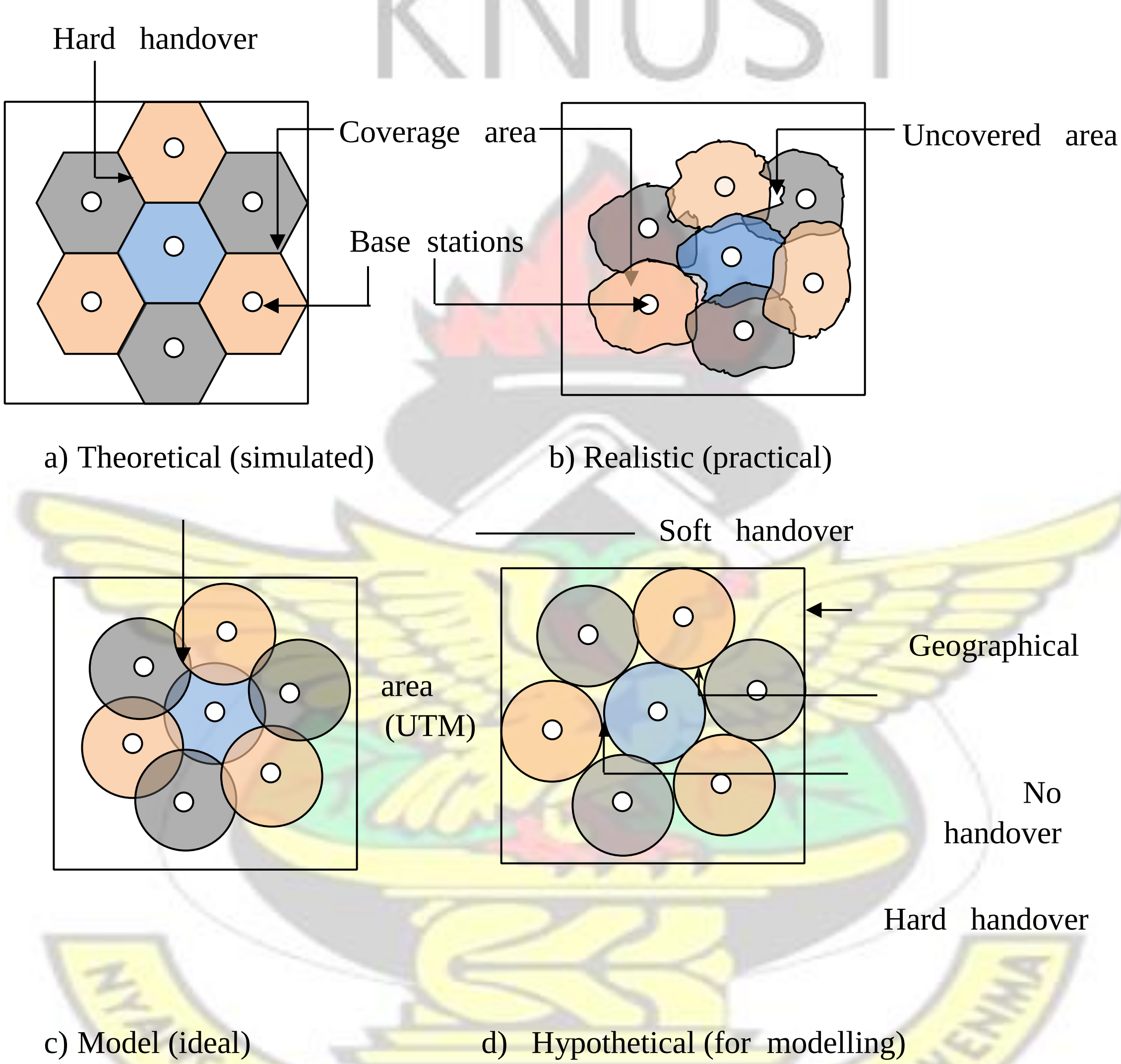

Figure 4.5: GSM cell shapes in radio networks

4.5 CO - CHANNEL RE-USE RATIO IN GSM NETWORK

Frequency re-use is a technique of reusing frequencies and channels within a communication system to improve capacity and spectral efficiency. Commercial wireless systems are based on this concepts in partitioning of an RF radiating area into cells. The increase in capacity in a commercial wireless network compared with a single transmitter network, comes from the fact that the same frequency can be used in different area for completely different transmission. The repeating regular pattern of cells is called cluster. Since each cell is designed to use radio frequencies only within it boundaries, the same frequencies can be reused in other cells not far without interference. Such cells are called cochannel cells. We consider two cases of frequency configuration that eliminate interference in GSM network design.

4.5.1 FREQUENCY RE-USE FOR UNIFORM CELL RANGE

4.5.1.1 THEOREM 4.1

For a hexagonal geometry with side ratio $1:1$ or $N:N$, the co-channel re-use ratio is given by

$$f_{ij} = \begin{cases} 3i \qquad , & for\ i = j \\ \sqrt{3(i^2 + ij + j^2)}, & for\ i \neq j \end{cases} \tag{4.10}$$

Where $n = i^2 + ij + j^2$ is the cluster size for $i, j \in \mathbb{Z} \geq 0$.

Proof:

Consider the hexagonal geometric tessellation with seven different cells as shown in the Figure 4.6. The chain of hexagons is either along j vertical or 60^0

rotation of i cells.

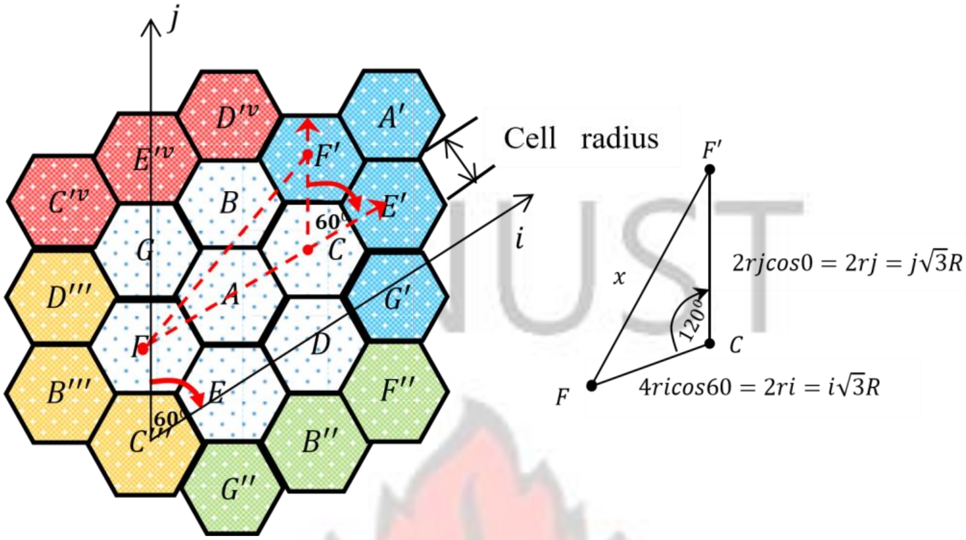

(a) n- cluster cell $(n = 7)$ (b) x –reuse distance

Figure 4.6: Co- channel re-use ratio

Generally, for $n = i^2 + ij + j^2$ we can find the nearest co-channel neighbors of a particular cell:

a) Move $i = 2$ cells along any chain of hexagons and then

b) Turn 120^0 clockwise and move $j = 1$ cells.

c) $n \in \mathbb{N}$- Cluster size of cell

d) $R \in \mathbb{R}$- radius of circle equivalent to any one side of the hexagon

e) $r = \frac{R\sqrt{3}}{2}$ – apothem of a hexagon

Using the cosine rule to find x from ΔACF:

$$x^2 = \left(i\sqrt{3}R\right)^2 + \left(j\sqrt{3}R\right)^2 - 2i \times \left(\sqrt{3}R\right)j \times \left(\sqrt{3}R\right)cos120^0$$

$$= 3R^2i^2 + 3R^2j^2 - 6ijR^2\left(\frac{-1}{2}\right)$$

$$x = \sqrt{3} \times R\sqrt{(i^2 + j^2 + ij)}$$

$$x = R\sqrt{3n} = |FF'|$$

For $i \neq j$

$$\therefore f_{ij} = \frac{x}{R} = \sqrt{3(i^2 + j^2 + ij)}$$

For $i = j$, $$f_{i,i} = \frac{x}{R} = \sqrt{3(i^2 + i^2 + i \times i)}$$

$$f_{i,i} = \sqrt{3 \times 3i^2}$$

$$f_{i,i} = 3i$$

Equation (4.10) is the re-use factor (ratio) and $x = Rf_{ij} = R\sqrt{3n}$ is the reuse distance. For a fixed cell size, small n decreases the size of the cluster which in turn results in the increase of the number of clusters and hence the capacity. However for small n, co-channel cells are located much closer and hence more interference. The value of n is determine by calculating the amount of interference that can be calculated for a sufficient quality communication. In a given coverage area (say cluster size of $n = 7$), there are several cells that use the same set of frequencies (frequency re-use). These cells are called cochannel cells and interference between signals from these cells is called cochannel interference. This co-channel interference cannot be combated by simply increasing the carrier power of transmitter. To reduce such interference these co-channel cells can be physically separated by a minimum distance to provide sufficient isolation due to propagation. When the size of each cell is approximately the same and the base station transmits the same power, the cochannel interference ratio is independent of the transmitted power and becomes a function of the radius of the cell (R) and the distance between the centers of the nearest co-channel cells (f_{ij}).

4.5.1.2 REMARK 4.1

For a hexagonal geometry with $f_{ij} = \frac{x}{R} = \sqrt{3n}$ a small value of f_{ij} provides larger capacity since the cluster size is small (requires more of the same frequency) whereas because of smaller level of co-channel interference a large value for f_{ij}

improves the transmission quality. Table 4.1 Shows the possible cluster size and frequency re-use factor of Theorem 4.1.

Table 4.1: Possible Cluster size and Frequency Re-use factor

Movement of cells	Cluster size (n)	Co-channel re-use ratio $\left(f_{ij} = \frac{x}{R} = \sqrt{3n}\right)$	Transmission Quality	Traffic Capacity
$i = 1,\ j = 0$	1	1.732	Lowest	Highest
$i = 1,\ j = 1$	3	3		
$i = 2,\ j = 0$	4	3.46		
$i = 2,\ j = 1$	7	4.58		
$i = 3,\ j = 0$	9	5.20		
$i = 2,\ j = 2$	12	6		
$i = 3,\ j = 1$	13	6.24		
$i = 4,\ j = 0$	16	6.93	Highest	Lowest

4.5.2 GENERALIZED FREQUENCY RE-USE (GFR) FOR NON-UNIFORM CELL RANGE

Frequency Reuse (FR) is an efficient Interference Management technique, which offers significant capacity enhancement and improves cell edge coverage with low complexity of implementation. The performance of cellular system greatly depends on the spatial configuration of Base Stations (BSs). FR is useful in designing Hexagon Tessellation Model (HTM) for densely and sparsely geographical distribution of subscribers of GSM network. GFR is an extension of the frequency re-use for uniform cell range or assignment model stated in Theorem 4.1. We generalize the results to non-uniform cell range of hexagonal tessellation with side ratio $N:\aleph$ for $\aleph > N$ using Theorem 4.2.

4.5.2.1 THEOREM 4.2: For a hexagonal geometry with side ratio $N:\aleph$, the co-channel re-use ratio for non-uniform cell range is given by

$$f_{ij} = \sqrt{3(N^2i^2 + N\aleph ij + \aleph^2j^2)} \text{ , for } \aleph \geq N$$

Where $n = N^2i^2 + N\aleph ij + \aleph^2j^2$ is the cluster size for $i, j \in \mathbb{Z} \geq$ and $N, \aleph \in \mathbb{Z}^+$

Movement along the ith cells $= 4\text{N}ricos60^0$

$$= 2Nri$$

$$= 2Ni\frac{\sqrt{3}}{2}R \qquad (4.11)$$

$$= \sqrt{3}NRi$$

Movement along the jth cells $= 2\aleph rjcos0^0$

$$= 2\aleph rj$$

$$= 2\aleph\frac{\sqrt{3}}{2}Rj$$

$$= \sqrt{3}\aleph Rj$$

Then,

$$x^2 = \left(iN\sqrt{3}R\right)^2 + \left(j\aleph\sqrt{3}R\right)^2 - 2 \times \left(N\sqrt{3}R\right)i \times \left(\aleph\sqrt{3}R\right)j \times cos120^0$$

$$x = R\sqrt{3(N^2i^2 + N\aleph ij + \aleph^2j^2)}$$

$$f_{ij} = \frac{x}{R} = \sqrt{3(N^2i^2 + N\aleph ij + \aleph^2j^2)}$$

Where

$$n = N^2i^2 + N\aleph ij + \aleph^2j^2 \qquad (3.11a)$$

Case 1: Uniform cell range: $N:\aleph = 1:1$

$n = i^2 + ij + j^2$ as in Theorem 4.1

Case 2: Non-uniform cell range: $N : \aleph = 1 : 2$

Then, $N = 1$ and $\aleph = 2$

$$n = i^2 + 2ij + 4j^2 \tag{3.11b}$$

Table 4.2: Cluster size and Frequency Re-use factor for non-uniform cells

Movement of cells	$N : \aleph = 1 : 2$		$N : \aleph = 1 : 3$	
	Cluster size (n)	Co-channel re-use ratio $(f_{ij} = \sqrt{3n})$	Cluster size (n)	Co-channel re-use ratio $(f_{ij} = \sqrt{3n})$
$i = 1,\ j = 0$	1	1.732	1	1.732
$i = 0,\ j = 1$	4	3.464	9	5.196
$i = 1,\ j = 1$	7	4.583	13	6.245
$i = 2,\ j = 0$	4	3.464	4	3.464
$i = 0,\ j = 2$	16	6.928	36	10.392
$i = 2,\ j = 1$	12	6	19	7.550
$i = 1,\ j = 2$	21	7.937	43	11.358
$i = 3,\ j = 0$	9	5.196	9	5.196
$i = 0,\ j = 3$	36	10.392	81	15.588
Sequence	1, 4, 7, 9, 12, 16, 21, 36, ...		1,4,9,13,19,36,43,81, ...	

4.6 TESSELLATING A PLANE FOR MAXIMUM AREA COVERAGE

4.6.1 HONEYCOMB CONJECTURE

STATEMENT: It states that hexagonal tessellation is the most efficient way to tessellate the plane in terms of the total perimeter per area coverage. A related property of hexagons in comparison to squares is how closely each shape approximate a circle as shown in Theorem 4.2 and Table 4.2 . Since the area of circle is defined as the locus of points at or within a certain distance from the centre of the circle, a circle is the most compact shape in $\mathbb{R}^2$. Any regular polygon that covers its circumcircle more completely is a closer approximation of the circle than another regular polygon which covers less.

4.6.2 COVER PATTERNS USING REGULAR POLYGONS

Triangles, squares and hexagons are known to be the only Archimedean tiling's with lattice polygon (Ding, 2010). Any regular polygon that can tile has the property of covering. It is often useful to consider the single regular polygon whose area approximates that of a circle. This regular polygon could be a guide in our geometric disks covering of GSM antenna in telecommunication network. We therefore state a theorem and give a proof to ascertain the choice of regular polygon.

4.6.2.1 TESSELLABLE REGULAR POLYGONS

4.6.2.1.1 THEOREM 4.2: The area of a regular hexagon is closer to its circumcircle than to any tessellable regular polygon (like a square, equilateral triangle) to that of its circumcircle.

Proof

Consider the circle with radius r inscribed in a hexagon, the other by a square and the third by a triangle as shown in Figure 4.7.

Case I: Hexagon $ABCDEF$

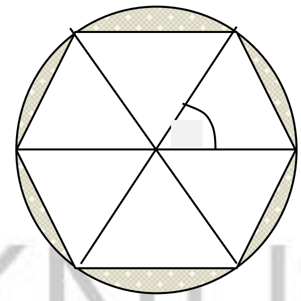

Figure 4.7 : Hexagon inscribed in a circle

It is evident that each of the triangle in Figure 4.7 is equilateral. So we consider ΔDOC where characteristically $\angle DOC = 60^0$.

$$\text{Area of hexagon} = 6 \times \text{area of } \Delta DOC$$

$$= 6 \times \frac{1}{2} \times |OD||OC| Sin60^0$$

$$= 6 \times \frac{1}{2} \times r \times r \times \frac{\sqrt{3}}{2}$$

$\cong 2.598r^2$ square units to 3decimal places.

Case II: Square $ABCD$

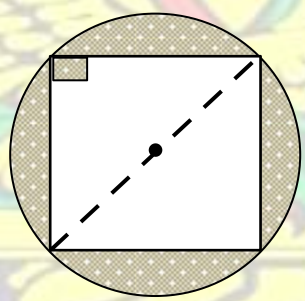

Figure 4.8: Square inscribed in a circle

We consider the isosceles right triangle ABC and apply Pythagoras theorem:

$$(2r)^2 = s^2 + s^2$$

$$\Rightarrow s = r\sqrt{2} \text{ units.}$$

But area of square $ABCD = |AB| \times |BC|$

$$= s \times s$$

$= 2r^2$ square units.

Case III: Triangle ABC

Consider the equilateral triangle ABC inscribed in a circle with centre O, radius r and side s.

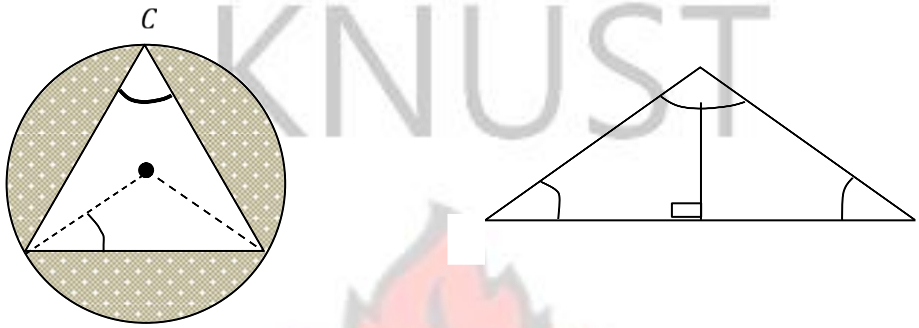

a) Equilateral triangle ABC (b) Isosceles triangle ABO

Figure 4.9: Triangle inscribed in a circle

Area of $\Delta ABC = \sqrt{s(s-a)(s-b)(s-c)}$ where

$s = \frac{a+b+c}{2}$ is the semi-perimeter

$= \frac{s+s+s}{2}$

$= \frac{3s}{2}$

Area of $\sqrt{-(- \quad)(- \quad)(- \quad)}$

Area of $\Delta ABC = 0.4330s^2$

But in Figure $4.8\ (c)(ii)$ we can find $s = f(r)$

$$\cos 30^0 = \frac{s/2}{r}$$

$$s = r\sqrt{3}$$

From equation (1) area of $\Delta ABC = 0.4330 \times r^2 \times 3$

$$= 1.299r^2$$

Case IV: Circle $ABCDEF$

Area $= \pi \times r^2$

$\cong 3.142r^2$ to 3 decimal places.

The common area of circles based on three polygons and occupying ratio in a circle has been shown in Table 4.3.

Table 4.3: Occupying Ratio Comparison of Tessellable Lattice Polygon.

Shape	Triangle	Square	Hexagon
Area (A)	$1.299r^2$	$2r^2$	$2.598r^2$
Area of circle (B)	$3.142r^2$	$3.142r^2$	$3.142r^2$
Ratio $(A{:}B)$	41.34%	63.65%	82.69%

Comparing the areas obtained for the three geometrical shapes we conclude that hexagons approximate circles more closely than squares, regular triangles and generally than any other regular tessellable geometrical 2-dimensional polygon. The proof is complete.

4.6.2.1.2 COROLLARY 4.1

Hexagons, because they approximate circles more closely are more compact than squares. This fact has direct application to any point of set sensors arranged on a plane or similar surface and can be reflected in nature (e.g. most animal vision organs have rods and cones arranged in nearly hexagonal tessellations in the eyes fovea), (Raposo, 2011).

4.6.2.3 NON-TESSELLABLE REGULAR POLYGON

Let A_n be the area of the inscribed polygon with n sides. As n increases, it appears that A_n becomes closer and closer to the area of the circle. We say that the area of the circle is the limit of the areas of the inscribed polygons, and we write

$$A = \lim_{n\to\infty} A_n \qquad (4.12)$$

4.6.2.3.1 THEOREM 4.3: The area of an n sided regular polygon inscribed in a circle is closer to its circumcircle as n increases.

Proof:

Non-lattice Archimedean non-tillable regular polygon includes pentagon, heptagon, octagon, nonagon, decagon, etc. We shall give a proof that as the number of sides of a regular polygon increases its area approximates that of it circumcircle . We shall give the percentage occupying area proof using numerical approach by considering the following cases.

Case I**:** Pentagon $ABCDE$

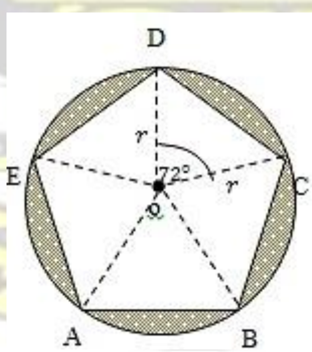

Figure 4.10 : Pentagon inscribed in a circle

It is evident that each of the triangle in Figure 4.10 is isosceles. So we consider ΔDOC where characteristically $\angle DOC = \frac{2\pi}{5} = 72^0$.

Area of Pentagon$= 5 \times$ area of ΔDOC

$$= 5 \times \frac{1}{2} \times |OD||OC| Sin\left(\frac{2\pi}{5}\right)$$

$$= 5 \times\times \tfrac{1}{2} \times r \times r \times 0.9511$$

$$\cong 2.3780r^2$$

Case II**:** Heptagon $ABCDEFG$

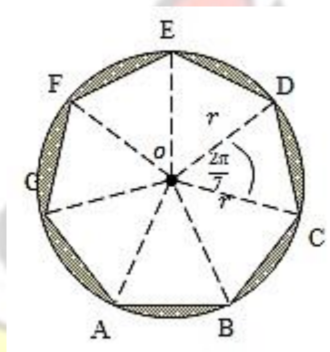

Figure 4.11: Heptagon inscribed in a circle

Area of Heptagon $= 7 \times$ Area of ΔDOC

$$= 7 \times \frac{1}{2} \times |OD||OC| Sin\left(\frac{2\pi}{7}\right)$$

$$= 7 \times \tfrac{1}{2} \times r \times r \times 0.7818$$

$$\cong 2.7363r^2$$

Case III: Octagon $ABCDEFGH$

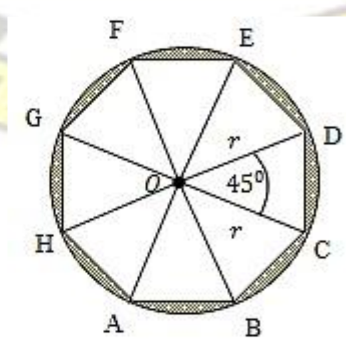

Figure 4.12: Octagon inscribed in a circle

$$\text{Area of Octagon} = 8 \times \text{Area of } \Delta DOC$$

$$= 8 \times \frac{1}{2} \times |OD||OC| Sin\left(\frac{\pi}{4}\right)$$

$$= 8 \times \frac{1}{2} \times r \times r \times \frac{\sqrt{2}}{2}$$

$$\cong 2.8284r^2$$

Case IV: n sided polygon

Generally, area of polygon inscribed in a circle with sides n is

$$A_n = n \times \text{area of a single } \Delta \text{ with origin as one vertex}$$

$$= n \times \frac{1}{2} \times r \times r \times sin\left(\frac{360^0}{n}\right)$$

$$A_n = \frac{nr^2}{2} sin\left(\frac{2\pi}{n}\right) \quad (4.13)$$

Case V: Circle

$$\text{Area} = \pi \times r^2$$

$$\cong 3.142r^2 \text{ to 3 decimal places.}$$

The common area of circles based on some non-tessallable regular polygons and occupying ratio in a circle has been shown in Table 4.4.

Table 4.4: Occupying Ratio Comparison of non-tilling Archimedean shapes

Non-tessellable Shape	Pentagon	Heptagon	Octagon	n-sided polygon
Area $(\boldsymbol{A})$	$2.3780r^2$	$2.7363r^2$	$2.8284r^2$	$\frac{nr^2}{2} \times sin\left(\frac{2\pi}{n}\right)$

Area of circle$(\boldsymbol{B})$	$3.142r^2$	$3.142r^2$	$3.142r^2$	$3.142r^2$
Ratio $(\boldsymbol{A}:\boldsymbol{B})$	75.68%	87.71%	90.02%	$\frac{n}{2\pi} \times sin\left(\frac{2\pi}{n}\right)\%$

Table 4.4 shows the area of an n sided regular polygon approaching the area of a circle as n increases. We shall state a theorem to that effect and give the first formal analytical proof.

4.6.2.3.2 THEOREM 4.4

Recall $A_n$as in equation (4.13). Then

$$\lim_{n\to\infty} A_n = \pi r^2.$$

REMARK: The above theorem states that the area A_n of an n –sided regular polygon inscribed in a circle with radius r approximates the area πr^2 of the circle , as n becomes large.

Proof

We shall give the first analytical proof.

Given $\quad A_n = \frac{nr^2}{2} sin\left(\frac{2\pi}{n}\right)$

$$\lim_{n\to\infty} A_n = \lim_{n\to\infty} \frac{nr^2}{2} sin\left(\frac{2\pi}{n}\right)$$

$$= \frac{r^2}{2} \lim_{n\to\infty} n \times sin\left(\frac{2\pi}{n}\right)$$

$$= \frac{r^2}{2} \lim_{n\to\infty} n \times sin\left(\frac{2\pi}{n}\right) \times \frac{2\pi/n}{2\pi/n}$$

$$= \frac{r^2}{2} \lim_{n\to\infty} n \times 2\pi/n \times \frac{sin\left(\frac{2\pi}{n}\right)}{2\pi/n}$$

$$= \pi r^2 \times \lim_{n\to\infty} \frac{sin\left(\frac{2\pi}{n}\right)}{2\pi/n}$$

$$\lim_{n\to\infty} A = \pi r^2 \text{(indeterminate type } \tfrac{0}{0} \text{ case)}$$

$$= \pi r^2 \times \lim_{n\to\infty} \frac{D_n\left[sin\left(\frac{2\pi}{n}\right)\right]}{D_n\left(\frac{2\pi}{n}\right)}$$

$$= \pi r^2 \times \lim_{n\to\infty} \frac{\left(\frac{-2\pi}{n^2}\right)cos\left(\frac{2\pi}{n}\right)}{\left(\frac{-2\pi}{n^2}\right)}$$

$$= \pi r^2 \times \lim_{n\to\infty} cos\left(\frac{2\pi}{n}\right) \times 1$$

$$= \pi r^2 \times cos0 \times 1$$

$$\lim_{n\to\infty} A_n = \pi r^2$$

This establishes the fact that the area of a non-tessellable regular polygon with sides n inscribed in a circle of radius r approaches πr^2 as n becomes large. Table 4.5 illustrates the percentage occupying ratio of some non-tessellable regular polygon.

Table 4.5: Occupying Ratio Comparison of non-tessellable regular polygon.

(4.14)

Non-tessellable Shape	Pentagon	Heptagon	Octagon	$n - gon \to \infty$
Area (A)	$2.3780r^2$	$2.7363r^2$	$2.8284r^2$	πr^2
Area of circle(B)	πr^2	$\pi 2r^2$	πr^2	πr^2
Ratio $(A{:}B)$	75.68%	87.71%	90.02%	100%

4.6.2.3.3 PROPOSITION 4.1: For any positive constant c(where$c = r^2/2$as in equation 4.13), the function $x \mapsto A(x)$ given by

$$A(x) = cxsin\left(\frac{2\pi}{x}\right)$$

is strictly increasing on $[2, \infty)$.

Proof

Note that A is at least twice continuously differentiable on $\mathbb{R}$ and

$$A'(x) = c\sin\left(\frac{2\pi}{x}\right) - \frac{2\pi c}{x}\cos\left(\frac{2\pi}{x}\right) \text{ and}$$

$$A''(x) = -\frac{2\pi c}{x^2}\cos\left(\frac{2\pi}{x}\right) + \frac{2\pi c}{x^2}\cos\left(\frac{2\pi}{x}\right) - \frac{4\pi^2 c}{x^3}\sin\left(\frac{2\pi}{x}\right)$$

$$= -\frac{4\pi^2 c}{x^3}\sin\left(\frac{2\pi}{x}\right)$$

Note that $A'(2) = c\left[\sin\left(\frac{2\pi}{2}\right) - \frac{2\pi}{2}\cos\left(\frac{2\pi}{2}\right)\right]$

$A'(2) = \pi > 0$ and $A''(x) < 0$ for $x \in (2, \infty)$, therefore $A'(x)$ is strictly decreasing on $(2, \infty)$. Furthermore $\lim_{x\to\infty} A'(x) = 0$. Hence $A'(x)$ is strictly positive on $[2, \infty)$, which implies that $A(x)$ is strictly increasing on $[2, \infty)$. The monotonic strictly increasing function A indicates that the area of a regular polygon inscribed in a disk increases with respect to the number of sides .i.e

$A_3 < A_4 < \cdots . A_n < A_{n+1} < \cdots$

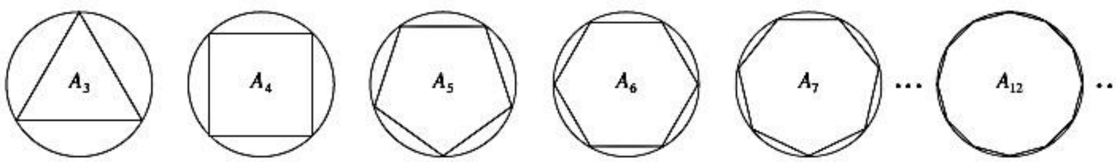

Figure 4.13: Strictly increasing function $A(x)$

4.7 POSITIONING CELLULAR NETWORKS

A simpler assumption, the circular-shaped cell, is also common in the literature. A reasonable approximation of this assumption is provided when signal propagation follows path loss models that consider constant signal power level along a circle around the base station (Goldsmith, 2005). In fact, a base station with an omni-directional antenna may cover a circular area that is defined as the area for which the propagating downlink signal go beyond a certain threshold; however, even in this case, this is only an approximation due to the impact of the environment. The major shortcoming of the circular approximation is that circular cells must moderately or partially overlap in order to avoid gaps.

4.8 OVERLAP FOR OPTIMAL DISKS COVERING

We consider simple layouts as depicted in Figure 4.15. Figure 4.15(a) illustrates the hexagonal cell layout. The inradius and the circumradius of the hexagonal cell are r_1 and R_1, respectively. In Figure 4.15(b), cells are partially overlapped because R_1 equals to the hexagon's circumradius. In this case, the model considers nodes not belonging to the cell of interest. Algebraically the best positioning of the GSM network is where the hexagonal and circular cells overlap to give us a difference of $2(R_1 - r_1)$ as shown in Figure 4.14(a).

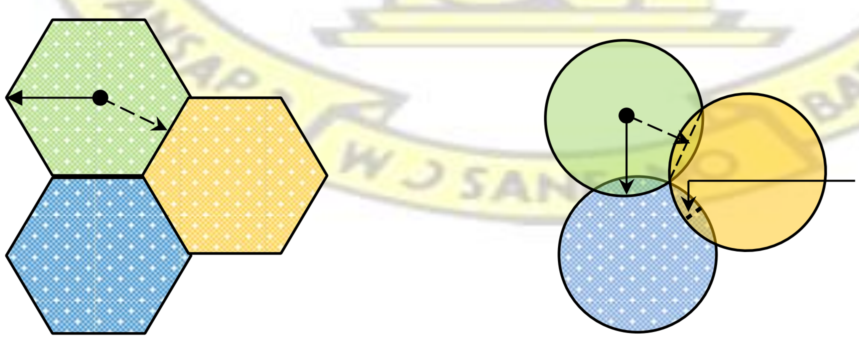

(a) Hexagonal cell layout (b) Idealized circular layout

Figure 4.14: Cell Layout Models For GSM Networks.

The idealized circular layout created by hexagonal tessellation yield a connected cover set with least overlap difference such that $\bigcap_{i=1}^{\infty} A_i \neq \emptyset$.

4.9 OVERLAP DIFFERENCE IN HEXAGON-INSCRIBED DISKS

Overlap in cell planning ensures smooth handover in GSM network. This overlap has a differential effect such as fading and attenuation in signals and therefore must be kept as minimal as possible. Overlap may occur for smooth handover of cells (frequency) and has the disadvantage of increasing the number of GSM masts as well as antenna required in a given area. A typical overlap may arise as a result of uniform cell radius (disks) or non-uniform cell radius. We shall however minimize the overlap difference for both uniform and nonuniform cell range in mobile telephony.

4.9.1 TYPE I: UNIFORM DISKS

It has been established (proven) that to cover a given plane or point sets with disks of radius R_1 and hexagonal apothem r_1, we require an overlap difference of $2(R_1 - r_1)$. We shall, however deduce formulas for calculating the width of any hexagonal disks covering in terms of the apothem (r_1) or the radius of the disks (R_1) or the height of the overlap area (H). Consider two intersecting uniform disks shown in Figure 4.15.

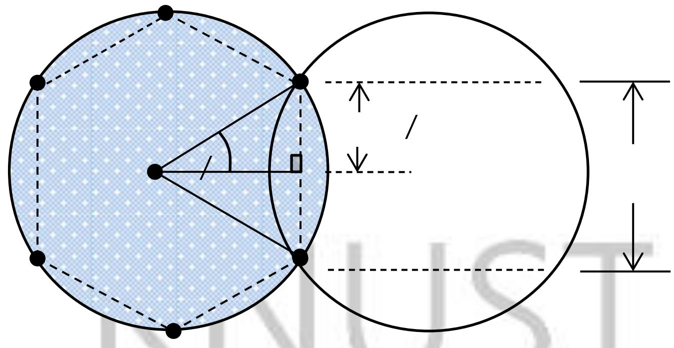

Figure 4.15: Overlap width for uniform disks(cell radius)

Consider triangle OAB in Figure 4.15.

Case I: $sin\left(\frac{\pi}{6}\right) = \frac{AB}{OA}$

$$\frac{1}{2} = \frac{H/2}{R_1}$$

$$H = R_1$$

Width = $2(R_1 - r_1)$

$\therefore$ Width $= 2(H - r_1)$

Case II: $Cos\left(\frac{\pi}{6}\right) = \frac{OB}{OA}$

$$\frac{\sqrt{3}}{2} = \frac{r_1}{R_1}$$

$r = \frac{\sqrt{3}}{2}R$ or $r = \frac{\sqrt{3}}{2}H$ where (4.15)

Width $= 2(R_1 - \frac{\sqrt{3}}{2}R_1)$

$\therefore$ width $= \left(2 - \sqrt{3}\right)R_1$ or width $= \left(2 - \sqrt{3}\right)H$ (4.17)

Generally for n full overlaps the difference is obtain to be

$$d = \sum_{i=1}^{n} 2(R_i - r_i)$$

(4.16)

$$d = \sum_{i=1}^{n} \left(2 - \sqrt{3}\right)R_i$$

$$d = (2-\sqrt{3})\sum_{i=1}^{n} R_i$$

But $R_i = R_j$ for all $i, j \in \mathbb{N}$, hence

$$d = (2-\sqrt{3})nR_i \tag{4.18}$$

Case III : $tan\left(\frac{\pi}{6}\right) = \frac{AB}{OB}$

$$\frac{1}{\sqrt{3}} = \frac{H/_2}{r_1}$$

$$H = \frac{2r_1}{\sqrt{3}}$$

$$H = R_1 = \frac{2\sqrt{3}r_1}{3}$$

$$\text{Width } = 2\left(\frac{2\sqrt{3}r_1}{3} - r_1\right)$$

$$\therefore \text{width} = \frac{2}{3}(2\sqrt{3}-3)r_1 \tag{4.19}$$

Equation (4.15), (4.17) and (4.19) establish the formula for calculating the width of a disks covering via hexagonal tilling. Table 4.6 shows the overlap difference and their percentage occupying ratio for tessellable regular polygon.

Table 4.6: Occupying overlap difference and ratio for uniform disks.

Regular Polygon	Hexagon	Square	Equilateral triangle
Overlap Difference (A)	$2(R_1 - r_1)$	$\frac{2}{3}(3R_1 - \sqrt{6}r_1)$	non
	$(2-\sqrt{3})R_1$	$(2-\sqrt{2})R_1$	R_1
	$\frac{2}{3}(2\sqrt{3}-3)r_1$	$\frac{2}{3}(2\sqrt{3}-\sqrt{6})r_1$	$\frac{2\sqrt{3}}{3}r_1$
Overlap difference of disks (B)	$2R_1$	$2R_1$	$2R_1$

Ratio$(A\colon B)$	13.397%	29.289%	50%

4.9.1.1 THEOREM 4.5 The apothem $r_n$created by n sided regular polygon inscribed in a disk of radius R_1 is $r_n = R_1 cos\left(\frac{\pi}{n}\right)$.

Proof.

Consider the circle as shown in Figure 4.16. Inscribed in the circle are three regular tessellable regular polygon, square, equi-lateral triangle and the hexagon.

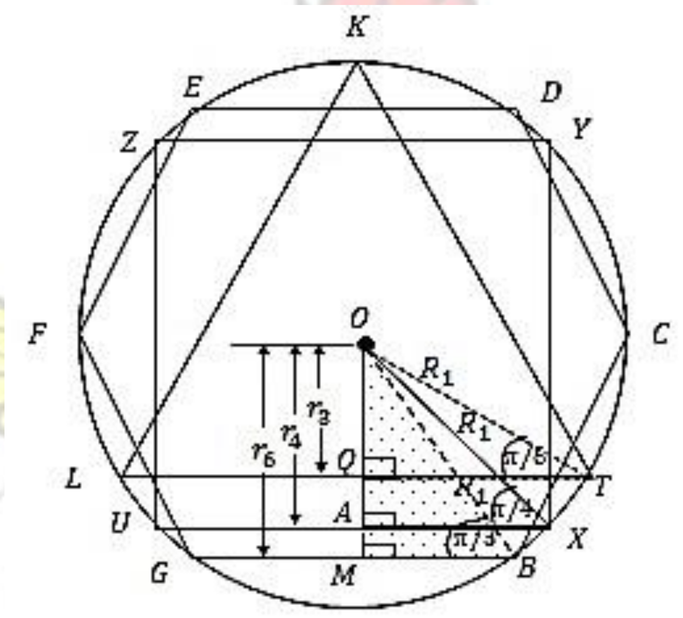

Figure 4.16: Apothem for regular polygon inscribed in disks

Let the apothem of an n sided regular polygon be r_n.

Case I: Equilateral triangle KLT.

Consider ΔQOT, in Figure 4.16. Then

$$\cos 60^0 = \frac{r_3}{R_1}$$

$$r_3 = R_1 cos60^0$$

$$r_3 = R_1 cos\left(\frac{\pi}{3}\right)$$

Case II: Square $XYZU$.

Consider $\Delta AOX,$ in Figure 4.16 then

$$\cos 45^0 = \frac{r_4}{R_1}$$

$$r_4 = R_1 cos 45^0$$

$$r_4 = R_1 cos\left(\frac{\pi}{4}\right)$$

Case III: Hexagon $BCDEFG$

Consider ΔMOB, in Figure 4.16. Then

$$cos 30^0 = \frac{r_6}{R_1}$$

$$r_6 = R_1 cos 30^0$$

$$r_6 = R_1 cos\left(\frac{\pi}{6}\right)$$

Generally for an $n$sided regular polygon

$$r_n = R_1 cos\left(\frac{\pi}{n}\right) \tag{4.20}$$

The apothem formulae in equation (4.20) lessen computation and helps us propose the total overlap difference formula in Theorem 4.6.

4.9.1.2 THEOREM 4.6: The total overlap difference created by n sided tessellable regular polygon inscribed in a disk for covering with radius is $2nR_1\left[1 - cos\left(\frac{\pi}{n}\right)\right]$. Each overlap difference is $2R_1\left[1 - cos\left(\frac{\pi}{n}\right)\right]$.

Proof.

Let d_n denote the overlap difference of an n sided regular tessellable polygon. From equation (4.15) each overlap difference is given as

$$d = 2(R_1 - r_1)$$

But R_1 is fixed where as r_1 is a dummy variable and will be replace by for $n \geq 3$. Then equation (4.15) becomes

$$d_n = 2(R_1 - r_n)$$

$$= 2\left[R_1 - R_1 cos\left(\frac{\pi}{n}\right)\right] \qquad R_1$$

$$d_n = 2R_1\left[1 - cos\left(\frac{\pi}{n}\right)\right]$$

But a tessellable regular polygon with n sides have n overlaps. So for n sided tessellable regular polygon

$$d_n = 2nR_1\left[1 - cos\left(\frac{\pi}{n}\right)\right] \text{ or}$$

$$d_n = 4nR_1 sin^2\left(\frac{\pi}{2n}\right) \qquad r_n$$

We shall illustrate this with example that when $n \geq 3$ theorem 4.6 is true.

For $n = 3$; $d_3 = 2R_1\left[1 - cos\left(\frac{\pi}{3}\right)\right].$

$d_3 = R_1$ as shown in Table 4.5.

For $n = 4$; $d_4 = 2R_1\left[1 - cos\left(\frac{\pi}{4}\right)\right].$

$$(4.21)$$

$d_4 = (2 - \sqrt{2})R_1$ as shown in Table 4.5.

For $n = 6$; $d_6 = 2R_1\left[1 - cos\left(\frac{\pi}{6}\right)\right].$

$$= 2R_1\left(1 - \frac{\sqrt{3}}{2}\right)$$

$$(4.22)$$

$d_6 = (2 - \sqrt{3})R_1$ as shown in Table 4.5.

In wireless telecommunication network design the overlap difference d_n help engineers to estimate before hand the overlap cost per choice of tessellable regular polygon, since it is a function of the coverage area. As the overlap difference increase with a decrease in the size of the regular tessellable polygon.

4.9.1.3 THEOREM 4.7: The total overlap area created by n sided tessellable regular polygon inscribed in a disks for covering of uniform radius R_1 is $2\left[\pi - \frac{n}{2}sin\left(\frac{2\pi}{n}\right)\right]R_1^2$ or $\left(\frac{d_n}{4n}\right)^2 cosec^4\left(\frac{\pi}{2n}\right)\left[2\pi - nsin\left(\frac{2\pi}{n}\right)\right]$

Proof.

From Figure 3.8, the area of each overlap difference is

$$A_n = \frac{area\ of\ circle - area\ of\ polygon}{n} \times 2$$

$$= \frac{2}{n} \times \left[\pi R_1^2 - \frac{nR_1^2}{2} sin\left(\frac{2\pi}{n}\right)\right]$$

$$A_n = \frac{2}{n} \times \left[\pi - \frac{n}{2} sin\left(\frac{2\pi}{n}\right)\right] R_1^2 \qquad (4.23)$$

Deductively, from equation (4.20)

$$R_1 = \frac{d_n}{2\left[1 - cos\left(\frac{\pi}{n}\right)\right]}$$

$$R_1 = \frac{d_n}{4sin^2\left(\frac{2\pi}{n}\right)} = \frac{d_n}{4} Cosec^2\left(\frac{\pi}{2n}\right) \qquad (4.24)$$

Equation (4.22) becomes

$$A_n = \frac{2}{n} \times \left[\pi - \frac{n}{2} sin\left(\frac{2\pi}{n}\right)\right]\left[\frac{d_n}{4} Cosec^2\left(\frac{\pi}{2n}\right)\right]^2$$

$$A_n = \frac{1}{n} \times \left(\frac{d_n}{4n}\right)^2 cosec^4\left(\frac{\pi}{2n}\right)\left[2\pi - nsin\left(\frac{2\pi}{n}\right)\right]$$

$$A_n = \left(\frac{d_n}{4}\right)^2 cosec^4\left(\frac{\pi}{2n}\right)\left[\frac{2\pi}{n} - sin\left(\frac{2\pi}{n}\right)\right]$$

*A*polygon with n sides have n overlaps, thus total overlap area

$$A_n = n \times \frac{2}{n} \times \left[\pi - \frac{n}{2} sin\left(\frac{2\pi}{n}\right)\right] R_1^2$$

$$A_n = 2\left[\pi - \frac{n}{2} sin\left(\frac{2\pi}{n}\right)\right] R_1^2$$

Deductively, from (23)

$$R_1 = \frac{d_n}{4nsin^2\left(\frac{\pi}{2n}\right)} \qquad (4.27)$$

$$A_n = 2\left[\pi - \frac{n}{2}sin\left(\frac{2\pi}{n}\right)\right] \times \left(\frac{d_n}{4nsin^2\left(\frac{\pi}{2n}\right)}\right)^2$$

$$A_n = \left(\frac{d_n}{4n}\right)^2 cosec^4\left(\frac{\pi}{2n}\right)\left[2\pi - nsin\left(\frac{2\pi}{n}\right)\right] \quad (4.25)$$

Is the total overlap area. Table 4.6 shows the total overlap area for the three tessellable regular polygons

(4.26)

Table 4.7 Total overlap area for all tessellable regular polygon

	Triangle (T)	Square (S)	Hexagon(H)
$\Delta_n = 2\left[\pi - \frac{n}{2}sin\left(\frac{2\pi}{n}\right)\right]R_1^2$ Overlap area	$\left(2\pi - \frac{3\sqrt{3}}{2}\right)R_1^2$	$2(\pi - 2)R_1^2$	$\left(2\pi - 3\sqrt{3}\right)R_1^2$
Area of disks (D)	πR_1^2	πR_1^2	πR_1^2
$A_0 = \left(\frac{T}{D} : \frac{S}{D} : \frac{H}{D}\right)$ Total occupying area ratio	117.3%	72.7%	34.6%

(28)

Table 4.7 shows that hexagon has the least overlap area hence least waste when covering with disks using hexagonal tessellation. This minimizes the number of disks suing for covering in GSM network design. Our study also reveals that equation (4.20) is useful in computing the total overlap area for tessellable regular polygon. This reduces algebraic computation in field work for telecommunication network design.

4.9.1.4 THEOREM 4.8: Given a circle of radius $R_{1,}$ we can inscribe a regular polygon of side length $2R_1 sin\left(\frac{\pi}{n}\right),$ where n is the number of sides of the regular polygon.

Proof.

Suppose the regular polygon has n sides. Then the two successive radii connecting two internal angle is $\frac{2\pi}{n}, n \geq 3.$ Consider an n-gon inscribed in a disk as shown in Figure 4.17.

(a) $n - gon$ inscribed in a disk (b) Angle at the centre of an $n - gon$

Figure 4.17 Polygon inscribed in a disk

Then
$$\theta = \frac{\pi - \frac{2\pi}{n}}{2}$$
$$\theta = \left(\frac{\pi}{2} - \frac{\pi}{n}\right)$$

Then, area of ΔAOB is equivalent to area of $\Delta OAB.$ Mathematically,

$$\frac{1}{2}R_1^2 sin\left(\frac{2\pi}{n}\right) = \frac{1}{2}SR_1 sin\left(\frac{\pi}{2} - \frac{\pi}{n}\right) \tag{4.29}$$

$$S = \frac{\frac{1}{2}R_1^2 sin\left(\frac{2\pi}{n}\right)}{\frac{1}{2}R_1 sin\left(\frac{\pi}{2} - \frac{\pi}{n}\right)}$$

$$= \frac{R_1 sin\left(\frac{\pi}{n} + \frac{\pi}{n}\right)}{sin\left(\frac{\pi}{2}\right) cos\left(\frac{\pi}{n}\right) - \cos\left(\frac{\pi}{2}\right) sin\left(\frac{\pi}{n}\right)}$$

$$= \frac{2R_1 sin\left(\frac{\pi}{n}\right) cos\left(\frac{\pi}{n}\right)}{sin\left(\frac{\pi}{2}\right) cos\left(\frac{\pi}{n}\right)}$$

$$S = 2R_1 sin\left(\frac{\pi}{n}\right) \quad \text{for} \quad n \geq 3 \tag{4.30}$$

4.9.1.5 COROLLARY 4.2 : In any circular disks of radius $R_{1,}$ hexagonal apothem r_1 and centre O, we can inscribe the following simultaneously:

a) A hexagon of side $R_{1,}$ or apothem

b) A square of side $s = \frac{2\sqrt{6}}{3}r_1$ or $R_1\sqrt{2}$

c) An equilateral triangle of sides $2r_1$ or $\sqrt{3}R_1$

Proof.

Figure 4.17 shows a disks with radius R_1 hexagonal apothem r_1, a square with dimensions s and an equilateral triangle with dimensions $\sqrt{3}R_1$. We find a relatiosnship between the variables R_1 , r_1 and s. Consider the following cases.

Case I: $s = f(R_1)$

We realize that triangle OQT is similar to triangle OMB, with $OT = BO = R_1$. From triangle OQT,

$$cos30^0 = \frac{QT}{R_1}$$

$$QT = \frac{\sqrt{3}}{2} R_1$$

$$\therefore LT = 2QT = \sqrt{3} R_1 \qquad (4.31)$$

Considering triangle $OAX,$

$$R_1^2 = \frac{s^2}{4} + \frac{s^2}{4}$$

$$2R_1^2 = s^2$$

$$R_1 = \frac{s\sqrt{2}}{2} \qquad (4.32a)$$

or $s = R_1\sqrt{2}$ $\qquad (4.32b)$

Case II: $r_1 = f(R_1)\ or\ f(s)$

Also, in ΔOMB which is similar to OQT.

$$R_1^2 = r_1^2 + \left(\frac{R_1}{2}\right)^2$$

$$3R_1^2 = 4r_1^2$$

$$R_1 = \frac{2r_1}{\sqrt{3}} = \frac{2r_1\sqrt{3}}{3} \text{ or} \qquad (4.33a)$$

$$r_1 = \frac{R_1\sqrt{3}}{2} \qquad (4.33b)$$

Substituting equation (4.33b) into (4.33a) we have

$$S = \frac{2r_1\sqrt{3}}{3} \times \sqrt{2}$$

$$S = \frac{2\sqrt{6}}{3} r_1$$

Or $\frac{\ }{\sqrt{\ }} \quad \frac{\sqrt{\ }}{\ }$

Then $AM = r_1 - \frac{S}{2}$

$$= \frac{S\sqrt{6}}{4} - \frac{S}{2}$$

$$AM = \frac{1}{4}\left(\sqrt{6} - 2\right)s = f(s) \quad (4.34c)\ (4.34e)$$

$(4.34d)$

Also $AM = r_1 - \frac{s}{2}$

$$= r_1 - \frac{1}{2} \times \frac{2\sqrt{6}}{3} r_1$$

$$AM = \frac{1}{3}\left(3 - \sqrt{6}\right) r_1$$

4.10 OVERLAP DIFFERENCE IN CYCLIC TESSELLABLE REGULAR POLYGON

Tessellable regular polygons inscribed in disks overlap with difference (d). This overlap difference can be expressed in terms of R_1 or r_1 which can be compared to determine the best covering technique in GSM cell design or tilling in ancient or contemporary art. We consider the three tessellable regular polygons namely regular triangle, square and hexagonal polygon. $(4.34f)$

Type I: Equi-triangular Polygon

Consider triangle OQT in Figure 4.16 which is congruent to triangle OMB. Then $MB = OT = \frac{R_1}{2}$ and $OM = QT = r_1$. Thus, equation (4.33a) and (4.33b) holds.

$$R_1^2 = \left(\frac{R_1}{2}\right)^2 + (r_1)^2$$

$$\frac{3}{4} R_1^2 = r_1^2$$

$$R_1 = \frac{2}{\sqrt{3}} r_1 = \frac{2\sqrt{3}}{3} r_1$$

Case I: $d = f(R_1)$

$$d = 2\left(R_1 - \frac{R_1}{2}\right)$$

$$d = R_1 \tag{4.40a}$$

Case II: $d = f(r_1)$

$$d = \frac{2r_1}{\sqrt{3}} = \frac{2\sqrt{3}}{3} r_1 \tag{4.40b}$$

Case III : $d = f(R_1, r_1)$

$d = 2\left(R_1 - \frac{R_1}{2}\right)$ but $R_1 = \frac{2\sqrt{3}r_1}{3}$ as in equation (4.33b)

$$= 2\left(R_1 - \frac{\frac{2\sqrt{3}}{3} r_1}{2}\right)$$

$$d = 2\left(R_1 - \frac{\sqrt{3}}{3} r_1\right)$$

$$d = \frac{2}{3}\left(3R_1 - \sqrt{3}r_1\right) \tag{4.40c}$$

Type II: Square Polygon

Consider square U, X, Y, Z in Figure 4.16 with centre O and dimension s by s. We compute the overlap difference for this polygon and study the occupying difference ratio to that of a disk.

Case I: $d = f(R_1, r_1)$

$$d = 2(R_1 - OA) = 2AM$$
$$= 2\left(R_1 - \frac{S}{2}\right)$$

$$= 2\left(R_1 - \frac{1}{2} \times \frac{2\sqrt{6}}{3} r_1\right)$$

$$d = \frac{2}{3}\left(3R_1 - \sqrt{6}\, r_1\right) \tag{4.41a}$$

Case II: $d = f(R_1)$

$$d = \frac{2}{3}\left(3R_1 - \sqrt{6}\, r_1\right)$$

$$= \frac{2}{3}\left(3R_1 - \sqrt{6}\ \times R_1\sqrt{3}\right)$$

$$d = \left(2 - \sqrt{2}\right)R_1 \qquad (4.41b)$$

Case III: $d = f(s)$

$$d = \left(2 - \sqrt{2}\right)R_1$$

$$= \left(2 - \sqrt{2}\right) \times \frac{S}{\sqrt{2}}$$

$$d = \left(\sqrt{2} - 1\right)S \qquad (4.41c)$$

Case IV: $d = f(r_1)$

$$d = \frac{2}{3}\left(3R_1 - \sqrt{6}\, r_1\right)$$

$$= \frac{2}{3}\left(3 \times \frac{2r_1}{\sqrt{3}} - \sqrt{6}\, r_1\right)$$

$$d = \frac{2}{3}\left(2\sqrt{3} - \sqrt{6}\right)r_1 \qquad (4.41d)$$

Type III: Hexagon

Consider $BCDEFG$ in Figure 4.16 with radius R_1. It is observed that triangle OMB is similar to triangle OQT. Thus equation (4.33a) and (4.33b) holds. We consider the following cases:

Case I: $d = f(R_1, r_1)$

$$= 2(R_1 - r_1) \qquad (4.42a)$$

Case II: $d = f(r_1)$

$$d = 2\left(\frac{2\sqrt{3}r_1}{3} - r_1\right)$$

$$d = \frac{2}{3}\left(2\sqrt{3} - 3\right)r_1 \qquad (4.42b)$$

Case III: $d = f(R_1)$

$$d = 2\left(R_1 - \frac{\sqrt{3}}{2}R_1\right)$$

$$d = (2-\sqrt{3})R_1 \quad (4.42c)$$

4.11 OVERLAP AREA IN CYCLIC TESSELLABLE REGULAR POLYGON

Similarly, the areas of regular tessellable polygons inscribed in disks can be expressed as a function of the disk radius R_1, hexagonal apothem r_1 and overlap difference d. We consider the three regular tessellable polygons namely equitriangular, square and hexagonal polygon.

Case I: Equi-triangular Polygon

From ΔKLT in Figure 4.16, we can calculate the area of triangle (A_T) to be

$$A_T = \frac{1}{2} \times \text{base} \times \text{perpendicular height}$$

$$= \frac{1}{2} \times \sqrt{3}R_1 \times \left(R_1 + \frac{R_1}{2}\right)$$

$$= \frac{3\sqrt{3}}{4} R_1^2 \quad (4.43)$$

But in equation (4.33a) $R_1 = \frac{2r_1\sqrt{3}}{3}$, implies

$$A_T = \sqrt{3}\, r_1^2 \quad (4.44)$$

But from equation (4.32) $d_3 = \frac{2r_1}{\sqrt{3}} = \frac{2\sqrt{3}}{3} r_1$, implies $r_1 = \frac{3d_3}{2\sqrt{3}}$

$$A_T = \sqrt{3} \times \frac{9d_3^2}{6}$$

$$A_T = \frac{3\sqrt{3}}{4} d_3^2 \quad (4.45)$$

Case II: Square Polygon

From square $UXYZ$ in Figure 4.17 we can calculate the area to be

$$A_s = s \times s$$

$$= R_1\sqrt{2} \times R_1\sqrt{2}$$

$$A_s = 2R_1^2 \quad (4.46)$$

Recall from equation (4.33a) $R_1 = \frac{2r_1\sqrt{3}}{3}$, then

$$A_s = \frac{8}{3} r_1^2 \tag{4.47}$$

Also, equation (3.41d) indicates that $d_4 = \frac{2}{3}(2\sqrt{3} - \sqrt{6})r_1$ which means $r_1 = \frac{(2\sqrt{3}+\sqrt{6})}{4} d_4$

Thus, our new area can be written in the form

$$A_s = \frac{8}{3} \times \frac{\left(2\sqrt{3} + \sqrt{6}\right)^2}{16} d_4^2$$

$$A_s = \left(3 + 2\sqrt{2}\right) d_4^2 \tag{4.48}$$

Case III: Hexagonal Polygon

Consider hexagon $BCDEFGU$ as shown in Figure 4.16. We have the area to be

$$A_H = 6 \times \frac{1}{2} \times R_1 \times R_1 \times sin60^0$$

$$A_H = \frac{3\sqrt{3}}{2} R_1^2 \tag{4.49}$$

Recall from equation (4.33a) $R_1 = \frac{2r_1\sqrt{3}}{3}$, then

$$A_H = \frac{3\sqrt{3}}{2} \times \frac{2r_1\sqrt{3}}{3}$$

$$A_H = 2\sqrt{3}\, r_1^2 \tag{4.50}$$

Also, in equation (4.42b) $d_6 = \frac{2}{3}(2\sqrt{3} - 3)r_1$, implies $r_1 = \frac{(2\sqrt{3}+3)}{2} d_6$ where d_6 is the overlap difference of hexagon inscribed in a circle. Then

$$A_H = 2\sqrt{3} \times \frac{\left(2\sqrt{3} + 3\right)^2}{4} d_6^2$$

$$A_H = \frac{3}{2}\left(12 + 7\sqrt{3}\right) d_6^2 \tag{4.51}$$

THEOREM 4.9: Disks have an overlap difference of $2R_1$ or $\frac{4\sqrt{3}}{3} r_1$ for covering since it does not tile. The area and overlap difference are respectively $\pi R_1^2 = \frac{4}{3}\pi r_1^2$ and $\frac{\pi}{4} d_\infty^2$.

Proof

From Figure 4.16, we know that equi-triangular polygon has an overlap difference of R_1 as in equation (4.40a). But the diameter of the disks is $2R_1$ which is twice that of the overlap difference of an equi-triangular polygon. Figure 4.18 illustrates equi-triangular tile with side s, apothem $\frac{R_1}{2}$ inscribed in a disk with radius R_1.

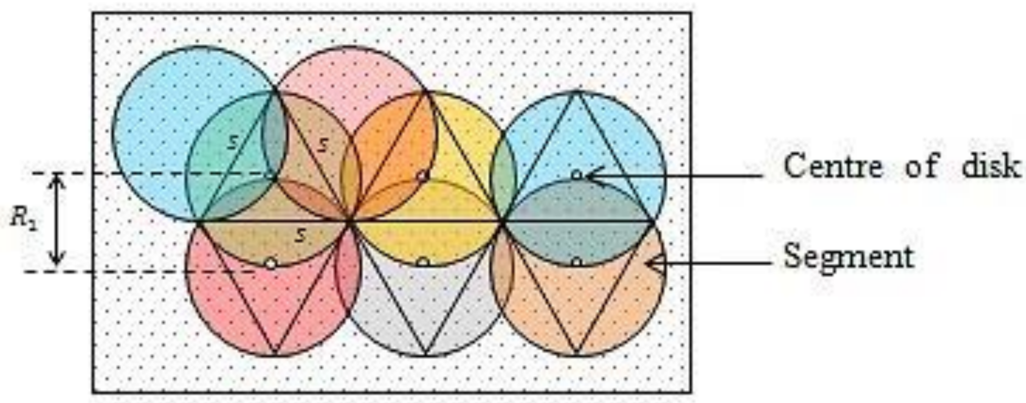

Figure 4.18: Equi-triangular tilling in disks

From Figure 4.18, six (6) equal segments completely cover a disks circumscribed on equi-triangular tilling whereas three (3) equal segments completely covers each equi-triangular tile. So the relationship between their overlap difference in covering will be $2R_1$ is to R_1 respectively. Thus disks cover with overlap difference of $2R_1$.

It follows from equation (4.33a) that $R_1 = \frac{2r_1\sqrt{3}}{3}$. Hence diameter of circle (overlap difference of regular polygon of n sides as n approaches infinity), d_∞ is

$$d_\infty = 2 \times \frac{2r_1\sqrt{3}}{3}$$

$$d_\infty = \frac{4\sqrt{3}}{3} r_1 \tag{4.52}$$

Similarly, the area of circle is

$$A_c = \pi R_1^2$$

$$A_c = \frac{4\pi}{3} r_1^2 \tag{4.53}$$

From equation (4.52) $r_1 = \frac{3d_\infty}{4\sqrt{3}}$ then

$$A_c = \frac{4\pi}{3} \times \frac{9d_\infty^2}{48}$$

$$A_c = \frac{\pi}{4} d_\infty^2 \tag{4.54}$$

4.12 RATIO OF OVERLAP DIFFERENCE AND AREA FOR TESSELABLE REGULAR POLYGONS INSCRIBED IN DISKS.

Table 4.8 shows the relationship between the overlap difference and area for three tessellable regular polygons inscribed in a disk with radius R_1, hexagonal apothem r_1 and their occupying ratio or covering fraction to that of the disks. Table 4.8: Overlap difference , area and their ratio for cyclic tessellable regular polygons

Tessellable Regular Polygon Vrs. Disks	(D) Disks	Triangle (T)	Square (S)	Hexagon (H)
$d = f(R_1, r_1)$	non	$\frac{2}{3}(3R_1 - \sqrt{3}r_1)$	$\frac{2}{3}(3R_1 - \sqrt{6}\,r_1)$	$2(R_1 - r_1)$
$d = f(R_1) = g(r_1)$	$2R_1$	R_1	$(2 - \sqrt{2})R_1$	$(2 - \sqrt{3})R_1$
	$\frac{4\sqrt{3}}{3} r_1$	$\frac{2\sqrt{3}}{3} r_1$	$\frac{2}{3}(2\sqrt{3} - \sqrt{6})r_1$	$\frac{2}{3}(2\sqrt{3} - 3)r_1$
$d_* = \left(\frac{D}{D} : \frac{T}{D} : \frac{S}{D} : \frac{H}{D}\right)$ Overlap difference ratio	100%	50%	29.3%	13.4%
Area $= f(R_1) = g(r_1)$	πR_1^2	$\frac{3\sqrt{3}}{4} R_1^2$	$2R_1^2$	$\frac{3\sqrt{3}}{2} R_1^2$
	$\frac{4}{3}\pi r_1^2$	$\sqrt{3} r_1^2$	$\frac{8}{3} r_1^2$	$2\sqrt{3} r_1^2$
$d_0 = \left(\frac{D}{D} : \frac{T}{D} : \frac{S}{D} : \frac{H}{D}\right)$ Overlap area ratio	100%	41.3%	63.7%	82.7%
$Area = f(d)$	$\frac{\pi}{4} d_\infty^2$	$\frac{\sqrt{\ }}{\ }$	$(3 + 2\sqrt{2})d_4^2$	$\frac{3}{2}(12 + 7\sqrt{3})d_6^2$

From Table 4.8 as radius increases overlapped area decreases according to inverse square law because curvature of circular shape of signal gets larger and larger. We deduce that for a Hexagon (H), Square (S) and Equi-triangular (T)

polygon, the following inequality holds for their overlap difference terms of

a) Radius of disks(R_1): $H_{(2-\sqrt{3})R_1} < S_{(2-\sqrt{2})R_1} < T_{R_1}$

b) Radius of disks and apothem (R_1, r): $H_{2(R_1-r_1)} < S_{2/3(3R_1-\sqrt{6}\,r_1)} < T_{2/3(3R_1-\sqrt{3}r_1)}$

c) Apothem (r): $H_{\frac{2}{3}(2\sqrt{3}-3)r_1} < S_{\frac{2}{3}(2\sqrt{3}-\sqrt{6})r_1} < T_{\frac{2\sqrt{3}}{3}r_1}$.

Thus, (a), (b) and (c) implies that the hexagon has the least overlap width and therefore is best suited for geometric covering using polygons. Hexagonal tiling with least overlap difference implies least overlap area or widest non overlapping area. It is expected that the hexagonal covering defined in terms of the overlap area will be greater than that of a square and an equi- triangular polygon. This coverage area defined in terms of

d) Radius of disks (R_1): $H_{\frac{3\sqrt{3}}{2}R_1^2} > S_{2R_1^2} > T_{\frac{3\sqrt{3}}{4}}$.

e) Overlap difference (d): $H_{\frac{3}{2}(12+7\sqrt{3})d^2} > S_{(3+2\sqrt{2})d^2} > T_{\frac{3\sqrt{3}}{4}d^2}$

It is evident that regular hexagon has the maximum coverage area 82.7% of disk area or least overlap difference 13.4% of disk difference and is therefore the best geometric object for optimal disk covering in a plane.

4.12.1 TYPE II: NON-UNIFORM DISKS

Non-uniform cell radius for two different GSM antenna masts with radii R_1 and R_2 ($R_2 > R_1$) and corresponding respective apothem's r_1 and r_2 would have the least cell overlap difference of $R_1 - r_1 + 2R_2 - r_2$. A mixture of nonuniform cell radius results in large overlap difference in effect increases interference (like cross talk, background noise, error in digital signaling-missed

calls, blocked calls, dropped calls). The difference $R_2 - r_2 + 2R_1 - r_1 > 2(R_1 - r_1)$, has the effect of increasing the number of overlap difference thereby increasing the number of GSM masts to be erected. Figure 4.19 shows overlap difference for two different cell range radii R_1 and R_2

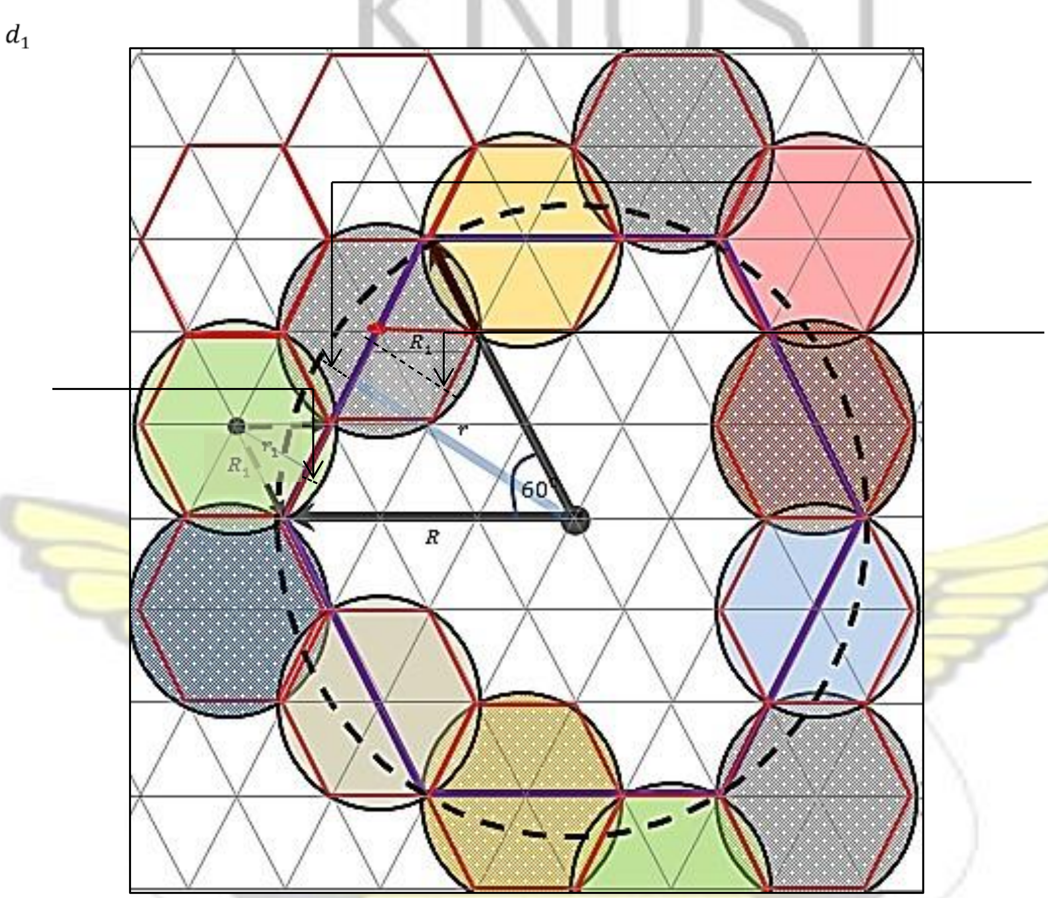

Figure 4.19: Overlap Difference for non-uniform Disks

Let $d_{R_2,R_1} = R_2 - r_2 + 2R_1 - r_1$ represents the least overlap difference for two different size disks superimposed on tessellable hexagon. Then for R_1, R_2 size tessellable regular polygons where $R_2 > R_1$

$$d_{R_2,R_1} = R_2 - r_2 + 2R_1 - r_1 \tag{4.55}$$

From equation (4.20) $r_n = R_1 cos\left(\frac{\pi}{n}\right)$

$$d_{R_2,R_1} = R_2 - R_2 cos\left(\frac{\pi}{n}\right) + 2R_1 - R_1 cos\left(\frac{\pi}{n}\right)$$

$$d_{R_2,R_1} = R_2\left[1 - cos\left(\frac{\pi}{n}\right)\right] + R_1\left[2 - cos\left(\frac{\pi}{n}\right)\right] \quad (4.56)$$

Since the polygon is a hexagon $n = 6$sided but with different radii. Thus

$$d_{R_2,R_1} = R_2\left[1 - cos\left(\frac{\pi}{6}\right)\right] + R_1\left[2 - cos\left(\frac{\pi}{6}\right)\right]$$

$$d_{R_2,R_1} = \frac{1}{2}\left[(2 - \sqrt{3})R_2 + (4 - \sqrt{3})R_1\right] \quad (4.57)$$

Equation (4.57) has the least overlap difference for GSM network design using two different radii since the $1:3$ size hexagon tile completely.

4.12.1.1 MASTING CONJECTURE 4.1: Generally for k different tessellable regular polygons $n_1, n_2, \dots n_l$ inscribed in disks with respective radii $R_l, R_{l-1}, \dots, R_1$ $(where\ R_l > R_{l-1})$ the least overlap difference is

$$d_{n_l,n_{l-1},\dots n_1} = R_k\left[1 - cos\left(\frac{\pi}{n_1}\right)\right] + R_{k-1}\left[2 - cos\left(\frac{\pi}{n_2}\right)\right] + \cdots + R_1\left[k - cos\left(\frac{\pi}{n_k}\right)\right]$$

.

$$= \sum_{l=1}^{k} R_{k-l+1}\left[l - cos\left(\frac{\pi}{n_l}\right)\right] \quad (4.58)$$

Since we are tilling with hexagon $n_l = 6,\ \forall\, l \in \mathbb{Z}^+$

$$d_{n_k,n_{k-1},\dots n_1} = \sum_{l=1}^{k} R_{k-l+1}\left[l - cos\left(\frac{\pi}{6}\right)\right]$$

$$d_{n_k,n_{k-1},\dots n_1} = \sum_{l=1}^{k} R_{k-l+1}\left[l - \frac{\sqrt{3}}{2}\right] \quad (4.59)$$

For three different tessellable regular hexagon the least overlap difference obtained from equation (4.59) is

$$d_{n_3,n_2,n_1} = \sum_{l=1}^{3} R_{3-l+1}\left[l - \frac{\sqrt{3}}{2}\right]$$

$$= R_3\left(1 - \frac{\sqrt{3}}{2}\right) + R_2\left(2 - \frac{\sqrt{3}}{2}\right) + R_1\left(3 - \frac{\sqrt{3}}{2}\right)$$

$$= R_3 - R_3\frac{\sqrt{3}}{2} + 2R_2 - R_2\frac{\sqrt{3}}{2} + 3R_1 - R_1\frac{\sqrt{3}}{2}$$

$$= R_3 - R_3 cos30^0 + 2R_2 - R_2 cos30^0 + 3R_1 - R_1 cos30^0$$

$$d_{n_3,n_2,n_1} = R_3 - r_3 + 2R_2 - r_2 + 3R_1 - r_1 \quad (4.59a)$$

This is the one sided least overlap difference of triple non-uniform hexagonal tessellation for masting in GSM network. Figure 4.20 illustrate's this concept.

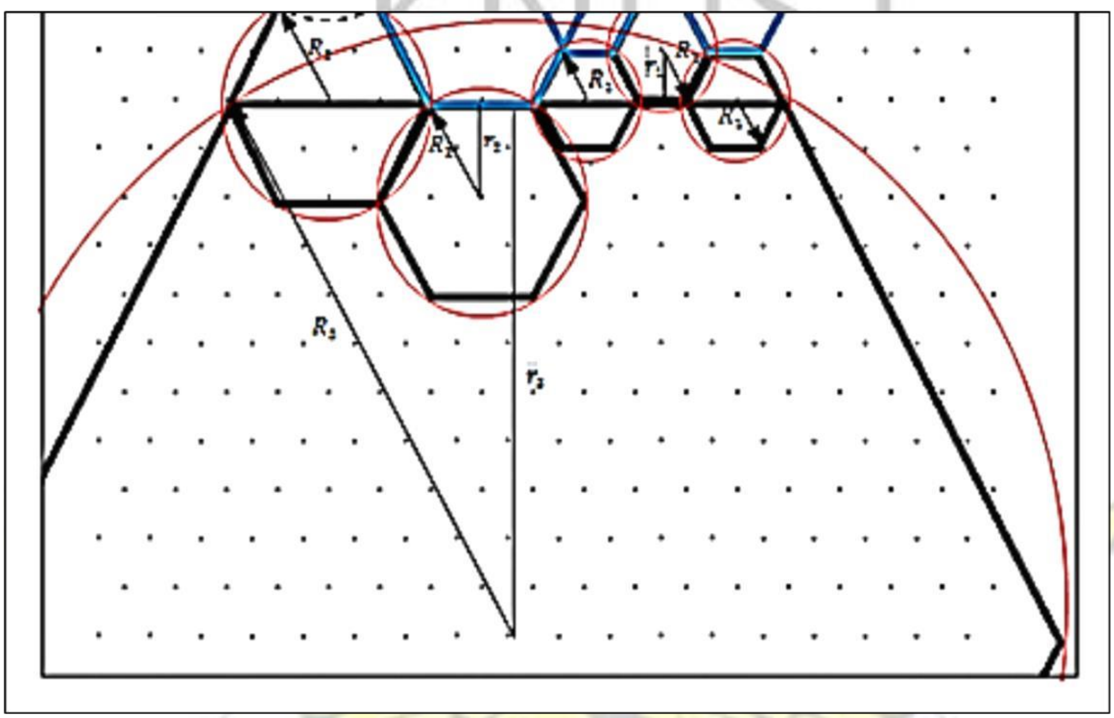

Figure 4.20(a): Triple different size hexagonal tessellation

Continuous tiling will lead us to the following overlap differences

Case I: Hexagon with Radius R_2

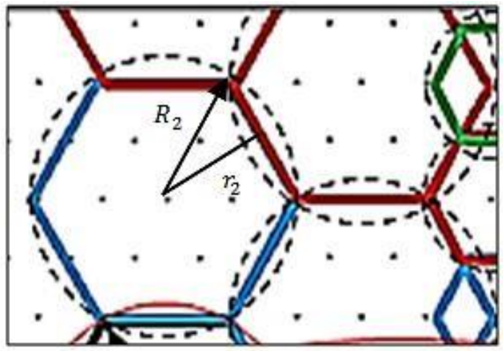

Figure 4.20(b): Section of hexagonal tiling with radius R_2 Overlap

difference will be

$$d = 2(R_2 - r_2)$$

$$d = \left(2 - \sqrt{3}\right)R_2$$

For k overlaps, the difference will be

$$d = \left(2 - \sqrt{3}\right)kR_2 \qquad (4.59b)$$

Case II: Hexagons with radii R_2 and R_1

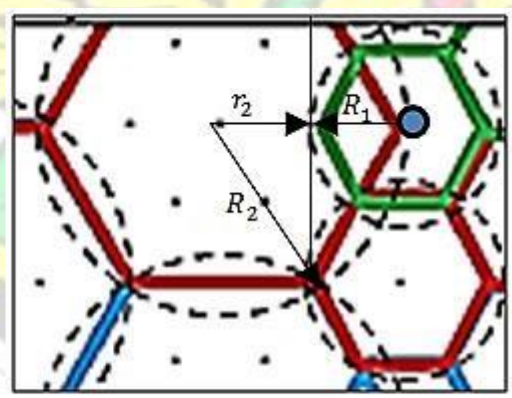

Figure 20(c): Section of hexagonal tessellation with radii R_2 and R_1 Overlap

difference will be

$$d = R_2 - r_2 + R_1 - r_1$$
$$d = R_2(1 - cos30^0) + R_1(1 - cos30^0)$$

$$d = \frac{1}{2}\left(2 - \sqrt{3}\right)(R_1 + R_2)$$

For m such overlaps, the difference will be

$$d = \frac{1}{2}(2-\sqrt{3})(R_1+R_2)m \qquad (4.59c)$$

Case III: Hexagons with Radii R_2 and R_1

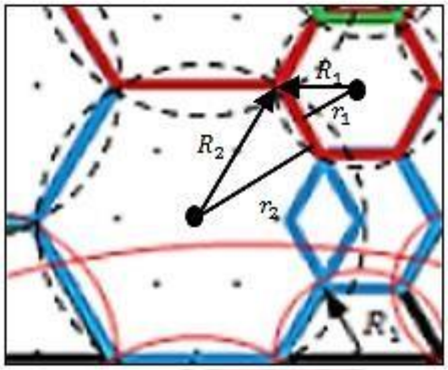

Figure 20(d): Section of hexagonal tiling with radii R_2 and R_1 Overlap difference is

$$d = R_2 - r_2 + R_1 - r_1$$

$$d = R_2(1-cos30^0) + R_1(1-cos30^0)$$

$$d = \frac{1}{2}(2-\sqrt{3})(R_1+R_2)$$

For p such overlaps, the difference will be

$$d = \frac{1}{2}(2-\sqrt{3})(R_1+R_2)p \qquad (4.59d)$$

Case IV: Hexagons with Radius R_1

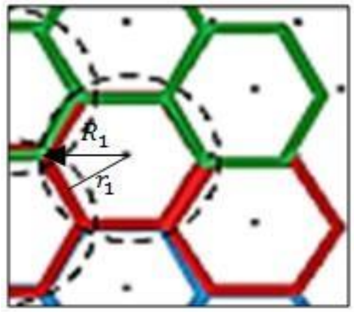

Figure 21(e): Section of least uniform hexagonal tessellation Overlap difference will be

$$d = 2(R_1 - r_1)$$

For n such overlaps, the difference will be

$$d = 2(R_1 - R_1 cos 30^0)$$

$$d_n = (2 - \sqrt{3})nR_1 \qquad (4.59e)$$

Generally, the various cases put together gives us Figure 4.21.

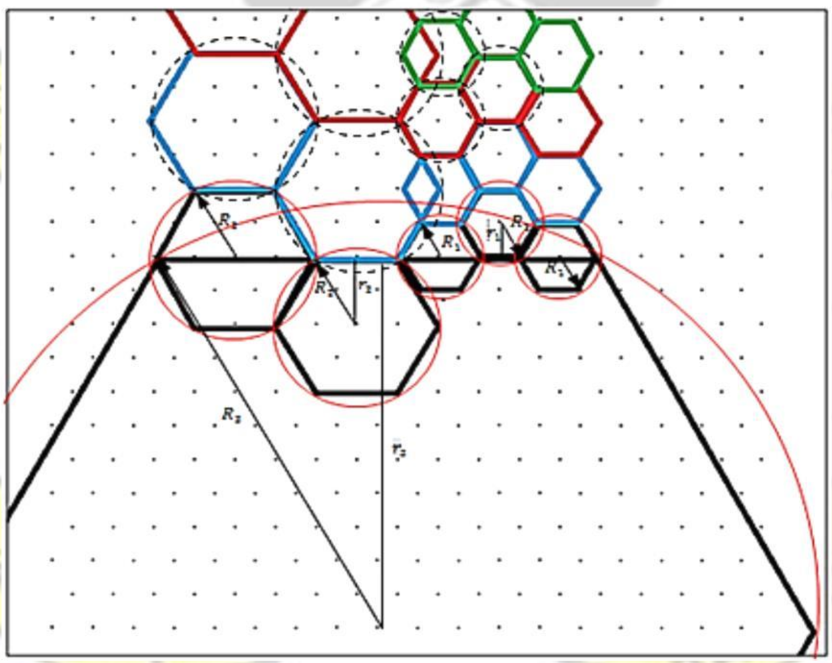

Figure 4.20: Triple tessellable different size hexagon for GSM design The total overlap difference is

$$d = 1(R_3 - r_3 + 2R_2 - r_2 + 3R_1 - r_1) + (2 - \sqrt{3})kR_2 +$$

$$\frac{1}{2}(2 - \sqrt{3})(R_1 + R_2)p + \frac{1}{2}(2 - \sqrt{3})(R_1 + R_2)m + (2 - \sqrt{3})nR_1$$ or

$$d = \left[R_3\left(1-\frac{\sqrt{3}}{2}\right)+R_2\left(2-\frac{\sqrt{3}}{2}\right)+R_1\left(3-\frac{\sqrt{3}}{2}\right)\right]+(2-\sqrt{3})(kR_2+nR_1)$$
$$+\frac{1}{2}(2-\sqrt{3})(R_1+R_2)(m+p) \qquad (4.59f)$$

4.12.1.2 PROPERTIES

For m, n and k tessellable different size regular polygon, we have

1. Asymmetry: $d_{m,n} \neq d_{n,m}$
2. Positive: $d_{m,n} > 0$
3. Triangle Inequality: $d_{m,n,k} < d_{m,n} + d_{n,k}$.

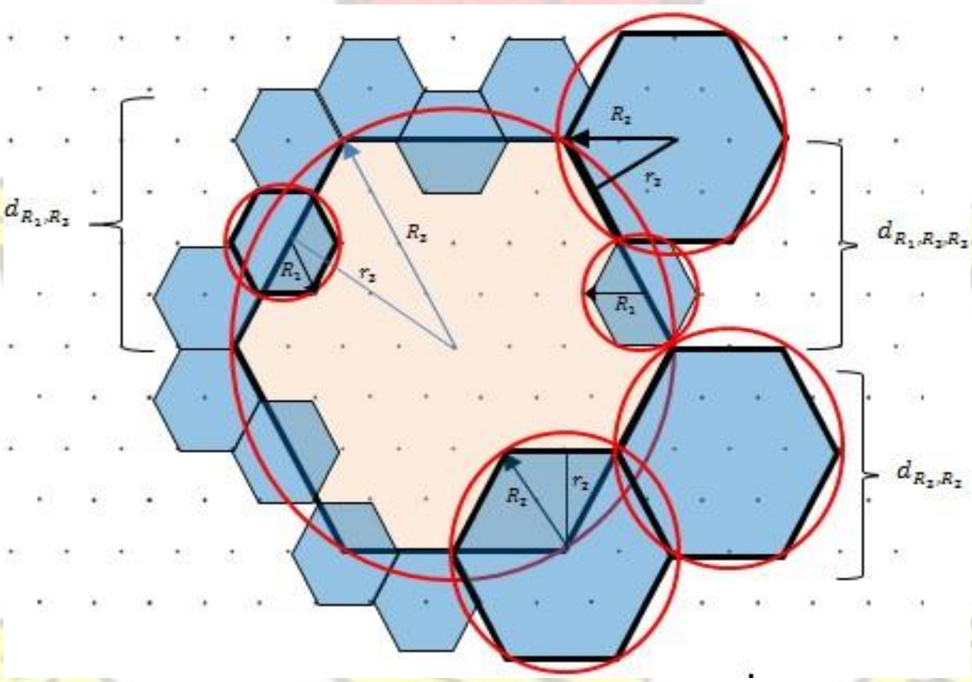

Figure 4.21: Overlap difference for m, n and k size hexagons

From Figure 4.21 we obtain the relation

$$d_{R_1,R_2,R_3} < d_{R_1,R_3} + d_{R_3,R_2}$$

This $(R_3 - r_3 + r_1 + R_2 - r_2) < (R_3 - r_3 + r_1) + (R_3 - r_3 + 2R_2 - r_2)$ simplifies to

$$(R_3 - r_3 + r_1 + R_2 - r_2) < [2(R_3 - r_3) + 2R_2 - r_2 + r_1]$$

$0 < R_3 - r_3 + R_2$ which is true for all $i \in \mathbb{Z}^+, R_i > r_i$ where

$R_i, r_i \in \mathbb{R}$. Hence property (3) above is true.

Table 4.9 illustrates the occupying overlap difference in hexagonal tiling for both uniform and non-uniform cell radius.

Table 4.9: Occupying width for uniform and non-uniform cell range.

GSM Cell Design Type	Uniform Cell Radius	Non-uniform Cell Radius
Overlap Difference (d_n)	$2(R_1 - r_1)$	$R_2 - r_2 + 2R_1 - r_1$
	$(2-\sqrt{3})R_1$	$\frac{1}{2}[(2-\sqrt{3})R_2 + (4-\sqrt{3})R_1]$
	$\frac{2}{3}(2\sqrt{3}-3)r_1$	$\frac{1}{3}[(2\sqrt{3}-3)r_2 + (4\sqrt{3}-3)r_1]$

Table 4.9 shows that it is only possible to compute the width of a hexagonal disks covering if either the radius of the disks is known or the apothem of the inscribed hexagon. It is also an establish fact that $R_2 > r_2$ and as R_2 increases the overlap difference (width - d_*) increases. This is due to the fact that the multipliers $(2-\sqrt{3})$ and $(4\sqrt{3}-3)$ for both uniform and non-uniform disks respectively are both greater than one (1), hence as $R_2 = f(r_2) \to \infty$ or $R_2 = f(R_i, r_i) \to \infty$, then $d_n \to \infty$.

4.13 AREA OF A SINGLE OVERLAP

$$(4.58b)$$

4.13.1 Type I: UNIFORM DISKS

We have proven (the proof was establish as a result of hexagon approximating circle closely) that optimal disks covering is achieved when the cells overlap to give us a difference of $2(R_1 - r_1)$.

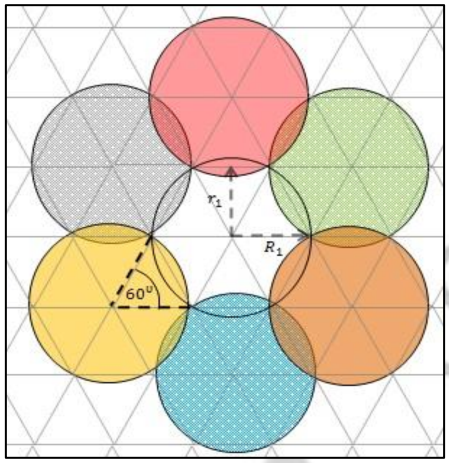

Figure 4.22: Area of a single Overlap for uniform Disks

We shall however established a formula for calculating the area of a pair of overlap for optimal covering of cells. From Figure 4.21 we have:

Area of single overlap $= 2 \times ($area of sector AOB –area of triangle $AOB)$.

$$= 2 \times \left(\frac{1}{2}{R_1}^2\theta - \frac{1}{2}{R_1}^2 sin\theta\right)$$

$$A_s = {R_1}^2(\theta - sin\theta) \qquad (4.58a)$$

For n –overlaps the total overlap area (A_T) is given by

$$A_T = n{R_1}^2(\theta - sin\theta)$$

For a hexagon, $\theta = \frac{\pi}{3}$ and a single area is

$A_s = {R_1}^2\left(\frac{\pi}{3} - sin\frac{\pi}{3}\right)$

$$= {R_1}^2\left(\frac{\pi}{3} - \frac{\sqrt{3}}{2}\right)$$

$$A_s = \frac{R_1^2}{6}(2\pi - 3\sqrt{3}) \qquad (4.58c)$$

Equation (4.54) is the formula for calculating excess area coverage loss (due to overlaps) when a pair of GSM masts are positioned with an overlap difference of $2(R_1 - r_1)$. The multiplier $0 < \frac{(2\pi - 3\sqrt{3})}{6} < 1$ widens the quadratic relationship between the area overlap and the radius of the inscribed hexagon in equation

(4.54). In field work, an overlap has the differential disadvantage of reducing coverage area, causing interferences which leads to block and dropped calls, cross talk when frequencies are not properly clustered. So the overlap area must be kept as small and few as possible - optimization. From equation (4.17),

$d = (2 - \sqrt{3})R_1$ becomes

$$R_1 = (2 + \sqrt{3})d$$

Hence (4.58c) becomes

$$A = \frac{(2+\sqrt{3})^2 \; (2\pi - 3\sqrt{3})}{6} d^2 \qquad (4.59)$$

Equation (4.59) is used to compute the overlap area for MTN Kumasi (Ghana), MTN River State (Nigeria), GLO Accra East (Ghana) and GLO River State (Nigeria) as shown in Tables L.1,P.1,T.1,X.1 and Appendix Z.5.

4.13.2 TYPE II: NON-UNIFORM CELL RADIUS

Non-uniform cell radius for two different GSM antenna masts with radii R_2 and R_1 with corresponding apothem of r_2 and r_1 would have a cell overlap difference of $R_2 - r_2 + 2R_1 - r_1$. This is illustrated in Figure 4.23.

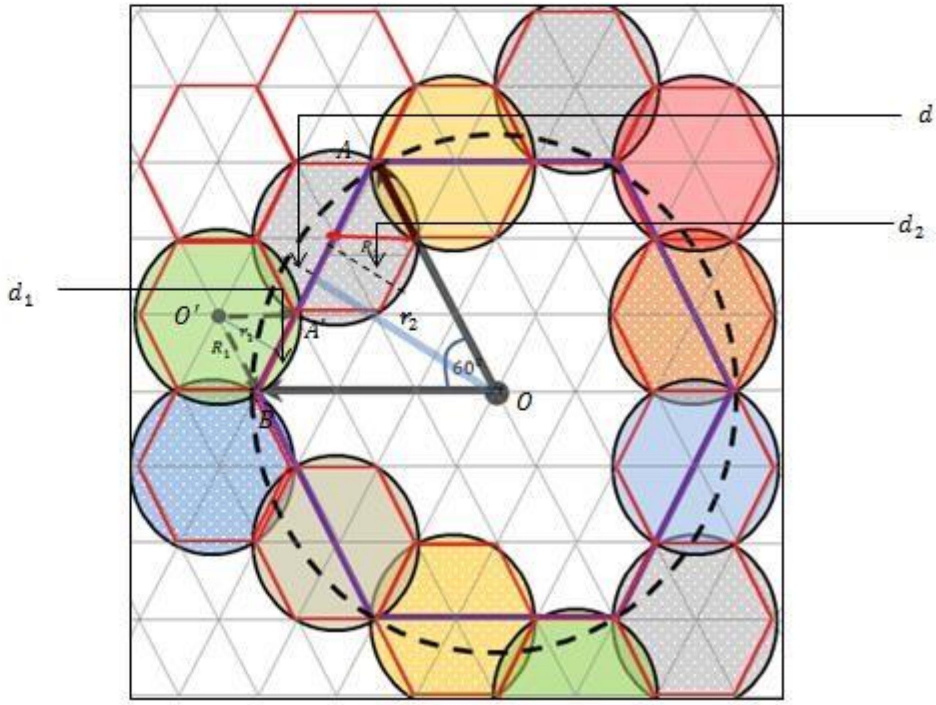

Figure 4.23: Area of overlap for non-uniform disks

The actual expression for the overlap difference can be calculated from Figure 4.23 considering the following two cases.

Overlap difference $= R_2 - r_2 + R_1 - r_1 + R_1.$

Case I: Triangle AOB

$$\text{Overlap difference} = R_2 - r_2$$

$$Sin60^0 = \frac{r_2}{R_2}$$

$$\therefore r_2 = \frac{R_2\sqrt{3}}{2}$$

Overlap difference $(d) = \left(1 - \frac{\sqrt{3}}{2}\right) R_2 = \frac{1}{2}(2 - \sqrt{3})R_2$

Case II: Triangle $A'OB$

$$\text{Overlap difference}(d_1) = R_1 - r_1$$

Similarly, triangle $A'OB$ is equilateral so $\frac{\sqrt{\ }}{\ }$. Thus $d_1 = \frac{1}{2}(2 - \sqrt{3})R_1$.

Case III: Circle with diameter AA''.

Circle with diameter AA' has an overlap difference of $d_2 = R_1$.

Generally, for non-uniform cell range we have

Overlap difference$(d_{m,n}) = d + d_1 + d_2$

$$= R_2 - r_2 + R_1 - r_1 + R_1.$$

$$= \frac{1}{2}(2-\sqrt{3})R_2 + \frac{1}{2}(2-\sqrt{3})R_1 + \frac{2R_1}{2}$$

$$= \frac{1}{2}(2-\sqrt{3})R_2 + \frac{1}{2}(4-\sqrt{3})R_1$$

$$d_{m,n} = \frac{1}{2}\left[(2-\sqrt{3})R_2 + (4-\sqrt{3})R_1\right] \tag{4.60}$$

But this expression is far greater than $2(R_1 - r_1)$. Thus it is not prudent to consider when covering with disks using non-uniform radii. Applicably, GSM network design for non-uniform cell range is economically unwise as well as inefficient in time complexity. The resulting area is calculated by the following approaches.

Area of a single repeated overlap

$A_{m,n}$ = area of bigger sector AOB _area ofΔAOB +area of smaller sector $A'O'B$ –area of$\Delta A'O'B$ + (area of circle with diameter $AA' \div 2$)

$$= \frac{1}{2}R_2^2\theta - \frac{1}{2}R_2^2 sin\theta + \frac{1}{2}{R_1}^2\theta_1 - \frac{1}{2}{R_1}^2 sin\theta_1 + \frac{1}{2}\pi R_1^2$$

$$A_{m,n} = \frac{1}{12}\left[R_2^2(2\pi - 3\sqrt{3}) + {R_1}^2(5\pi - 3\sqrt{3})\right] \tag{4.61}$$

But this expression for the area is repeated six(6) times for non-uniform disks covering. Hence the required total area is

$$A_{m,n} = \frac{6}{12}\left[R_2^2(2\pi - 3\sqrt{3}) + {R_1}^2(5\pi - 3\sqrt{3})\right] \tag{4.61a}$$

Equation (4.23) can be defined in terms of equation $(4.18a)$ connecting the two different areas. The relationship is

$$A_{m,n} = \frac{1}{2}\left[R_2^2(2\pi - 3\sqrt{3}) + 3\pi{R_1}^2 + {R_1}^2(2\pi - 3\sqrt{3})\right]$$

$$A_{m,n} = \frac{1}{2}\left[R_2^2\left(2\pi - 3\sqrt{3}\right) + 3\pi {R_1}^2 + A_n\right] \tag{4.61b}$$

Since $R_2 > R_1 > 0$ the expression $R_2^2\left(2\pi - 3\sqrt{3}\right) + 3\pi {R_1}^2 >> 0$ as well as $R_2^2\left(2\pi - 3\sqrt{3}\right) + 3\pi {R_1}^2 > A_n$. Thus, there is no possibility that $A_{m,n} = A_n$; therefore making the value of $A_{m,n} > A_n$. Thus, the area of a single overlap difference in the uniform cell radius is smaller than that of the non-uniform cell radius. It is not cost efficient for telecom engineers as well as industrial mathematicians to consider non-uniform GSM cell radius with number of intersecting cells more than that with an overlap difference of $2(R_1 - r_1)$. We shall however find a relationship between the inner angle θ and the outer angle θ_1 as well as inner radius R and outer radius R_1 for a regular polygon of side n.

Case I: $\theta_1 : f \mapsto \theta$

$$\theta_1 = k_n \theta$$

where

$$k_n \begin{cases} > 1\,, for\; n > 6 \\ = 1\,, for\; n = 6 \\ < 1\,, for\; n < 6 \end{cases} \tag{4.62}$$

Geometrically,

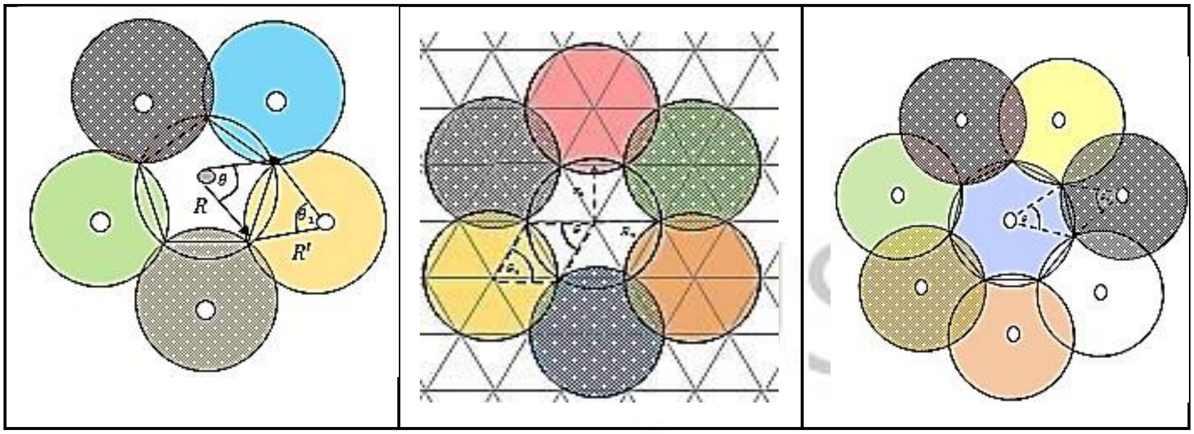

(a) Pentagon $(\theta_1 < \theta)$ (b) Hexagon $\left(\theta_1 = \theta = \frac{\pi}{3}\right)$ (c) Heptagon $(\theta_1 > \theta)$

Figure 4.24: Angular and Radii relationship for uniform and non-uniform disks

Case II: $R_1 : f \mapsto R$

There is a linear relationship between R and R_1. For a GSM with large cell radius as centre and small cell radius as rings covering it circumference as in Figure 4.24, we have the mathematical linear relationship.

$$R = k_n R_1$$

Where

$$K_n \begin{cases} > 1\,, \ for\ n > 6 \\ = 1\,, for\ n = 6 \\ < 1\,, for\ n < 6 \end{cases} . \tag{4.63}$$

Table 4.9 illustrates example of the linear relationship between R_1 and R in equilateral triangle, square, pentagon and hexagon.

4.14 THEOREM 4.9

Let E_n represent the edge lengths of an n sided regular polygon with radius Rinscribe in a disks . Mathematically,

$$E_n \begin{cases} > R, & for\ n < 6 \\ = R, & for\ n = 6 \\ < R, & for\ n > 6 \end{cases} \tag{4.64}$$

The relationship between these two lengths $(E_n$ and $R)$ is linear;.i.e $E_n = K_n R$ Proof.

We shall consider two polygons that sandwich the hexagon, namely the pentagon and the heptagon. We establish this sandwich method of proof with the aim of investigating whether the number of sides n of the polygon inscribed in a circle (disks) has a relationship with it radius.

Case I: Pentagon (E_5)

Consider pentagon $ABCDE$ in Figure 4.25 which has fewer number of sides as compared to hexagon. We use the fact that each interior angle is $\frac{540}{5} = 108^0$ with $\angle AOB = 72^0$ and $\angle OBA = 54^0$.

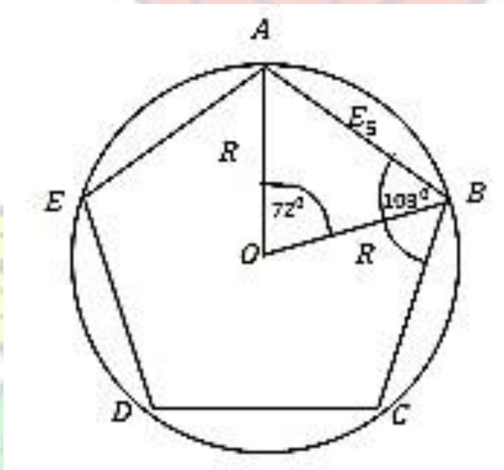

Figure 4.25: Relationship between edge and radius of pentagon

$$|AB|^2 = |AO|^2 + |OB|^2 - 2|AO||OB|\cos(72^0)$$

$$E_5{}^2 = R^2 + R^2 - 2R \times R\cos(72^0)$$

$$= 2R^2[1 - \cos(72^0)] \qquad = 2R\left[\sin\left(\frac{\pi}{5}\right)\right] \text{ or}$$

$$= 4R^2[\sin^2 36] \qquad = 2R^2\left[1 - \left(\frac{\sqrt{5}-1}{4}\right)\right]$$

$$E_5 = \frac{R}{2}\sqrt{10 - 2\sqrt{5}} \tag{4.65}$$

Where the multiplier $K_5 = 2\left[\sin\left(\frac{\pi}{5}\right)\right] > 1$, hence $E_5 > R$. The proof of the exact value of $cos(72^0)$ is shown in Appendix A.

Case II: Heptagon(E_7)

Consider heptagon $ABCDEFG$ in Figure 4.26, which have more number of sides as compared to hexagon. We use the fact that each interior angle is $\frac{(n-2)\times 180}{n} = \frac{5\pi}{7} \cong 128.6^0$ with $\angle AOB = \frac{2\pi}{7}$ and $\angle OBA = \frac{5\pi}{14} \cong 64.3^0$.

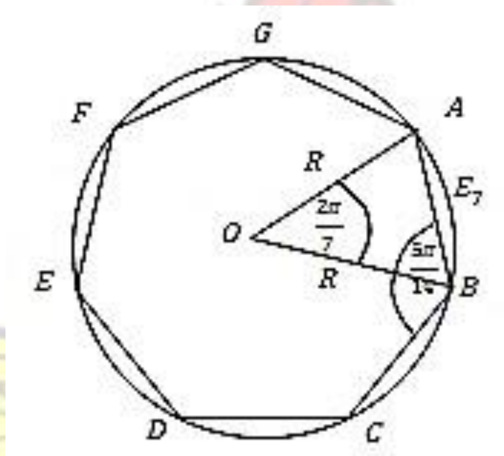

Figure 4.26: Relationship between edge and radius of heptagon

$$|AB|^2 = |AO|^2 + |OB|^2 - 2|AO||OB|cos\left(\frac{2\pi}{7}\right)$$

$${E_7}^2 = R^2 + R^2 - 2 \times R \times Rcos\left(\frac{2\pi}{7}\right)$$

$$= 2R^2\frac{\left[1 - cos\left(\frac{2\pi}{7}\right)\right]}{2} \times 2$$

$$= 4R^2 sin^2\left(\frac{\pi}{7}\right)$$

$$E_7 = 2Rsin\left(\frac{\pi}{7}\right)$$

Where the multiplier $K_7 = 2sin\left(\frac{\pi}{7}\right) < 1$, hence $E_7 < R$.

Therefore $R < E_n \leq R$ depending on the value of n. The proof is complete. Table 4.9 and Figure 4.26 shows the linear relationship between the edge and the radius of sample regular polygons inscribed in a circle. The value of the multiplier

$$(4.66)$$

$K_n \in \mathbb{R}^+$ depends on the number of sides, n. We perform our test for circular disks of radius $R = 2, 3$ and 4 units as shown in Table 4.10.

Table 4.10**:** The Relationship $E_n = K_nR$

Regular polygon $K_n = 2sin\left(\frac{\pi}{n}\right)$	Triangle $(K_3 = \sqrt{3})$	Square $(K_4 = \sqrt{2})$	Pentagon $\left(K_5 = 2\left[sin\left(\frac{\pi}{5}\right)\right]\right)$	Hexagon $(K_6 = 1)$	Heptagon $\left(K_7 = 2sin\left(\frac{\pi}{7}\right)\right)$
$E_n = K_nR$	$\sqrt{3}R$	$\sqrt{2}R$	$2\left[sin\left(\frac{\pi}{5}\right)\right]R$	R	$2Rsin\left(\frac{\pi}{7}\right)$
$E_n = 2K_n$	$2\sqrt{3}$	$2\sqrt{2}$	$4\left[sin\left(\frac{\pi}{5}\right)\right] = 2.351$	2	$4sin\left(\frac{\pi}{7}\right) = 1.736$
$E_n = 3K_n$	5.196	4.243	3.527	3	2.603
$E_n = 4K_n$	6.928	5.657	4.702	4	3.472

The linear relationship is plotted with matlab as illustrated in Figure 4.28. Appendix C shows the matlab code for this program.

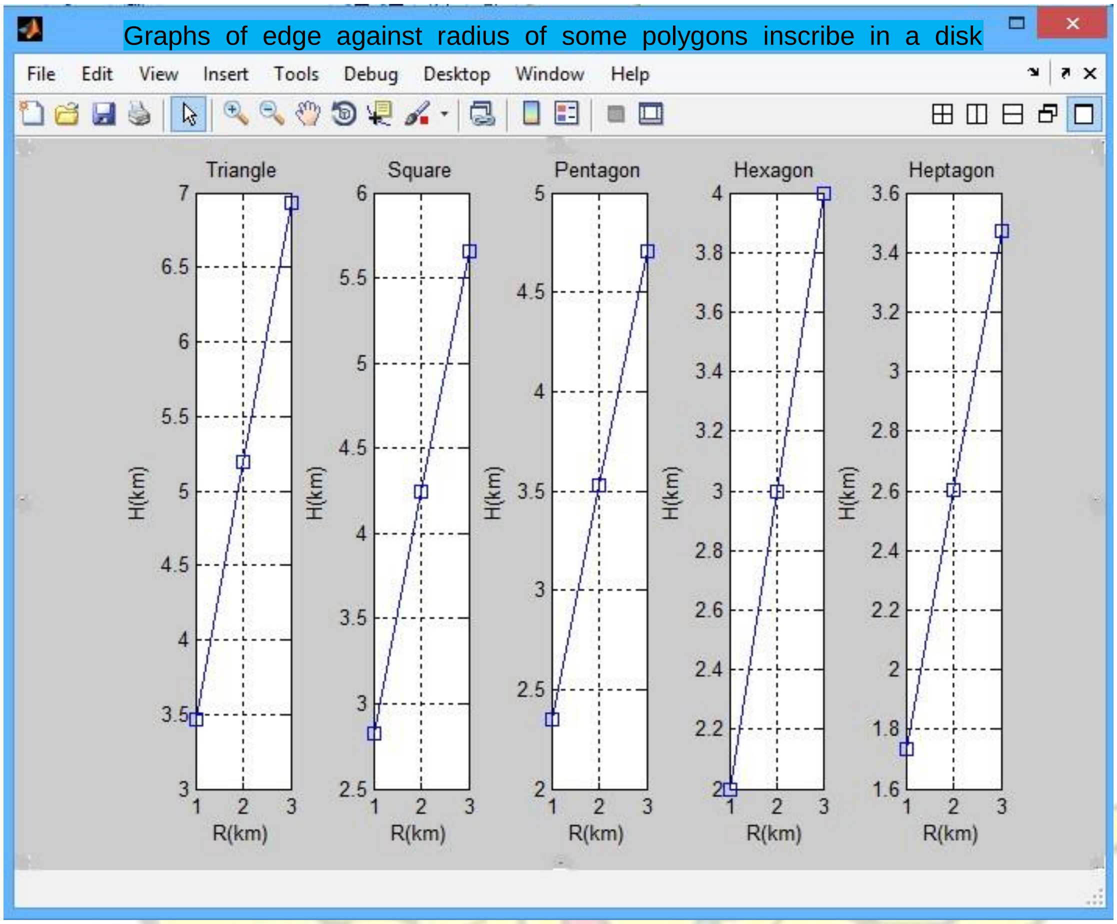

Figure 4.27: The linear relationship of $E_n = K_n R$

From Table 4.9 and Figure 4.27 it can be seen that there is a direct relationship between the number of sides n of a regular polygon and it edge length E_n inscribed in a disk with fixed radius. The slope of the relationship is positive, thus for a fixed circular disks an increase in the number of sides n of the inscribed polygon results in a decrease in (the edge length is smaller than the radius of it circumcircle) the edge length (E_n) of the polygon. Mathematically, as $n \to \infty,\ K_n \to$ decreases, resulting in $E_n < R$.

4.16 ANTENNA CHARACTERISTICS

Base and mobile stations and their antennas may be described by a number of parameters: Location (position on terrain), height above ground, carrier frequency, effective power, cable loss, radiation patterns, and tilt (mechanical and electrical) among others.

In this subsection we are mainly interested in antenna location and area coverage in open flat area environment. An area is considered to be open if there are no obstacles over a plane in the direction of the base station and in general, around the position of the mobile station.

4.16.1 HANDOVER OPERATION AND GEOMETRY OF CELL OVERLAP IN GSM NETWORKS

User mobility in mobile communication network can essentially be supported by handover. In handover operation there is the automatic transfer of the subscriber from one cell to another during the call process, without causing any interference to the call (Mishra, 2004). When the user moves from the coverage area of one cell (cell 1) to another (cell 2), a new connection with the latter has to be set up and the connection with the old cell may be freed. The handover may be smooth or interrupted (hard). A smooth handover requires that the cells are not tangent (reduced area maximization) with or without different carrier-wave frequencies. Figure 4.28 shows a hard handover of cells.

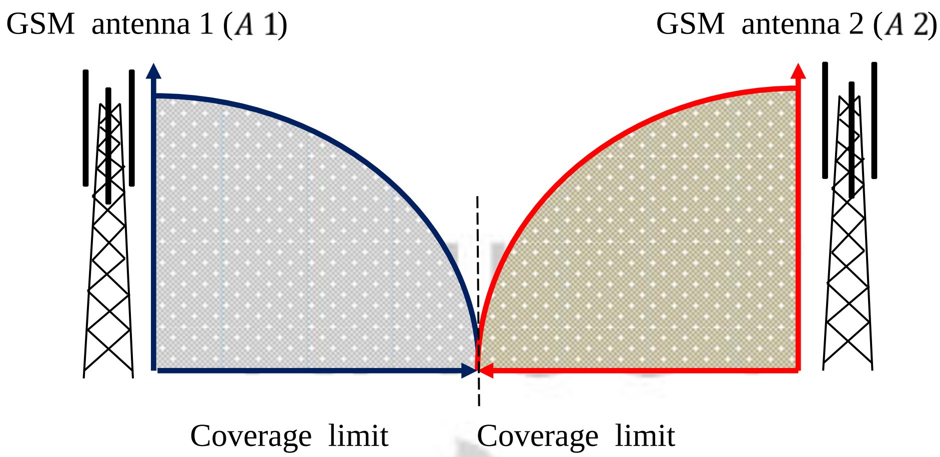

Figure 4.28: Geometry of two non-overlapping cells

The overlapping cells allow for smooth (soft) handover when the band of carrierwave frequencies allocated to neighbouring base stations are the same. This allows a user to have two (or even more) simultaneous connections with base stations and therefore, when moving from one cell to another, a new connection can be set up before the old one is released. In other words in order that interference between phone cells does not occur near the boundary between two cells where the signals from the two base stations overlap, the band of carrierwave frequencies allocated to neighbouring base stations should be the same.

Figure 4.29 explains this concept.

GSM antenna 1(A 1) GSM antenna 2 (A 2)

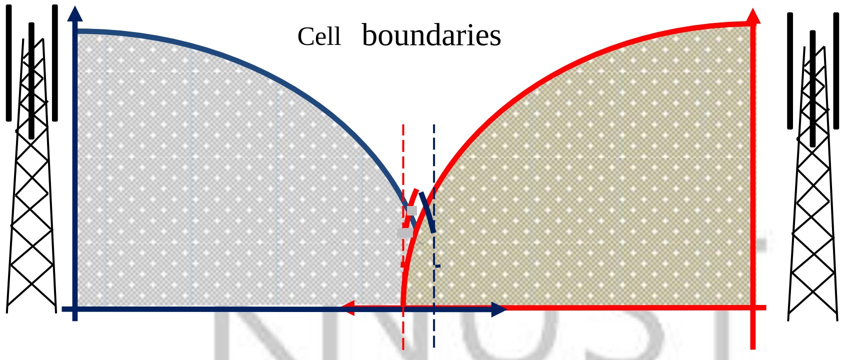

Figure 4.29: Geometry of two overlapping cells (smooth handover)

Theoretically, a handover should be initiated at the centre of the handover area since the signal levels received from both links are similar. But the signal level received from both links does not follow smooth variation, this results in either pre-mature handover or delayed handover. Frequent pre-mature handover results in higher probability of unnecessary handover and delayed handover results in higher call dropping probability. Thus an ideal handover position is crucial to obtain good handover performances. (n)

4.17 FORMULA FOR CALCULATING NUMBER OF OVERLAPS IN GSM NETWORK DESIGN.

Overlaps form a significant portion of covering problems using disks in hexagonal tessellation. The number of overlaps (N) depend on the cluster size of the hexagonal tessellation in the GSM network. Figure 4.30 shows a cluster size of three (3).

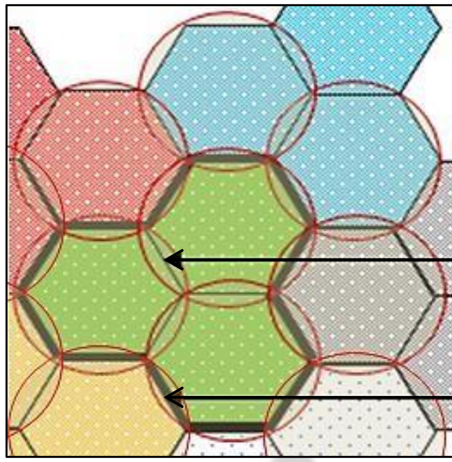

Figure 4.30: Overlaps in 3 cluster size

A formula for calculating the overlaps in non-rectilinear form is given by:

Number of overlaps for a cluster of size n,

$$N_n = \frac{1}{2}(Number\ of\ External\ edges\ (E_e))\ + Internal\ edges(E_i)$$

$$N_n = \frac{1}{2}E_e + E_i = 3n, \quad \text{for } n \in \mathbb{Z}^+ \geq 1 \tag{4.71}$$

Table 4.11 shows the number of overlaps in some cluster sizes in hexagonal tessellation.

Table 4.11: Number of overlaps for uniform cell range in different cluster size

Cluster size (n)	1	3	4	7	9
Number of overlap	$6 \times \frac{1}{2} + 0$	$12 \times \frac{1}{2} + 3$	$14 \times \frac{1}{2} + 5$	$18 \times \frac{1}{2} + 12$	$24 \times \frac{1}{2} + 15$
$N_n = 3n$	3	9	12	21	27
Each overlap difference (d_n)	$(2-\sqrt{3})R_1$				
Total overlap difference $T_n = N_n \times d_n$	$3(2-\sqrt{3})R_1$	$9(2-\sqrt{3})R_1$	$12(2-\sqrt{3})R_1$	$21(2-\sqrt{3})R_1$	$27(2-\sqrt{3})R_1$

From Table 4.11 it is evident that cluster sizes in hexagonal tessellation is made up of overlaps (full and partial). The number of overlaps increases with an increase in the cluster size which in turn increases the total number of overlap difference. This is important in determining the cost associated to each cluster or cost of an overlap for optimal covering in telecommunication network design. We provide the cost for different GSM cell range's for MTN and GLO – Ghana and Nigeria provided by ATC Tower (Ghana/ Nigeria) Limited in Table I.1 of Appendix I. and use it to quantify the cost associated with the number of overlaps (N_n).

4.18 OPTIMAL HEXAGONAL COVERING OF POINT SETS PROBLEM

The maximal covering of point sets problem using minimum number of tiled hexagons is a new area in set cover problem in computational geometry and optimization. The problem seeks to find the minimum number of hexagons that can be used to cover a given set of randomly scattered points. Consider the WGS-84 data points in UTM $(x_1, y_1), (x_2, y_2)\ldots, (x_n, y_n)$ representing positions of GSM masts for a given (fixed) cell range r as shown in Figure 4.34. How can we efficiently cover the data points with the least number of hexagons?

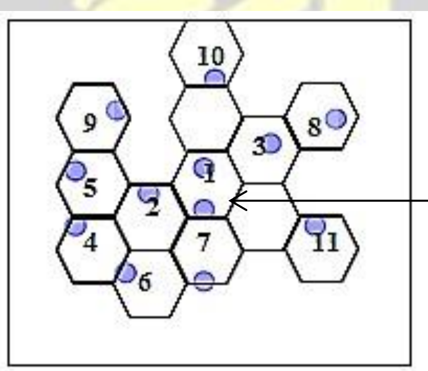

Figure 4.31: Covering of Point Set

Start covering

4.18.1 PROCEDURE

Consider a regular hexagon with given radius r. The following procedure covers the point sets with least number of hexagons.

(i) Place the hexagon in a way so that it can contain the maximum number of points given $n \geq 2$. When there is a tie between two hexagons containing most points we choose the one whose edge has more points closest.

(ii) Hexagon one (1) covers two points and therefore has the maximum covering so we labelled as the start covering. We look for the next set of point that is either closer to hexagon one or can contain the next set of most points.

(iii) Continue this pattern till all points are exhausted. The hexagonal tile can be rotated at the centre of the starting covering with an angle $0^0 < \theta < 60^0$ for better orientation.

(i) A point that is farthest can be covered by tiling from the closest edge. A cover that has no points inside is not numbered and counted.

This yield the optimal covering of point sets using hexagons for disks covering. The concepts of points sets can be extended to regular and irregular polygons (geographical area) where the vertices denote the point sets.

4.18.2 MOTIVATION 1:

Consider a township with settlements (buildings) representing point sets. A mobile company wanted to provide network services by erecting GSM masts with directional antennas to cover the entire settlements. Given a specific cell range, how can this be done optimally. Assuming the subscribers in these settlements can roam.

4.18.2.1 PROBLEM 1: Consider a point set $S = \{S_1, S_2, S_3, \dots S_n\}$ in an n-

dimensional Euclidean space, E^n, where $n \geq 2$. We therefore make the assumption that no $(n+1)$points in S lie in a common hyperplane or a vertical hyperplane. Find the minimum cardinality of disks with radius r, that covers the entire points with the condition that at least two points lie in a disks.

4.18.3 MOTIVATION 2: Consider a township with settlements representing a well define geographical area. A mobile company wanted to provide network services by erecting GSM masts to cover the entire geographical area of the township. With a specified cell range, how can this be done, optimally? Assuming the subscriber can roam.

4.18.3.1 PROBLEM 2: Consider a point set $S = \{S_1, S_2, S_3, \ldots S_n\}$ in a plane evenly spaced. Find the minimum cardinality of disks with radius r, that covers the entire points and the convex hull.

4.18.4 MOTIVATION 3: Consider a township with settlements representing a well define geographical area (regular shape). A mobile company wanted to provide network services by erecting GSM masts to cover the entire geographical area of the township.

With a specified cell range, how can this be done, optimally? Assuming the subscriber can roam.

4.18.4.1 PROBLEM 3: Given a regular polygon P design the minimum cardinality of disks with radius r needed to cover P.

4.18.5 MOTIVATION 4: The interest in this problem is revived with the rise of research in wireless networks. For example, in cellular networks, we need to deploy base stations such that every client in a designated geographical region can be served – receive signal. Assuming the subscriber can roam.

4.18.5.1 PROBLEM 4: Consider an irregular polygon P in a plane. Find the minimum number of disks that covers the entire polygon.

4.19 SECTOR HOMOGENEITY OF GSM ANTENNA FOR AREA FRACTALS IN GEOMETRY.

Practically, sectoring is basically a technique which increase the signal to interference ratio (SIR) without necessitating an increase in the cluster size. That is to say sectorization reduces co-channel interference in GSM antenna coverage. Consider the classical uniform sectoring of directional GSM antenna into 180^0, 120^0, 90^0, 72^0, 60^0. The following cases has been considered before we generalize.

Case I**:** Two Sector Site Square (180^0)

Consider a regular polygon such as a square inscribed in a circle with centre O, radius r and each interior angle $\left(\frac{360^0}{n}\right)$ 90^0 as shown in Figure 4.32.

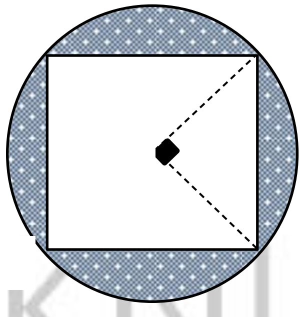

Figure 4.32: Area of a square inscribed in a circle

$\therefore$ area of square $ABCD = 4 \times \Delta AOB$

$$= 4 \times \frac{1}{2} \times r \times r \times sin\, 90^0$$

$$= 2r^2 \text{ square units}$$

We now consider a two sector site square as shown in Figure 4.33(a) applied to a GSM antennae with only two sectors as shown in Figure 4.33(b). The sector refers to the area covered by the GSM antennae.

(a) Area Fractal in square (b) Two sector GSM antennae

Figure 4.33: Two Sector Sites Topology

In the two sector GSM antennae site the fractal area is calculated by

Area of shaded $(A_{4/2}) = \frac{\text{Area of square}}{2}$

$$= \frac{2r^2}{2}$$

$$= r^2 \text{ square units.}$$

$$= \sin(90^0) \times r^2$$

$\Leftrightarrow$Area of fractal$(A_{2nd}) = sin(\text{each interior angle}) \times r^2$.

Case II: 3 sector site Hexagon (120^0)

Consider the 3 sector site hexagon of radius r and each interior angle $\left(\frac{360^0}{n}\right)$ 120^0 with centre O as shown in Figure 4.34(a).

(a) Area fractal in Hexagon (b) Three sector GSM antennae

Figure 4.34: Three Sector Site Topology

$$\text{Area of fractal}(A_{6/2}) = \frac{\text{area of hexagon}}{3}$$

$$= \frac{6\sqrt{3}r^2}{4} \div 3$$

$$= \frac{\sqrt{3}}{2} \times r^2$$

$$= sin(120^0) \times r^2$$

$\Leftrightarrow$Area of fractal$(A_{3rd}) = \sin(\text{each interior angle}) \times r^2$ sq. units

Case III: 4 Sector Site Octagon (90^0)

We shall establish area fractal by first considering the area of an octagon. Consider the octagon with centre O and radius r and each interior angle 45^0 shown in Figure 4.35.

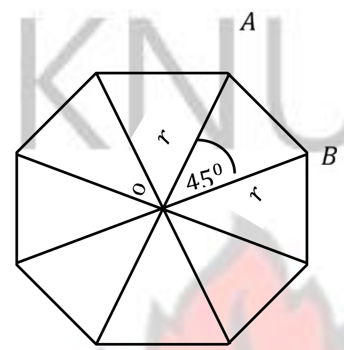

Figure 4.35: Area of an Regular Octagon

$$\text{Area of octagon} = 8 \times \left(\frac{1}{2} \times \text{r} \times \text{r} \times sin45^0\right)$$

$$= 2\sqrt{2}\, r^2 \text{ square units.}$$

Consider the four (4) sector site octagon of apothem a and each interior angle $\left(\frac{360^0}{n}\right)$ 90^0 with centre O as shown in Figure 4.36.

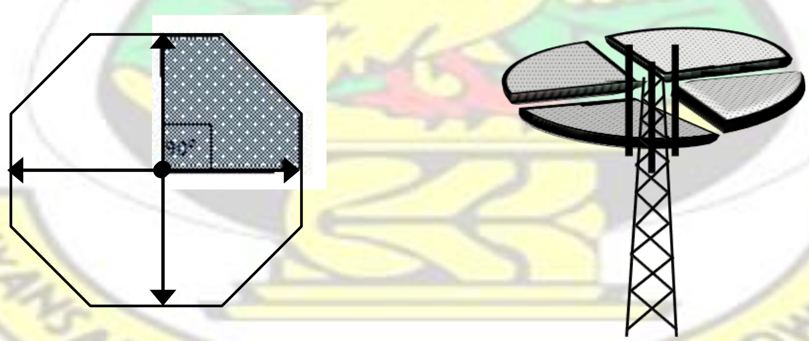

O

(a) Area Fractal in Octagon (b) Four sector GSM antennae

Figure 4.36: Four Sector Site Topology

$$\text{Area of shaded} \left(\frac{8}{2}\right) \text{fractal} = \frac{area\ of\ octagon}{4} = \frac{2\sqrt{2}\, r^2}{4}$$

$$= sin\left(\frac{90^0}{2}\right) \times r^2$$

Area of shaded (A_{4th}) fractal $= sin(\text{each interior angle}) \times r^2$.

Case IV: 5 Sector Site Decagon (72^0)

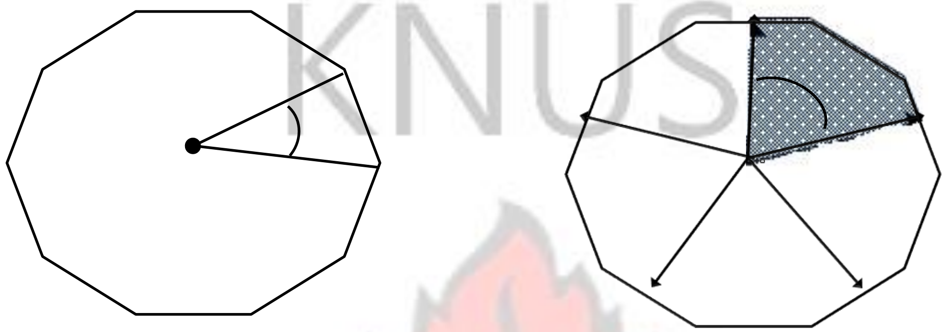

We shall establish fractal area for a five (5) sector GSM antennae of a decagon by first considering the area of a decagon. Consider the decagon with centre and radius r and interior angle 36^0 shown in B Figure 4.37 (a).

(a) Area of Regular decagon (b) Area fractal in decagon

Figure 4.37: Five Sector Site Topology

Area of $\Delta AOB = \frac{1}{2} \times \mathrm{r} \times \mathrm{r} \times sin36^0$

$$= \frac{r^2}{2} \times sin\,36^0$$

Area of decagon $= 10 \times \frac{r^2}{2} \times sin\,36^0$

$$= 5\,sin\,36^0 \times r^2.$$

$$= 5r^2 \times \frac{\sqrt{10 - 2\sqrt{5}}}{4}$$

Area of a fifth $(A_{10/2})$ fractal $= \frac{\text{area of decagon}}{5}$

$$= \frac{5\, sin\, 36^0 \times r^2}{5}$$

$$= sin\, 36^0 \times r^2 \tag{4.56}$$

$$= \frac{\sqrt{10 - 2\sqrt{5}}}{4} \times r^2$$

Area of shaded $(A_{5th}) = sin(each$ interior angle$) \times r^2$.

Case n: n sector site $\left(\frac{2\pi}{n}\right)$

Generally, for a regular polygon with sides $2n$. The fractal area is calculated by using the formula:

R

$$A_{2n/2}\text{fractal} = sin\left(\frac{2\pi}{n}\right) \times r^2.$$

The proof is complete.

4.19.1 THEOREM 4.10

In any regular hexagon inscribed in a circle of radius r, the perpendicular height(H) is $r\sqrt{3}$.

Proof

Consider hexagon $ABCDEF$ inscribed in a circle with radius r, diameter with the hexagon's perpendicular height (H) and apothem h as shown in Figure 4.38.

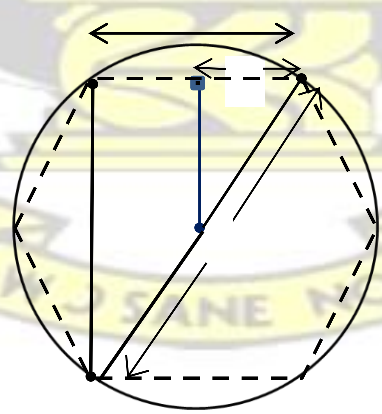

F C

Figure 4.38: Height and Radius of inscribed hexagon.

From Pythagoras theorem

$$R^2 = H^2 + L^2$$

But $L = 2l = r$ and $R = 2r$

$$(2r)^2 = H^2 + (2l)^2$$

$$H^2 = 4r^2 - 4l^2$$

$$H = 2\sqrt{r^2 - l^2}$$

$$= 2\sqrt{r^2 - \frac{r^2}{4}}$$

$$H = r\sqrt{3} \tag{4.57}$$

4.19.2 THEOREM 4.11

The apothem (h) of any regular hexagon inscribed in a circle with radius r and diameter R is given by $\frac{\sqrt{}}{}$ or $\frac{r\sqrt{3}}{2}$.

Proof

From Figure 4.68 ΔADE is similar to $\Delta\, RDM$ then;

Ratio: $\frac{AD}{RD} = \frac{DE}{DM} = \frac{EA}{MR}$

$$\frac{R}{r} = \frac{L}{l} = \frac{H}{h}$$

$\Rightarrow$ $$\frac{R}{r} = \frac{H}{h}$$

$\Rightarrow$ $h = \frac{r}{R} \times H$ where $H = r\sqrt{3}$

$\therefore$ $$h = \frac{r}{R} \times r\sqrt{3}$$

$\frac{\sqrt{}}{}$. The proof is complete.

Similarly, $R = 2r$

$$\frac{\sqrt{}}{}$$

$$h = \frac{r\sqrt{3}}{2}. \tag{4.58}$$

4.20 MAP PROJECTIONS

A map projection is the systematic drawing of lines representing meridians and parallels on a flat surface. Different projections have unique characteristics and serving different purposes. They are depicted by projecting the parallels and meridians of the ellipsoid onto the plane. Common projections include Mercators projection, Stereographic projection, Conic projections etc.

4.20.1 GEODESY OF THE EARTH

Geodesy is the science concerned with the study of the exact size and shape of the Earth in conjunction with the analysis of the variations of the Earth's gravitational field. The topographic surface of the Earth is very unsuitable as a reference surface since it has a complicated shape, varying in height by up to twenty kilometres from the deepest oceans to the highest mountains (Osborne, 2013). However, for the purpose of high precision geodetic surveys, the undulating surface is mathematically replaced by the oblate ellipsoid of revolution which is a closer representation of the true shape of the earth and provides for accurate position, azimuth and distance information, as opposed to a spherical model of the earth (Hager, 1996). The modern satellite ellipsoids used in the World Geodetic System such as WGS-84 are defined with respect to the Earth's centre of mass and a defined orientation of axes.

4.20.2 THE ELLIPSOID

An ellipsoid is a closed quadric surface that is a three-dimensional analogue of an ellipse. The standard equation of an ellipsoid centered at the origin of a Cartesian coordinate system and aligned with the axes is

$$\frac{x^2}{a^2}+\frac{y^2}{b^2}+\frac{z^2}{c^2}=1$$

The points (*a*,0,0), (0,*b*,0) and (0,0,*c*) lie on the surface and the line segments from the origin to these points are called the semi-principal axes of length a, b, c. They correspond to the semi-major axis and semi-minor axis of the appropriate ellipses.

There are four distinct cases of which one is degenerate:

- $a > b > c$ −tri-axial or (rarely) scalene ellipsoid;
- $a = b > c$ − oblate ellipsoid of revolution (oblate spheroid); □ $a = b < c$ − prolate ellipsoid of revolution (prolate spheroid);
- $a = b = c$ − the degenerate case of a sphere.

4.20.3 COORDINATES OF THE ELLIPSOID

The Earth is more accurately modelled as an oblate ellipsoid of revolution. If the symmetry axis is taken as OZ the Cartesian equation with respect to its centre is

$$\frac{X^2}{a^2}+\frac{Y^2}{a^2}+\frac{Z^2}{b^2}=1, \qquad a>b \tag{4.59}$$

The definition of longitude λ is exactly the same as on the sphere. The geodetic latitude ϕ,which is the angle at which the normal at P intersects the equatorial plane $(Z = 0)$.

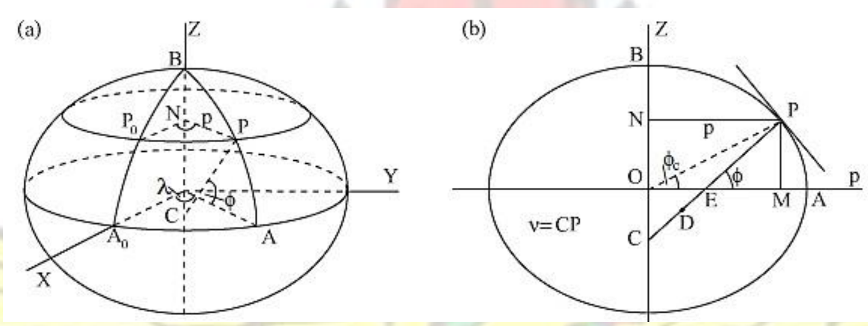

$p(\phi)$

$v(\phi)$

(a) Ellipsoid (b) Cross-section of the ellipsoid

Figure 4.39: Condition of the ellipsoid

The new feature is that the normal does not pass through the centre of the ellipsoid (except when P is on the equator and at the poles). The line joining P to the centre defines the geocentric latitude ϕ_c. We introduce the notation for the distance PN of a point P from the central axis and we also set for the length CP of the normal at P to its intersection with the symmetry axis. Therefore

e

$$p(\phi)=v(\phi)cos\phi=\sqrt{X^2+Y^2} \tag{4.60}$$

4.20.4 THE PARAMETERS OF THE ELLIPSOID

The parameter a is the equatorial radius and the parameter b is the distance from centre to pole often called the polar radius. These parameters are the major and minor semi-axes of a meridional ellipse defined by any meridian and its continuation over the poles. Instead of using (a, b) as the basic parameters of the ellipse we can use the combination (a, e) where is the eccentricity, or (a, f) where f is the (first) flattening. These parameters are defined and related by

$$\left.\begin{aligned} b^2 &= a^2(1-e^2) \\ f &= \frac{a-b}{a} \\ e^2 &= f(2-f) \end{aligned}\right\} \tag{4.61}$$

The flattening of the Earth is small at the poles (Artic and Antarctic).

4.20.5 PARAMETERIZATION BY GEODETIC LATITUDE

The equation of any meridian ellipse follows from (4.59) and (4.60):

$$\frac{P^2}{a^2} + \frac{Z^2}{b^2} = 1 \tag{4.62}$$

Differentiating this equation with respect to p gives

$$\frac{dZ}{dP} = -\frac{pb^2}{Za^2} \tag{4.63}$$

Since the normal and tangent are perpendicular the product of their gradients is 1 and therefore the gradient of the normal is

$$tan\phi = -\left(\frac{dZ}{dp}\right)^{-1} = \frac{Za^2}{pb^2} = \frac{Z}{p(1-e^2)} \tag{4.64}$$

Eliminating Z from equations (4.62) and (4.61) gives

$$p^2[1 + (1-e^2)tan^2\phi] = a^2 \tag{4.65}$$

Thus the required parameterization is

$$PN = p(\phi) = \frac{acos\phi}{[(1-e^2)sin^2\phi]^{1/2}} \tag{4.66}$$

$$PM = Z(\phi) = \frac{a(1-e^2)sin\phi}{[1-e^2sin^2\phi]^{1/2}} \tag{4.67}$$

Since $v = CP = PNsec\phi = psec\phi$ we have

$$CP = v(\phi) = \frac{a}{[1-e^2sin^2\phi]^{1/2}} \tag{4.68}$$

In terms of which

$$p(\phi) = v(\phi)cos\phi \tag{4.69}$$

$$Z(\phi) = (1-e^2)v(\phi)sin^2\phi \tag{4.70}$$

4.20.6 THE TRIANGLE OCE

We shall require the sides of the triangle ΔOCE defined by the normal and its intercepts on the axes

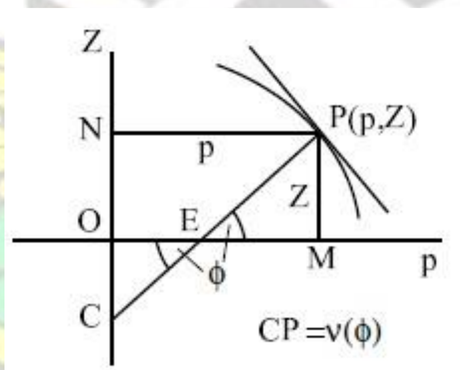

Figure 4.40: Triangle OCE

$$OE = OM - EM = p - Zcot\phi$$
$$= vcos\phi - (1-e^2)vcos\phi$$
$$= ve^2cos\phi$$
$$CE = ve^2$$
$$OC = ve^2sin\phi \tag{4.71}$$

The sides of this small triangle are all of order ae^2

4.20.7 THE RELATION BETWEEN GEODETIC AND GEOCENTRIC LATITUDES

From Figure 4.40 and equations (4.69) and (4.70) we immediately obtain the relation between ϕ and ϕ_c:

$$tan\phi_c = \frac{Z}{p} = (1 - e^2)tan\phi \tag{4.72}$$

Clearly ϕ and ϕ_c are equal only at the equator, $\phi = 0$, or at the poles, $\phi = \frac{\pi}{2}$. Since $e^2 \cong 0{:}0067$ the difference $\phi - \phi_c$ at any other angle is small (and positive). We find the position and magnitude of the maximum difference. First we write

$$\tan(\phi - \phi_c) = \frac{tan\phi - tan\phi_c}{1 + tan\phi tan\phi_c}$$

$$= \frac{e^2 tan\phi}{1+(1-e^2)tan^2\phi} \tag{4.73}$$

Differentiating with respect to ϕ gives

$$\sec^2(\phi - \phi_c)\frac{d(\phi-\phi_c)}{d\phi} = \frac{e^2 sec^2\phi[1-(1-e^2)tan^2\phi]}{1+(1-e^2)tan^2\phi} \tag{4.74}$$

Therefore $\phi - \phi_c$ has a turning point, clearly a maximum when the right hand side vanishes at $\tan\phi = \frac{1}{\sqrt{1-e^2}}$. Using the value of e for the WGS ellipsoid shows that the maximum difference occurs at $\phi \cong 45^0.095$, for which $\phi_c \cong 44^0.904$ and the latitude difference $\phi - \phi_c \cong 11.50'$. (Note that $e^2 \cong 0.00667$ is the radian measure of $22.9'$).

4.20.8 CARTESIAN AND GEOGRAPHIC COORDINATES

Using (4.69) and (4.70) the Cartesian coordinates of a point on the surface are

$$X(\phi) = p(\phi)cos\lambda = v(\phi)cos\phi cos\lambda \tag{4.75}$$

$$Y(\phi) = p(\phi)sin\lambda = v(\phi)cos\phi sin\lambda \tag{4.76}$$

$$Z(\phi) = (1 - e^2)v(\phi)sin\phi \tag{4.77}$$

For given X, Y, Z the inverse relations for ϕ and λ are

$$\lambda = tan^{-1}\left(\frac{Y}{X}\right) \tag{4.78}$$

$$\phi = tan^{-1}\left(\frac{Z}{(1-e^2)\sqrt{X^2+Y^2}}\right) \tag{4.79}$$

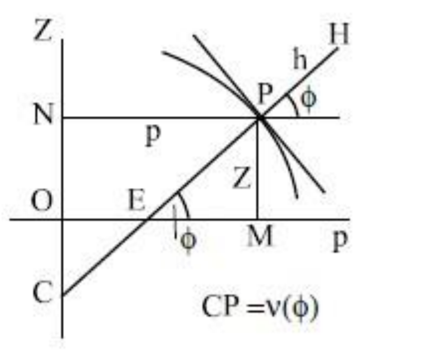

Figure 4.41: Cartesian and geographic coordinates

The two dimensional coordinate system describing points on the surface may be extended to a three dimensional coordinate system. Let H be a point at a height h $p +$ on the normal to the surface at the point P with geographical coordinates ϕ and λ. The distance of this point from the axis is now $hcos\phi$. Also, from (4.71), we have $EP = CP = CE = v(1-e^2)$. The coordinates of H are

$$X(\phi) = [v(\phi) + h]cos\phi cos\lambda \tag{4.80}$$

$$Y(\phi) = [v(\phi) + h]cos\phi sin\lambda \tag{4.81}$$

$$Z(\phi) = [(1-e^2)v(\phi) + h]sin\phi \tag{4.82}$$

For the inverse relations dividing equation (4.81) by (4.80) gives λ explicitly, as in equation (4.78). To find ϕ and h we can eliminate λ from (4.80) and (4.81) and rewrite equation (4.82) for Z to give

$$\sqrt{X^2+Y^2} = [v(\phi) + h]cos\phi \tag{4.83}$$

$$Z + e^2 v(\phi) sin\phi = [v(\phi) + h] sin\phi \quad (4.84)$$

Dividing these equations gives an implicit equation for ϕ:

$$\phi = tan^{-1}\left[\frac{Z + e^2 v(\phi) sin\phi}{\sqrt{X^2 + Y^2}}\right] \quad (4.85)$$

There is no closed solution to this equation but we can develop a numerical solution by considering the following fixed point iteration:

$$\phi_{n+1} = g(\phi_n) = tan^{-1}\left[\frac{Z + e^2 v(\phi_n) sin\phi_n}{\sqrt{X^2 + Y^2}}\right], \quad n = 0,1,2, \ldots \quad (4.86)$$

Now in most applications we will have $h \ll a$ so that a suitable starting approximation is the value of ϕ obtained by using $h = 0$ solution, equation (4.79)

$$\phi_0 = tan^{-1}\left[\frac{Z}{(1 - e^2)\sqrt{X^2 + Y^2}}\right] \quad (4.87)$$

If the iteration scheme converges so that $\phi_{n+1} \to \phi^*$ and $\phi_n \to \phi^*$ in (4.86) then ϕ^* must be the required solution of equation (4.85). The condition for convergence of the fixed point iteration is that $|g'(\phi)| < 1$: this is true here since $g'(\phi) = O(e^2)$. Once we have found ϕ it is trivial to deduce from equation (4.83)

$$h = sec\phi\sqrt{X^2 + Y^2} - v(\phi) \quad (4.88)$$

4.20.9 THE UNIVERAL TRANSVERSE MERCATOR'S PROJECTION

The Mercator's projection can be visualized as an ellipsoid projected onto a cylinder with tangency established at the equator and with the polar axis of the ellipsoid in coincidence with the cylinder. The origins of the projection line s vary. When the cylinder is opened and flattened a distortion appears in the polar regions. Distortions becomes pronounced as the distance north and south of the equator increases. A Universal Transverse Mercator's (UTM) projection is where the cylinder has been rotated or transversed 90^0. The ellipsoid and cylinder are thus tangent along a meridian as in the case of Mercator's projection.

UTM is a set of 60 TME projections based on the WGS (1984) ellipsoid. The areas extend 15^0 in longitude from the central meridians as shown in Figure 4.42.

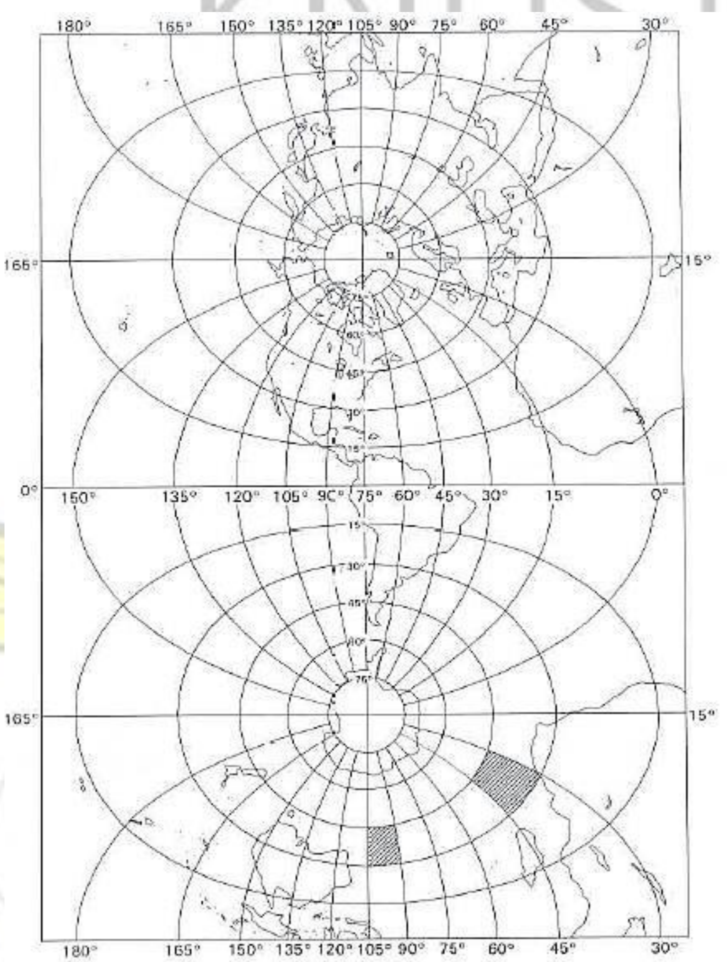

Figure 4.42: UTM projections of the earth **4.20.10**

DISTANCES ON THE ELLIPSOID

Starting from the parameterization of the Cartesian coordinates

$$X(\phi) = p(\phi)cos\lambda = v(\phi)cos\phi cos\lambda \tag{4.75}$$

$$Y(\phi) = p(\phi)sin\lambda = v(\phi)cos\phi sin\lambda \tag{4.76}$$

$$Z(\phi) = (1 - e^2)v(\phi)sin\phi \tag{4.77}$$

We have

$$dX = \dot{p}cos\lambda d\phi - psin\lambda d\lambda, \quad \text{where DOT} \equiv \frac{d}{d\phi}$$

$$dY = \dot{p}sin\lambda d\phi \qquad + pcos\lambda d\lambda,$$

$$dZ = \dot{Z}d\phi$$

The metric arc length is written as

$$dS^2 = dX^2 + dY^2 + dZ^2$$
$$= \left(\dot{p}^2 + \dot{Z}^2\right)d\phi^2 + p^2 d\lambda^2$$

The cross-section coordinates and their derivatives are

$$p(\phi) = v(\phi)cos\phi, \qquad Z(\phi) = Z(\phi) = (1 - e^2)v(\phi)sin\phi \tag{4.89}$$

$$\frac{dp}{d\phi} = -\rho sin\phi, \qquad \frac{dZ}{d\phi} = \rho cos\phi \tag{4.90}$$

Using (4.89) and (4.90) we obtain two useful forms

$$dS^2 = \rho^2 d\phi^2 + p^2 d\lambda^2 \tag{4.91}$$

$$dS^2 = \rho^2 d\phi^2 + v^2 cos^2\phi d\lambda^2 \tag{4.92}$$

On the meridian we have $d\lambda = 0$ and on the parallel circle we have $d\phi = 0$. Therefore

$$dS_{meridian} = \rho d\phi \tag{4.93}$$

$$dS_{parallel} = vcos\phi d\lambda \tag{4.94}$$

4.20.11 THE INFINITESIMAL ELEMENT ON THE ELLIPSOID

We define a map projection by two functions $x(\phi, \lambda)$ and $y(\phi, \lambda)$ which specify the plane Cartesian coordinates (x, y) corresponding to the latitude and longitude coordinates (ϕ, λ). The projection equations are written in terms of a modified Mercator parameter ψ usually called the isometric latitude.

$$x(\lambda, \phi) = a\lambda \qquad y(\lambda, \phi) = a\psi(\phi)$$

From equations (4.93) and (4.94) we see that the infinitesimal element on the ellipsoid is approximated by a planar rectangular quadrilateral with sides of length $\rho\delta\phi$ on the meridians and $v cos\phi d\lambda$ on a parallel. This is shown in Figure 4.43.

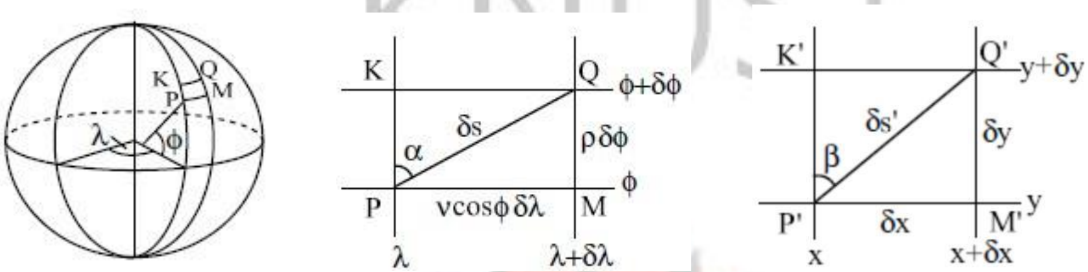

(a) Point on an ellipsoid (b) Projection plane KPMQ (c) Reflected projection plane

Figure 4.43: Infinitesimal element and it projection planes

Comparing the infinitesimal element on the ellipsoid and the projection plane and imposing the conformality condition geometrically,

$$\left.\begin{aligned} tan\alpha &= \frac{v cos\phi\delta\lambda}{\rho\delta\phi} \\ tan\beta &= \frac{\delta x}{\delta y} = \frac{a\delta\lambda}{a\psi'(\phi)\delta\phi} \end{aligned}\right\} \tag{4.95}$$

So that

$$tan\beta = \frac{\rho sec\phi}{v\psi'(\phi)} tan\alpha \tag{4.96}$$

The projection is conformal if $\alpha = \beta$. Therefore

$$\frac{d\psi}{d\phi} = \frac{\rho(\phi) sec\phi}{v(\phi)} \tag{4.97}$$

$$\int_0^{\phi} d\psi = \int_0^{\phi} \frac{\rho(\phi) sec\phi}{v(\phi)} d\phi$$

$$\psi(\phi) = \int_0^{\phi} \frac{(1-e^2) sec\phi}{1-e^2 sin^2\phi} d\phi$$

$$\psi(\phi) = \int_0^{\phi} \frac{(1-e^2)}{cos\phi} . \frac{1}{1-e^2sin^2\phi} d\phi$$

$$= \int_0^{\phi} \left[\frac{1}{cos\phi} - \frac{e^2cos\phi}{2}\left(\frac{1}{1+esin\phi} + \frac{1}{1-esin\phi}\right)\right] d\phi$$

$$= \int_0^{\phi} \left[\frac{1}{cos\phi} - \frac{e}{2}\left(\frac{ecos\phi}{1+esin\phi} + \frac{ecos\phi}{1-esin\phi}\right)\right] d\phi$$

$$= In\left[tan\left(\frac{\phi}{2} + \frac{\pi}{4}\right) - \frac{e}{2} In\left(\frac{1+esin\phi}{1-esin\phi}\right)\right]$$

$$= tanh^{-1}(sin\phi) - etanh^{-1}(esin\phi) \tag{4.98}$$

The formula used to derived the conformal ellipsoid Mercator's coordinates (xEastings and y-Northings) from ellipsoid Latitude (ϕ) and Longitude (λ) are:

$$x(\lambda, \phi) = a\lambda$$

$$y(\lambda, \phi) = a\psi(\phi)$$

$$= aIn\left[tan\left(\frac{\phi}{2} + \frac{\pi}{4}\right) - \frac{e}{2} In\left(\frac{1+esin\phi}{1-esin\phi}\right)\right]$$

$$= atanh^{-1}(sin\phi) - aetanh^{-1}(esin\phi)$$

$$h = k = \frac{\sqrt{1-e^2sin^2\phi}}{cos\phi}$$

where the transformation parameters from WGS-84 to local datum uses the following

λ –Ellipsoid longitude in radians

ϕ – Ellipsoid latitude in radians

a – Ellipsoid semi-major axis $(6{,}378{,}137.000m)$

e – Ellipsoid eccentricity $(e = 8.1819190842622 \times 10^{-2})$

h – Central meridian scale factor (0.9996012717)

k – Parallel scale factor

$\frac{1}{f}-$ Inverse flattening (298.257223563)

rX –Rotations X $(0.000")$

$rY-$ Rotations Y $(0.000")$ $rZ-$

Rotations Z $(0.000")$

$dS-0.0000$ parts per million (ppm) (Hagger et al., 1996).

The above equations with their geodetic parameters are all embedded in coordinate converter software's like GIS, Fugro etc. WGS-84 local coordinates in Degrees Minutes Seconds (DMS) format was obtained from American Tower Company Ghana (ATC) (A. Owuahene, Kumasi, Ghana. WGS-84 Local Geographic coordinates).This was converted to WGS-84 showing both geographical and grid coordinates using Fugro coordinate converter and the result was plotted in

Autocad environment.

CHAPTER 5

VARIANT GSM CELL FOR OPTIMAL DISKS COVERING WITH

LEAST OVERLAP DIFFERENCE AND AREA

This chapter will identify using the developed algorithms outlined in the previous chapter for efficient time complexity and optimal geometric disks covering algorithm for point sets, regular and irregular plane. The chapter will experiment with the data set provided by ATC Ltd - Ghana/ Nigeria. GPS in local grid coordinates will be projected to WGS 84 using Fugro to obtain the geographical and grid coordinates. The WGS-84 coordinates and cell range was plotted in Autocad for easy computation and analysis. We shall compare using cost-benefit analysis to determine the efficient disks covering for a single site MTN-Kumasi East (Ashanti Region) with cell range 0.6km, GLO- Accra East (Greater Accra) with cell range 0.8km, MTN River State (Southern Nigeria) with multiple cell range 0.6km, 1.3km and 2.5km and GLO- River State (Nigeria) with 1 and 3km.

5.1 MONETARY VALUATION OF OVERLAP AREA AND OVERLAP DIFFERENCE FOR GSM NETWORK DESIGN

Data from ATC (Tower), Helios and EATON Ghana and Nigeria Ltd as shown in Table I.1 was collected and analyzed for Huawei BTS with specific cell ranges as at Apr- Aug. 2014. We compute the overlap area and overlap difference for both uniform and non-uniform cell range for the network design.

The computation is illustrated in Appendices Z.1, Z.2 and Z.3

5.2 LOCAL COORDINATES OF GSM MASTS FOR MTN AND GLO NETWORKS (GHANA AND NIGERIA)

Data from ATC (Ghana and Nigeria) Ltd showing local coordinates of MTN GSM masts in Kumasi East-Ghana, River State- Nigeria and GLO masts in SouthEast of Accra - Ghana, River State - Nigeria was obtained. This is shown in Table

J.1 of Appendix J.1, Table N.1 of Appendix N.1, Table R.1 of Appendix R.1 and Table V.1 of Appendix V.1 respectively. This was projected to WGS-84 using Fugro as shown in Table J.2 of Appendix J.2, Table N.2 of Appendix N.2, Table R.2 of Appendix R.2 and Table V.2 of Appendix Y. Figure 4.42 shows a map with population density of Ghana and Nigeria that our study covers .

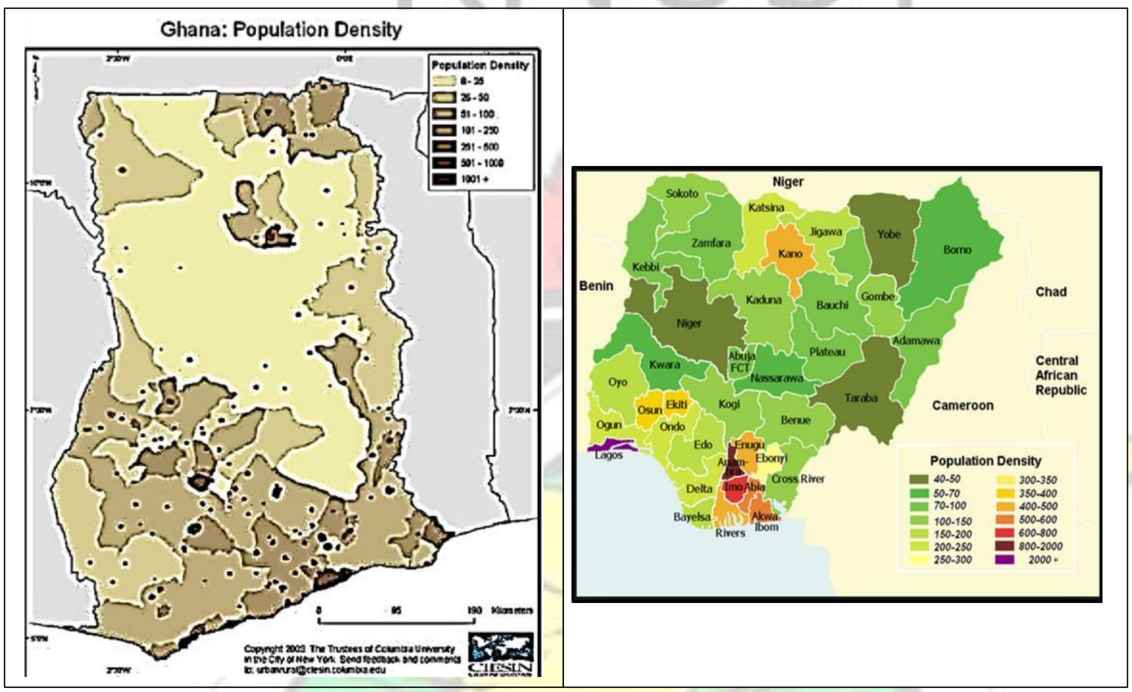

(a) Regions in Ghana b) States in Nigeria

Figure 4.42: Population density in Ghana and Nigeria in thousands

5.3 OVERLAP COST OF ORIGINAL LAYOUT VRS. PROPOSED HEXAGONAL TESSELLATED DESIGN.

We compute the overlap cost of both the original layout and the proposed hexagonal tiled design for a single cluster size. The values were obtained in Appendix Z.3. For MTN Kumasi East, Ghana the hexagonal design accounted for $4,970,000 for 35 masts out of $7,100,000 for 50 masts. MTN River State accounted for \$5,344,569.86 for 36 masts out of \$7,190,569.86 for 50 GSM masts. GLO Accra East accounted for \$6,075,382.28for 44 masts out of \$7,064,398.00 for 50 GSM masts. Finally, GLO River State, accounted for \$5,610,227.954 for 38 masts out of \$6,634,713.434 for 45 GSM masts. Costbenefit analysis shows that the most efficient and cost effective way of the cell design is by the use of the hexagonal tessellation. Table Z.3 in Appendix Z.3 shows the cost of the original layout as compared to the cost incurred when the proposed hexagonal tessellation design was adopted.

5.4 DISCUSSION OF RESULTS

From the economic standpoint, the hexagonal tessellation design option emerges as the least costly and is technically feasible.

The hexagonal tessellated design covering obtained by maximal node covering is preferred over the current approach practice by –telecommunication engineers. For instance MTN Ghana, used 50 GSM masts to cover an area of $25.04km^2$ at Kumasi East, instead of using 35 GSM masts to cover an area of $32.74km^2$ if the hexagonal approach is used. This is equivalent to using 2GSM masts to cover approximately $1km^2$ in their design where as the hexagonal tessellation model uses approximately 1GSM masts to cover the same area. GLO Ghana uses 50 GSM masts to cover $74.50km^2$ for Accra East instead of 43 GSM masts to cover $71.50km^2$ proposed by the hexagonal tessellation. Furthermore, GLO Nigeria uses 45 GSM masts to cover $111.48km^2$ at River State whereas the hexagonal tessellation model uses 38 GSM masts to cover $119.51km^2$. Finally, MTN Nigeria uses 50 GSM masts to cover $21.48km^2$ at River State whereas our model uses 36 GSM masts to cover $148.71km^2$. This will consequently reduce environmental impacts such as habitat destruction and economic costs. This is shown in Table 4.12.

Table 4.12: GSM masts and their total area coverage.

	Original Layout		Hexagonal Tessellation Model	
Case Study	Number of masts	Area covered (km^2)	Number of masts	Area covered (km^2)
MTN Ghana, Kumasi-East	50	25.04	35	32.74
Ratio	1mast	$0.50km^2$	1mast	$0.94km^2$
GLO Ghana, Accra-East	50	74.50	43	71.50
Ratio	1 mast	$1.49km^2$	1 mast	$1.66km^2$
MTN Nigeria, River State	50	21.48	36	148.71
Ratio	1 mast	$0.43km^2$	1 mast	$4.13km^2$
GLO Nigeria, River State	45	111.48	38	119.51
Ratio	1 mast	$2.48km^2$	1 mast	$3.15km^2$

The computation of the coverage area is also shown in Appendix Z.2 and Z.3. Table 4.12 shows that the Hexagonal Tessellation Model uses single mast to cover wider area or fewer masts to cover more area than the original design for all cases considered and is therefore recommended for design network. Geometrically, this cover uses the minimum connected disks (GSM masts) with the property that each disk (D_i) is a superset of the hexagon (H), $(D_i \supset H)$.

It is important to note also that the percentage change area coverage of the hexagonal tessellation model over our design the original layout is 30.75% for MTN Kumasi East, 4.03% for GLO Accra, 592.32% for MTN River State and 7.20% for GLO River State as shown in Appendix Z.6. However, it is important to note that the telecom engineers were probably unaware of or disinterested in any techniques, which would achieve a global minimum and thus masting by hexagonal tessellation model is probably the more appropriate measure.

CHAPTER 6

CONCLUSIONS AND RECOMMENDATIONS

This thesis recognized network analysis techniques to the design of GSM coverage in wireless telecommunication problem in an effort to develop straight forward analytical tools for mobile network industry or cell planners. Varied and newly developed network design concepts, theorems, propositions, applications are presented in the actual work. Included are the techniques for solving the disks covering problem in GSM network design environment. A case study of MTN -

Kumasi East (Ghana) and River State (Nigeria), GLO – South Eastern Accra (Ghana) and River State (Nigeria), was used to exemplify the proposed covering design. Specific and significant contributions in each of the above fields are discussed in the sections that follows.

6.1 SIGNIFICANT FINDINGS IN THIS RESEARCH

The findings in this study provide a formula $\frac{nR_1^2}{2} sin\left(\frac{2\pi}{n}\right)$, for computing the area of a regular polygon inscribed in a disk. This was proved analytically to be strictly increasing with respect to the number n of sides of the regular polygon. Geometry of tessellable regular polygon, of side length R_1, resulted in hexagonal area $\frac{3\sqrt{3}}{2} R_1^2$, which approximate closely the area of a circle than any other tessellable regular polygon for disk covering. This occupies 82.70% of the disks (see table 4.2). We use both geometrical and analytical approaches to establish the strictly increasing property of the area of regular polygons as the number of sides n increases. The limiting area is the area of a circle. Hexagon has a

segment overlap of 5.767% compared to 18.175% for square and 29.33% for regular triangular tilling in disk covering. Hence hexagon has the least overlap area and with least material cost for disk covering. This implies that regular hexagon has the minimum width and is the best geometric object for optimal disk covering in a plane. A formulae for apothem $r_n = R_1 os\left(\frac{\pi}{n}\right)$, and least total overlap difference $d_n = 2nR_1\left[1 - cos\left(\frac{\pi}{n}\right)\right]$ for tessellable regular polygon inscribed in disks was put forward. That of the area was found to be

$$2\left[\pi - \frac{n}{2} sin\left(\frac{2\pi}{n}\right)\right] R_1^2.$$

The study also led us to a formula

$$f_{ij} = \begin{cases} 3i & , \quad for\ i = j \\ \sqrt{3(i^2 + ij + j^2)}, & for\ i \neq j \end{cases}$$

for calculating the co-channel re-use ratio and the cluster size (n) for uniform cell range and generally

$$f_{ij} = \sqrt{3(N^2 i^2 + N\aleph ij + \aleph^2 j^2)}, \qquad \text{for } \aleph \geq N$$

where $n = N^2 i^2 + N\aleph ij + \aleph^2 j^2$ for any cell range. The least overlap difference for non-uniform cell range was conjectured to be $d_{R_1,R_2} = \frac{1}{2}[(2-\sqrt{3})R_2 + (4-\sqrt{3})R_1]$ for two (2) different size hexagonal cell range and generally as $d_{R_1,R_2,\ldots,R_k} = \sum_{l=1}^{k} R_{k-l+1}\left[l - \frac{\sqrt{3}}{2}\right]$ for $R_1, R_2, \ldots R_l$ different size tessellable regular polygons for our Multiple Size Hexagonal Tessellation Model (MSHTM).

Given a circle of radius R_1, we have shown that this circle circumscribes the family of n-sided regular polygons with side length $2R_1 sin\left(\frac{\pi}{n}\right)$. The tessellable regular polygons among this family of polygons are those with $n = 3,\ 4$ and 6. Among the tessellable regular polygons the hexagon has the least overlap difference of $(2-\sqrt{3})R_1$, compared to $(2-\sqrt{2})R_1$ for a square and R_1 for regular triangle. This is known to be 13.4% as compared to 29.3% for a square and 50% for a regular triangle of the total diameter of the circle. The area of the circle occupied by the hexagon is $\frac{3\sqrt{3}}{2}R_1^2$, which is approximately 82.70% of the area of the disks. The square and regular triangle occupy approximately 63.7% and 41.3% respectively. These values are consistent with respect to the honeycomb conjecture

(Pappus, c.290 – c.350 CE, cited in Raposo, 2011) that the hexagon is the most efficient way to tessellate the plane in terms of the total perimeter per area coverage. Overlap area for uniform cell range expressed as a function of the overlap difference was determined to be

$$A_n = \left(\frac{d_n}{4n}\right)^2 cosec^4\left(\frac{\pi}{n}\right)\left[2\pi - nsin\left(\frac{2\pi}{n}\right)\right],$$

for all regular polygons. This practically informs telecom engineers ahead of time the cost to be incurred when making the choice of overlap area and type of tessellable regular polygon in GSM network design.

The findings in this thesis proved that for a cluster of n regular tessellable Hexagons, the number of overlaps is given by

$$N_n = \frac{1}{2}E_e + E_i = 3n$$

This simplifies computation in field work as cumbersome counting is avoided. Finally, the ideas were experimented on two different cellular network namely MTN and GLO in two different regions (state) of Ghana and Nigeria each. The hexagonal tessellation model for GSM network design for both uniform and non-uniform cell ranges was known to be economically feasible in terms of monetary cost and habitat destruction.

6.2 STRENGTHS AND WEAKNESS

The novelty of this thesis lies in the way comprehensive theory has been established for practical design of GSM network of masts. A unique feature in this thesis is the masting conjecture and the development and extension of cochannel re-use with cluster size for hexagons of different dimensions. It also focuses in the way ideas in the theory of network optimization has been made tractable in solving pragmatic GSM network design problem. Theorems, conjectures, lemma's etc that support the hexagonal tiled design in field work has illuminated and merge both mathematics and related discipline including

Civil, Geodetic and Telecom engineering. In fact, confirming Carl Friedrich Gauss 18th century quotes: "Mathematics is the Queen of the Sciences" (Boyer, 2012) and Lobachevsky's 19th century quotes: " There is no branch of mathematics, however abstract which may not in someday be applicable to the phenomena of the real world (O'Connor et al., 1997).

Secondly, the ideas presented here will form a basis for further research in grid pattern design for planting of crops for effective sprinkler watering, erecting of sirens in a continuous space for maximum covering.

In light of the strength cast by this thesis, it has but few weakness that the author deem important to spell out for potential future research. First the inability to obtain data for VODAFON and AIRTEL Ghana to widen up the research pose a problem. Secondly, the inability to obtain GPS of GSM masts for the whole country (Ghana and Nigeria) on a large scale project was also a great challenge.

6.3 FURTHER RESEARCH

Generally, it is evident that more research needs to be done to determine rational values for environmental damage caused by GSM masts layout. Besides, future research must determine the effects of common environmental concerns in the industry including electromagnetic radiation and destruction of various ecosystems such as forest and mountainous regions. The most useful area of suggested further research relates to the application of hexagonal tessellation to disks covering is design pattern in planting for effective watering of crops using sprinkler and erecting of sirens for maximum covering. Future research should aim to;

- Develop a software package for the models proposed in this thesis to make the results accessible for practitioners.
- Extend the results to the cases where multiple monopole antennas are used so as to produce a signal that is non-circular in motion. For example, two dipoles (or monopoles) antenna at a distance of one quarter wavelength and feed them 90^0 out of phase (Munk, 1979). Here the disks used in this work could be replaced by cardioid's. Similar modelling can be done for other special plane curves like Hypocycloids with cusps, lemniscate, cycloid, limacon of Pascal, n –leaved rose among others.
- Develop a software package as in (FUN, MATLAB,OPNET ITGURU, ATOLL etc) and include the extended models.

Drawing from the previous section, the ideas presented here aims at forming the basis for potential future research in network of design of GSM. In view of this, the author seeks a critical examination of the ideas presented herein.

6.4 SUMMARY AND RECOMMENDATIONS

We found that GSM cell site planning requires a lot of geometric and algebraic calculations that aid in planning and analyzing of wireless networks. For instance the overlap difference $2(R_1 - r_1)$ for uniform cell range in GSM design network and $R - r + 2R_1 - r_1$ is that of non-uniform cell range where $R_1 > r_1$ and

$R > r$. This results in uniform cell design having wider coverage area with fewer masts than non-uniform cell design. We used geometry to establish a formula for the co-channel re-use ratio and the cluster size which is systematic and transparent as compared to the arbitrary selection of frequency in telecommunication network design. This mathematical ideas will aid in time and resource efficiency in GSM network design.

Calculation of amount of overlapping coverage area is important in cellular system as the total amount of signal interference depends on the overlapping coverage area, spectral congestion (Ghassemlooy, 2014) and wrong assignment of frequency's. This amount of overlap plays an important role in making the decision of handover. The current practice of erecting GSM masts may lead to a high level of hard handover or uneconomical amount of soft handover. The cases of MTN Ghana, Kumasi, MTN Nigeria, River State, GLO Ghana, Accra and GLO Nigeria, River State are typical examples where our proposed hexagonal r_1 design model outperforms the current practice of GSM network design. A closed form formula $(2-\sqrt{3})R_1$ for optimal overlap difference of hexagonal coverage is presented in this thesis and the calculation of minimum overlapping coverage area $\frac{3\sqrt{3}}{2}R_1^2$ as compared to that of a square or equi-triangular tile. The study also shows that in a disk of radius R_1 and hexagonal apothem we can inscribe a regular polygon of dimension $2R_1 sin\left(\frac{\pi}{n}\right)$. This formulae helps geometrically in least time complexity for inscribing a regular polygon in a disk. Overlap difference formulae for hexagons of different dimensions is conjectured for optimal cell planning. An application of the hexagonal tessellation model reduces from 50 MTN Ghana masts at Kumasi east to 35, 50 GLO Ghana masts at Accra East to 44, 50 MTN Nigeria masts at River State to 36 and 45 GLO Nigeria masts to 38 at River State.

Geometric disk covering which is an important study in computational geometry, geometric topology (rubber sheet geometry) as well as optimization of telecommunication network design can best be achieved in least time complexity using Hexagonal Tessellation Model. Therefore Mathematicians, Computer Scientists as well as Telecommunication engineers should not lose sight of this important findings when covering with disks.

REFERENCES

Aloupis G. and Hearn R.A. (2012). Covering Points with Disjoint Unit Disks. In Proceedings of the 24th Canadian Conference on Computational Geometry, Charlottetown.

Alt. H. and Arkin .E. (2011). How to Water Carrots: Geometric Coverage Problems in Points Sets. Institute of Computer Science, Freie Universit¨ at Berlin, D14195 Berlin, Germany.

Arora .S, Raghavan P. and Rao S. (1998). Approximation Schemes for Euclidean k-Medians and related Problems. In STOC ’98: Proc. of the 30th Annual ACM Symp. Theory Comput.,pp. 106–113.

Azad R. I. M. (2012). Multiple Antenna Technique (MIMO). Bachelor’s Thesis Thesis, Helsinki Metropolia University of Applied Sciences.

Bai X, C. Zhang, D. Xuan, J. Teng, and W. Jia (2009). Low-connectivity and Fullcoverage Three Dimensional Wireless Sensor Networks. In Proc. Of ACM MobiHoc.

Bai X., S. Kumar, D. Xuan, Z. Yun, and T. Lai (2006). Deploying Wireless Sensors to Achieve Both Coverage and Connectivity. In Proc. of ACM MobiHoc.

Balachandran K. and R. Ejzak, E.A. (1999). GPRS-136: High-Rate Packet Data Service for North American TDMA Digital Cellular Systems. IEEE Personal

Balanis C. A, Panayiotis I. and Ioannides (2007). Introduction to Smart Antennas. United States, Morgan & Claypool Publishers.

Baltzis, K. B. (2008). A Geometrical-based Model for Co-channel Interference Analysis and Capacity Estimation of CDMA Cellular Systems. EURASIP Journal on Wireless Communications and Networking, pp. 1-7, doi:10.1155/2008/791374.

Baltzis, K. B. (2010a). Analytical and Closed-form Expressions for The Distribution of Path loss in Hexagonal cellular Networks. Wireless Personal Communications, pp. 1-12, doi:10.1007/s11277-010-9962-2

Baltzis, K. B. (2010b). Closed-form description of microwave signal attenuation in cellular systems. Radio Engineering, Vol. 19, no. 1, Apr. 2010, 11-16.

Baltzis K. B (2011). Hexagonal vs Circular Cell Shape: A Comparative Analysis and Evaluation of the Two Popular Modeling Approximations, Cellular Networks - Positioning, Performance Analysis, Reliability, Dr. Agassi Melikov (Ed.), ISBN: 978-953- 307-246-3, InTech. Available from: http://www.intechopen.com/books/cellular-networks-positioning-performanceanalysis-reliability/hexagonal-vscircular-cell-shape-a-comparative-analysis-andevaluation-of-the-two-popular-modeling-a.

Bambah R. P. and Rogers C. A. (1952). Covering the plane with convex sets. J. London Math. Soc, 27:304–314.

Bharucha, Z. and Haas, H. (2008). The distribution of path losses for uniformly distributed nodes in a circle. Research Letters in Communications, Vol. 2008, 4 pages, doi:10.1155/2008/376895.

Boroczky K. (2005). Finite coverings in the hyperbolic plane. Discrete & Computational Geometry, 33:165–180.

Boyer C. B. and Merzbach U. C. (2012). History of Mathematics. John Wiley and

Sons. 3rd ed. Pp.496.

Brasche G. and Bernard Walke B. (1997). Concepts, Services, and Protocols of the New GSM Phase 2+ General Packet Radio Service. IEEE Communications Magazine, pp. 94-104.

Brewer, C. A. (1996). Prediction of simultaneous contrast between map colors with Hunt's model of color appearance. Color Research and Application, 21(3), 221235.

Capacity and Efficiency. (2009). IEEE Transactions on Communications, Vol. 48, no. 4, pp. 658-669.

Carbrera D. A., Cione L. A, Cozzuol . M. A. (2012). Tridimensional Angel Shark Jaw Elements (Elasmobranchii, Squatinidae) From the Miocene of Southern Argentina, Vol.49(1), ISSN 0002-7014, pp 126.

Carr, D. B., Olsen, A. R., & White, D. (1992). Hexagon mosaic maps for display of univariate and bivariate geographical data. Cartography and Geographic Information Science, 19(4), 228-236.

Chan T. M (2005). Output- Sensitive Construction of Convex Hull. Ph.D Thesis in Computer Science, University of British Columbia, USA.

Chidume C.E. (1989). Functional Analysis, An Introduction to Metric Space. Department of Mathematics, University of Nigeria, Nsuka.Pp.135

Cho H.-S.; Kwon, J. K. & Sung D. K. (2000). High reuse efficiency of radio resources in urban microcellular systems. IEEE Transactions on Vehicular Technology, Vol. 49, no. 5, Sep. 2000, 1669-1667.

Christaller, W. (1933). Die zentralen Orte in Suddeutschland. Jena: Gustav Fischer.

Corney .J, Rea .H, Clark .D, Pritchard .J, Breaks .M, and MacLeod . R (2002). Coarse filters for shape matching," Computer Graphics and Applications, IEEE, vol. 22, pp. 65-74.

Culberson J. C. and Reckhow R .C. (1994). Covering Polygon is Hard, Journal of Algorithms, Vol.17, pp. 2- 44.

Darweesh T. H. (1999). Capacity and Performance Analysis of A Multi-User, Mixed Traffic GSM Network, Masters Thesis, University of Calgary, Canada, pp 10-11

Ding R. (2010). On Counting Problems in Archimedean Tiling's- A Survey. Bernoulli Conference on Discrete and Computational Geometry. Hebei Normal University, pp. 7.Document Nr: LZTB 151 002 r1A.

Drane C., Macnaughtan M., Scott C. (1998). Positioning GSM Telephones. IEEE Communication Magazine, 0163-6804, pp. 49.

Fan G. and Zhang J. (2004). A Novel Geometric Diagram and Its Applications in Wireless Networks. IEEE INFOCOMM, pp. 2 ISSN. 0-7803-8356-7/04.

Furuskär A. et. al (1998). System Performance of the EDGE Concept for Enhanced Data Rates in GSM and TDMA/136., Proceedings of IEEE VTC'

Garey M.L and Johnson D.S (1979). Computers and Intractability: A Guide to the Theory of NP-Completeness. San Francisco: W. H. Freeman.

Ghassemlooy (2014). Lecture Notes on Mobile communication Systems. Retrieved from URL: http://soe.northumbria.ac.uk/ocr/

Goldsmith A. (2005). Wireless Communications, Cambridge University Press, New York.

Graham, M. D. (1990). Comparison of Three Hexagonal Tessellations through Extraction of Blood Cell Geometric Features. Analytical and Quantitative Cytology and Histology, 12(1), 56-72.

Griffin, A. L., MacEachren, A. M., Hardisty, F., Steiner, E., & Li, B. (2006). A Comparison of Animated Maps with Static Small-Multiple Maps for Visually

Identifying Space-Time Clusters. Annals of the Association of American Geographers, *96*(4), 740-753.

Grunbaum B. and. Shepard G.S (1986). Tiling and Patterns, Freeman, New-York.

Hales, T. C. (2001). The Honeycomb Conjecture. Discrete and Computational

Hagger J. W, Fry, L. L, Jacks, S. S, Hill, D. R (1996).Datums, Ellipsoids, Grids and Grid Reference Systems. DMA Technical Manual 8358.1, USA

H˙m˙l˙inen .J. (2008).Cellular Network Planning and Optimization, Part V: GSM. Helsinki University of Technology, Communication and Network Department TKK, 18.1, pp. 4.

Haenggi M , Andrews J. G, Baccelli F, Dousse O, Franceschetti M. (2009). Stochastic Geometry and Random Graphs for the Analysis and Design of Wireless Networks. IEEE Journal on Selected Areas in Communications 27 (7), 1029-1046.

Hochbaum D and Maass W. (1985). Approximation schemes for covering and packing problems in image processing and VLSI. Journal of the ACM, 32(1):130– 136.

Hu N. (2013). Approximation Algorithms for Geometric Covering problems for disks and Squares. Masters Thesis, University of Waterloo, Ontario, Canada.

Igarashi Y. and Suzuki H. (2011). Cover geometry design using multiple convex hulls," Computer_Aided Design, vol. 43, pp. 1154_1162.

Inaba N. (2008). http //inabapuzzle com/hirameki/suuri_ans4 html.

Ioachim A. and Toacsan M. I. (2001). Microwave Characteristics of BaO-PbONd_2O_3-TiO_2 Dielectric Resonators. Proceedings of the 16_{th} Hertzian Optics and Dielectrics Biennial Colloquium, OHD 2001, Le Mans, France, pp. 133-136.

Jraifi A., Laamara R. A., Belhaj A., and Saidi E. H. (2010). A proposal solution for interference inter-operators, Progress In Electromagnetics Research C, Vol. 12 Issue 15.

Keating K and King J. (1999), Signed Tiling's with Squares, Journal of Combinatorial Theory - Series A, Vol.85, No.1, pp. 83-91.

Kershner R. (1939). The number of circles covering a set. American Journal of Mathematics, 61:665–671.

Kidd R. (2005). NWP Discrete Global Grid Systems. ASCAT, Soil Moisture Report Series, No. 4, Institute of Photogrammetry and Remote Sensing, Vienna University of Technology, Austria.

Lawler E. L, Lenstra J. K., Rinnooy K., Shmoys D. B. (1985). The traveling salesman problem", John Wiley.

Lessard D. (2000). Optimal Polygon Placement on a Grid. Masters Thesis, Ottawa-Carleton Institute for Computer Science, Carleton University, Canada, pp. 17.

Li Z. L. H. X. W. (2002). Convex Hull Based Point Pattern Matching under Perspective Transformation.

Mee C. (2010). International AS/A level Physics, Hodder Education, pp 425-426.

Melissen J. and Schuur P. (1996). Improved coverings of a square with six and eight equal circles. Electronic Journal of Combinatorics, Vol.3, Issue 1.

Miller M. J. , Vucetic B. and Berry L (1993). Satellite Communications – Mobile and Fixed Services. Kluwer Academic, Boston.

Mishra .A. R (2004). Second-Generation Network Planning and Optimization. Pp. 26. John Wiley & Sons, Ltd. ISBN: 0-470-86267-X.

Munk .B. A and Larson C. J (1979). A Cavity-Type Broadband Antenna with a Steerable Cardioid Pattern. Ohio State University, ElectrioScience Laboratory, Department of Electrical Engineering.

Nurmela K and P. Ostergard (2000). Covering a square with up to 30 equal circles. Research Report A62, Laboratory for Theoretical Computer Science, Helsinki University of Technology.

O' Connor, J. and Robertson, E. (1997). The Mac Tutor History of Mathematics. University of St Andrews- School of Mathematical and Computational Sciences: St Andrews, GB, Vol. 3.,No.17. Retrieved from URL: wwwhistory.mcs.stand.ac.uk/Quotations/Lobachevsky.html.December, 2013.

Okayama Y., Kiyomi M., and Uehara R. (2011). On Covering of any point configuration by disjoint unit disks. In Proceedings of the 23rd Canadian Conference on Computational Geometry, pp 393-397.

Osbrone P. (2013). The Normal and The Transverse Mercator's Projections on the Sphere and the Ellipsoid with full Derivations of all Formulae. Edinburgh, UK.

Paredes R.., Aragon .J. L and Barrio .A. (1998). Non periodic Hexagonal Square-Triangle Tiling's, Physical Review B, Vol.58, No.18, pp. 11990-11995.

Pirinen P. (2006). Cellular topology and outage evaluation for DS-UWB system with correlated lognormal multipath fading, Proceedings of IEEE 17th International Symposium on Personal, Indoor and Mobile Radio Communications (PIMRC'06), pp. 1-5, Helsinki, Sep. 2006, doi:10.1109/PIMRC.2006.254343.

Peng R. C., Wang J.Y., Tian Z., Guo L. X, and Chen Z. P. (2005).A Research for Selecting Baseline Point of the Territorial Sea Based on Technique of the Convex

Hull Construction. Cehui Xuebao / Acta

Raisanen L. (2005). Multi-objective site selection and analysis for GSM cellular network planning, Ph.D Thesis, Cardiff University, Department of Computer Science, Wales, pp. 1.

Rappaport T. S. (2005). Wireless Communications: Principles and Practice, (2nd Ed.), Prentice Hall.

Raposo P. (2011). Scale-Specific Automated map Line Simplification by Vertex Clustering on A Hexagonal Tessellation, pp.37.

Reid J. B. (2005). The carrot calculator: a decision support tool for carrot crop management. Acta Hort. (ISHS) 670:131- 136. http: // www. actahort. Org /books/670/67014.htm

Richard C., Hoffe. M., Hermisson. J. and Baake M . (1998). Random Tilings: Concepts and Examples, Journal of Physics A, Mathematical and General, Vol.31, No.30, pp. 6385-6408.

Saunders S. R. (1999). Antennas and Propagation for Wireless Communication systems. Great Britain. John Wiley & Sons Ltd.

Shankar S. R & Kalivarathan G. (2013). Feasibility Studies of Wireless Sensor Networks and its Implication. International Journal of Electrical Engineering & Technology (IJEET), ISSN 0976-6553, Volume 4, Issue 2, pp. 105-111

Sperduto E. (2009). Combinatorial Structures For Communication Networks. Ph.D Thesis, Department of Informatics & Automation, Roma Tre University, Bulgaria.

Stavroulakis P. (2003). Interference Analysis and Reduction for Wireless Systems, Artech House, Inc., Norwood.

Stojmenovic I. (1997). "Honeycomb Networks: Topological Properties and Communication Algorithms," IEEE Transactions on Parallel and Distributed Systems, vol. 8, no. 10, pp. 1036-1042.

Toth G. (1987).Finite coverings by translates of centrally symmetric convex domains. Discrete Computer Geometry, 2:353–363.

Wang X, Liu .J and Zhuang .D (2003). "Application of convex hull in identifying the types of urban land expansion," ACTA GEOGRAPHICA SINICA - CHINESE EDITION-, vol. 58, pp. 885-892.

Wikepedia (2013). Circle Packing. Retrieved from URL: http://en.wikipedia.org/wiki/Circle_packing. World

Time Zone (2014). Retrieved from URL:http://www.worldtimezone.com/gsm.html

Wen C. and Guo T. (2009). An Efficient Algorithm for Fingerprint Matching Based on Convex Hulls in Computational Intelligence and Natural Computing. CINC'09. International Conference , pp. 66-69.

Xu X. and Whang Z. (2011). Wireless Coverage Via Dynamic Programming. Illinois Institute of Technology, Chicago, USA. WASA , LNCS 6843, pp. 108 – 118.

Yang S., F. Dai, M. Cardei, and J. Wu (2006). On Connected Multiple Point Coverage in WirelessSensor Networks. Journal of Wireless Information Networks.

Yang Z. and Cohen F.S (1999). Image Registration and Object Recognition using Affine Invariants and Convex Hulls. Image Processing, IEEE Transactions on, vol. 8, pp. 934-946, 1999.

Yu Z., J. Teng, X. Bai, D. Xuan, and W. Jia (2013). On Wireless Nnetwork Coverage in in Bounded Areas. In INFOCOM, Proc. of IEEE, pp. 1195 1203.

APPENDIX A

EXACT VALUE OF Cos 72^0

In figure 4.17 we want to find a relationship between the side H of a nontessellable regular polygon-pentagon and it radius. The cosine rule was used to compute the length of the side and we obtain the relationship $\sqrt{2R^2\left[1 - cos\left(\frac{2\pi}{5}\right)\right]}$. The exact value of $cos\left(\frac{2\pi}{5}\right)$ can be calculated. Consider the $36^0 - 72^0 - 72^0$ isosceles triangle in figure $A.1$

$ABD.$

x

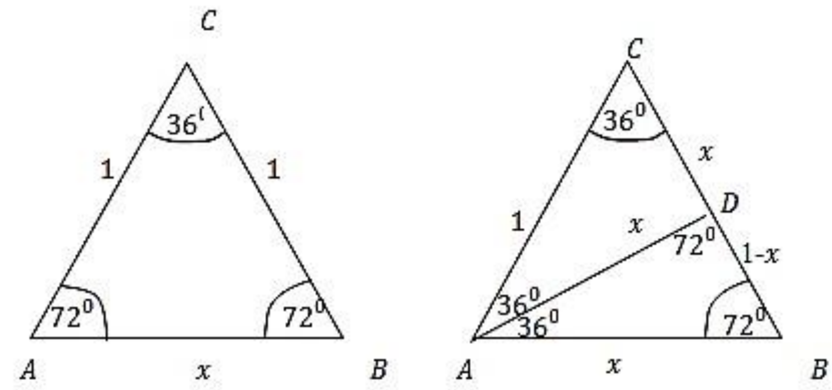

(a) Actual $36^0 - 72^0 - 72^0$ triangle (b) bisected $36^0 - 72^0 - 72^0$ triangle

Figure A.1: The $36^0 - 72^0 - 72^0$ isosceles triangle.

Let the side length $|AB| = x$, $|AC| = 1$ and $|BC| = 1$. We now bisect $\angle CAB$ to obtain $\angle CAD = 36^0$ and $\angle DAB = 36^0$. Triangle ABC is similar to triangle

Therefore,

Ratio: $k = \frac{CA}{AB} = \frac{AB}{BD} = \frac{BC}{DA}$ where k is a scalar multiplier.

$$\frac{1}{x} = \frac{x}{1-x} = \frac{1}{x}$$

$$x^2 = 1 - x$$

$x^2 + x - 1 = 0$ which is a quadratic equation in.

$$x = \frac{-1 \pm \sqrt{1^2 - 4(1)(-1)}}{2(1)}$$

$x_1 = \frac{-1+\sqrt{5}}{2}$ and

x_1 is unreasonable and therefore discarded as the side of a triangle is nonnegative.

Hence the only possible value is .

Using the cosine rule in ΔABD:

$$|AB|^2 = |AD|^2 + |BD|^2 - 2|AD||BD|cos72^0$$

$$x^2 = x^2 + (1-x)^2 - 2(x)(1-x)cos72^0$$

$$cos72^0 = \frac{(1-x)^2}{2x(1-x)}$$

$$cos72^0 = \frac{1-x}{2x}$$

$$= \frac{1-x}{x} \times \frac{1}{2}$$

But $\frac{1}{x} = \frac{x}{1-x}$

$$= \frac{x}{1} \times \frac{1}{2}$$

$$= \frac{-1+\sqrt{5}}{2} \times \frac{1}{2}$$

$$\therefore \quad cos72^0 = \frac{\sqrt{5}-1}{4}.$$

The proof is complete.

APPENDIX B

EXACT VALUE OF Sin 36^0

In figure 4.64 we were challenged with computing the sine of 36^0 for five sector site decagon in area fractal leaving our answer in surd form. Consider triangle ABD in Figure A.1(b) in Appendix A and using the sine rule:

$$\frac{\sin 36^0}{1-x} = \frac{sin72^0}{x}$$

$$sin36^0 = \frac{1-x}{x} \times sin72^0$$

But from similar triangles we know that

$\frac{1}{x} = \frac{x}{1-x} = \frac{1}{x}$ with $\frac{\sqrt{\ }}{\ }$ Which

implies that $sin36^0 = \frac{x}{1} \times sin72^0$

$$= \frac{\sqrt{5}-1}{2} \times \sqrt{(1-(cos72^0)^2)}$$

$$= \frac{\sqrt{5}-1}{2} \times \sqrt{1-\left[\frac{\sqrt{5}-1}{4}\right]^2}$$

$$= \frac{\sqrt{5}-1}{2} \times \frac{\sqrt{5+\sqrt{5}}}{2\sqrt{2}}$$

$$= \frac{\sqrt{(\sqrt{5}-1)^2 \times (5+\sqrt{5})}}{4\sqrt{2}}$$

$$= \frac{1}{4}\sqrt{\frac{(6-2\sqrt{5})(5+\sqrt{5})}{2}}$$

$$-\sqrt{\quad \sqrt{\ }}.$$

APPENDIX C

MATLAB CODE FOR GRAPHING $E = K_nR$

```
>> %The first line is a triangle
>> x_1=[1,2,3];
>> y_1=[3.464,5.196,6.928];
>> y_2=[2.828,4.243,5.657];
>> y_3=[2.351,3.527,4.702]; >>
y_4=[2,3,4];
>> y_5=[1.736,2.603,3.472];
>> subplot(1,5,1);
>> plot(x_1,y_1);
>> grid on
```

```
>> xlabel('R(km)');
>> ylabel('H(km)');
>> title('Triangle');
>>%The second line is a Square
>> subplot(1,5,2);
>> plot(x_1,y_2);
>> grid on
>> xlabel('R(km)');
>> ylabel('H(km)');
>> title('Square');
>> %The third line is a Pentagon
>> subplot(1,5,3);
>> plot(x_1,y_3);
>> grid on
>> xlabel('R(km)');
>> ylabel('H(km)');
>> title('Pentagon');
>> %The fourth line is a Hexagon
>> subplot(1,5,4);
>> plot(x_1,y_4);
>> grid on
>> xlabel('R(km)');
>> ylabel('H(km)');
>> title('Hexagon');
>> %The fifth line is a heptagon
>> subplot(1,5,5);
>> plot(x_1,y_5);
>> grid on
>> xlabel('R(km)');
>> ylabel('H(km)');
>> title('Heptagon');
```

APPENDIX D GSM SPECIFICATIONS FOR URBAN AND RURAL AREAS

Table D.1 shows the BTS for MTN and GLO (Ghana and Nigeria) with their prices and specification. Since our model was for outdoor we only considered the outdoor equipment's for Huawei brand. The commonly used sectorization for both urban and rural areas is also indicated in Table D.2

Table D.1 Price list of two brands of Huawei BTS from April- August 2013/ 2014

Date	HS Code	Description (Package)	Unit	Per Unit (USD)
19/04/14 (Huawei)	85238020	DBS3900 Outdoor S111 128 CE45 Codes 20W Carrier SW Node B (H3BTS0124) (IT SW IN CD Form)(Non SDH),1CD Containing 10NOS S/W	NOS	2,027.318
30/03/13 (Huawei)	85238020	BT 292035, Huawei BTS / DBS3900 / 3900A-SW Expansion S222 to S444, MRFU 1800MHZ (Inv.0003651313020I001) (Software on CD) (Captive consumption for Cellular telephone network)	NOS	2,344.283

Table D.2: GSM specifications for urban and rural design.

Locations	Urban (Southern sector)	Rural (Northern sector)
Height from base	15m-36m	25m-56m
Cell Range (dBi antennas)	1.5km, 4km,6km	6km, 10km, 15km
	0.4, 0.6, 0.8, 0.9km	1.5km
Sectorization (Angle)	$60^0, 120^0, 180^0, 240^0, 300^0, 360^0$	$120^0, 240^0, 360^0$
	$90^0, 180^0, 270^0, 360^0$	$180^0, 360^0$
	_	$30^0, 150^0, 270^0, 360^0$

Source: ATC, Helios and Eaton Ghana (April. – Aug., 2014)

APPENDIX F

CONVERSION OF THE GRID COORDINATES TO WGS-84

The local geographic coordinates in degree decimal coordinates provided in Table J.1 of Appendix J.1, Table N.1 of Appendix N.1, Table R.1 of Appendix R.1 and

Table V.1 of Appendix J.1 by ATC (Ghana and Nigeria) was converted using FUGRO using the geodetic parameters. Illustrative example of the geodetic parameters for conversion for West Africa is shown in Figure F.1

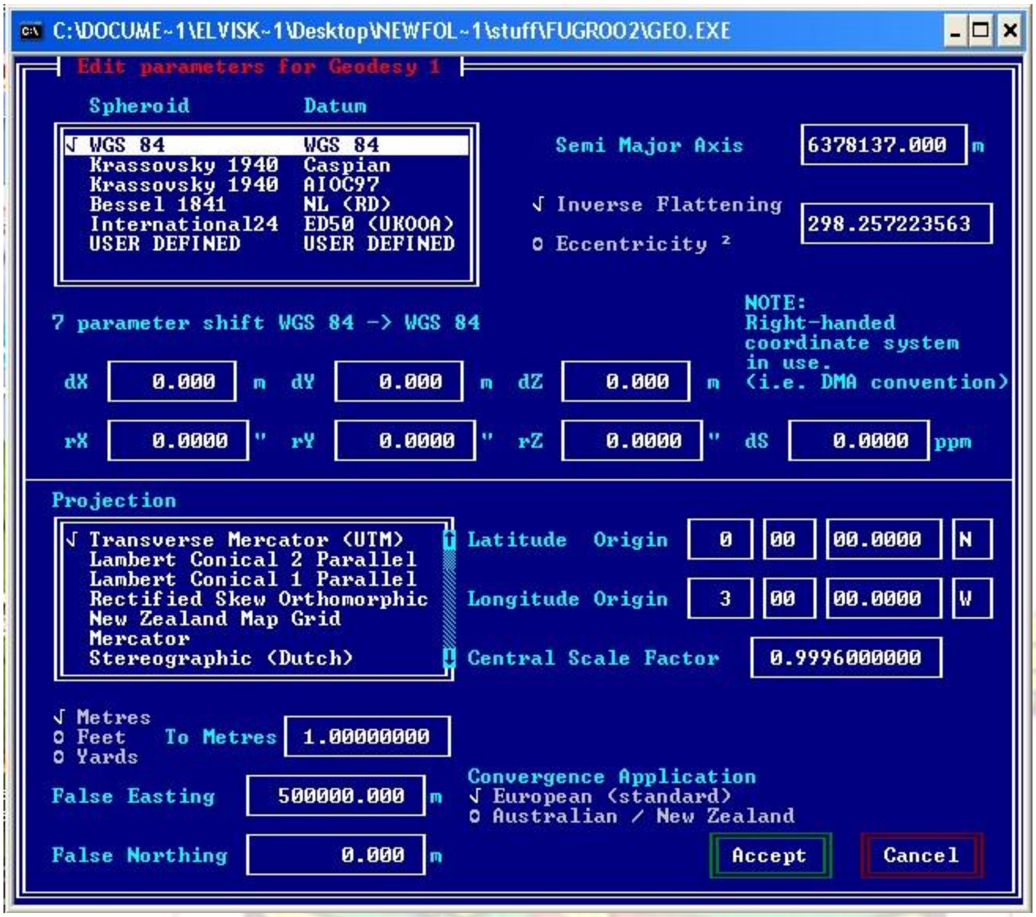

Figure F.1: West Africa Parameter's for conversion between coordinates systems

Sample coordinate conversion using KNUST, Kumasi East Ghana from geographical to UTM is illustrated in Figure F.2

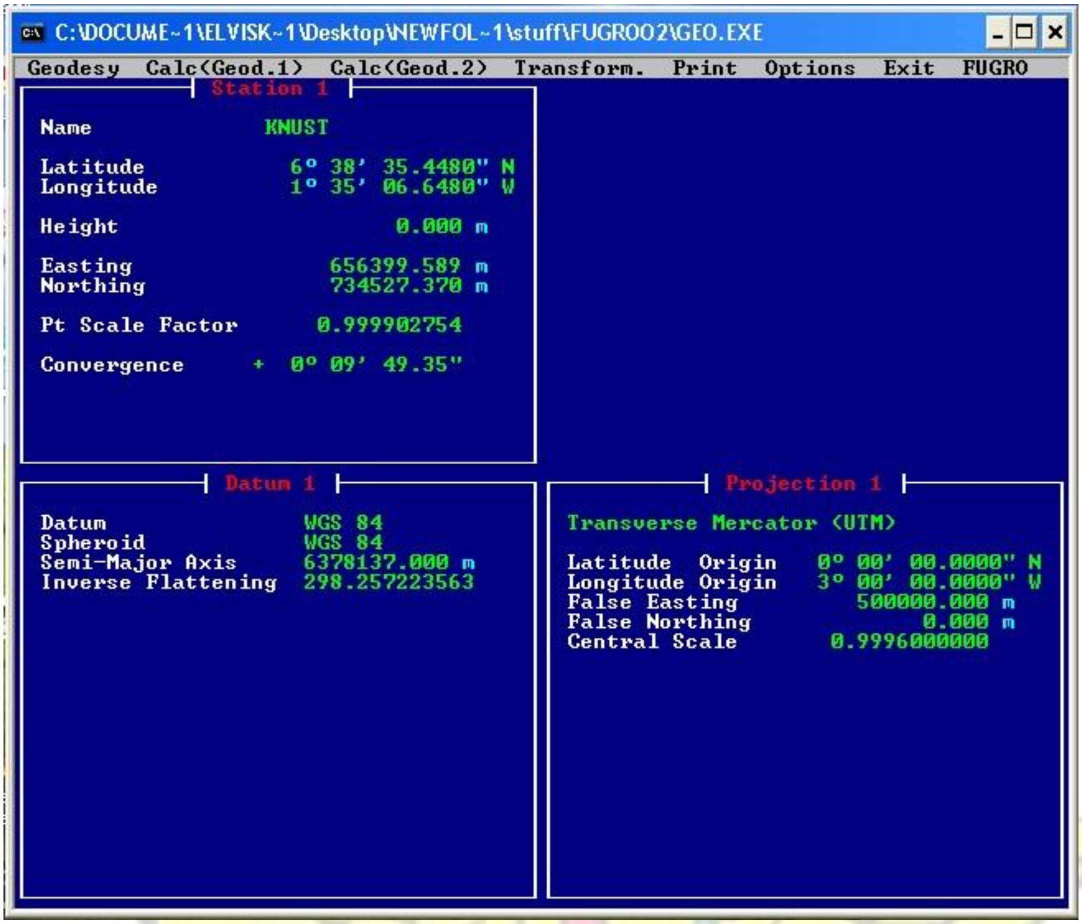

Figure F.2: Sample coordinate conversion of KNUST GSM masts, Ghana.

APPENDIX G GSM BANDS FOR WEST AFRICAN COUNTRIES

Table G.1 shows the GSM bands used in West African countries.

Table G.1: GSM bands used in some African countries.

Country	900MHz	1800MHz	3G	4G (live LTE WiMA HSPA+, test, license)
GHANA	900	1800	3G 900 / 2100 Scancom;	4G LTE Surfline 2600Mhz;
NIGERIA	900	1800	3G 2100 AirtelNG; 3G 2100 Glo Mobile; 3G 2100 Etisalat; 3G 2100 MTN;	4G LTE Smile 800Mhz; 4G LTE Spectranet 2300Mhz;
IVORY COAST	900	1800	-	-
TOGO	900	-	3G 2100 Togocel Togo;	-
BENIN	900	1800	3G 2100 Moov Benin; 3G 2100 MTN;	-
BURKINA FASO	900	-	-	-
MALI	900		3G 2100 Orange;	-
GAMBIA	900	1800	3G 2100 QCell	4G WiMAX Airspan, 4G WiMAX Alvarion
GUINNEA	900	1800	3G 2100 Cellcom;	900
Guinea-Bissau	900	1800	-	-
LIBERIA	900	1800	3G 2100 Cellcom; 3G 2100 Novafone;	4G Cellcom, HSPA+
SENEGAL	900	1800	3G 2100 Expresso Senegal; 3G 2100 Tigo; 3G 2100 Orange;	-
SIERRA LEONE	900	1800	3G 2100 SMART; 3G 900 Africell; 3G 900 Airtel;	-
CAMEROON	900	1800	-	4G Africa /Alvarion
NIGER	900	1800	-	-
MAURITANIA	900	1800	3G 2100 Chinguitel; 3G 2100 MATTEL; 3G 2100 Mauritel;	-
GABON	900	1800	-	-
ALGERIA	900	1800	3G 2100 Mobilis; 3G 2100 Ooridoo; 3G 2100 Djezzy;	4G LTE Algerie , Telecom

,

Source: http://www.worldtimezone.com/gsm.html

APPENDIX H COMPONENTS OF GSM TOWER AND THEIR COSTS

Table H.1 shows a range of cost price of components of GSM cell tower for 6dBi/8dBi antennas for 1.5km -6km cell range.

Table H.1: Components of GSM tower and their costs

Components (Huawei Brand)		Costs ($)
1.Civil Works (Installations)	- Standard building materials, - The mast and its erection, - Backup generators, - Fencing, - Tiny air-conditioned shack, - Security systems (Personnel). - Base Transmitters Station (BTS) - Land Acquisition / Roof tops etc	$85,000 – $105,000
2.Telecommunications Guts	- Base band processors, - Transceivers, - Power supplies, amplifiers, etc	$40,000.00
	- Installation	$12,000.00
3. Electrical Works (Installations)	- Connecting Tower to core networks	$5000.00
Total (1+2+3)		$142,000 -$162, 000
4.Operational costs (On going monthly costs) - Variable Costs	- Repair and maintenance, - Diesel fuel for back-up generators - etc	$ 29,000.00
Total (1+2+3+4)		$171,000-$191,000.

Source: ATC (Ghana, April- Aug.,2014)

APPENDIX I

CELL TOWER COSTS FOR RANGE OF GSM MASTS

The price lists of GSM masts with full equipment's provided by ATC, Helios and EATON Ghana and Nigeria with estimated price for the month of April to August, 2014 is shown in Table I.1

Table I.1: Cell Tower costs for various GSM cell range.

Cell Tower Costs Huawei Brand (GSM 900Mhz)		Differences in costs for cell range	Full Cost of GSM Masts (HUAWEI-DXX-824-960/1710 - 2170-65/65-17.5/18dBi-M/M)	Cost of GSM Antenna (No BTS-)
0.6 km		\$000.00	\$142,000 – \$162, 000	-
0.8 km		\$712.04	\$141,287.96 – \$162,712.04	-
1.2km		\$9,369.32	\$151,369.32 – \$171,369.32	-
1.5km		\$12,934.48	\$154,934.48 – \$174,934.48	-
2.5km		\$24,050.31	\$166,050.31 – \$186,050.31	-
Estimated Price:	1.0km	-	\$146,328.64 - \$167,040.68	-
	1.6km	-	\$159,669.135 – \$178,381.175	-
	1.8km	-	\$161,709.815 – \$178,709.815	-
	3.0km	-	\$196,253.274 – \$205,447.652	-
	6.6km	-	\$223,200.540 – 238,278.230	-

Source: ATC (Ghana, April- Aug., 2014)

APPENDIX J.1

LOCAL GEOGRAPHIC COORDINATES OF MTN GSM MASTS IN KUMASI-EAST, GHANA

Table J.1 shows 50 local grid coordinates of MTN GSM masts for Kumasi-East (Ghana) in zone 30N provided by ATC (Ghana).

Table J.1: WGS-84 Geographic coordinate for MTN masts in Kumasi-East

POINT ID	SITE NAME	LATITUDE	LONGITUDE	TRIG. HEIGHT
mtnGH.1	OFORIKROM	6.68105	-1.59203	25m
mtnGH.2	ASAFO	6.68873	-1.61083	25m
mtnGH.3	MARKET 1	6.69647222	-1.62411111	25m
mtnGH.4	MARKET 3	6.69931	-1.62027	25m
mtnGH.5	ASAFO MOSQUE	6.68371	-1.61152	25m
mtnGH.6	STADIUM	6.67944	-1.60587	25m
mtnGH.7	AYIGYA	6.69706	-1.57949	25m
mtnGH.8	OFORIKROM	6.68914	-1.58572	25m
mtnGH.9	RAILWAYS	6.68393	-1.61854	25m
mtnGH.10	MARKET 4	6.69653	-1.61727	25m
mtnGH.11	ABOABO	6.69966	-1.59477	25m
mtnGH.12	KUM ACADEMY	6.71163	-1.56032	25m
mtnGH.13	SOCIAL CLUB	6.70800	-1.62652778	25m
mtnGH.14	KASSE	6.65596	-1.60800	25m
mtnGH.15	ASOKWA 2	6.68713	-1.60507	25m
mtnGH.16	ATONSU 2	6.6573	-1.59194	25m
mtnGH.17	ATONSU 1	6.649	-1.59166	25m
mtnGH.18	GYINYASI	6.66247	-1.56939	25m
mtnGH.19	AYIDUASI	6.67523	-1.56376	25m
mtnGH.20	KNUST	6.68488	-1.5763	25m
mtnGH.21	EMENA	6.67077	-1.54285	25m
mtnGH.22	ATONSU 3	6.64318	-1.58518	25m
mtnGH.23	KASSE 2	6.64813	-1.60967	25m
mtnGH.24	GYINYASI 2	6.65709	-1.58149	25m

mtnGH.25	AHINSAN 2	6.66312	-1.60012	25m
mtnGH.26	KENTINKRONO	6.69907	-1.55726	25m
mtnGH.27	KENTINKRONO 2	6.69208333	-1.55966667	25m
mtnGH.28	AMAKOM	6.68238	-1.59926	25m
mtnGH.29	ANLOGA	6.67706	-1.5922	25m
mtnGH.30	OLD AHINSAN	6.67552	-1.58845	25m
mtnGH.31	OFORIKROM 3	6.68799	-1.59253	25m
mtnGH.32	AYIDUASE 2	6.67907	-1.5484	25m
mtnGH.33	KNUST 2	6.66837	-1.58469	25m
mtnGH.34	KOTEI	6.66175	-1.55644	25m
mtnGH.35	KAASE 3	6.6385	-1.60575	25m
mtnGH.36	BOMSO	6.68192	-1.58182	25m
mtnGH.37	GYINYASI 3	6.65604	-1.57262	25m
mtnGH.38	ODUOM	6.69308	-1.54204	25m
mtnGH.39	ATONSO 4	6.65433	-1.58522	25m
mtnGH.40	AYIGYA 2	6.69086	-1.57234	25m
mtnGH.41	KAASE 4	6.65485	-1.59939	25m
mtnGH.42	KNUST AYIGYA	6.6871	-1.57036	25m
mtnGH.43	ASOKORE MAMPG	6.70863889	-1.56855556	25m
mtnGH.44	KTI	6.69125	-1.60628	25m
mtnGH.45	DECABIN	6.68332	-1.58673	25m
mtnGH.46	AYEDUASE 3	6.67358	-1.55300	25m
mtnGH.47	DEDUAKO	6.65545	-1.54674	25m
mtnGH.48	ATONSU 4	6.6439	-1.59665	25m
mtnGH.49	AYIGYA 3	6.68909	-1.57865	25m
mtnGH.50	ESERESO	6.62925	-1.56134	25m

APPENDIX J.2

WGS-84 COORDINATES OF LOCAL GSM MASTS FOR MTN, KUMASI EAST, GHANA.

Table J.2 shows the 50 WGS-84 coordinates of towns in Kumasi East (Ashanti region-Ghana) for a fixed antenna height of 25m and a cell range of 0.6km.

Table J.2: WGS-84 coordinates of MTN masts of Kumasi East-Ghana

MTN Masts with Node Points (WGS-84)				
	Geographical Coordinates		Grid Coordinates (UTM)	
Location	Latitude	Longitudes	Easterns (Xm)	Northerns (Ym)
1. Oforikrom	$6^0 40' \; 51''.7800 \; N$	1 35 31.30800 W	655630.273	738712.788
2. Ayigya	6 41 19.4280 N	1 36 38.98800 W	653549.412	739556.115
3. Oforikrom_2	6 41 47.29999 N	1 37 26.80000 W	652078.734	740408.094
4. Ayiduase	6 41 57.51600 N	1 37 12.97200 W	652502.496	740723.077
5. KNUST_1	6 41 01.35600 N	1 36 41.47200 W	653474.696	739000.804
6. Ahinsan_2	6 40 45.98400 N	1 36 21.13200 W	654100.673	738530.405
7. Old Ahinsan	6 41 49.41600 N	1 34 46.16400 W	657011.548	740487.130
8. Ayiduase_2	6 41 20.90400 N	1 35 08.59200 W	656325.318	739609.364
9. KNUST_2	6 41 02.14800 N	1 37 06.74400 W	652698.529	739022.947
10. Bomso	6 41 47.50800 N	1 37 02.17200 W	652835.016	740416.607
11. Ayigya_2	6 41 58.77600 N	1 35 41.17200 W	655321.466	740769.774
12. KNUST Ayigya	6 42 41.86800 N	1 33 37.15200 W	659126.150	742104.442
13. Ayiduase_3	6 42 28.80000 N	1 37 35.50001 W	651808.000	741682.046
14. Ayigya_3	6 39 21.45600 N	1 36 28.80000 W	653872.512	735933.392
15. Oforikrom_3	6 41 13.66800 N	1 36 18.25200 W	654186.708	739380.994
16. Gyinyase	6 39 26.28000 N	1 35 30.98400 W	655647.720	736086.596
17. Gyinyase_1	6 38 56.40000 N	1 35 29.97600 W	655681.292	735168.889
18. Kaase	6 39 44.89200 N	1 34 09.80400 W	658139.257	736665.449
19. Gyinyase_2	6 40 30.82800 N	1 33 49.53600 W	658757.615	738078.245
20. Atonsu_1	6 41 05.56800 N	1 34 34.68000 W	657368.116	739141.305
21. Ayeduase	6 40 14.77200 N	1 32 34.26000 W	661070.886	737591.845
22. KNUST	6 38 35.44800 N	1 35 06.64800 W	656399.589	734527.370
23. Emena	6 38 53.26800 N	1 36 34.81200 W	653690.308	735067.055

24. Atonsu 3	6 39 25.52400 N	1 34 53.36400 W	656803.166	736066.679
25. Kaase 2	6 39 47.23200 N	1 36 00.43200 W	654741.498	736727.586
26. Gyinyase_3	6 41 56.65200 N	1 33 26.13600 W	659468.522	740716.558
27. Ahinsan 2	6 41 31.49999 N	1 33 34.80001 W	659204.719	739943.196
28. Kentinkrono	6 40 56.56800 N	1 35 57.33600 W	654830.529	738857.577
29. Kentinkrono 2	6 40 37.41600 N	1 35 31.92000 W	655612.740	738271.529
30. Amakom	6 40 31.87200 N	1 35 18.42000 W	656027.820	738102.426
31. Anloga	6 41 16.76400 N	1 35 33.10800 W	655572.800	739480.040
32. Old Ahinsan	6 40 44.65200 N	1 32 54.24000 W	660454.566	738507.848
33. Oforikrom 3	6 40 06.13200 N	1 35 04.88400 W	656445.790	737312.985
34. Ayiduase 2	6 39 42.30000 N	1 33 23.18400 W	659571.275	736590.000
35. KNUST 3	6 38 18.60000 N	1 36 20.70000 W	654126.716	734003.419
36. Kotei	6 40 54.91200 N	1 34 54.55200 W	656758.786	738812.231
37. Kaase 3	6 39 21.74400 N	1 34 21.43200 W	657784.196	735953.396
38. Bomso	6 41 35.08800 N	1 32 31.34400 W	661153.135	740059.153
39. Gyinyase 3	6 39 15.58800 N	1 35 06.79200 W	656391.641	735760.301
40. Oduom	6 41 27.09600 N	1 34 20.42400 W	657804.002	739803.834
41. Atonso 4	6 39 17.46000 N	1 35 57.80400 W	654824.800	735813.340
42. Ayigya 2	6 41 13.56000 N	1 34 13.29600 W	658024.111	739388.694
43. Kaase 4	6 42 31.10000 N	1 34 06.80002 W	658216.663	741771.021
44. KNUST Ayigya	6 41 28.50000 N	1 36 22.60800 W	654051.645	739836.193
45. Asokore Mampg	6 40 59.95200 N	1 35 12.22800 W	656215.505	738965.479
46. KTI	6 40 24.88800 N	1 33 10.80000 W	659947.776	737899.269
47. Decabin	6 39 19.62000 N	1 32 48.26400 W	659947.776	735896.493
48. Ayeduase3	6 38 38.04000 N	1 35 47.94000 W	655131.176	734603.377
49. Deduako	6 38 38.04000 N	1 35 47.94000 W	657106.962	739606.089
50. Esereso	6 62 92.50000N	1 56 13.40000W	659039.962	732994.599

APPENDIX K 1

ORIGINAL LAYOUT OF GSM MASTS LOCATION OF MTN KUMASI EAST, GHANA

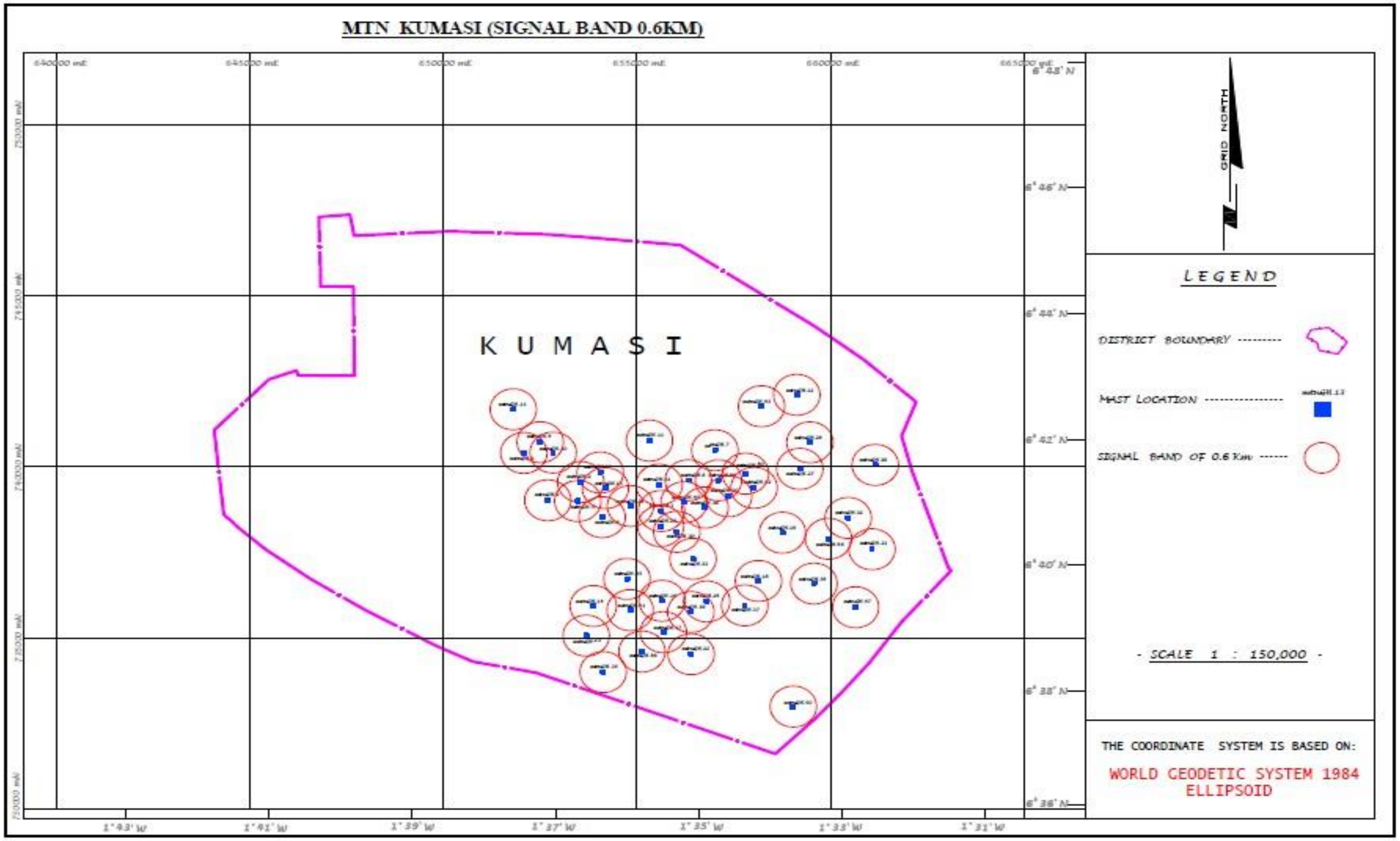

Figure K.1: Original Layout of GSM Masts, MTN Kumasi East, Ghana.

APPENDIX K. 2

MATLAB CODE FOR PLOTTING 50 MTN GSM MASTS WITH MINIMAL HEXAGONAL COVERING.

```
load set1 scatter(set1(:,1),set1(:,2),'fill') n=6.65; m=7.45;
figure(1),hold on for i=6.4695:.015:n     for j =
7.295:0.015:m         hexagon(0.005,i,j)     end end  for
i=6.4695:.015:n      for j = 7.295:0.015:m
hexagon(0.005,i+0.0075,j+0.0075)      end  end  axis([6.5
6.64 7.30 7.44])  xlabel('Easterns (xkm)')
ylabel('Northerns (ykm)')  title('Hexagonal Tessellation
of MTN - GHANA Masts')
```


APPENDIX K.3

MATLAB PLOT OF 50 MTN GSM MASTS POSITIONS WITH MINIMUM HEXAGONAL COVERING

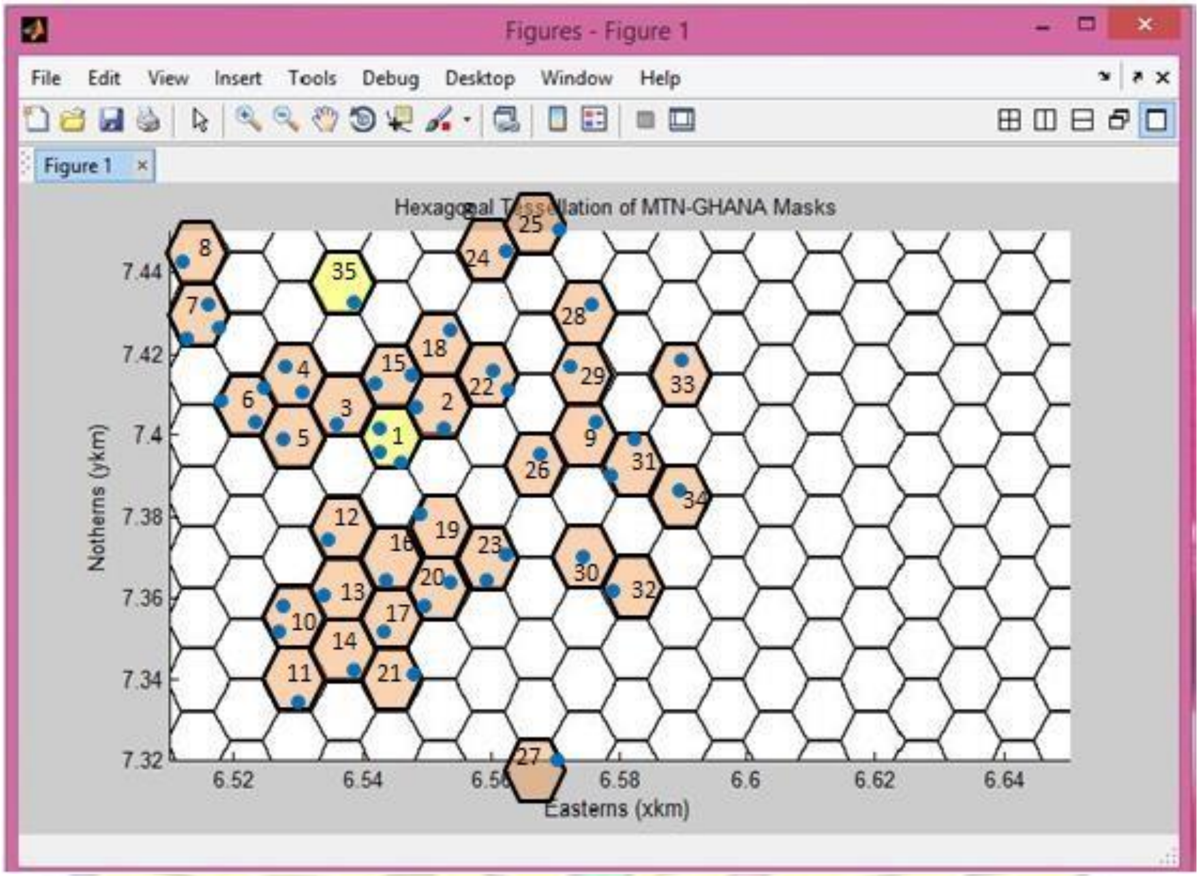

Figure K.3: Graph showing position of 50 MTN GSM Masts with hexagonal covering, Kumasi East, Ghana.

APPENDIX K.

MAXIMAL NODE COVERING USING HEXAGONS OF MTN GSM MASTS, KUMASI-EAST

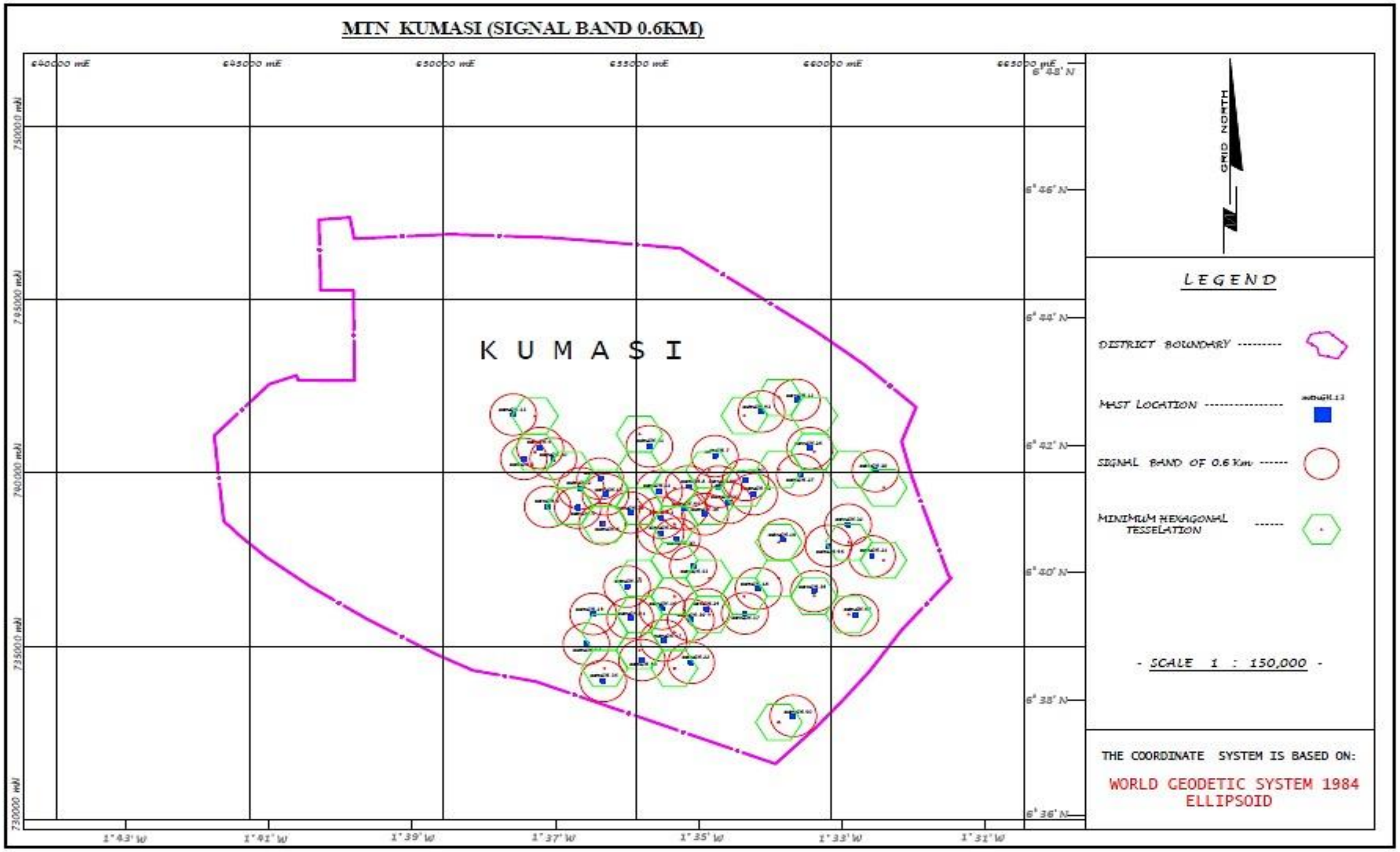

Figure K.4: Maximal node covering using hexagons for MTN Kumasi-East

APPENDIX K.

MINIMUM HEXAGONAL TESSELLATION OF GSM MASTS FOR MTN KUMASI EAST

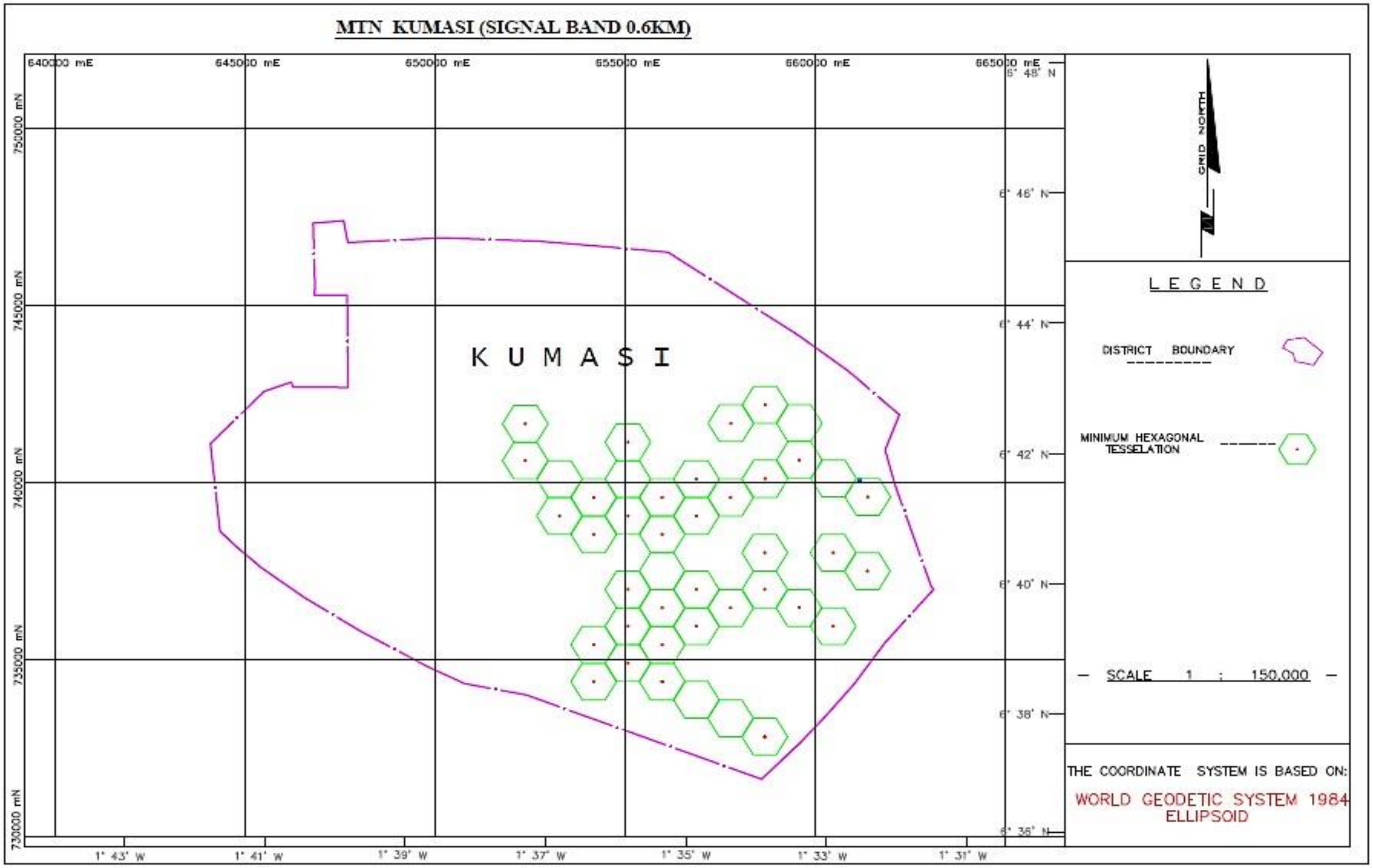

6

Figure K.5: Minimum Hexagonal Tessellation of WGS-84 for MTN Kumasi-East

APPENDIX K.

OPTIMAL DISKS COVERING FOR MTN GHANA GSM MASTS, KUMASI EAST

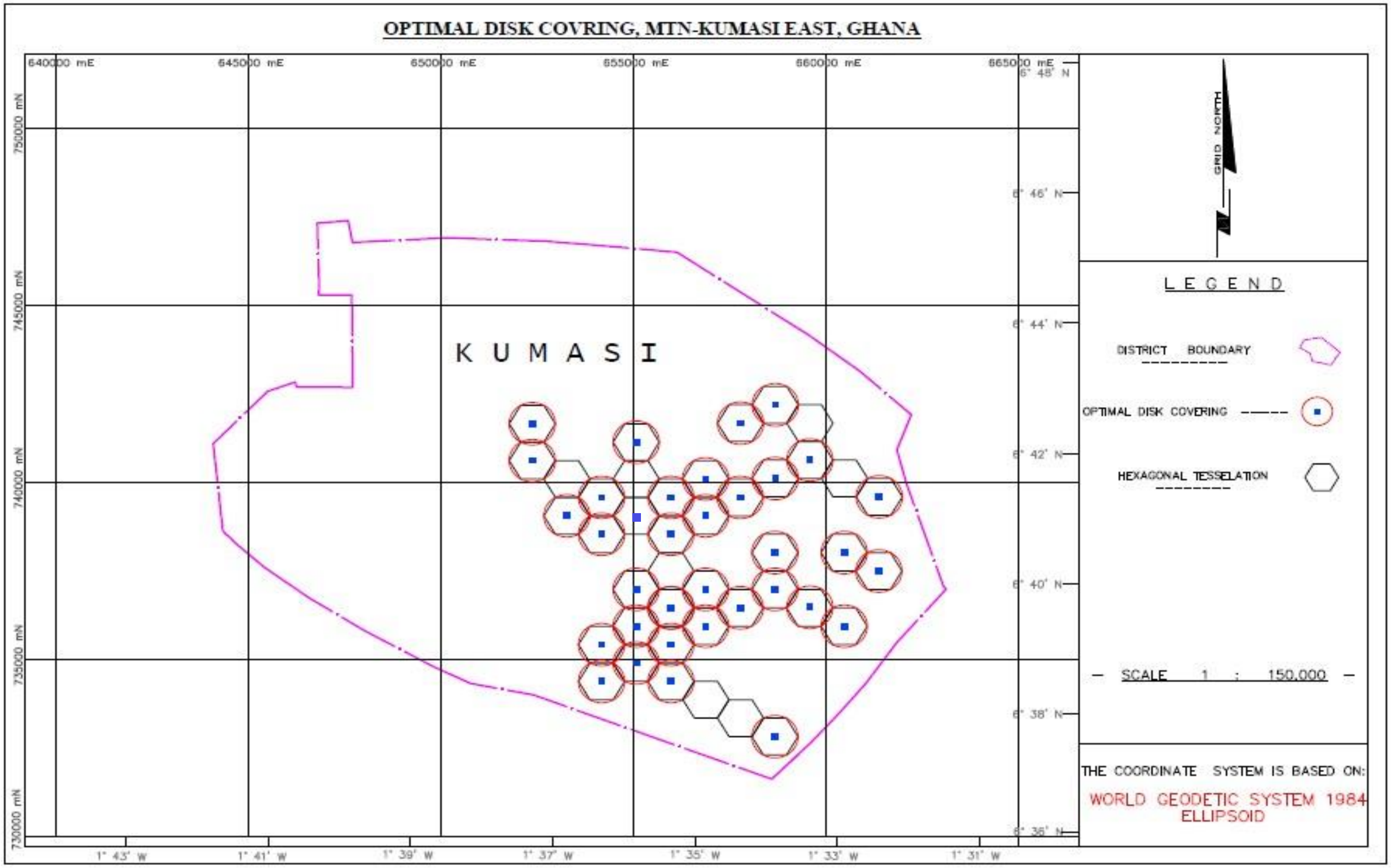

Figure K.6: Optimal Disks Covering for MTN GSM Masts, Kumasi East-Ghana

APPENDIX L

TABLE L.1 OVERLAP DIFFERENCE FOR 0.6KM MTN CELL RANGE – KUMASI EAST, GHANA.

Serial	Overlap Difference $d = d_m - d_n$	Value(m)	(A_d) Overlap Area	Serial	Overlap Difference $d = d_m - d_n$	Value(m)	(A_d) Overlap Area
1.	$d_3 - d_4$	671.9845	1139475.623	22.	$d_{31} - d_1$	430.5960	480672.144
2.	$d_3 - d_{10}$	443.6543	496679.1365	23.	$d_1 - d_{45}$	562.5434	467871.412
3.	$d_4 - d_{10}$	747.7813	1411028.312	24.	$d_1 - d_{29}$	758.3914	798543.529
4.	$d_{10} - d_2$	81.5865	16796.66778	25.	$d_1 - d_{30}$	471.5853	1451353.906
5.	$d_9 - d_2$	195.8562	96796.839	26.	$d_1 - d_8$	65.5667	561186.281
6.	$d_2 - d_{44}$	624.9433	985525.2592	27.	$d_1 - d_{36}$	67.1068	10848.0875
7.	$d_2 - d_5$	639.5699	1032196.922	28.	$d_{29} - d_{30}$	751.7942	11363.6955
8.	$d_9 - d_5$	423.5040	452586.4634	29.	$d_{29} - d_{45}$	280.8178	1426213.256
9.	$d_5 - d_{44}$	184.7302	86111.73269	30.	$d_8 - d_{49}$	418.3507	198992.080
10.	$d_{44} - d_{15}$	725.1811	1327026.149	31.	$d_8 - d_{20}$	56.9784	441639.111
11.	$d_{15} - d_5$	392.8305	389400.8782	32.	$d_8 - d_{36}$	292.6341	8192.322
12.	$d_{15} - d_2$	539.0729	733299.7325	33.	$d_8 - d_{45}$	546.8182	216090.857
13.	$d_{15} - d_6$	345.0611	300454.3748	34.	$d_8 - d_7$	85.8279	754522.941
14.	$d_{15} - d_{28}$	370.2505	345921.7222	35.	$d_{45} - d_{36}$	635.5204	18588.464
15.	$d_5 - d_6$	416.9689	438726.4873	36.	$d_{45} - d_{49}$	280.8178	1019167.389
16.	$d_6 - d_{28}$	400.1605	404068.4681	37.	$d_{45} - d_{30}$	316.7741	198992.080
17.	$d_6 - d_2$	35.5237	3184.365533	38.	$d_{30} - d_1$	471.5853	253212.918
18.	$d_{28} - d_{31}$	231.2698	134966	39.	$d_{30} - d_{36}$	181.1123	561186.281
19.	$d_{28} - d_1$	387.2503	378416.4898	40.	$d_{30} - d_{33}$	306.7387	82771.804

20.	$d_{28} - d_{29}$	222.5975	125033.7026	41.	$d_7 - d_{40}$	153.6429	237423.483
21.	$d_{31} - d_8$	436.4467	1139475.623	42.	$d_7 - d_{49}$	313.7318	59567.7943
43.	$d_{31} - d_{45}$	376.6861	358051.6806	60.	$d_{21} - d_{46}$	35.6022	3198.455
44.	$d_{49} - d_{42}$	257.4450	167245.8885	61.	$d_{49} - d_{40}$	475.3484	570178.189
45.	$d_{49} - d_{20}$	666.8751	1122213.608	62.	$d_{25} - d_{16}$	89.9902	20435.109
46.	$d_{49} - d_{36}$	333.1484	280067.0331	63.	$d_{25} - d_{41}$	281.9598	200613.851
47.	$d_{20} - d_{42}$	498.9126	628109.6581	64.	$d_{41} - d_{16}$	332.8930	279637.785
48.	$d_{20} - d_{40}$	406.9473	417890.8575	65.	$d_{41} - d_{17}$	128.1286	41426.543
49.	$d_{20} - d_{36}$	507.4910	649895.0312	66.	$d_{48} - d_{17}$	411.0528	426365.199
50.	$d_{20} - d_{45}$	34.0597	2927.306275	67.	$d_{48} - d_{35}$	29.9943	2270.199
51.	$d_{36} - d_{45}$	635.5204	1019167.389	68.	$d_{16} - d_{39}$	387.6659	379229.165
52.	$d_{36} - d_{29}$	67.1146	11366.33729	69.	$d_{16} - d_{17}$	281.6768	200211.345
53.	$d_{40} - d_{42}$	730.1218	1345169.955	70.	$d_{17} - d_{39}$	275.6814	191779.180
54.	$d_{26} - d_{27}$	382.8960	369954.3906	71.	$d_{17} - d_{22}$	236.9324	141656.150
55.	$d_{32} - d_{46}$	408.0549	420168.7239	72.	$d_{17} - d_{48}$	411.0528	426365.199
56.	$d_{32} - d_{21}$	95.9846	23248.21674	73.	$d_{39} - d_{24}$	686.9509	1190797.518
57.	$d_{14} - d_{41}$	239.9851	145329.9365	74.	$d_{24} - d_{37}$	212.4569	113901.176
58.	$d_{14} - d_{23}$	314.6990	249906.3278	75.	$d_{37} - d_{18}$	404.3385	412550.121
59.	$d_{23} - d_{35}$	50.3005	6384.562331	76.	$d_{43} - d_{12}$	231.3354	135042.577
Total$(\sum d)$ =26,884.4603m				Total$(\sum A_d) = 31{,}508{,}849.82$m^2			

APPENDIX M WGS-84 COORDINATES OBTAIN FROM HEXAGONAL TESSELLATION FOR MTN GSM MAST MASTS, KUMASI-GHANA

The hexagonal design model resulted in thirty five (35) coordinates with their UTM and WGS-84 coordinates shown in table M.1.

Table M.1: WGS-84 coordinates of MTN GSM masts in Kumasi-East Ghana.

MTN Masts with Node Points (WGS-84)				
Location (Node)	Geographical Coordinates		Grid Coordinates	
	Latitudes	Longitudes	Easterns (Xm)	Northerns(Ym)
1.	-1.62148	6.707602	652366.2443	741639.6407
2.	-1.57255	6.707603	657775.2501	741655.2391
3.	-1.5644	6.712279	658675.2501	742174.8544
4.	-1.54004	6.688712	661375.2501	739576.7782
5.	-1.54018	6.669775	661366.2443	737482.7187
6.	-1.54836	6.655702	660466.2443	735923.873
7.	-1.54831	6.674498	660466.2443	738002.334
8.	-1.55641	6.660566	659575.2501	736459.0867
9.	-1.58897	6.688714	655966.2443	739561.1797
10.	-1.59707	6.702834	655066.2443	741120.0254
11.	-1.6134	6.684084	653266.2443	739041.5645
12.	-1.62151	6.698204	652366.2443	740600.4102
13.	-1.60528	6.679362	654166.2443	738521.9492
14.	-1.60525	6.68876	654166.2443	739561.1797
15.	-1.56459	6.674546	658666.2443	738002.334
16.	-1.56473	6.627556	658666.2443	732806.1816
17.	-1.56462	6.665148	658666.2443	736963.1035
18.	-1.57277	6.660473	657766.2443	736443.4883
19.	-1.5809	6.665195	656866.2443	736963.1035
20.	-1.58092	6.655797	656866.2443	735923.873
21.	-1.58905	6.660519	655966.2443	736443.4883
22.	-1.58908	6.651121	655966.2443	735404.2578
23.	-1.5891	6.641723	655966.2443	734365.0273
24.	-1.59718	6.665242	655066.2443	736963.1035
25.	-1.5972	6.655843	655066.2443	735923.873
26.	-1.59723	6.646445	655066.2443	734884.6425
27.	-1.58082	6.693389	656866.2443	740080.7949
28.	-1.5563	6.698158	659575.2501	740616.0086
29.	-1.60536	6.651167	654166.2443	735404.2578
30.	-1.57269	6.688667	657766.2443	739561.1797

31.	-1.56445	6.693483	658675.2501	740096.3934
32.	-1.60538	6.641769	654166.2443	734365.0273
33.	-1.58084	6.683991	656866.2443	739041.5645
34.	-1.589	6.679315	655966.2443	738521.9492
35.	-1.56472	6.627555	658666.244	732806.182

APPENDIX N.1 LOCAL GEOGRAPHICAL COORDINATES FOR GLO GSM MASTS IN RIVER STATE, NIGERIA

Table N.1 shows 50 local grid coordinates of GLO GSM masts for River State-Nigeria in zone 32N provided by ATC (Nigeria).

Table N.1: Local Grid coordinate of GLO masts in River State, Nigeria.

POINT ID	SITE NAME	Easterns (m)	Northerns(m)	TRIG. HEIGHT
GloNG.1	62 NSUKKA STREET, MILE 1 DIOBU	504097.391	87454.996	25m
GloNG.2	PEOPLES CLUB COMPOUND, RUMUOLA ROAD	504382.027	92155.78	25m
GloNG.3	APEX MILL LTD. TRANS AMADI INDUSTRIAL AREA	507225.032	89580.753	25m
GloNG.4	EJOVINA ESTATE, RUMUOKWUTA, MILE 5	503014.371	92410.726	25m
GloNG.5	By LINSOLOA EYE CLINIC, 180 NTA ROAD, MGBOUBA	501278.34	94654.151	25m
GloNG.6	RUMUPIRIKOM VILLAGE, OWABIE CLOSE	501996.61	92038.215	25m
GloNG.7	COLLEGE OF EDUCATION ROAD, RUMUOLEMENI	496872.068	89469.317	25m
GloNG.8	NPA BY INDUSTRY ROAD, CONOIL FILLING STATION	505678.527	84989.028	25m
GloNG.9	50 ABEL JUMBO STREET, DIOBU, PHC	503020.163	88085.294	25m
GloNG.10	AIRPORT	498785.214	110438.126	25m
GloNG.11	DELTA PARK UNIPORT, BY SENIOR STAFF CLUB-ASSU	493836.54	99918.621	25m
GloNG.12	RUMUOBIAKANI (NWOGU STREET) CLOSE TO SHELL I.A	507399.774	92570.022	25m
GloNG.13	25 NZIMIRO STREET, OLD GRA, PORT HARCOURT	505571.649	87711.662	25m
GloNG.14	PLOT 127 TRANS AMADI INDUSTRIAL LAYOUT, PHC	508847.914	90198.406	25m
GloNG.15	AGIP RD, BY NEW BIBLE PRIESTHOOD CHURCH	502025.28	89703.398	25m
GloNG.16	PH-BORI EXPRESS WAY, AKPAJOELEME	514502.192	91196.519	25m
GloNG.17	PH-ABA EXPRESS WAY, PORT HARCOURT	513077.589	95141.976	25m
GloNG.18	CHIEF CHINDA NNOKAM, RD, MILE 3	503031.927	89221.918	25m
GloNG.19	SIB POLIC BARRACKS PREMISES	507010.918	84610.143	25m
GloNG.20	MOBILE BARRACK HARBOUR ROAD	505842.893	84039.427	25m
GloNG.21	SEED TIME MODEL NUSERY AND PRIMARY SCHOOL, RUMUKALAGBOR, OFF ELEKAHIA	506131.72	90172.95	25m

GloNG.22	28, RUMUCHAKARA STREET, CHOBA.	493564.873	98416.982	25m
GloNG.23	OKPORO ROAD EXTENSION, 2ND ARTILLERY, PORT HARCOURT	508473.643	93264.415	25m
GloNg.24	75 HAROLD WILSON DRIVE, OKARKI STREET, BOROKIRI	508292.659	82146.762	25m
GloNG.25	7A ELIDORLU STREET, RUMUKWURUSHI	510743.761	94852.03	25m
GloNG.26	7A HARLEY STREET BY GOVT. HOUSE DRIVE, OLD GRA	505875.27	86182.992	25m
GloNG.27	8 JONNY LANE, AGIP ESTATE	500842.875	90136.137	25m
GloNG.28	ALONG OKILO STREET, ABULOMA	510587.982	85922.246	25m
GloNG.29	ALONG PH-ABA EXPRESS WAY, RUMUKRUSHI	509400.894	93710.306	25m
GloNG.30	BEHIND CONOIL FILLING STATION, ALONG ABULOMA ROAD	508066.075	52083.834	25m
GloNG.31	BY PALACE STREET, WOJI TOWN	509812.817	91810.957	25m
GloNG.32	By RCCG CHURCH (GETHSEMANE AREA, 20 EGONU STREET,	503197.722	94477.794	25m
GloNG.33	BY TANTUA SECONDARY SCHOOL, ELEKAHIA	507387.154	91016.244	25m
GloNG.34	CHIEF GABRIEL AMADI LANE OFF IKWERRE ROAD	503021.761	93648.739	25m
GloNG.35	CHINDAH AVENUE, OFF STADIUM ROAD, OROMERUEZIMGBU, ELEKAHIA	505696.849	91696.382	25m
GloNG.36	EAGLE CEMENT FACTORY ROAD, RUMULUMENI	497936.665	88726.5	25m
GloNG.37	FEDERAL HOUSING ESTATE, ROAD 25, NO. 23, WOJI	511061.216	91120.797	25m
GloNG.38	INFORMATION CENTER BY NIGER STR.	507568.4	84166.584	25m
GloNG.39	OFF RAILWAY ROAD, WOJI TOWN	509707.461	92688.53	25m
GloNG.40	OMAGWA-IGWRUTA ROAD	505734.011	105645.04	25m
GloNG.41	POLICE STATION, ELIMGBO, ENEKA	510239.575	96825.3	25m
GloNG.42	RUMUONUKEM CLOSE, OFF EAST WEST ROAD, RUMUODARA	509243.655	95384.246	25m
GloNg.43	UPE MODEL PRIMARY SCHOOL COMPD. BOROKIRI	508742.233	83128.22	25m
GloNG.44	WEATHER-HEAD COMPANY, RUMUODIMAYA, BY BENO PETROL	504104.438	96199.173	25m
GloNG.45	13 CHUKWUDARA STREET, RUMUODARA	507966.355	94647.902	25m
GloNG.46	8 JONNY LANE AGIP	500842.875	90136.137	25m
GloNG.47	2 AGUDAMA STREET, D/LINE	504971.55	88940.545	25m
GloNG.48	CONOIL PREMISES, RECLAMATION LAYOUT, OFF HARBOUR ROAD	505353.778	83603.648	25m
GloNG.49	ELELENWO OFF ACMG SCHOOL ROAD	512070.184	93490.8	25m
GloNG.50	TRANS AMADI INDUSTRIAL LAYOUT, BY FAITH LOVE OF GOD INT'L INC	509157.367	88785.873	25m

APPENDIX N.2 WGS-84 COORDINATES OF LOCAL GLO MASTS IN RIVER STATE, NIGERIA

Table N.2shows the WGS-84 coordinates of the 25m height of 45 GSM masts nodes for two different cell range 1km and 3km used by GLO Nigeria in River State.

Table N.2: WGS-84 and UTM coordinates of GLO masts River State - Nigeria

GLO Masts with Node Points (WGS-84)				
	Geographical Coordinates		Grid Coordinates	
Location (Node)	Latitudes	Longitudes	Easterns (Xm)	Northerns (Y)
1. 62 Nsukka Street, Mile 1 Diobu	4^0 47, 24.30457,, N	$6^0$59, 55.25222,, E	278031.137	529784.462
2. Peoples club Compd, Rumuola Rd	4^0 49, 57.34415,, N	7^0 00, 04.15197,, E	278319.201	534485.576
3. Apex Mill Ltd, Trans Amdi Industrial Area	4^0 48 ,33.72452 N	7^0 01, 36.59181,, E	281160.660	531908.203
4. Ejovina Estate, Rumuokwuta, Mile 5	4^0 50 ,05.54406,, N	6^0 59, 19.75207,, E	276951.573	534741.544
5. By Linsolua Eye Clinic, Mgbouba	4^0 51 ,18.44378,, N	6^0 58, 23.25213,, E	275216.972	536986.493
6. College of Educatn Road, Rumuolemeni	4^0 49 ,53.34403,, N	6^0 58, 46.75220,, E	275933.424	534369.728
7. 50 Abel Jumbo Street, Diobu, PHC	4^0 48 ,29.3440,, 3 N	6^0 56, 00.65280,, E	270806.405	531804.229
8. Airport		7^0 00, 46.73219,, E	279610.683	527317.081
9. Delta Park Uniport, Senior Staff Club-	4^0 46 ′ 04.14488″ N 4^0 47 ′ 44.74447″ N	6^0 59, 20.25229,, E	276954.239	530415.607
10. Plot 127 Trans Amadi Industrial Layout, PHC.	4^0 50 ,11.04425,, N	7^0 01, 42.05168,, E	281337.586	534897.674
11. Agip Road,By new Bible Priesthood Ch.	4^0 47 ,32.76463,, N	7^0 00, 43.07206,, E	279505.747	530040.097

12. Ph-Bori Express way, Akpajo -Eleme	4^0 48 ,53.94452,,	N	7^0 02, 29.21164,, E	282784.165	532524.751
13. Ph-Aba express way, Port Harcourt	4^0 48 ,37.34428,,	N	6^0 58, 47.85231,, E	275960.407	532034.617
14. Sib Police Barracks Premises	4^0 49 ,26.82469,,	N	7^0 05, 32.63106,, E	288439.752	533518.877
15. Mobile Barack Harbour Road	4^0 51 ,35.16426,,	N	7^0 04, 46.13103,, E	287017.873	537465.767
16. Seed Time Model Sch., Rumukalagbor,	4^0 48 ,21.74434,,	N	6^0 59, 20.55222,, E	276966.824	531552.354
17. 28, Rumuchakara Street,Choba	4^0 45 ,51.90498,,	N	7^0 01, 29.99207,, E	280942.951	526937.200
18. Okporo road Ext., Port Harcourt	4^0 45 ,33.24497,,	N	7^0 00, 52.13220,, E	279774.388	526367.256
19. 75 HAROLD WILSON DRIVE, BOROKIRI	4^0 48 52.92440	N	7^0 01 ,01.0718,, 8 E	280067.655	532501.256
20. 7A HARLEY STREET, OLD GRA	′ ″ ′ ″ 4^0 50 ,33.72421,,	N	7^0 02 ,16.85155,, E	282412.076	535591.362
21. 8 JONNY LANE, AGIP ESTATE	4^0 44 31.80526	N	7^0 02, 11.75208,, E	282223.075	524472.636
22. ALONG OKILO STREET, ABULOMA	4^0 51 ,25.56417,,	N	7^0 03, 30.41123,, E	284683.592	537177.493
23. ALONG PH-ABA EXP. WAY RUMUKRUSHI	4^0 46 ,43.02478,,	N	7^0 00, 53.03210,, E	279808.304	528511.037
24. CONOIL FILLING STN., ABULOMA RD	4^0 48 ,51.34418,,	N	6^0 58, 09.45240,, E	274778.175	532468.261
25. BY PALACE STREET, WOJI TOWN	4^0 46 ,34.86502,,	N	7^0 03, 25.97167,, E	284521.340	528246.883
26. By RCCG CHURCH , 20 EGONU STREET	4^0 50 ,48.30424,,	N	7^0 02, 46.91144,, E	283339.751	536036.626
27. CHIEF GABRIEL AMADI LANE	4^0 49 ,46.50445,,	N	7^0 03, 00.41146,, E	283750.339	534136.776
28. CHINDAH AVE., ELEKAHIA	4^0 51 12.84387	N	6^0 59, 25.55197,, E	277136.449	536808.717
29. EAGLE CEMENT, RUMULUMENI	′ ″ ′ ″ 4^0 49 ,20.46441,,	N	7^0 01, 41.75173,, E	281323.838	533343.735
30. FEDERAL HOUSING ESTATE, NO. 23, WOJI	4^0 50 45.84394	N	6^0 59, 19.90203,, E	276959.864	535979.694
31. INFORMATION CENTER, NIGER STR.	4^0 49 ,42.48424,,	N	7^0 00, 46.85187,, E	279633.839	534025.172
32. OFF RAILWAY ROAD, WOJI TOWN	4^0 48 05.24417	N	6^0 56, 35.25271,, E	271870.597	531060.552
33. OMAGWA-IGWRUTA ROAD	′ ″ ′ ″ 4^0 49 ,24.12455,,	N	7^0 03, 40.97141,, E	284998.369	533445.639
34. POLICE STATN, ELIMGBO, ENEKA	4^0 45 37.50504	N	7^0 01, 48.11205,, E	281500.177	526493.194

35. RUMUONUKEM CLOSE, RUMUODARA	4^0 50 ′15.06433″ N	7^0 02′ 56.93144″ E	283645.608	535014.519
36. WEATHER-HEAD COMP., RUMUODIMA.	4^0 52 ′29.76399″ N	7^0 03′ 13.91119″ E	284180.795	539151.339
37. 13CHUKWUDARA STR., RUMUODARA	4^0 51 ′42.78406″ N	7^0 02′ 41.69136″ E	283183.716	537710.860
38. 8 JONNY LANE AGIP	″ N 4^0 45 03.78519″	7^0 02′ 26.27199″ E	282673.396	525453.880
39. 2 AGUDAMA STREET, D/LINE	′ 4^0 52 ′08.94373 N	6^0 59′ 54.85179″ E	278044.526	538529.631
40. CONOIL PREMISES, OFF HARBOUR RD	4^0 51 ′18.72408″ N	7^0 02′ 00.29151″ E	281905.741	536975.368
41. ELELENWO OFF ACMG SCHOOL RD	4^0 48 ′51.34418″ N	6^0 58′ 09.45240″ E	278424.107	532786.477
42. TRANS AMADI INDUSTR. LAYOUT,	4^0 48 ′12.72449″ N	7^0 00′ 23.51206″ E	278906.465	531269.550
43. 75 HAROLD WILSON DRIVE, BOROKIRI	4^0 45 19.02501 N	7^0 00′ 36.29229″ E	279284.907	525931.777
44. 7A ELIDORLU STR, RUMUKWURUSHI	′ ″ ′ ″ N 4^0 50 ′41.34436″	7^0 04′ 13.55120″ E	286009.162	535815.155
45. 7A HARLEY STREET, OLD GRA	4^0 48 07.98467 N	7^0 02′ 39.35169″ E	283092.632	531111.843

APPENDIX O. 1

ORIGINAL LAYOUT OF GSM MASTS LOCATION OF GLO RIVER STATE, NIGERIA.

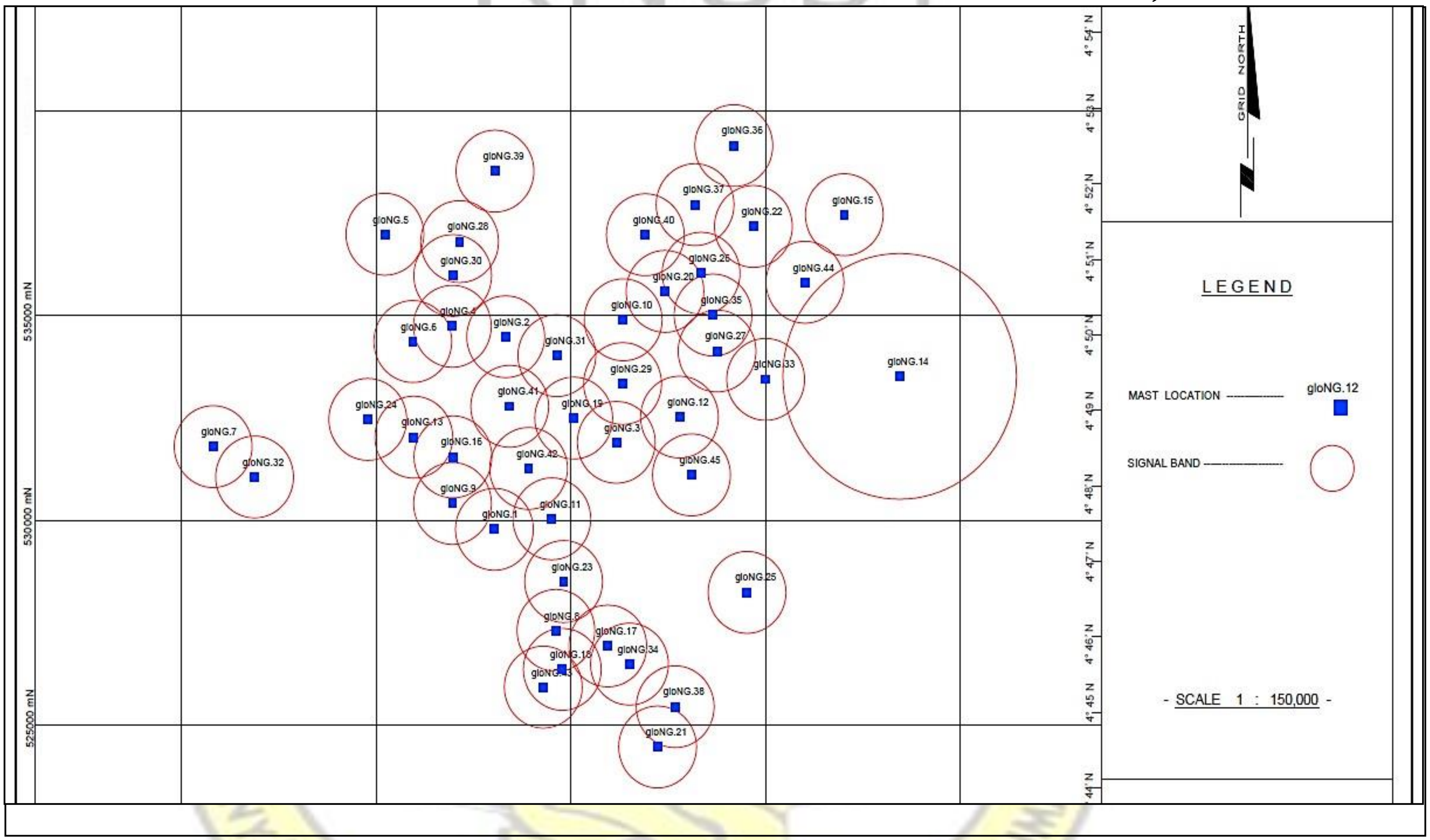

Figure O.1: Original Layout of GSM Masts, GLO River State, Nigeria.

APPENDIX O.2

MATLAB CODE FOR GSM MASTS POSITION WITH MINIMAL HEXAGONAL COVERING

```
load set2

scatter(set2(:,1),set2(:,2),'fill')

n=2.99; m=5.59;

figure(1),hold on for

i=2.594:.03:n     for j =

5.1:0.03:m

hexagon(0.01,i,j)     end end


 for i=2.594:.03:n      for j = 5.1:0.03:m

hexagon(0.01,i+0.015,j+0.015)      end  end  axis([2.7 2.9

5.23 5.4])  xlabel('Easterns (xkm)')  ylabel('Northerns

(ykm)')  title('Hexagonal Tessellation of GLO -

NIGERIA Masts')
```


APPENDIX O.3

MATLAB PLOT OF 45 GLO GSM MASTS POSITIONS WITH HEXAGONAL COVERING

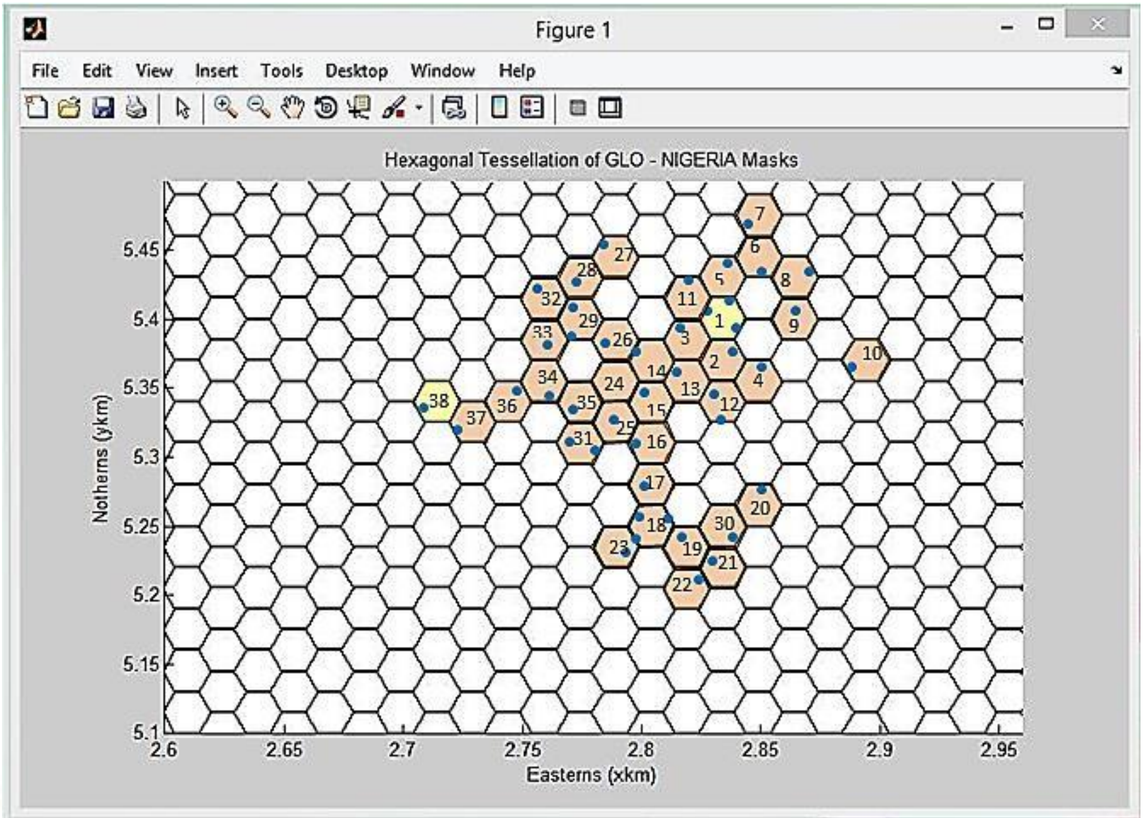

Figure O.3: Graph showing position of 45 GLO GSM Masts with hexagonal covering, River State, Nigeria.

APPENDIX O.

MAXIMAL NODE COVERING USING HEXAGONS OF GLO GSM MASTS, RIVER STATE- NIGERIA

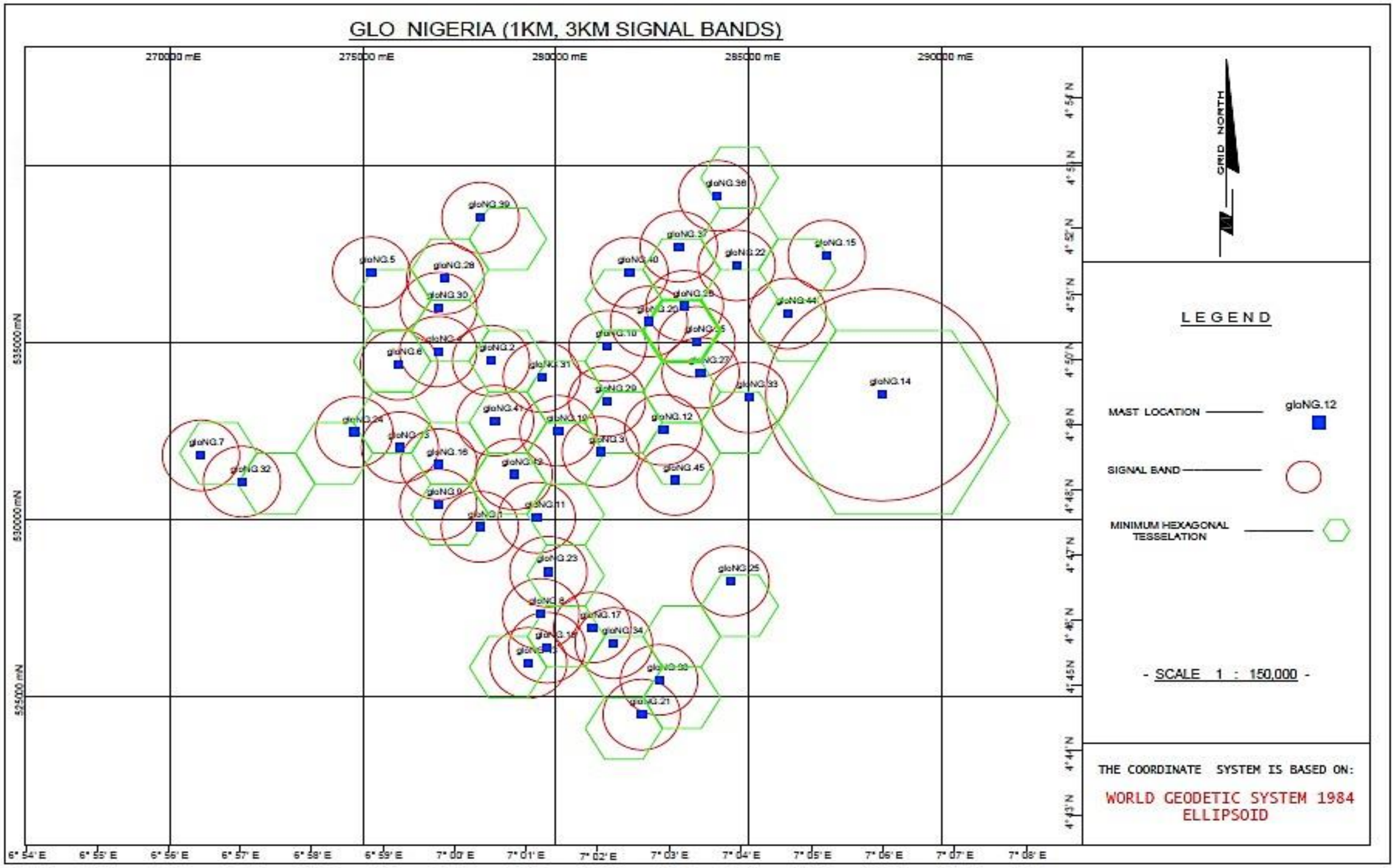

Figure O.4: Maximal node covering using hexagons for GLO River State, Nigeria

APPENDIX O.

MINIMUM HEXAGONAL TESSELLATION OF GLO GSM MASTS, RIVER STATE-NIGERIA

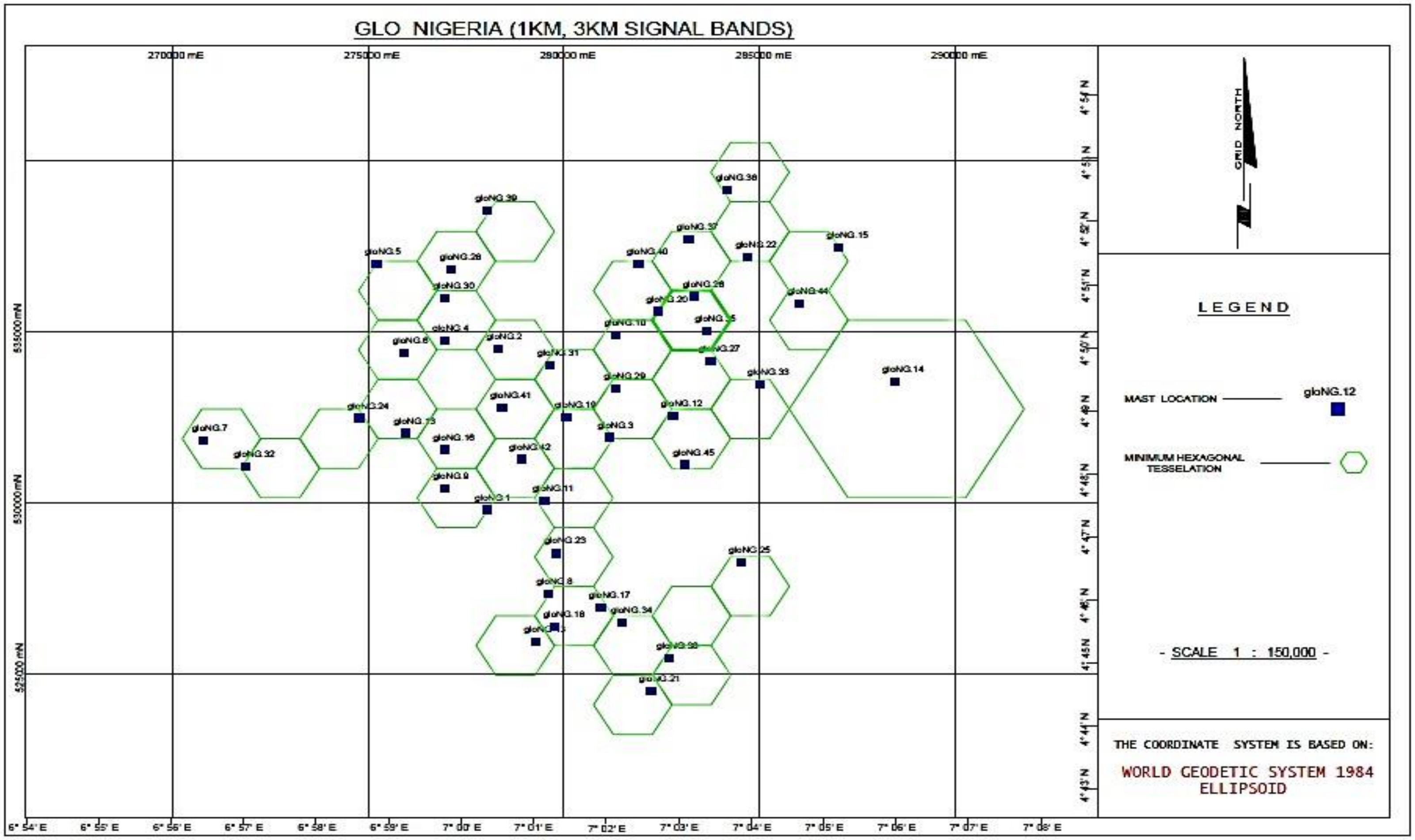

6

Figure O.5: Minimum Hexagonal Tessellation for GLO River State, Nigeria

APPENDIX O.

OPTIMAL DISKS COVERING FOR GLO MASTS, RIVER STATE-NIGERIA.

7

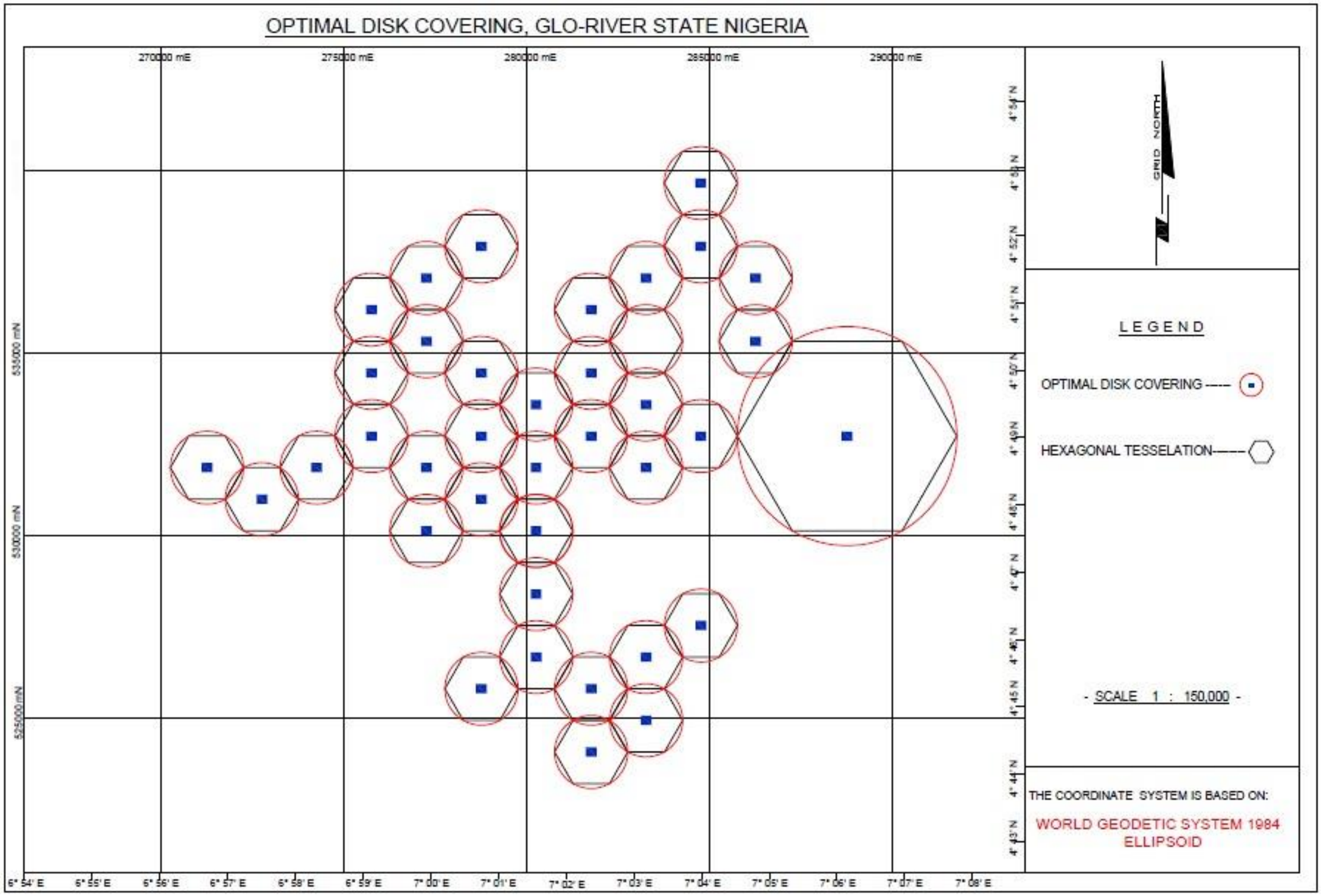

Figure O.6: Optimal Disks covering, GLO River State-Nigeria.

APPENDIX P TABLE P.1 OVERLAP DIFFERENCE FOR 1km and 3km GLO CELL

RANGE– RIVER STATE –NIGERIA.

Serial	Overlap Difference $d = d_m - d_n$	Value (m)	Area of (A_d) overlap	Serial	Overlap Difference $d = d_m - d_n$	Value (m)	(A_d) Area of overlap
1.	$d_5 - d_{28}$	72.3080	13193.47583	22.	$d_{16} - d_{42}$	39.8507	4007.360711
2.	$d_{28} - d_{39}$	54.1971	7412.054852	23.	$d_{16} - d_{41}$	90.3580	20602.49163
3.	$d_{28} - d_{30}$	1152.3790	3351021.374	24.	$d_{41} - d_{19}$	331.8871	277950.3797
4.	$d_{36} - d_{37}$	248.1021	155327.1621	25.	$d_{41} - d_{42}$	408.2288	420526.9253
5.	$d_{37} - d_{40}$	525.4938	696821.7852	26.	$d_{42} - d_{19}$	307.2325	238188.5259
6.	$d_{37} - d_{22}$	408.1117	420285.7045	27.	$d_{42} - d_{11}$	632.2670	1008759.314
7.	$d_{37} - d_{26}$	318.5107	255996.8257	28.	$d_{10} - d_{20}$	721.0427	1311923.452
8.	$d_{40} - d_{20}$	526.2810	698911.0543	29.	$d_{10} - d_{29}$	446.0002	501945.5796
9.	$d_{40} - d_{26}$	287.4071	208440.2149	30.	$d_{29} - d_{12}$	325.6972	267679.17
10.	$d_{26} - d_{20}$	971.0000	2379167.326	31.	$d_{29} - d_3$	555.2235	777897.196
11.	$d_{26} - d_{35}$	933.1114	2197118.686	32.	$d_{29} - d_{19}$	487.4635	599612.5745
12.	$d_{26} - d_{22}$	237.1937	141968.7722	33.	$d_{27} - d_{35}$	1116.0309	3142960.809
13.	$d_{22} - d_{44}$	99.1842	24823.98594	34.	$d_{27} - d_{33}$	573.3784	829600.8415
14.	$d_{15} - d_{44}$	65.5704	10849.31186	35.	$d_{27} - d_{12}$	120.6073	36705.71746
15.	$d_{44} - d_{14}$	656.2505	212116	36.	$d_{27} - d_{26}$	56.2890	7995.278454
16.	$d_7 - d_{32}$	701.7088	1242511.374	37.	$d_{27} - d_{20}$	23.4453	1387.069159
17.	$d_6 - d_4$	916.0837	2117662.951	38.	$d_{12} - d_3$	263.3653	175026.4297
18.	$d_6 - d_{30}$	90.6625	20741.58344	39.	$d_{12} - d_{45}$	553.8116	773945.9346
19.	$d_4 - d_{30}$	761.8222	1464514.835	40.	$d_1 - d_9$	751.7799	1426159

20.	$d_4 - d_2$	608.6244	934727.9863	41.	$d_1 - d_{42}$	276.1423	192420.9713
21	$d_2 - d_{31}$	607.0733	929969.6852	42.	$d_1 - d_{11}$	503.3959	639448.9449
43.	$d_2 - d_{41}$	297.6651	223584.8455	54.	$d_{11} - d_{23}$	441.2937	491407.7279
44.	$d_{31} - d_{10}$	85.8387	18593.14219	55.	$d_{23} - d_8$	789.7996	1574056.605
45.	$d_{31} - d_{19}$	415.5391	435722.831	56.	$d_{23} - d_{17}$	59.7972	9022.943219
46.	$d_{31} - d_{29}$	177.7890	79762.0489	57.	$d_8 - d_{18}$	1036.1707	2709250.374
47.	$d_{31} - d_{41}$	268.5793	182025.2358	58.	$d_8 - d_{43}$	1036.1707	2709250.374
48.	$d_{24} - d_{13}$	740.7464	1384604.141	59.	$d_{17} - d_8$	614.6309	953268.643
49.	$d_{13} - d_{16}$	884.0014	1971934.261	60.	$d_{17} - d_{34}$	1287.5099	4182998.235
50.	$d_{13} - d_9$	100.2907	25380.94875	61.	$d_{17} - d_{18}$	699.8555	1235956.788
51.	$d_9 - d_{16}$	863.1833	1880150.376	62.	$d_{17} - d_{43}$	699.8555	1235956.788
52.	$d_{34} - d_{38}$	432.6403	472324.4953	63.	$d_{34} - d_{18}$	269.6220	183441.3251
53.	$d_{38} - d_{21}$	920.3571	2137466.225	64	$d_{33} - d_{14}$	557.8378	785239.9847
Total $(\sum d) =$ 31,503.75m				Total $(\sum A_d) = 55{,}019{,}724.45$ m^2			

APPENDIX Q

WGS-84 COORDINATES OBTAIN FROM HEXAGONAL TESSELLATION MODEL FOR GLO GSM MAST, RIVER STATE – NIGERIA.

The hexagonal design model resulted in thirty eight (38) coordinates with their WGS-84 coordinates shown in table Q.1.

Table Q.1: Coordinate for Hexagonal Tessellation

GLO Masts with Node Points (WGS-84)				
Location (Node)	Geographical Coordinates		Grid Coordinates	
	Latitudes	Longitudes	Easterns (Xm)	Northerns (Ym)
1.	7.072676	4.840455	286256.9	535331.9
2.	7.095276	4.817028	288756.9	532733.9
3.	7.005099	4.83243	278756.9	534465.9
4.	6.937573	4.808739	271256.9	531867.8
5.	7.04559	4.856038	283256.9	537064
6.	7.059396	4.770016	284761.4	527545.5
7.	7.005007	4.863749	278756.9	537930
8.	7.059222	4.816926	284756.9	532733.9
9.	7.00519	4.80111	278756.9	531001.8
10.	7.018731	4.793319	280256.9	530135.8
11.	7.059089	4.863907	284756.9	537930
12.	7.072632	4.856116	286256.9	537064
13.	7.045943	4.746488	283261.4	524947.5
14.	7.005144	4.81677	278756.9	532733.9
15.	7.018686	4.808979	280256.9	531867.8
16.	7.018641	4.824639	280256.9	533599.9
17.	7.059044	4.879567	284756.9	539662.1
18.	7.032138	4.832509	281756.9	534465.9
19.	7.032183	4.816849	281756.9	532733.9
20.	7.045725	4.809057	283256.9	531867.8
21.	7.04568	4.824718	283256.9	533599.9
22.	7.032093	4.848169	281756.9	536198
23.	7.045635	4.840378	283256.9	535331.9
24.	6.951115	4.80095	272756.9	531001.8
25.	6.96461	4.80882	274256.9	531867.8

26.	6.978059	4.832349	275756.9	534465.9
27.	6.991694	4.793241	277256.9	530135.8
28.	6.978106	4.81669	275756.9	532733.9
29.	6.991648	4.8089	277256.9	531867.8
30.	6.978013	4.848009	275756.9	536198
31.	6.991556	4.840219	277256.9	535331.9
32.	7.032447	4.738619	281761.4	524081.4
33.	7.032403	4.754279	281761.4	525813.5
34.	7.018862	4.762071	280261.4	526679.5
35.	7.005366	4.754202	278761.4	525813.5
36.	7.018777	4.77766	280256.9	528403.7
37.	6.99151	4.855879	277256.9	537064
38.	7.045899	4.762148	283261.4	526679.5

APPENDIX R.1

LOCAL GEOGRAPHICAL COORDINATES FOR MTN MASTS IN RIVER STATE, NIGERIA.

Table R. 1 shows the local coordinates of 50 900MHz GSM masts in part of River State provided by ATC Nigeria.

Table R.1: Local Grid coordinate of MTN masts in River State, Nigeria.

POINT ID	SITE NAME	Easterns (m)	Northerns(m)	TRIG. HEIGHT
mtnNG.1	AGUDAMA STREET, BY GARRISON	505014.182	88988.374	25m
mtnNG.2	11B ELECHI BEACH, DIOBU	503674.114	86687.308	25m
mtnNG.3	16 NHEDIOHANMA, DIOBU, PHC	502955.208	87977.917	25m
mtnNG.4	APEX MILL LTD. TRANS AMADI INDUSTRIAL AREA	507210.232	89577.099	25m
mtnNG.5	BY 3 KING'S AVENUE, ABULOMA, OZUBOKO	508524.316	86733.931	25m
mtnNG.6	EJUAN COMM., BEHIND DAY SPRING INFANT AND JUNIOR SCH. ABULOMA	508885.176	87739.533	25m
mtnNG.7	NZIMIRO STREET SHELL RA, OLD GRA	505886.993	87323.904	25m
mtnNG.8	OCO MILLER INDUSTRIAL SERVICES LTD., TRANS AMADI	508323.086	89467.793	25m
mtnNG.9	OFF JOHN OGBODA STREET, NGWOR STREET	505741.092	89101.063	25m
mtnNG.10	OKIS AWO CLOSE, AMADI-AMA, RAINBOW	507647.423	88247.219	25m
mtnNG.11	OLD GRA FORCE AVENU BY OLUMENI JUNCTION	505254.113	86245.167	25m
mtnNG.12	OPP GIGGLES CYBERCAFE, UPE SCH JUNCTION BOROKIRI	508858.127	82844.127	25m
mtnNG.13	OPP NANA'S HOTELS, MOORE HOUSE STREET	508379.432	83823.867	25m
mtnNG.14	ORUTA COMPOUND, OZUBOKOAMA	509023.15	85673.043	25m
mtnNG.15	PLOT 305 BOROKIRI SAND FILLED AREA, UPE SAND FILLED AREA	508006.727	83339.905	25m

mtnNG.16	NKPOGU BYE-PASS ALONG TOKI HOTEL ROAD	506479.738	88944.012	25m
mtnNG.17	ST MARY'S CATHOLIC CHURCH BY LAGOS BUS STOP	506350.236	84355.361	25m
mtnNG.18	CHINDAH ESTATE, UST, PORT HARCOURT	502756.96	88909.182	25m
mtnNG.19	23 DICK TIGER, STREET, DIOBU	503085.76	87368.752	25m
mtnNG.20	MILE ONE POLICE STATION	503971.878	87556.649	25m
mtnNG.21	OPP 100 ABEL JUMBO STREET, MILE 2 DIOBU PHC	502578.838	87800.573	25m
mtnNG.22	OMEGA BEACH BY APOSTOLIC ARMY CHURCH EASTERN BY PASS	506692.885	86332.364	25m
mtnNG.23	NNOKAM-OFF ADA-GEORGE RD., RUMUOKWOKUNU VILLAGE	502409.69	89343.111	25m
mtnNG.24	OPP 3 DICK NWOKE STREET, OGBUNABALI	505623.723	87849.788	25m
mtnNG.25	4 NZIMIRO STREET, OPP CFC BUS STOP, PORT HARCOURT	504868.008	88098.428	25m
mtnNG.26	IMMACULATE CATHOLIC HEART PARISH, 51 EKWE STREET, MILE 3, DIOBU	502820.823	88525.036	25m
mtnNG.27	9 EZEBUNWO CLOSE, OROWURUKWO	504635.142	89833.394	25m
mtnNG.28	BY ADARI-OBU LANE, ABULOMA	509679.153	86349.937	25m
mtnNG.29	ROAD E, UST CAMPUS	501909.117	87362.76	25m
mtnNG.30	CHIEF ODUM CLOSE OFF OGBUNABALI, EASTERN BYE-PASS	505752.33	88319.523	25m
mtnNG.31	ROAD 3, AGIP ESTATE	501664.501	89605.899	25m
mtnNG.32	11 WONODI STREET, GRA PHASE III	504136.013	89600.407	25m
mtnNG.33	31B FORCES AVENUE, PHC CLUB STAFF QUARTERS, OLD GRA	505259.064	86820.235	25m
mtnNG.34	CHRISTIAN COUNCIL COLLEGE, BY C.C.C ROAD, ELEKAHIA	506032.804	89751.075	25m
mtnNG.35	OUR LADY FATIMAH'S COLLEGE, CREEK ROAD BY NEW MARKET LAYOUT	507747.078	83845.489	25m
mtnNG.36	BY RESURRECTION MINISTRIES, BOROKIRI SAND FILLED BEHIND NOWA MKT	508502.089	82371.185	25m
mtnNG.37	5 ABUJA BYPASS, BESIDES FLEET OIL FILLING STATION, MILE 3, DIOBU	503610.492	88861.21	25m
mtnNG.38	6 ABOBIRI STREET, OFF INDUSTRY ROAD, P.H	505777.349	84513.27	25m
mtnNG.39	ABONNEMA WHARF ROAD, BY RCCG KIDNEY PARISH	504609.789	85859.5	25m
mtnNG.40	BY MARINE BASE COMMUNITY BANK PREMISES	506662.517	85112.239	25m
mtnNG.41	8 RECLAMATION LAYOUT OFF HARBOUR ROAD	505550.548	83955.272	25m
mtnNG.42	3 ENWENABURU AVENUE, ELIOGBOLU	505964.067	95502	25m
mtnNG.43	BY AGGREY ROAD HOUSING ESTATE, PORT HARCOURT	507844.425	84403.764	25m

mtnNG.44	BEHIND CHINDAH BAR, OFF IHUNWO OROGBUM ROAD	503161.883	89458.176	25m
mtnNG.45	FACULTY OF LAW BUILDING, UST CAMPUS	501818.854	88346.015	25m
mtnNG.46	UST CAMPUS	501698.625	88327.851	25m
mtnNG.47	INSIDE EL-SHADDAI INT'L INC. PREMISES, AMADI AMA	506982.21	88447.719	25m
mtnNG.48	OPP 6A WOKE LANE OGBUNABALI	505238.592	88453.355	25m
mtnNG.49	CHIEF AKAROLO ESTATE, ELEKAHIA	507001.541	90541.538	25m
mtnNG.50	DANGOTE PREMISES, TRANS AMADI, OGINIGBA	508440.784	90890.473	25m

APPENDIX R.2

WGS-84 COORDINATES FOR MTN GSM MASTS IN RIVER STATE, NIGERIA

The local GSM zone 32 coordinates of GLO Nigeria in River State is converted to WGS-84. This is shown in table R.2 for a fixed antenna height of 25m and cell ranges of 0.6km, 1.3km and 2.5km

Table R.2: WGS-84 and UTM coordinates for MTN masts River State - Nigeria

MTN Masts with Node Points (WGS-84)				
Location	Geographical Coordinates		Grid Coordinates	
	Latitude	Longitudes	Easterns (Xm)	Northings(Ym)
1. AGUDAMA STR., BY GARRISON	4^{0} 48′ 14.28446″ N	7^{0} 00′ 24.89204″ E	278949.137	531317.354
2. 11B ELECHI BEACH, DIOBU	4^{0} 46′ 59.28462″ N	6^{0} 59′ 41.57230″ E	277607.260	529016.990
3. 16 NHEDIOHANMA, DIOBU, PHC	4^{0} 47′ 41.24449″ N	6^{0} 59′ 18.15230 E	276889.199	530308.265
4. APEX MILL LTD. TRANS AMADI INDUS. AREA	4^{0} 4′ 33.60453″ N	7^{0} 01′ 36.11181″ E	281145.856	531904.560
5. BY 3 KING'S AVENUE, ABULOMA, OZUBOKO	4^{0} 47′ 01.14485″ N	7^{0} 02′ 18.95184″ E	282458.036	529060.136

6. EJUAN COMMUNITY, ABULOMA	4^0 47, 33.90477,, N	7^0 02, 30.59174 ,, E	282819.658	530065.587
7. NZIMIRO STREET SHELL RA, OLD GRA	4^0 47, 20.16467,, N	7^0 00, 53.33206 ,, E	279820.847	529652.068
8. OCO MILLER IND.. SERV. LTD., TRANS AMADI	4^0 48, 30.12458,, N	7^0 02, 12.23173 ,, E	282258.753	531794.438
9. OFF JOHN OGBODA STREET, NGWOR STR.	4^0 48, 18.00450,, N	7^0 00, 48.47199 ,, E	279676.210	531429.531
10. OKIS AWO CLOSE, RAINBOW	4^0 47, 50.34468,, N	7^0 01, 50.39185 ,, E	281582.136	530574.219
11. OLD GRA FORCE AVENU	4^0 46, 45.00473,, N	7^0 00, 32.87214 ,, E	279187.121	528573.665
12. OPP GIGGLES CYBER CAFE, BOROKIRI	4^0 44, 54.54525,, N	7^0 02, 30.05200 ,, E	282789.100	525169.673
13. OPP NANA'S HOTELS, MOORE HOUSE STR.	4^0 45, 26.40512,, N	7^0 02, 14.45200 ,, E	282311.053	526149.861
14. ORUTA COMPOUND, OZUBOKO-AM	4^0 46, 26.64496,, N	7^0 02, 35.21184 ,, E	282956.163	527998.775
15. PLOT 305 BOROKIRI, UPE SAND FILL AREA	4^0 45, 10.62516,, N	7^0 02, 02.39203 ,, E	281937.962	525666.112
16. NKPOGU BYE-PASS, TOKI HOTEL ROAD	4^0 48, 12.94455,, N	7^0 01, 12.45193 ,, E	280414.825	531271.930
17. ST MARY'S CATHOLIC CH. LAGOS BUS STOP	4^0 45, 43.56496,, N	7^0 01, 08.57216 ,, E	280282.014	526682.863
18. CHINDAH ESTATE, UST, PORT HARCOURT	4^0 48, 11.54438,, N	6^0 59, 11.65228 ,, E	276691.599	531239.780
19. 23 DICK TIGER, STREET, DIOBU	4^0 47, 21.42455,, N	6^0 59, 22.43231 ,, E	277019.328	529698.935

7905.683	529886.217
6512.658	530131.171
0626.117	528659.839
6344.602	531674.010
9557.926	530178.201
8802.305	530427.412
6755.193	530855.544
8570.664	532162.743
3612.721	528675.271
5842.544	529693.789
9686.886	530647.896
5599.515	531937.367
8071.310	531930.090
9192.486	529148.794

532079.405
526171.937
524696.934
531191.187
526841.199
528188.416
527439.601
526283.300
537831.021
526730.203
531788.546
530677.224
534326.027
530775.220
530782.113
532869.255
533217.187

APPENDIX S.1

ORIGINAL LAYOUT OF GSM MASTS LOCATION OF MTN RIVER STATE-NIGERIA.

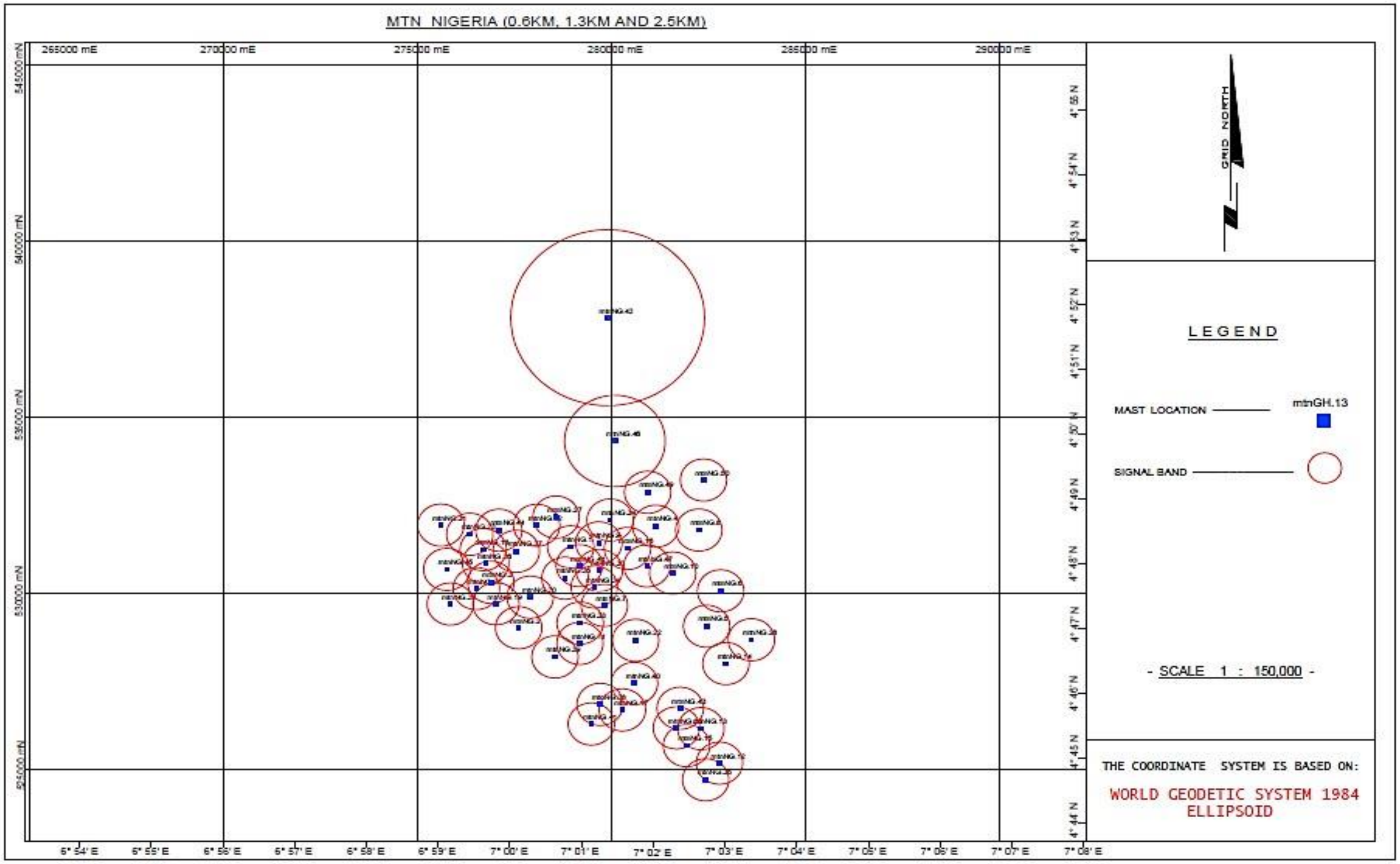

Figure S.1: Original Layout of GSM masts-MTN River State, Nigeria

APPENDIX S.2

MATLAB CODE FOR MTN GSM MASTS POSITION WITH MINIMAL HEXAGONAL COVERING, RIVER STATE-NIGERIA

```
load set3
scatter(set3(:,1),set3(:,2),'fil
l') n=5.1; m=0.96;
figure(1),hold on for
i=5.0008:.015:n     for j =
0.81325:0.015:m
hexagon(0.005,i,j)     end
end


 for i=5.0008:.015:n      for j = 0.81325:0.015:m
hexagon(0.005,i+0.0075,j+0.0075)      end  end  axis([5 5.1 0.8 0.96])
xlabel('Easterns (xkm)')  ylabel('Northerns (ykm)')  title('Hexagonal
Tessellation of MTN RIVER STATE, NIGERIA Masts')
```


APPENDIX S.3

MATLAB PLOT OF 50 MTN GSM MASTS POSITIONS WITH HEXAGONAL COVERING -RIVER STATE, NIGERIA

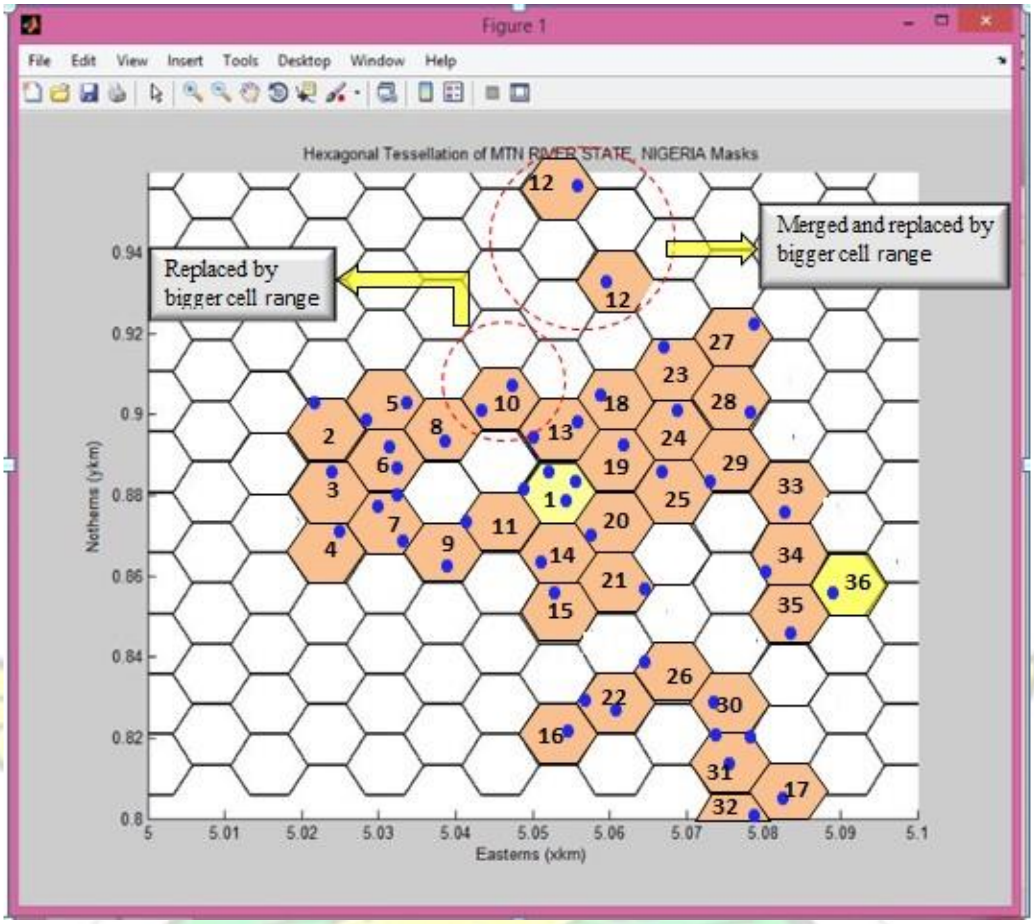

Figure S.3: Graph showing position of 50 MTN GSM Masts with hexagonal covering, River State, Nigeria

APPENDIX S. 4

MAXIMAL NODE COVERING USING HEXAGONS FOR MTN RIVER STATE-NIGERIA

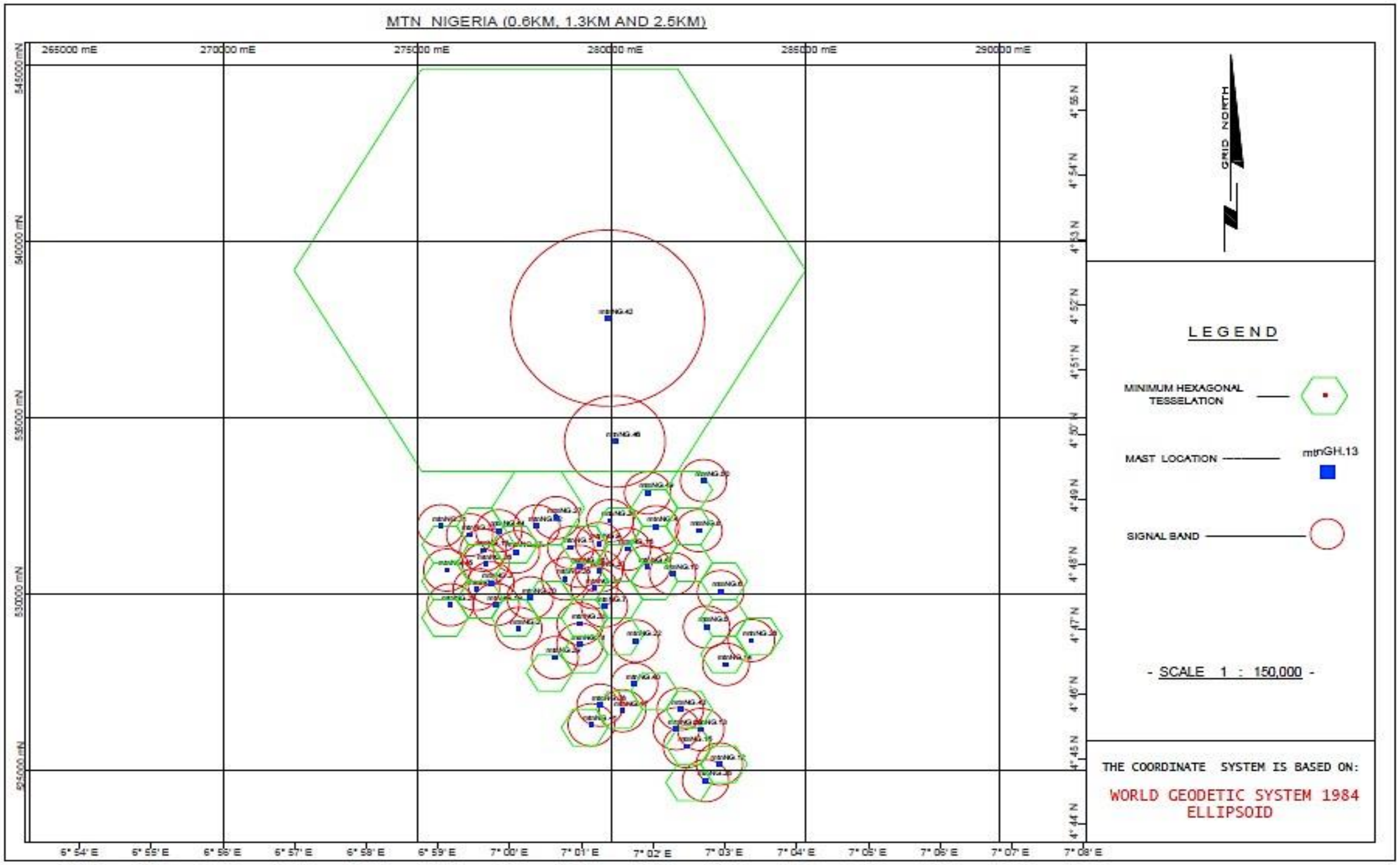

Figure S.4: Maximal node covering using hexagons of MTN River State, Nigeria

APPENDIX S.5

MINIMAL HEXAGONAL TESSELLATION OF GSM MASTS FOR MTN RIVER STATE-NIGERIA

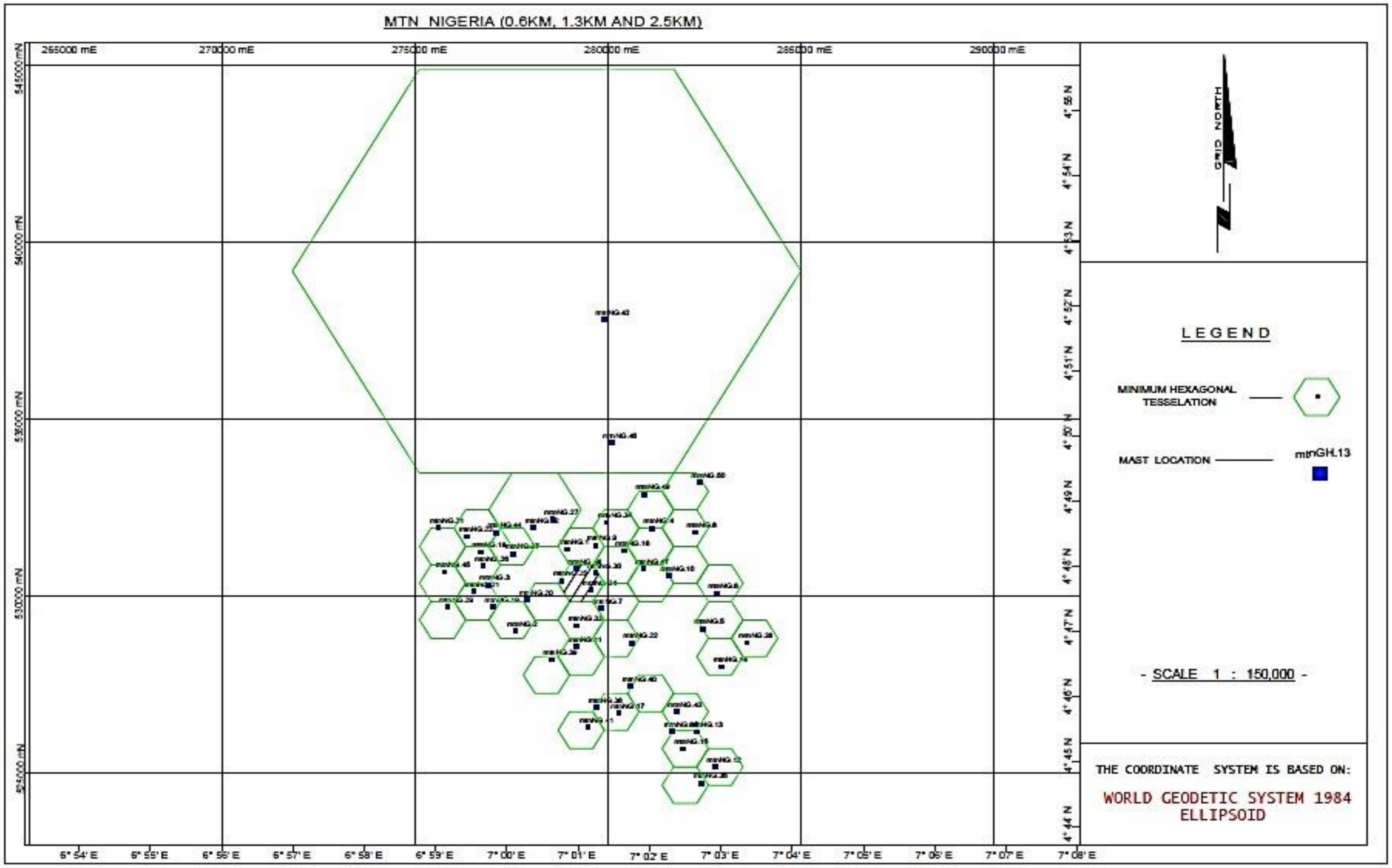

Figure S.5: Minimum Hexagonal Tessellation of MTN River State, Nigeria

APPENDIX S.6

OPTIMAL DISKS COVERING FOR MTN GSM MASTS, RIVER STATE-NIGERIA.

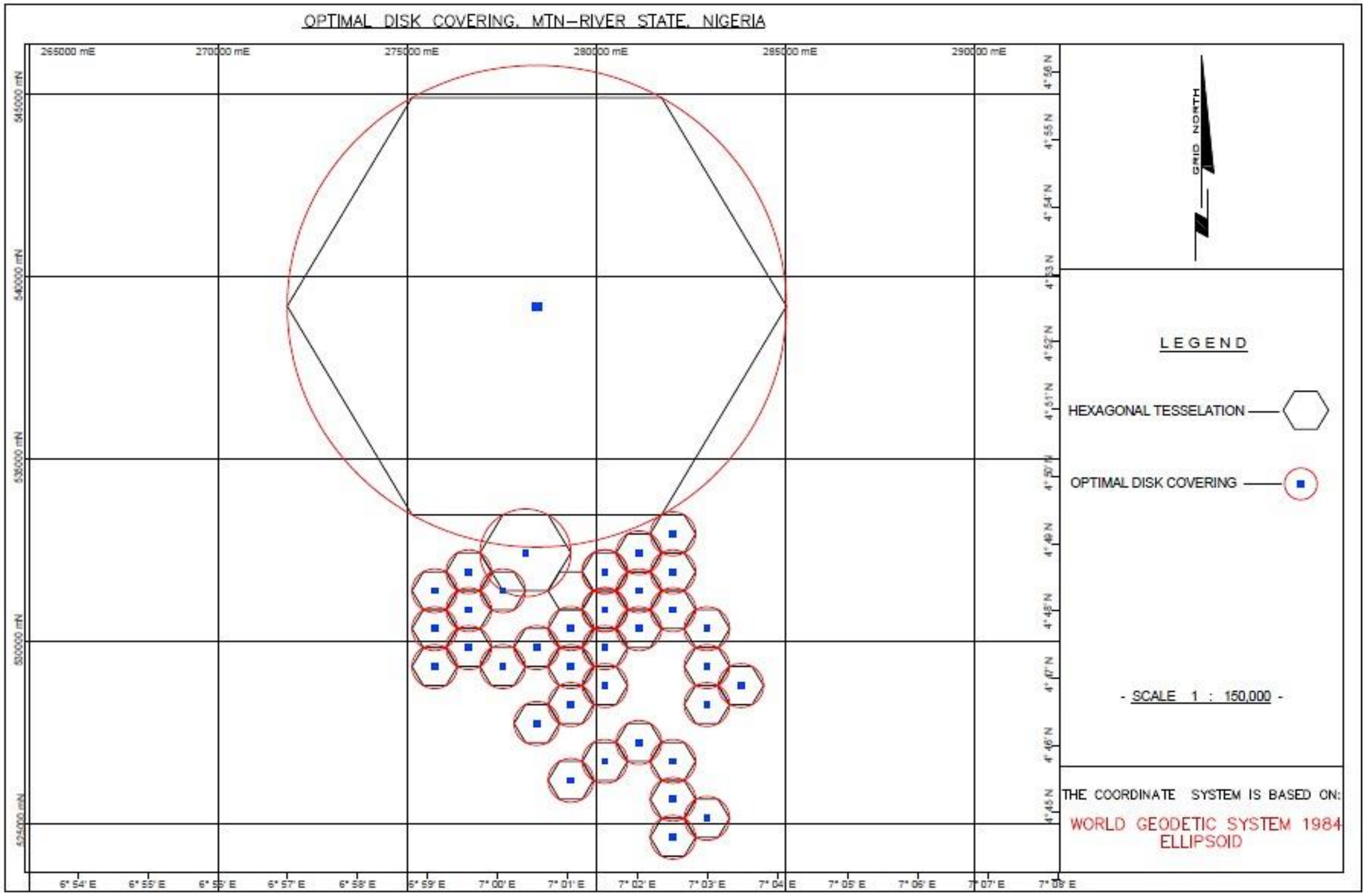

Figure S.6: Optimal Disks Covering of MTN Masts, River State-Nigeria

APPENDIX T

TABLE T.1: OVERLAP DIFFERENCE FOR 0.6km,1.3km, 2.5km MTN CELL RANGE– RIVER STATE (NIGERIA)

Serial	Overlap Difference $d = d_m - d_n$	Value (m)	Area of overlap (A_d)	Serial	Overlap Difference $d = d_m - d_n$	Value (m)	Area of (A_d) overlap
1.	$d_{42} - d_{46}$	289.9813	222044.00	22.	$d_{43} - d_{15}$	123.7141	38621.1256
2.	$d_{46} - d_{49}$	215.2717	124885.00	23.	$d_{13} - d_{35}$	567.2068	811838.0168
3.	$d_{49} - d_{4}$	212.9525	114433.1922	24.	$d_{13} - d_{12}$	109.4508	30229.0436
4.	$d_{4} - d_{8}$	81.6679	16830.20104	25.	$d_{13} - d_{15}$	589.0909	875691.5421
5.	$d_{4} - d_{16}$	233.2389	137274.0656	26.	$d_{15} - d_{35}$	567.2068	811838.0168
6.	$d_{4} - d_{47}$	47.7039	5742.411344	27.	$d_{15} - d_{12}$	214.6637	116279.6587
7.	$d_{4} - d_{34}$	9.6558	235.2681028	28.	$d_{12} - d_{36}$	607.9591	932685.5619
8.	$d_{16} - d_{47}$	493.6746	614990.0552	29.	$d_{31} - d_{23}$	409.7396	423645.3124
9.	$d_{16} - d_{34}$	277.3459	194102.0076	30.	$d_{23} - d_{44}$	438.9687	486243.3069
10.	$d_{16} - d_{9}$	444.7582	499153.8841	31.	$d_{23} - d_{26}$	810.5369	1657799.9
11.	$d_{16} - d_{30}$	241.1916	146794.8718	32.	$d_{23} - d_{45}$	40.8618	4213.2916
12.	$d_{47} - d_{10}$	505.1518	643917.6609	33.	$d_{44} - d_{32}$	215.4276	117108.7144
13.	$d_{6} - d_{5}$	131.4954	43632.25393	34.	$d_{44} - d_{37}$	453.1748	518224.6067
14.	$d_{5} - d_{14}$	27.5591	1916.534266	35.	$d_{44} - d_{26}$	206.3699	107468.0168
15.	$d_{40} - d_{38}$	131.1031	43372.29959	36.	$d_{32} - d_{1}$	129.4741	42301.16504
16.	$d_{40} - d_{17}$	381.1399	366568.6824	37.	$d_{32} - d_{37}$	292.9307	216529.1175
17.	$d_{43} - d_{35}$	633.2396	1011865.197	38.	$d_{27} - d_{1}$	273.7579	189112.3313
18.	$d_{43} - d_{13}$	633.2396	1011865.197	39.	$d_{34} - d_{9}$	487.4520	599584.2833
19.	$d_{9} - d_{30}$	418.2921	441515.3955	40.	$d_{24} - d_{25}$	404.3435	412560.3237

20.	$d_9 - d_{48}$	669.0557	1129564.61	41.	$d_{24} - d_{48}$	483.9451	590988.0793
21.	$d_9 - d_1$	464.3242	544037.9123	42.	$d_{29} - d_{21}$	399.7777	403295.761
43.	$d_{45} - d_{26}$	182.0447	83626.24686	63.	$d_{29} - d_{19}$	23.2047	1358.7465
44.	$d_{45} - d_{21}$	264.4319	176446.9753	64.	$d_{19} - d_{20}$	294.0752	218224.4106
45.	$d_{45} - d_{29}$	212.4948	113941.817	65.	$d_{19} - d_{21}$	534.0102	719590.8493
46.	$d_{26} - d_{37}$	341.6531	294548.8004	66.	$d_{19} - d_{26}$	13.6140	467.6899
47.	$d_{26} - d_3$	636.5535	1022483.593	67.	$d_{20} - d_2$	280.9723	199211.103
48.	$d_{26} - d_{19}$	13.6140	467.6899306	68.	$d_7 - d_{33}$	394.9396	393593.4759
49.	$d_3 - d_{21}$	783.8926	1550599.56	69.	$d_{33} - d_{11}$	624.8460	985218.4021
50.	$d_3 - d_{20}$	99.3801	24922.14313	70.	$d_{33} - d_{39}$	40.3124	4100.7551
51.	$d_3 - d_{19}$	576.9297	839909.1656	71.	$d_{39} - d_{11}$	448.9873	508691.6872
52.	$d_3 - d_{37}$	100.0536	25261.08301	72.	$d_{41} - d_{38}$	597.6027	901180.1747
53.	$d_3 - d_{45}$	5.3750	72.90267503	73.	$d_{41} - d_{17}$	305.7118	235836.4513
54.	$d_{25} - d_1$	298.0264	224127.9406	74.	$d_{38} - d_{40}$	131.1031	43372.2996
55.	$d_{25} - d_{48}$	686.8085	1190303.882	75.	$d_{18} - d_{44}$	517.7495	676434.7394
56.	$d_{25} - d_{30}$	288.3549	209817.2539	76.	$d_{18} - d_{23}$	644.1559	1047052.613
57.	$d_{25} - d_{20}$	152.7068	58844.14814	77.	$d_{18} - d_{37}$	345.0220	300386.2877
58.	$d_{24} - d_{30}$	712.9229	1282542.18	78.	$d_{18} - d_{26}$	810.5369	1657799.9
59.	$d_{24} - d_7$	611.8305	944601.809	79.	$d_{18} - d_3$	247.7574	154895.8552
60.	$d_{18} - d_{45}$	105.7063	28196.04989	80.	$d_{18} - d_{21}$	77.0424	14977.7347
Total $(\sum d) =$ 26,412.518m				Total $(\sum A_d) = 32{,}834{,}104.29$m^2			

APPENDIX U

WGS-84 COORDINATES OBTAIN FROM HEXAGONAL TESSELLATION FOR MTN GSM MAST, RIVER STATE – NIGERIA.

The hexagonal design model resulted in thirty six (36) coordinates with their WGS-84 coordinates shown in Table U.1.

Table U.1: WGS-84 coordinates of MTN GSM masts in River State, Nigeria.

MTN Masts with Node Points (WGS-84)				
Location (Node)	Geographical Coordinates		Grid Coordinates	
	Latitudes	Longitudes	Easterns (Xm)	Northerns (Ym)
1.	7.001829	4.875151	278408	539192.2
2.	6.999304	4.81407	278108	532437.2
3.	7.018272	4.800032	280208	530878.4
4.	6.977757	4.785819	275708	529319.5
5.	6.985854	4.790541	276608	529839.1
6.	7.010283	4.757727	279308	526201.8
7.	6.993979	4.785867	277508	529319.5
8.	7.01838	4.762448	280208	526721.4
9.	7.002076	4.790589	278408	529839.1
10.	7.002131	4.771797	278408	527760.7
11.	7.010201	4.785915	279308	529319.5
12.	7.010228	4.776519	279308	528280.3
13.	7.018299	4.790636	280208	529839.1
14.	7.018326	4.78124	280208	528799.9
15.	7.026478	4.76717	281108	527241.1
16.	7.034602	4.762495	282008	526721.4
17.	7.010183	4.795325	279309	530360.4
18.	7.02637	4.804753	281108	531398
19.	7.026397	4.795358	281108	530358.8
20.	7.034468	4.809475	282008	531917.6
21.	7.034495	4.800079	282008	530878.4
22.	7.04262	4.795404	282908	530358.8
23.	7.042673	4.776612	282908	528280.3
24.	7.042647	4.786008	282908	529319.5
25.	7.034629	4.753099	282008	525682.2
26.	7.042753	4.748424	282908	525162.6
27.	7.050771	4.781333	283808	528799.9
28.	7.034655	4.743703	282008	524643
29.	7.018245	4.809428	280208	531917.6

30.	7.026343	4.814149	281108	532437.2
31.	7.034441	4.818871	282008	532956.8
32.	6.985827	4.799937	276608	530878.4
33.	6.977729	4.795215	275708	530358.8
34.	6.977701	4.804611	275708	531398
35.	6.985799	4.809333	276608	531917.6
36.	6.993924	4.804659	277508	531398

APPENDIX V.1

LOCAL GEOGRAPHICAL COORDINATES OF GLO GSM MASTS FOR ACCRA EAST, GHANA.

Table V.1 shows 50 local grid coordinates of GLO GSM masts for Accra –East in zone 30N provided by ATC (Ghana).

Table V.1: Local Geographic coordinate of GLO masts in Accra-East

POINT ID	SITE NAME	LATITUDE	LONGITUDE	TRIG. HEIGHT
GloGH.1	OPEN SPACE AT OFANKOR HOUSE No 10, ACCRA	5.657466	-0.275807	36m
GloGH.2	ROOFTOP AT HSE NO PKB039, POKUASE JUNC.	5.68708	-0.282001	36m
GloGH.3	ROOFTOP ON HSE NO 29, NANA POKU ROAD TAIFA	5.659459	-0.2508203	36m
GloGH.4	OPEN SPACE OF LAND ON HSE NO CAB 14/7 ASHALE BOTWE	5.67808427	-0.25424116	36m
GloGH.5	ROOFTOP SPACE IN KWABENYA	5.67828064	-0.24235123	36m
GloGH.6	ROOFTOP SPACE ON HSE NO 275/25 DARKUMAN	5.68927135	-0.24483368	36m
GloGH.7	Rooftop space at Hse No.21, New Ashongman Estate	5.6951527	-0.22952464	36m
GloGH.8	Plot at HSE No 233, New Ashongman	5.684753	-0.231469	36m
GloGH.9	Rooftop at Chrisla Hotel, Dome Old Lorry Station. Dome	5.653364	-0.237725	36m
GloGH.10	COMPOUND AT OK36RESIDENTIAL AREA, DOME PILLAR	5.64821288	-0.22808006	36m
GloGH.11	PLOT OF LAND AT KWASHIEBU, ACCRA	5.60026758	-0.26838881	36m
GloGH.12	48, WINNEBA RD,LOWER MARCARTHY HILL	5.568974	-0.287663	36m
GloGH.13	SPACE ON H/N A885/14 MPOASE, DANSOMAN	5.528228	-0.271842	36m

GloGH.14	SPACE IN WEIJA NEW TOWN	5.568384	-0.328613	36m
GloGH.15	ROOFTOP ON H/N 1, DANSOMAN HIGH STREET, DANSOMAN.	5.56458253	-0.26823846	36m
GloGH.16	OPEN SPACE ON HSENO A156/12 NORTH SHIABU, DANSOMAN	5.526645	-0.259819	36m
GloGH.17	OPEN SPACE ON A 843/15 DANSOMAN	5.55017	-0.260567	36m
GloGH.18	ROOFTOP IN HSE NO A527/19 SHARPCURVE MATAHEKO, DANSOMAN	5.567448	-0.256825	36m
GloGH.19	OPEN SPACE ON B10/33/17 SOUTH ODORKOR	5.574238	-0.263441	36m
GloGH.20	OPEN SPACE ON H/N B795/5 AMONTIA ROAD, BUBUASHIE	5.57530563	-0.24821188	36m
GloGH.21	ROOFTOP IN DARKUMAN FIRST ROAD	5.588115	-0.251255	36m
GloGH.22	134 / 20 KWASHIEMAN, ADDY JUNCTION	5.587964	-0.265406	36m
GloGH.23	ONE STOREY BUILDING AT DARKUMAN, FADAMA JUNCTION	5.597083	-0.254072	36m
GloGH.24	OPEN SPACE AT TANTRA HILL	5.640711	-0.254282	36m
GloGH.25	ROOF TOP SPACE ON HSE NO.8, KOFI POTORPHY AVENUE,WEST LEGON.	5.64529852	-0.21386072	36m
GloGH.26	B259 / 24 BRAINYA STREET, MANCHE IMAN TESANO	5.6077	-0.23466672	36m
GloGH.27	OPEN SPACE ON HOUSE NO 23 3RD ROAD TESANO	5.601172	-0.230152	36m
GloGH.28	ROOFTOP ON H/N 222, TESANOHIGHWAY ACCRA.	5.60575926	-0.2256386	36m
GloGH.29	NO 213,AFUNYAN STREET, ABELEMKPE	5.6085279	-0.21689493	36m
GloGH.30	SOACE ON HOUSE NO 1, ABELEMKPE.	5.603851	-0.213805	36m
GloGH.31	ROOFTOP ON PLOT 88, BLOCK 10 ABEKA, ACCRA	5.594984	-0.236242	36m
GloGH.32	PLOT OF LAND AT KANESHIE, ACCRA	5.58491521	-0.23947272	36m

GloGH.33	ROOFTOP ON B1200/7 MANGOLANE1 BUBUASHIE	5.5795239	-0.23439328	36m
GloGH.34	OPEN SPACE ON HSENO 55 KANESHIE 1 ESTATE	5.56642	-0.230216	36m
GloGH.35	ROOFTOP ON B451/6, ABOSSEY OKAI ACCRA.	5.55767435	-0.23238517	36m
GloGH.36	ROOFTOP IN HSENO: A638/4 LARTEBIOKORSHIE, ADAMA ROAD	5.547922	-0.241557	36m
GloGH.37	ROOFTOP SPACE ON HSE NO A1184/3 MANPROBI	5.537049	-0.241004	36m
GloGH.38	ROOFTOP SPACE AT H/N A807/3, ARYEEQUAYE STR,	5.532907	-0.242222	36m
	BABTIST CH. MAMPROBI			
GloGH.39	OPEN SPACE ON HSENO A685/1 KPAKPO BROWN ROAD, KORLE GONNO,	5.533782	-0.226355	36m
GloGH.40	HSE NO F157/8, NORTH LABONE ESTATES	5.57460099	-0.1701683	36m
GloGH.41	OPEN SPACE ON ER.70/5A.254 MULES YARD, ST JAMES TOWN, ACCRA	5.535744	-0.213117	36m
GloGH.42	OPEN SPACE ON D554/4, THOMPSON ROAD ADABRAKA.	5.557939	-0.209928	36m
GloGH.43	Rooftop on H/N B748/10 Awodome Estate	5.572316	-0.225444	36m
GloGH.44	ROOFTOP IN HSENO 3 BARNABAS CRESCENT ADABRAKA, ACCRA	5.566291	-0.216229	36m
GloGH.45	OPEN SPACE ON HSE NO C435/4 GOODWILL ROAD, KOKOLEMLE	5.577878	-0.213108	36m
GloGH.46	OPEN SPACE ON HSENO C494/12 KOTOBABI	5.598745	-0.206155	36m
GloGH.47	ROOFTOP IN HSE NO C569/13 PIGFARM	5.598	-0.197816	36m
GloGH.48	SPACE BELONGING ON H/N D 626/14 DZOWOULU	5.61549	-0.195135	36m
GloGH.49	ROOFTOP SPACE ON H/N E463/16 SECOND MAMOBI LINK, KAWUKUDI	5.59335447	-0.18992832	36m
GloGH.50	OPEN SPACE AT OFANKOR HOUSE No 10, ACCRA	5.57431835	-0.18659207	36m

APPENDIX V.2

WGS-84 COORDINATES FOR GLO MASTS IN ACCRA, SOUTH EAST, GHANA.

Table V.2 shows 50 WGS-84 coordinates of GLO masts in South Eastern Accra - Ghana for a fixed antenna height of 25m and a cell range of 0.8km. Table V.2: WGS-84 coordinates for GLO masts in South East Accra - Ghana

GLO Masts with Node Points (WGS-84)				
Location	Geographical Coordinates		Grid Coordinates	
	Latitude	Longitude	Easterns (Xm)	Northerns(Ym)
1. OPEN SPACE AT OFANKOR HOUSE No 10, ACCRA	5^{0}39′ 26.87760″ N	0^{0}16′ 32.90520″ W	801779.992	626047.993
2. ROOFTOP AT HOUSE NO PKB039, POKUASE JUNCTION	5^{0} 41′ 13.48800″ N	0^{0} 16′ 55.20360 W	801077.948	629321.973
3. ROOFTOP ON HOUSE NO 29, NANA POKU ROAD TAIFA	5^{0} 39′ 34.05240 ″N	0^{0} 15′ 02.95308 W	804549.008	626281.605
4. OPEN SPACE OF LAND ON HSE NO CAB 14/7 ASHALE BOTWE	5^{0} 40′ 41.10337″ N	0^{0} 15′ 15.26818 W	804160.000	628341.000
5. ROOFTOP SPACE IN KWABENYA	5^{0} 40′ 41.81030 ″N	0^{0} 14′ 32.46443 W	805477.999	628369.000
6. ROOFTOP SPACE ON HSE NO 275/25 DARKUMAN	5^{0} 41′ 21.37686″ N	0^{0} 14′ 41.40125 W	805197.000	629584.000
7. Rooftop space at Hse No.21, New Ashongman Estate	5^{0} 41′ 42.54972 ″N	0^{0} 13′ 46.28870 W	806891.000	630243.000
8. Plot at HSE No 233, New Ashongman	5^{0} 41′ 05.11080 ″N	0^{0} 13′ 53.28840 W	806680.972	629091.047
9. Rooftop at Chrisla Hotel, Dome Old Lorry Station.	5^{0} 39′ 12.11040 ″N	0^{0} 14′ 15.81000 W	806003.996	625613.977

10. OPEN SPACE IN A COMPOUND AT OKO RESIDENTIAL AREA, DOME PILLAR	5^0 38′ 53.56637 ″N	0^0 13′ 41.08822 W	807076.000	625049.000
11. PLOT OF LAND AT KWASHIEBU, ACCRA	5^0 36′ 00.96329 ″N	0^0 16′ 06.19972 W	802632.000	619722.000
12. 48, WINNEBA ROAD,LOWER MARCARTHY HILL	5^0 34′ 08.30640 ″N	0^0 17′ 15.58680 W	800511.019	616249.044
13. SPACE ON H/N A885/14 MPOASE, DANSOMAN	5^0 31′ 41.62080 ″N	0^0 16′18.63120 W	802285.974	611748.003
14. SPACE IN WEIJA NEW TOWN	5^0 34′ 06.18240 ″N	0^0 19′ 43.00680 W	795971.020	616163.039
15. ROOFTOP ON H/N 1, DANSOMAN HIGH STREET, DANSOMAN.	5^0 33′ 52.49711 ″N	0^0 16′05.65846 W	802667.000	615773.000
16. OPEN SPACE ON HSENO A156/12 NORTH SHIABU, DANSOMAN	5^0 31′ 35.92200 ″N	0^0 15′ 35.34840 W	803619.959	611578.953
17. OPEN SPACE ON A 843/15 DANSOMAN	5^0 33′ 00.61200 ″N	0^0 15′38.04120 W	803524.993	614181.973
18. ROOFTOP IN HSE NO A527/19 SHARPCURVE MATAHEKO, DANSOMAN	5^0 34′ 02.81280 ″N	0^0 15′ 24.57000 W	803931.039	616095.977
19. OPEN SPACE ON B10/33/17 SOUTH ODORKOR	5^0 34′ 27.25680 ″N	0^0 15′ 48.38760 W	803193.979	616843.988
20. OPEN SPACE ON H/N B795/5 AMONTIA ROAD, BUBUASHIE	5^0 34′ 31.10027 ″N	0^0 14′ 53.56277 W	804881.999	616970.000
21. ROOFTOP IN DARKUMAN	5^0 35′ 17.21400 ″N	0^0 15′ 04.51800 W	804537.964	618385.991

802969.049	618361.964
804220.989	619376.985
804175.033	624205.019
808654.000	624734.000
806367.000	620562.047
806870.978	619841.969
807369.000	620352.000
808337.000	620663.000
808682.057	620147.037
806198.975	619153.972
805846.000	618038.000
806412.000	617444.000
806881.986	615995.992
806646.000	615027.000
805634.035	613942.982

54	612739.984
25	612280.974
26	612386.004
99	616932.999
52	612610.012
06	615067.995
46	616650.980
65	615989.012
70	617272.976
54	619585.990
61	619507.949
62	621445.014
00	618998.000
99	616893.000

308, ACCRA, 10 OSU AVE., EXT. CANTONMENT, ACCRA				

APPENDIX W.1

ORIGINAL LAYOUT OF GSM MASTS LOCATION OF GLO SOUTH EASTERN ACCRA - GHANA.

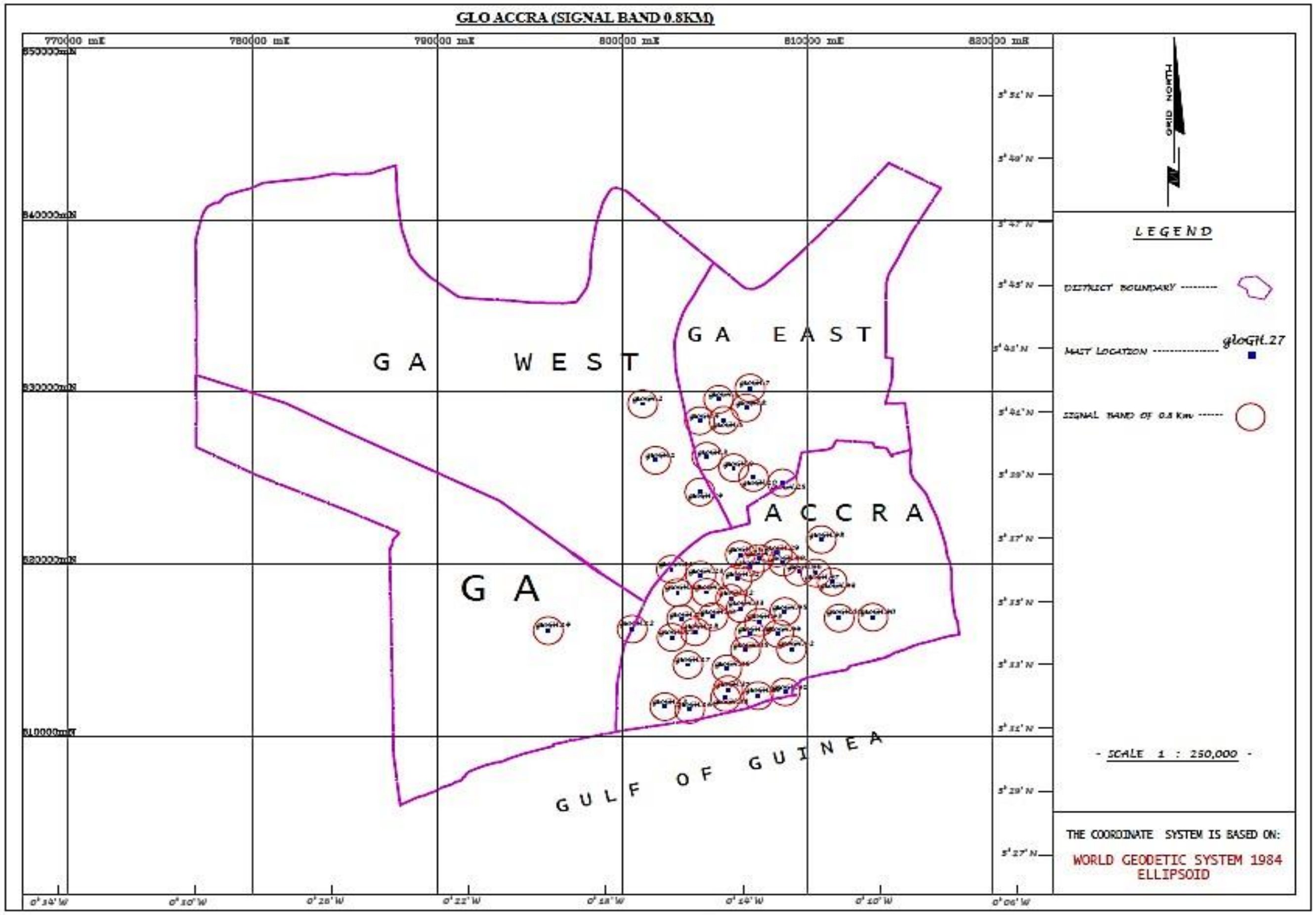

Figure W.1: Original layout of GSM masts, GLO Accra East, Ghana.

APPENDIX W. 2

MATLAB CODE FOR GLO GSM MASTS POSITION WITH MINIMAL HEXAGONAL COVERING, ACCRA EAST-GHANA.

```
load set4
scatter(set4(:,1),set4(:,2),'fill')
n=8.15; m=6.31;
figure(1),hold on for
i=7.945:1.5*.015:n     for j =
6.1009:1.5*0.015:m
hexagon(1.5*0.005,i,j)     end
end


 for i=7.945:1.5*.015:n      for j = 6.1009:1.5*0.015:m
hexagon(1.5*0.005,i+1.5*0.0075,j+1.5*0.0075)
    end  end  axis([7.95 8.15 6.1 6.31])  xlabel('Easterns (xkm)')
ylabel('Northerns (ykm)')  title('Hexagonal Tessellation of GLO ACCRA
EAST-GHANA Masts')
```


APPENDIX W. 3

MATLAB PLOT OF 50 GLO GSM MASTS POSITIONS WITH HEXAGONAL COVERING –ACCRA EAST, GHANA

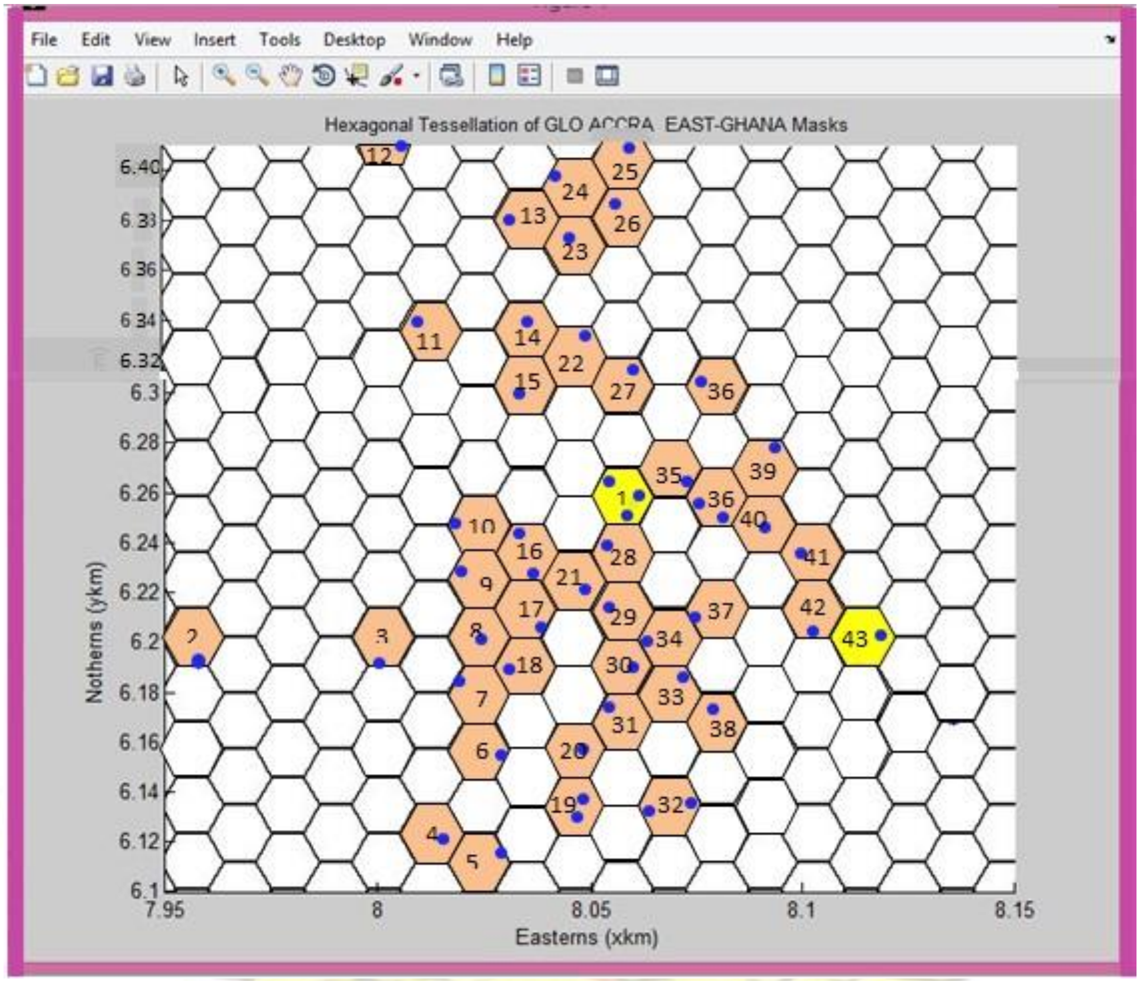

Figure W.3: Coverage Area of GLO South Eastern Accra for 50 WGS-84 Coordinates

APPENDIX W. 4

MAXIMAL NODE COVERING USING HEXAGONS FOR GLO ACCRA-EAST, GHANA.

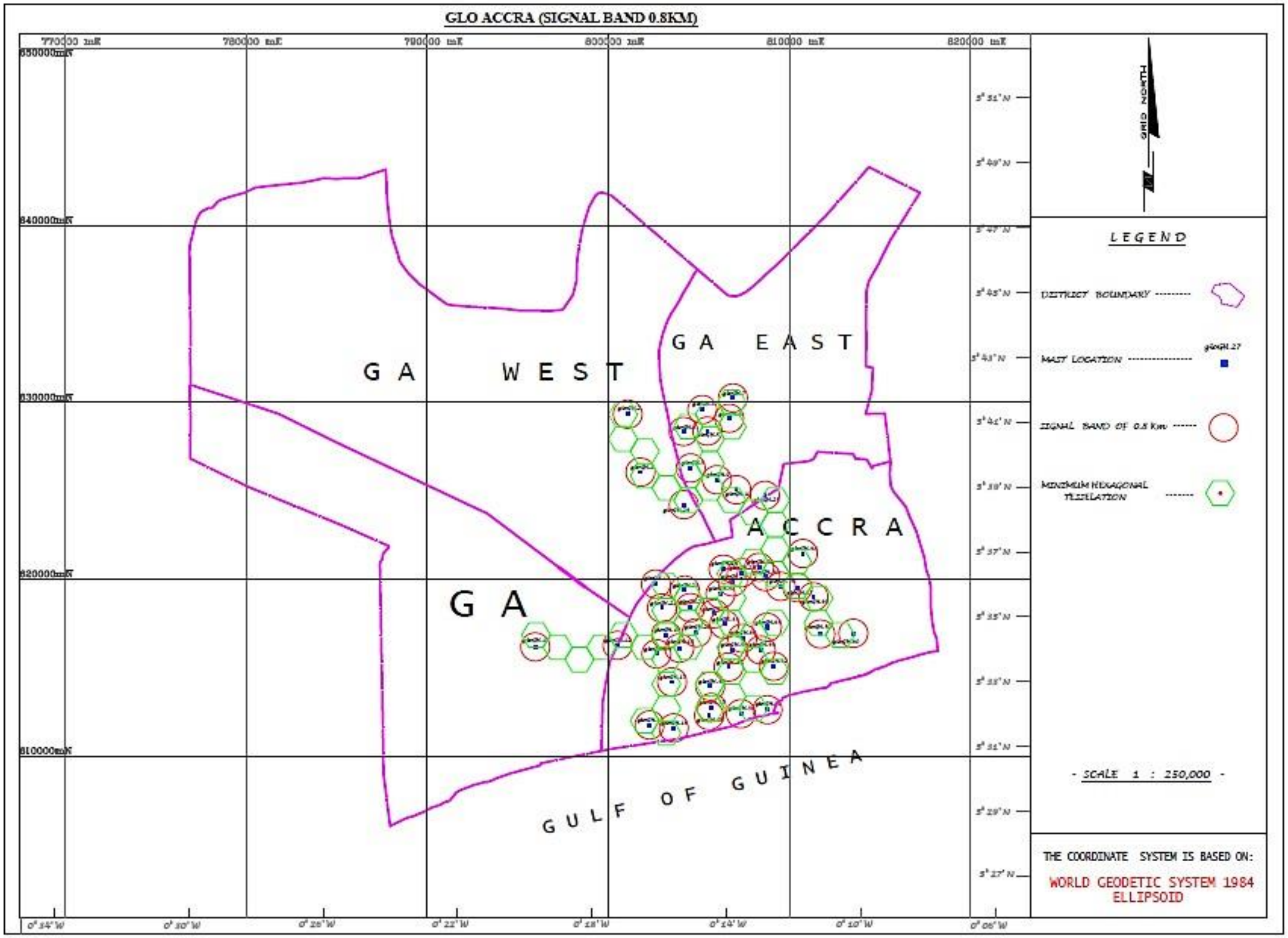

Figure W.4: Maximal node covering using hexagons for GLO Accra-East

APPENDIX W.5

MINIMUM HEXAGONAL TESSELLATION FOR GLO MASTS,ACCRA EAST- GHANA.

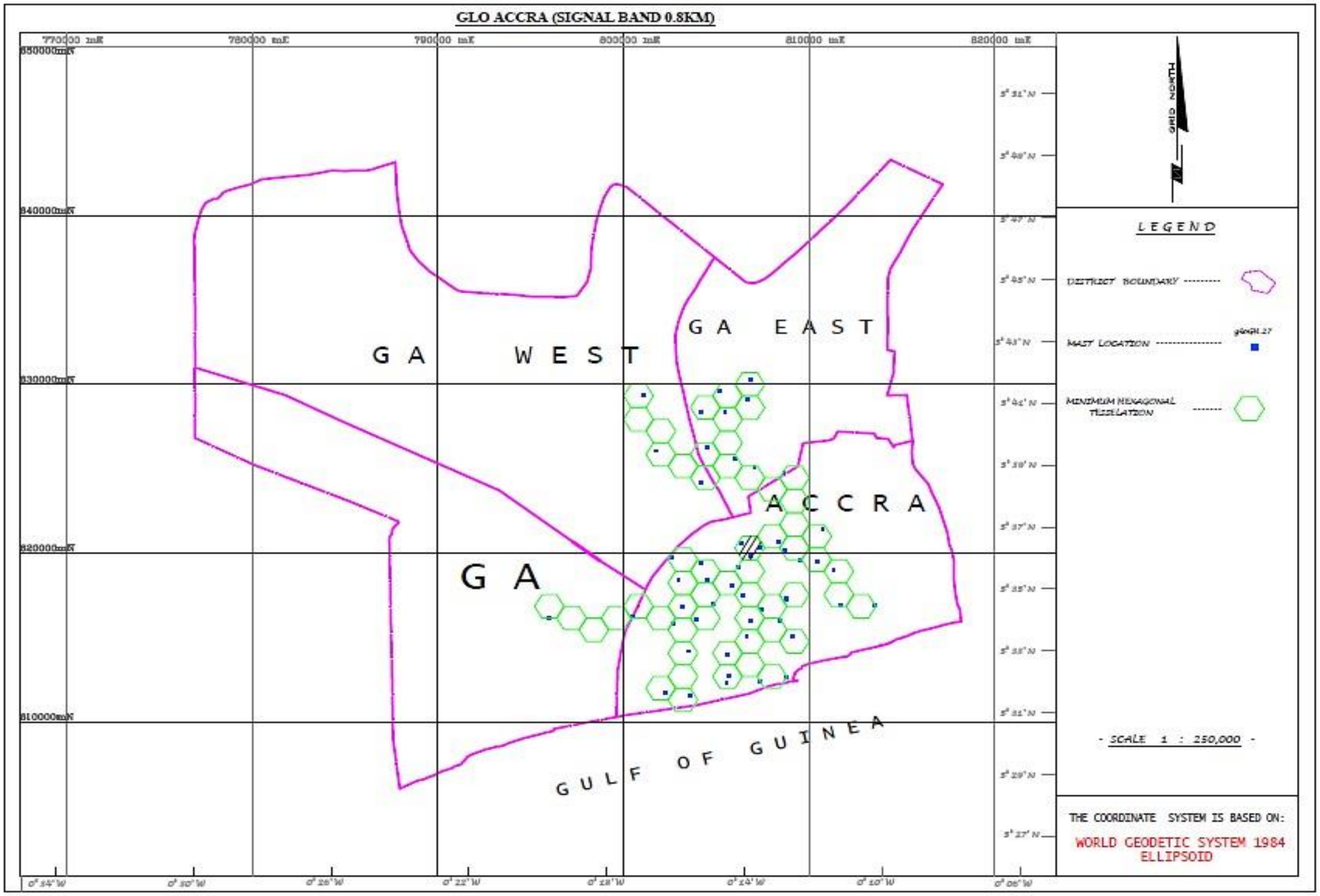

Figure W.5: Minimal Hexagonal Tessellation of GLO Accra East-Ghana

APPENDIX W. 6

OPTIMAL DISKS COVERING FOR GLO MASTS, ACCRA EAST-GHANA

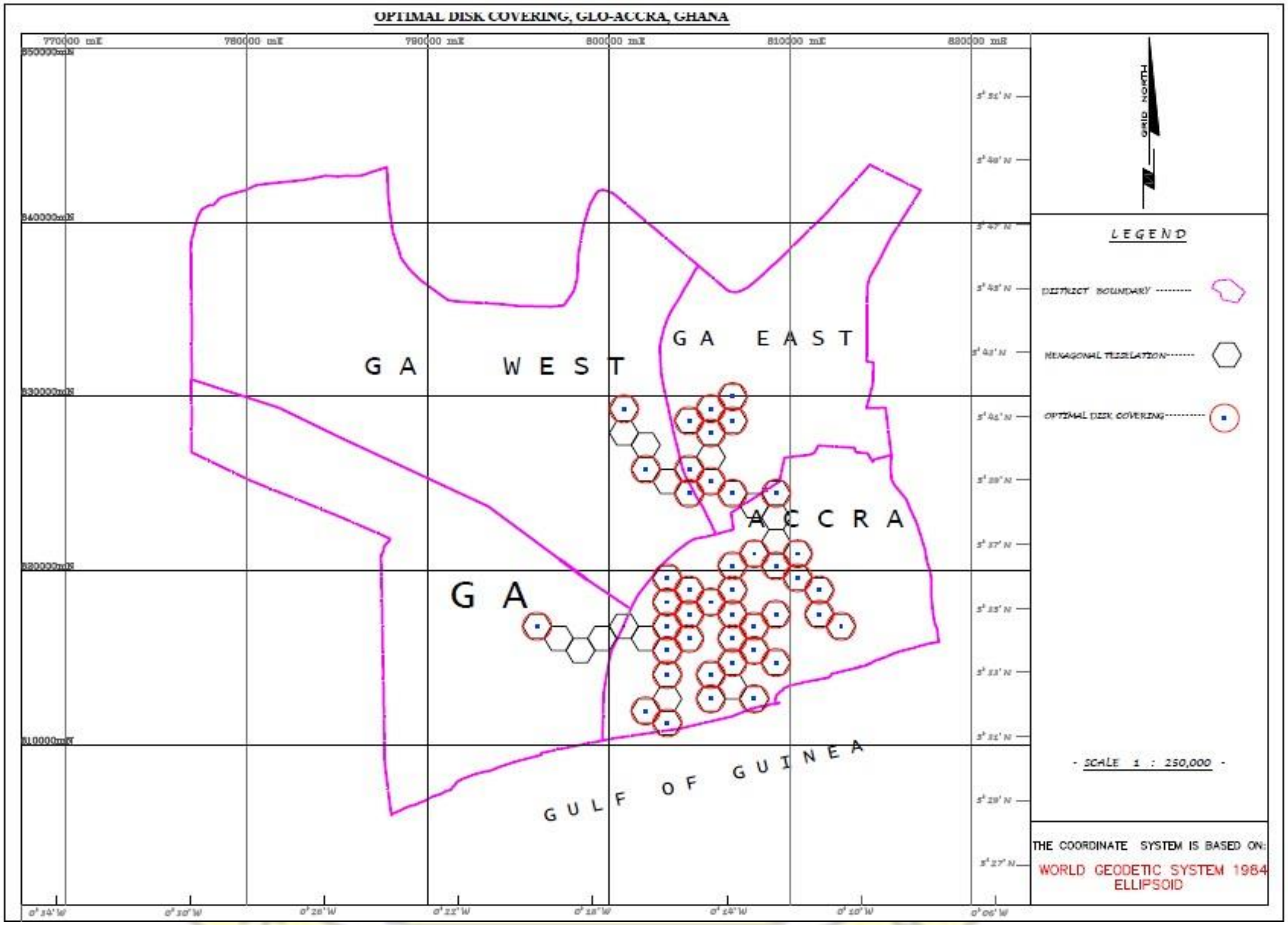

Figure W.6: Optimal Disks Covering of GLO masts, Accra East-Ghana

APPENDIX X

TABLE X.1: OVERLAP DIFFERENCE FOR 0.8KM GLO CELL RANGE– ACCRA EAST.

Serial	Overlap Difference $d = d_m - d_n$	Value (m)	Area of overlap (A_d)	Serial	Overlap Difference $d = d_m - d_n$	Value (m)	Area of overlap (A_d)
1.	$d_4 - d_5$	281.7036	200249.45	20.	$d_{32} - d_{33}$	779.5172	1533338.1
2.	$d_6 - d_5$	352.9293	314312.72	21.	$d_{33} - d_{43}$	77.6288	15206.605
3.	$d_5 - d_8$	196.9690	97899.909	22.	$d_{34} - d_{43}$	755.9221	1441918.2
4.	$d_9 - d_{10}$	388.2279	380329.5	23.	$d_{34} - d_{35}$	602.6862	916577.14
5.	$d_7 - d_8$	429.0570	464532.94	24.	$d_{35} - d_{36}$	117.0407	34566.893
6.	$d_{11} - d_{22}$	198.8219	99750.474	25.	$d_{36} - d_{37}$	1052.7667	2796731.7
7.	$d_{22} - d_{21}$	30.9010	2409.5259	26.	$d_{37} - d_{38}$	1122.1294	3177403.8
8.	$d_{19} - d_{15}$	406.3827	416732.1	27.	$d_{28} - d_{29}$	583.2675	858463.99
9.	$d_{15} - d_{18}$	295.3511	220122.13	28.	$d_{28} - d_{30}$	271.0423	185379.06
10.	$d_{13} - d_{16}$	255.3462	164530.09	29.	$d_{28} - d_{27}$	583.2675	858463.99
11.	$d_{23} - d_{21}$	559.5471	790059.55	30.	$d_{43} - d_{44}$	379.8932	364174.53
12.	$d_{21} - d_{32}$	853.1964	1836895.9	31.	$d_{39} - d_{41}$	116.0689	33995.252
13.	$d_{21} - d_{20}$	142.8142	51467.054	32.	$d_{29} - d_{30}$	979.2890	2419960.5
14.	$d_{20} - d_{32}$	161.2777	65634.952	33.	$d_{30} - d_{46}$	580.7849	851171.67
15.	$d_{21} - d_{18}$	142.8142	51467.054	34.	$d_{45} - d_{44}$	271.7805	186390.22
16.	$d_{26} - d_{28}$	576.2209	837846.65	35.	$d_{44} - d_{42}$	441.3202	491466.75
17.	$d_{26} - d_{27}$	721.0767	1312047.2	36.	$d_{44} - d_{34}$	49.0053	6060.0001
18.	$d_{26} - d_{31}$	181.9353	83525.766	37.	$d_{46} - d_{47}$	671.7068	1138534
19.	$d_{31} - d_{32}$	429.5365	465571.81	38.	$d_{47} - d_{49}$	585.4827	864997.12
					Total $(\sum A_d) = 26,030,184.0m^2$		

Total $(\sum d) = 16{,}624.7086m$	

APPENDIX Y

WGS-84 COORDINATES OBTAIN FROM HEXAGONAL TESSELLATION FOR GLO GSM MAST, ACCRA EAST-GHANA.

The hexagonal design model resulted in forty three (43) coordinates with their WGS-84 coordinates shown in table Y.1.

Table Y.1: WGS-84 coordinates of GLO GSM masts in Accra-East Ghana.

GLO Masts with Node Points (WGS-84)				
Serial	Geographical Coordinates		Grid Coordinates	
	Latitudes	Longitudes	Easterns (Xm)	Northerns (Ym)
1.	-0.23017	5.692946	806820.5	629998.5
2.	-0.23066	5.605304	806813	620299
3.	-0.23023	5.680426	806820.5	628612.8
4.	-0.27429	5.530382	802013	611985.2
5.	-0.27365	5.65559	802020.5	625841.6
6.	-0.26321	5.586676	803213	618220.5
7.	-0.26327	5.574155	803213	616834.9
8.	-0.26333	5.561634	803213	615449.3
9.	-0.26339	5.549114	803213	614063.6
10.	-0.2635	5.524072	803213	611292.3
11.	-0.25236	5.592886	804413	618913.4
12.	-0.25242	5.580365	804413	617527.7
13.	-0.25248	5.567844	804413	616142.1
14.	-0.252	5.655488	804420.5	625841.6
15.	-0.25206	5.642968	804420.5	624455.9
16.	-0.24157	5.586574	805613	618220.5
17.	-0.24174	5.549013	805613	614063.6
18.	-0.2418	5.536492	805613	612678
19.	-0.24109	5.674218	805620.5	627920
20.	-0.2412	5.649177	805620.5	625148.7
21.	-0.23071	5.592784	806813	618913.4
22.	-0.23077	5.580263	806813	617527.7
23.	-0.23083	5.567743	806813	616142.1
24.	-0.23089	5.555223	806813	614756.4
25.	-0.23041	5.642865	806820.5	624455.9

26.	-0.21998	5.573952	808013	616834.9
27.	-0.22004	5.561432	808013	615449.3
28.	-0.22016	5.536391	808013	612678
29.	-0.20913	5.580161	809213	617527.7
30.	-0.20925	5.555121	809213	614756.4
31.	-0.20876	5.642761	809220.5	624455.9
32.	-0.18743	5.592578	811613	618913.4
33.	-0.18749	5.580058	811613	617527.7
34.	-0.24108	5.68683	805614.7	629315.8
35.	-0.19809	5.611409	810420.5	620991.8
36.	-0.17669	5.573746	812813	616834.9
37.	-0.32821	5.574454	796013	616834.9
38.	-0.20901	5.605201	809213	620299
39.	-0.21974	5.611513	808020.5	620991.8
40.	-0.28432	5.686944	800820.5	629305.7
41	-0.25193	5.680621	804414.7	628623
42.	-0.26315	5.599197	803213	619606.2
43.	-0.19822	5.59889	810413	619606.2

APPENDIX Z.1

TOTAL COVERAGE AREA OF ORIGINAL NETWORK DESIGN

We compute the total coverage area of the original disks used by the various GSM networks in their design and compare it to the area coverage obtain by the hexagonal tessellation. For n different disks (A) we use the inclusionexclusion principle formula below.

$$Area\left|\bigcup_{i=1}^{n} A_i\right| = Area\sum_{i}|A_i|$$

$$- Area\sum_{i<j}\left|A_i \cap A_j\right|$$

$$+ Area\sum_{i<j<k}\left|A_i \cap A_j \cap A_k\right| - \cdots + (-1)^{n+1} Area\left|\bigcap_{i=1}^{n} A_i\right|$$

where the first sum is over all i the second sum is over all pairs $i.j$ with $i <$ j, the third sum is over all triples i, j, k with $i < j < k$ and so fourth.

Z.1 MTN GSM DESIGN, KUMASI EAST-GHANA

$$Area = 50 \times \pi \times 600^2 - 31{,}508{,}849.82$$

$$= 25{,}039{,}817.94 m^2$$

$$= 25.04km^2$$

Z.2 GLO GSM DESIGN, ACCRA EAST-GHANA

$$Area = 50 \times \pi \times 800^2 - 26{,}030{,}184.0$$

$$= 74{,}500{,}780.91m^2$$

$$= 74.50km^2$$

Z.3 MTN GSM DESIGN, RIVER STATE - NIGERIA

$$Area = 48 \times \pi \times 600^2 + 1 \times \pi \times 1300^2 + 1 \times \pi \times 6600^2 - 32{,}834{,}104.29$$

$$= 21{,}477{,}435.35m^2$$

$$= 21.48km^2$$

Z.4 GLO GSM DESIGN, RIVER STATE - NIGERIA

$$Area = 44 \times \pi \times 1000^2 + 1 \times \pi \times 3000^2 - 55{,}019{,}724.45$$

$$= 111{,}484{,}686.20m^2$$

$$= 111.48km^2$$

APPENDIX Z. 2

TOTAL COVERAGE AREA OF TILED HEXAGONAL NETWORK DESIGN

We compute the total coverage area of the proposed hexagonal tessellation employed in the design and compare with the existing coverage area. We use the formula in equation (4.49)

$$\text{Area of hexagon} = \frac{3\sqrt{3}}{2} R^2$$

$$\text{Total area of hexagon} = \text{sum of Number of hexagons} \times \text{unit area}$$

$$= \sum_{i=1}^{n} N_{R_i} \times \frac{3\sqrt{3}}{2} R_i^2$$

Where

$R_i =$ disks with radius i

$N_{R_i} =$ Number of disks with radius i

Z.1 MTN GSM DESIGN, KUMASI EAST-GHANA

$$Area = 35 \times \frac{3\sqrt{3}}{2} \times 600^2$$

$$= 32{,}735{,}760.26 m^2$$

$$= 32.74 km^2$$

Z.2 GLO GSM DESIGN, ACCRA EAST-GHANA

$$Area = 43 \times \frac{3\sqrt{3}}{2} \times 800^2$$

$$= 71{,}499{,}057.341 m^2$$

$$= 71.50km^2$$

Z.3 MTN GSM DESIGN, RIVER STATE - NIGERIA

$$Area = 34 \times \frac{3\sqrt{3}}{2} \times 600^2 + 1 \times \frac{3\sqrt{3}}{2} \times 1200^2 + 1 \times \frac{3\sqrt{3}}{2} \times 6600^2$$

$$= 148{,}713{,}882.3m^2$$

$$= 148.71km^2$$

Z.4 GLO GSM DESIGN, RIVER STATE - NIGERIA

$$Area = 37 \times \frac{3\sqrt{3}}{2} \times 1000^2 + 1 \times \frac{3\sqrt{3}}{2} \times 3000^2$$

$$= 119{,}511{,}505.722253m^2$$

$$= 119.51km^2$$

APPENDIX Z. 3

COSTS OF ORIGINAL LAYOUT VRS. PROPOSED HEXAGONAL TESSELLATION DESIGN.

The unit price provided by ATC (Ghana), Helios (Ghana) and EATON (Ghana) was used to calculate the cost incur by each design model. Table Z.3 shows the results.

Table Z.3: Costs of original layout versus hexagonal tessellation model.

Total Overlap Cost		Hexagonal Tessellation Design	Original layout
MTN- Kumasi East ($R_1 = 0.6km$)	Number of Overlaps (n)	36	76
	Total Overlap Difference $d_n = (2-\sqrt{3})nR_1$	$5{,}787.7026m$	26,884.4603m
	Cost (\$)= unit price × number of GSM masts	$35 \times 142000 = \$4{,}970{,}000$	\$7,100,000
	Number of GSM Masts (N)	35	50
GLO – Accra East ($R_1 = 0.8km$)	Number of overlaps (n)	45	38
	Total Overlap Difference: $d_n = (2-\sqrt{3})nR_1$	$9{,}646.171m$	$16{,}624.7086m$
	Cost (\$) = unit × price number of masts	43× \$141,287.96 = \$6,075,382.28	\$7,064,398.00
	Number of GSM Masts (N)	43	50

), , 2	80
10m	$26{,}412.518m$
, N_{R_3}-1	N_{R_1}-48, N_{R_2} -1 N_{R_3}-1
86	$7,190,569.86
	50
	63
$3m$	30,945.9100m
1	N_{R_1}-44, $N_{R_2} - 1$
954	$6,634,713.434
	45

APPENDIX Z.4

PERCENTAGE CHANGE IN THE GSM OVERLAP DIFFERENCE IN HEXAGONAL TESSELLATION VRS. ORIGINAL LAYOUT.

We calculate the percentage change of our GSM hexagonal coverage design over the original layout using the formula:

$$\text{Percentage Change} = \frac{Change\ in\ Value}{Actual\ Value} \times 100\%$$

Z.4.1 OVERLAP DIFFERNCE FOR MTN KUMASI EAST GHANA

$$\text{Percentage Change} = \frac{26{,}884.4603 - 5787.7026}{26{,}884.4603\text{m}} \times 100\%$$

$$= 78.50\%$$

Z.4.2 OVERLAP DIFFERNCE FOR GLO ACCRA- EAST GHANA

$$\text{Percentage Change} = \frac{16{,}624.7086 - 9{,}646.171}{16{,}624.7086} \times 100\%$$

$$= 41.98\%\%$$

Z.4.3 OVERLAP DIFFERNCE FOR MTN RIVER STATE, NIGERIA

$$\text{Percentage Change} = \frac{126{,}412.518 - 12{,}850.0185}{126{,}412.518} \times 100\%$$

$$= 89.83\%$$

Z.4.3 OVERLAP DIFFERNCE FOR GLO RIVER STATE, NIGERIA

$$\text{Percentage Change} = \frac{30{,}945.9100 - 16{,}344.90074}{30{,}945.9100} \times 100\%$$

$$= 47.18\%$$

APPENDIX Z.5

TOTAL OVERLAP AREA OF HEXAGONAL TESSELLATION.

We compute the total overlap area of the proposed hexagonal tessellation employed in the design and compare with the existing overlap area. We use the formula in equation (4.23) for n tessellable regular polygons or (4.58c) for a single overlap area.

Case I: Uniform Cell Range

$$A_n = \left(\frac{d_n}{4n}\right)^2 cosec^4\left(\frac{\pi}{2n}\right)\left[2\pi - nsin\left(\frac{2\pi}{n}\right)\right] \text{ or}$$

$$A = \frac{\left(2+\sqrt{3}\right)^2\left(2\pi-3\sqrt{3}\right)}{6} d^2$$

where $d = \left(2-\sqrt{3}\right)R_1$

For n overlaps,

$$A_n = \frac{\left(2+\sqrt{3}\right)^2\left(2\pi-3\sqrt{3}\right)}{6} d^2 \times n$$

Z.5.1 TOTAL OVERLAP AREA FOR MTN KUMASI –EAST, GHANA

$$A_{36} = \frac{\left(2+\sqrt{3}\right)^2\left(2\pi-3\sqrt{3}\right)}{6}\left[\left(2-\sqrt{3}\right)\times 600\right]^2 \times 36$$

$$= 2{,}347{,}991.03m^2$$

$$= 2.235km^2$$

Z.5.2 TOTAL OVERLAP AREA FOR GLO ACCRA-EAST, GHANA

$$A_{45} = \frac{\left(2+\sqrt{3}\right)^2\left(2\pi-3\sqrt{3}\right)}{6}\left[\left(2-\sqrt{3}\right)\times 800\right]^2 \times 45$$

$$= 5{,}217{,}757.84m^2$$

$$= 5.218km^2$$

Case II: Non-uniform Cell Range

$$A = \frac{\left(2+\sqrt{3}\right)^2\left(2\pi-3\sqrt{3}\right)}{6} \times n \times d^2 + autocad\ value\ (polyline)$$

Z.5.3 TOTAL OVERLAP AREA OF MTN RIVER STATE-NIGERIA

$$A = \frac{\left(2+\sqrt{3}\right)^2\left(2\pi-3\sqrt{3}\right)}{6} \times 600^2 \times 51 + autocad\ value(890{,}972.4509m^2)$$

$$= 47.22km^2$$

Z.5.4 TOTAL OVERLAP AREA OF GLO RIVER STATE –NIGERIA

$$A = \frac{\left(2+\sqrt{3}\right)^2(2\pi - 3\sqrt{3})}{6} \times 1000^2 \times 54 + autocad\ value\ (23{,}561{,}944.9m^2)$$

$$= 159{,}825{,}678.4m^2$$

$$= 159.83km^2$$

APPENDIX Z.6

PERCENTAGE CHANGE IN THE GSM TOTAL COVERAGE AREAS IN THE HEXAGONAL TESSELLATION VRS. ORIGINAL LAYOUT

We calculate the percentage change of coverage area of our GSM hexagonal coverage design over the original layout using the formula:

$$\text{Percentage Change} = \frac{Change\ in\ Value}{Actual\ Value} \times 100\%$$

Z.4.1 TOTAL OVERLAP AREA FOR MTN KUMASI –EAST, GHANA

$$\text{Percentage Change} = \frac{32.74 - 25.04}{25.04} \times 100\%$$

$$= 30.75\%$$

Z.4.2 TOTAL OVERLAP AREA FOR GLO ACCRA- EAST GHANA

$$\text{Percentage Change} = \frac{74.50 - 71.50}{74.50} \times 100\%$$

$$= 4.03\%$$

Z.4.3 TOTAL OVERLAP AREA FOR MTN RIVER STATE, NIGERIA

$$\text{Percentage Change} = \frac{148.71 - 21.48}{21.48} \times 100\%$$

$$= 592.32\%$$

Z.4.4 TOTAL OVERLAP AREA FOR GLO RIVER STATE, NIGERIA

$$\text{Percentage Change} = \frac{119.51 - 111.48}{111.48} \times 100\%$$

$$= 7.20\%$$

APPENDIX Z.7

RESEARCH PAPER'S PUBLISHED

This appendix contain a list of papers published from this research work.

1. Donkoh E.K.,Amponsah S.K.,Opoku A.A and Buabeng .I. (2015).Hexagonal Tessellation Model For Masting GSM Antenna: Case Study of MTN

Kumasi East-Ghana. International Journal of Applied Mathematics, Article ID:27704180, ISSN: 2051-5227, Vol. 30, Issue. 1, pp 1349 – 1357, UK.

2. Donkoh E. K., Amponsah S. K., Ansere A. J and Bonsu A. K. (2015). Masting Conjecture for Multiple Size Hexagonal Tessellation in GSM Network Design. International Journal of Mathematical and Computer Modelling. Article ID: 27704276, Vol. 20, Iss. 1, ISSN: 2051-4271,pp 1156-1167
3. Donkoh E. K., Amponsah S. K., Ansere A. J and Bonsu A. K. (2015). Application of Least Overlap Difference for Multiple Size Hexagonal Tessellation in GSM Network Design: Case Study of GLO River State, Nigeria. International Journal of Mathematical Sciences, Article ID: 27704275, ISSN:2051-5995, Vol. 35, Iss.1,pp 1712 – 1726, UK.
4. Donkoh E. K., Amponsah S. K. and Opoku A. A. (2015). Optimal Geometric Disks Covering using Tessellable Regular Polygons. Journal of Mathematics and Statistics, Maxwell Scientific Journal-Accepted.
5. Amponsah S. K, Donkoh E. K.. and Opoku A. A. (2015). Optimal Disks Overlap For Cell Planning in Telecommunication Network Design. International Journal of Mathematical Sciences, Article ID: 277042983, ISSN:2051-5995, Vol. 35, Iss.1,pp 1748-1756.
6. Donkoh E. K, Amponsah S. K., and Opoku A. A. (2015). Overlap Dimensions in Cyclic Tessellable Regular Polygons (2015). Research Journal of Mathematics and Statistics, Maxwell Scientific Journal, ISSN:2042-2024, e-ISSN:2040-7505,Vol.7, Issue 2,pp 11 – 16. Retrieved from URL: http://www.maxwellsci.com/print/rjms/v7-11-16.pdf